



**University of
Nottingham**

UK | CHINA | MALAYSIA

The Study of Troglitazone Liver Toxicity via *in vitro* and *in silico* Approaches

Mathias Nuamah

School of Life Sciences

Thesis submitted for the degree of Doctor of Philosophy

July 2021

Supervisors

Dr. Andrew Bennett

Prof. Guru Aithal

Abstract

Background: Drug-induced liver injury (DILI) is rare but potentially lethal, and it can cause liver disease attributable to all types of drugs. The adverse impact of most of the DILI incidents is mild, and it recovers after the removal of drugs. The harmful agents should be identified and removed as early as possible to avoid the development of chronic liver damage. Troglitazone (TGZ) was a derivative of a thiazolidinedione drug produced for the treatment of type 2 diabetes, in the late 1990s. However, it was withdrawn from the market due to reported cases of liver toxicities. Several molecular mechanisms have been proposed to underlie TGZ-induced liver toxicity. Understanding the interactions between these mechanisms could aid drug developers in predicting DILI more vigorously.

Aim: This thesis is aimed at using a combination of *in silico* and *in vitro* approaches to evaluate the interaction of TGZ with multiple biological systems and predict the emergent biological pathways in TGZ-induced liver toxicity.

Method: To evaluate TGZ toxicity pathways, a model was constructed using Petri net software termed "SNOOPY" to reconstruct the putative cellular effects of TGZ, including activation of PPAR γ , interaction with mitochondria, and activation of apoptosis. The model was imported into the MUFINS software suite and simulated. Activation of apoptosis was validated against the published systems biology markup language (SBML) model downloaded from BIOMODELS, upon which the model was created. The effects of TGZ on cellular activities were determined through an *in vitro* approach.

Results: The model created in SNOOPY and simulated in MUFINS could reproduce the behaviour of the original submission of BIOMODELS simulated in COPASI, validating the reconstruction. Other possible TGZ toxicity pathways have been predicted. TGZ-induced apoptosis is done through the activation of caspase 3/7 and 9, in a concentration-dependent manner. Also, a dose-dependent decrease in cellular processes has been recorded. However, caspase-8 activation in TGZ-treated cells has not been recorded.

Conclusion: These data support the activation of apoptosis via the intrinsic route. The *in silico* model reproduces the original model, and it can therefore be used to predict TGZ induced-liver toxicity. The *in vitro* assays were useful tools to elucidate TGZ-induced toxicity, making it a suitable model for this study.

Declaration

I declare that this thesis and the work to which it refers are the results of my efforts. In conjunction with Prof. Nick Plant (my external supervisor), we generated the *in silico* data. All sources of information have been justly recognised by means of reference. As a result of this, I declare that this thesis has been written by me and has not been submitted in any previous application for a degree. I agree that the university has the right to submit my work to the plagiarism detection service Turnitin for originality checks.

Acknowledgements

I wish to extend my appreciation to my supervisors, Dr. Andrew Bennett and Prof. Guru Aithal, for granting me permission to continue my research and for providing supervision and support while allowing me to work independently. I will always be grateful to my external supervisor, Prof. Nick Plant, who gave me the opportunity to undertake this research. Prof. Plant has supported me throughout my studies with total commitment. I attribute the usage of advanced research techniques to my supervisors' encouragement and support.

I am truly appreciative and thankful to my former tutor, Dr. Poorna Gunasekera, who encouraged and supported me during my toughest times. I am so thankful to Dr. Danso for his support and encouragement throughout my journey. Also, I thank the friendly technicians, Monika Owen and Nicola De Vivo, who kept me amply stocked with general supplies and assisted me in my laboratory experiences. Also, I must thank my colleagues, Amy Barber, Razan Al-Momani and Rawan Edan, for sharing their experiences and providing invaluable assistance.

Above all, I pay tribute to God for blessing me with wisdom and health throughout this research journey.

The list of abbreviations

ALT	Alanine transaminase
AP-1	Activator-protein-1
APAF-1	Apoptotic protease activating factor 1
APAP	Paracetamol (or acetaminophen)
AR	Androgen
ASK1	Apoptosis signal-regulating kinase 1
AST	Aspartate transaminase
ATP	Adenosine triphosphate
Bcl-2	B-cell lymphoma 2
BSEP	Bile salt export pump
Ca ²⁺	Calcium ion
cAMP	cyclic adenine monophosphate
CEs	Mammalian carboxylesterases
COPASI	Complex Pathway Simulator
CPS1	carbamoyl phosphate synthetase I,
CRMs	chemically reactive metabolites
CsA	Cyclosporin A
CyP	Cytochrome P450
Cyt. C	Cytochrome c
DAMPs	Danger-associated molecular pattern molecules
DBD	DNA-binding domain
DILI	Drug-induced liver injury
DISC	Death inducing signalling complex
DMEM	Dulbecco's Modified Eagle's Medium
DMSO	Dimethyl sulfoxide
DNA	Deoxyribonucleic Acid
DRIP	Vitamin D receptor-interacting proteins
DT	Doubling Time
ECACC	European Collection of Authenticated Cell Cultures
ER	Endoplasmic reticulum

ER	Estrogen receptor
ERK	Extracellular signal-regulated protein kinase
ETC	Electron transport chain
FADD	FAS-associated protein death domain protein
FBS	Foetal Bovine Serum
FFA	Free Fatty Acid
FMO	Flavin-containing monooxygenase
G6Pase	Glucose-6-phosphatase enzyme
GIP	Glucose-dependent insulinotropic peptide
GLPK	GNU Linear Programming Kit
GR	Glucocorticoid
GRN	Glucuronide
GS	Glutamine synthetase
GSH	Glutathione
GSMN	Genome Scale Metabolic Network
GSSG	Glutathione disulphide
GST	Glutathione S-transferase
H ₂ O ₂	Hydrogen Peroxide
HC	heavy α -chain
HCT-116	Human colorectal cancer cells
HDAC	Histone deacetylation
HMGCR	3-hydrogen-3methylglutaryl-coenzyme A reductase
HREs	hormone response elements
HSC	Hepatic stellate cells
Huh7	Human hepato cellular carcinoma cell
IDILI	Idiosyncratic drug-induced liver injury
IPLA ₂	Calcium-independent phosphate A (2)
IRS-1	Insulin receptor substrate 1
JNK	c-jun-terminal kinase
K _m	Michaelis-Menten constant

LFT	Liver function test
LSECs	Liver sinusoidal epithelial cells
MAPK	Mitogen-activated protein kinase
MCF-7	Human breast cancer cells MCF-7
MMAC1	Mutated in multiple advanced cancers 1
Mn-SOD	Manganese dismutase
MoMA	Minimisation of metabolic adjustment
MOMP	Mitochondrial outer membrane permeabilisation
MPC	Mitochondrial Pyruvate Carrier
MPTP	Mitochondrial permeability transition pore
MR	Mineralocorticoid
MRC	Mitochondrial respiratory chain
MuFINS	Multi Formalism Interaction Network Simulator
NAC	N-acetyl L-cysteine
NADPH	Reduced nicotinamide adenine dinucleotide phosphate
NAPBQI	N-acetyl-p-benzoquinone imine
NO	Nitric Oxide
NSD-1	Nuclear receptor-binding SET domain-containing protein 1
OQM	O-quinone methide
PARP	Poly (ADP-ribose) polymerase
PASMCs	Pulmonary artery smooth muscle cells
PC-3	Human prostate cancer cells
PCs	Positive cofactors
Pepck	Phosphoenolpyruvate carboxykinase
pH	Power of Hydrogen (Hydrogen ion concentration)
PIP3	P1P3 Phosphatidylinositol (3,4,5)-trisphosphate (PtdIns (3,4,5) P3),
PPAR γ	Peroxisome proliferator-activated receptor gamma
PTEN	Phosphatase and tensin homologue deleted from chromosome 10
Puma	p53 upregulated modulator of apoptosis
PXR	Pregnane X receptor

QSSPN	Quasi Steady State Petri Net
RAR	Receptors for all-trans retinoic acid
ROOM	Regulatory on/off minimization
ROS	Reactive oxygen species
R-S-H	Disulphide
SCAP	Sterol cleavage-activation protein
SF-1	Steroidogenic factor-1
SGK2	Serum and glucocorticoid-regulated kinase 2
SOD	Superoxide dismutase
SRC	Steroid receptor coactivator
SREBPs	Sterol regulatory element-binding proteins
SXR	Steroid and xenobiotic sensing receptor
tBid	Truncated Bid
TCA	Trichloroanisole
TGZ	Troglitazone
TNF α	Tumour necrosis factor alpha
Tox21	Toxicology in the 21st Century Tox21
ToxCast	Toxicity Forecaster
TRADD	Tumour necrosis factor receptor type 1-associated death protein
TRAIL	Tumour necrosis factor-related apoptosis-inducing ligand
TRAP	Thyroid receptor-associated proteins
TRAP	Thyroid receptor-associated proteins
Trx	Thioredoxin
TZD	Thiazolidinedione
VDR	Vitamin D3
Vmax	Maximum rate of reaction
XIAP	X-linked Apoptosis Protein Inhibitor

Table of Content

Chapter 1	Introduction	12
1.1	Toxicity testing in drug discovery and development	12
1.1.1	Drug target classification	14
1.1.2	Candidate drug selection	14
1.1.3	Preclinical development.....	15
1.1.4	Clinical trials	16
1.1.5	The physiological functions of the liver	17
1.1.5.1	Hepatocytes	18
1.1.5.2	Kupffer cells	19
1.1.5.3	Endothelial cells	21
1.1.5.4	Stellate cells.....	23
1.2	Drug-induced liver injury (DILI).....	25
1.2.1	Natural history of DILI	25
1.2.2	The role of immune reactions to DILI.....	27
1.2.3	Idiosyncratic drug Induced liver injury (IDILI).....	29
1.2.4	Mechanisms behind the development of idiosyncratic drug reactions ..	32
1.2.5	Bioactivation of drugs and the risk for Idiosyncratic drug-mediated hepatic injury.....	34
1.3	Hepatic glucose metabolism and diabetes	34
1.3.1	Hepatic glucose metabolism.....	35
1.3.2	Diabetes mellitus	38
1.3.3	Treatment and management of diabetes mellitus	40

1.3.3.1	The effect of insulin on glucose homeostasis.....	41
1.3.4	Nuclear receptors	43
1.3.5	Pregnane -X-Receptor in xenobiotic or drug biotransformation and its functions in DILI.....	50
1.3.6	Peroxisome proliferator-activated receptors	54
1.3.7	Mechanism of action of thiazolidinediones	55
1.3.7.1	Features of TGZ.....	58
1.3.7.2	Mechanism of action of TGZ	59
1.3.7.3	Bioavailability	61
1.4	Drug metabolism and metabolic detoxification	62
1.4.1.1	Phase I metabolism.....	63
1.4.1.2	Phase II metabolism.....	64
1.4.2	Metabolism of TGZ	66
1.4.3	The effect of TGZ on quinone formation and oxidative stress	70
1.4.4	From authorization to the removal of TGZ from the market.....	72
1.4.5	Proposed mechanism of TGZ-induced liver toxicity.....	74
1.4.5.1	The mitochondria as the primary organelle target of TGZ toxicity..	76
1.4.5.2	The effect of TGZ on metabolome	79
1.4.5.3	The effects of TGZ on Cell death	83
1.4.5.4	TGZ-induced JNK activation on apoptosis.....	86
1.4.5.5	The role of TGZ on necrotic cell death.....	87
1.4.5.6	Inhibition of bile transport by TGZ and its effects on hepatocytes..	89
1.4.5.7	The effect of TGZ on cholesterol synthesis.....	92
1.4.6	The necessity to study a drug that has been withdrawn from the market.....	95
1.5	<i>In silico</i> and metabolomics tools in modern toxicity studies	95
1.6	Hypothesis and aims.....	97

Chapter 2	Materials and general methods	98
2.1	Materials	98
2.1.1	Materials for <i>in vitro</i> studies	98
2.1.2	Materials for <i>in silico</i> studies	100
2.1.2.1	Software	100
2.1.2.2	File setups	100
2.1.2.3	Sample file	101
2.2	Methods	101
2.2.1	Systems biology	101
2.2.1.1	The read arcs	103
2.2.1.2	Inhibitory arcs	104
2.2.1.3	Animation of qualitative Petri nets in snoopy	104
2.2.2	The non-metabolic pathways of TGZ-induced hepatotoxicity	105
2.2.2.1	Using SurreyFBA for metabolic analysis	107
2.2.2.2	General description of the SurreyFBA software	109
2.2.3	<i>In vitro</i> assay	110
2.2.3.1	Cell culturing	110
2.2.3.2	Cryopreservation and thawing of cells	111
2.2.4	Determination of TGZ on cell viability using MTT assay	111
2.2.5	Determination of doubling time of Huh7 cells under various conditions	112
2.2.6	Determination of Vitamin C cytoprotective concentration in Huh7 cells	113
2.2.7	Assessment of apoptosis by caspase assay	113
2.2.8	Measurement of CYP3A4 induction	114
2.2.9	Quantification of ROS by 2',7'- dichlorofluorescein diacetate dye	114

2.2.10	Quantification of intracellular H ₂ O ₂ in Huh7 cells	115
2.2.11	ATP quantification	115
2.2.12	Urea quantification assay	116
2.2.13	Glutamate dehydrogenase activity assay	116
2.2.14	Pyruvate quantification assay	117
2.2.15	Ammonia quantification assay	118
2.2.16	Glutathione depletion assay	119
2.2.17	Determination of cholesterol levels in Huh7 cells	119
2.2.18	Determination of bile acid in HEK293 cells	120
2.2.19	Statistical analysis	121
Chapter 3	<i>In vitro</i> assesement of TGZ-induced Toxicity	123
3.1	The Effects TGZ in Huh7 cells viability	123
3.1.1	<i>In vitro</i> models to study the effects of liver toxicity	124
3.2	Results	126
3.2.1	The effects of TGZ on cell viability at different time points	126
3.2.2	The effects of TGZ on Huh7 cell viability by MTT method	127
3.2.3	Determination of doubling time in Huh7 cell growth	128
3.2.4	Effect of low doses of TGZ on Huh7 cell viability	130
3.2.5	Effects of TGZ on caspase activities in Huh7 cells	131
3.2.5.1	Results	133
3.2.5.2	The effect of TGZ on caspase 3/7 activity in Huh7 cells	133
3.2.5.3	The effect of TGZ on initiator caspase-9 activity in Huh7 cells	134

3.2.5.4	The effect of TGZ on initiator caspase-8 activity in Huh7 cells.....	136
3.3	Discussion.....	138
3.4	Other probable factors that might contribute to TGZ-induced liver hepatotoxicity	145
3.4.1	The effect of TGZ on glutamate dehydrogenase activity in Huh7 cells	147
3.4.2	The effect of TGZ on ammonia production and urea formation in Huh7 cells.....	148
3.4.3	The effect of TGZ on cholesterol homeostasis	152
3.4.4	TGZ-induced cholestasis as a contributing factor to liver toxicity	154
3.5	Discussion.....	156
Chapter 4	Effects of TGZ on mitochondrial impairment.....	166
4.1	Introduction	166
4.2	Results	169
4.2.1	Quantification of ROS levels in Huh7 cells treated with TGZ.....	169
4.2.2	Quantification of hydrogen peroxide levels in Huh7 cells	170
4.2.3	Effects of ascorbic acid on Huh7 cells viability	172
4.2.4	The effect of co-treatment of vitamin C and TGZ on Huh7 cells viability.....	173
4.2.5	Quantification of ROS levels in Huh7 cells co-treatment treated with TGZ and vitamin C.....	175
4.2.6	Effect of TGZ on glutathione homeostasis in Huh7 cells	176
4.2.7	Determination of CYP3A4 induction in TGZ-treated Huh7 cells	178
4.2.8	Effect of TGZ on cellular ATP levels in Huh7 cells	180

4.2.9	Effects of TGZ on intracellular pyruvate levels in Huh7 cells	181
4.3	Discussion.....	183
Chapter 5	The need for <i>in silico</i> system in drug discovery	193
5.1	Systems Biology.....	193
5.1.1	Model Development.....	195
5.1.2	Results of model development and prediction	196
5.1.2.1	Petri net creation of TGZ apoptotic pathway	198
5.1.2.2	Petri net representation of TGZ-induced PXR activation and its target genes	200
5.1.2.3	Petri net representation of TGZ-induced cholesterol signalling	201
5.1.3	Model simulation and prediction	203
5.1.4	TGZ receptor occupancy	204
5.1.5	TGZ apoptotic pathways.....	205
5.1.6	Effect of TGZ on Bcl-2/xL expression	208
5.1.7	Model simulation on the effect of TGZ on bile acid homeostasis	209
5.1.8	The effect of TGZ on cholesterol synthesis	213
5.1.9	Model simulation on the effect of TGZ on PTEN expression	215
5.1.10	Model simulation on the effect of TGZ on glucose homeostasis	217
5.1.11	TGZ metabolism and reactive metabolites	219
5.1.11.1	The effect of TGZ on CYP3A4 induction	220
5.1.11.2	Metabolism of TGZ to TGZ-quinone formation.....	221
5.1.11.3	Metabolism of TGZ toTGZ-SO4	223
5.1.12	Mitochondrial complex inhibition and hepatic injury.....	225
5.1.13	Effect of TGZ on cell number.....	226

5.2	Discussion.....	228
Chapter 6	General discussion	236
6.1	Future Work	239
6.2	Conclusion	240
Chapter 7	References.....	241
Appendix A.	Control file for simulations	298
Appendix B.	Standard curves for ammonia assay.....	299
Appendix C.	Standard curves for urea assays.....	300
Appendix D.	Standard curves for H₂O₂ assay	301
Appendix E.	Standard curves for cholesterol assay	302

Table of Figures

Figure 1-1 Drug discovery and development procedure.....	13
Figure 1-2 Three structural design of the liver lobule	18
Figure 1-3 Schematic representation of cellular respiration pathways	37
Figure 1-4 The Structure and function of the nuclear receptor	49
Figure 1-5 Structure of three thiazolidinediones along with tocopherol	59
Figure 1-6 Mechanism by which thiazolidinediones enhances insulin Action.....	61
Figure 1-7 Phase I and Phase II metabolism of APA	63
Figure 1-8 Primary metabolic pathways of TGZ	69
Figure 1-9 Schematic representation of the intrinsic and extrinsic apoptotic pathways	85
Figure 1-10 Morphological features of necrotic and apoptotic cell death.....	89
Figure 2-1 Petri net elements and their graphical representation.....	102
Figure 2-2 Graphical representations of Petri net operation.....	103
Figure 2-3 Petri net creation with Snoopy	105
Figure 2-4 Overview of the Quasi-State Petri net approach	106
Figure 2-5 Reduction of MTT to formazan.....	112
Figure 3-1 The effects of TGZ on Huh7 viability at both 24 and 48 hrs exposure ..	127
Figure 3-2 The effects of TGZ on Huh7 viability at 24 hrs exposure	128
Figure 3-3 Exponential growth curve of Huh7 cell line between 0-60 hrs.....	130
Figure 3-4 The effect of low doses of TGZ on Huh7 cell viability	131

Figure 3-5 The effects of TGZ on caspase 3/7 activity in Huh7 cell	134
Figure 3-6 TGZ activation of caspase-9 activities in Huh7 cells	135
Figure 3-7 TGZ activation of caspase-8 activities in Huh7 cells	137
Figure 3-8 Effect of TGZ on GDH activity in Huh7 cells	148
Figure 3-9 A-B The effect of TGZ on ammonia and urea production in Huh7 cells	151
Figure 3-10 The effect of TGZ on cholesterol levels in Huh7 cells	154
Figure 3-11 The effect of TGZ on extracellular bile acid concentration in HEK293 cells.....	156
Figure 4-1 ROS production by TGZ in Huh7 cells	170
Figure 4-2 The effects of TGZ on H ₂ O ₂ production in Huh7 cells	171
Figure 4-3 The effect of vitamin C in Huh7 cells viability	173
Figure 4-4 Effect of vitamin C and TGZ on Huh7 cell viability	174
Figure 4-5 Effect of co-treatment of Vitamin C and TGZ on ROS production in Huh7 cells.....	176
Figure 4-6 The effect of TGZ on GSH levels in Huh7 cells.....	178
Figure 4-7 The effect of TGZ on CYP3A4 induction in Huh7 cells	180
Figure 4-8 The effects of TGZ on ATP levels in Huh7 cell	181
Figure 4-9 The effects of TGZ on pyruvate levels in Huh7 cells.....	183
Figure 5-1 An outline of systems biology.....	195
Figure 5-2 Probable pathways of TGZ-induced liver toxicity for model creation.....	197
Figure 5-3 Petri net representation of TGZ-Bcl-2 interactions and induction of apoptosis.....	199

Figure 5-4 Petri Net representation of TGZ-induced PXR activation	201
Figure 5-5 Petri Net representation of cholesterol signalling	203
Figure 5-6 Model simulation output comparison with <i>in vitro</i> data on the effect of TGZ on Nuclear receptor occupancy.....	205
Figure 5-7 A- D and A1-D1 Comparison of simulation outputs.....	207
Figure 5-8A-B Comparison of model prediction and <i>in vitro</i> assessment of the effects of TGZ on Bcl-2/xL expression.....	209
Figure 5-9A-D Model simulation outputs of the effects of TGZ on BSEP and Bile acids compared with <i>in vitro</i> data on TGZ-induced BSEP inhibition.....	212
Figure 5-10 Model simulation output of the effect of TGZ on cholesterol levels at different time points.	215
Figure 5-11 A-B Model simulation output and <i>in vitro</i> data on the effect of TGZ on PTEN expression levels	217
Figure 5-12 Model simulation output and <i>in vitro</i> data on the effect of TGZ on glucose metabolism.....	219
Figure 5-13 Model simulation output of the effect of TGZ on CYP3A4 levels.....	221
Figure 5-14 Model simulation output of the of TGZ-quinone formation compared with <i>in vitro</i> and <i>in vivo</i> data on the effects of TGZ-quinone formation	222
Figure 5-15 A-B Model simulation output of the effect of TGZ-SO ₄ formation	224
Figure 5-16 A-C Model simulation output of TGZ on ATP and complex V and <i>in vitro</i> assessment on complex I-V	226
Figure 5-17 Model simulation output on the effect of TGZ on cell number	227

List of Tables

Table 1-1 Nuclear receptor subtypes and their signalling mechanisms.....	46
Table 1-2 Reactions categorised as phase I or phase II metabolism	66
Table 2-1 Materials and reagents.....	98
Table 2-2 SurreyFBA analysis displaying metabolic reactions	108
Table 2-3 Table showing external metabolite tag dialogue box.....	109

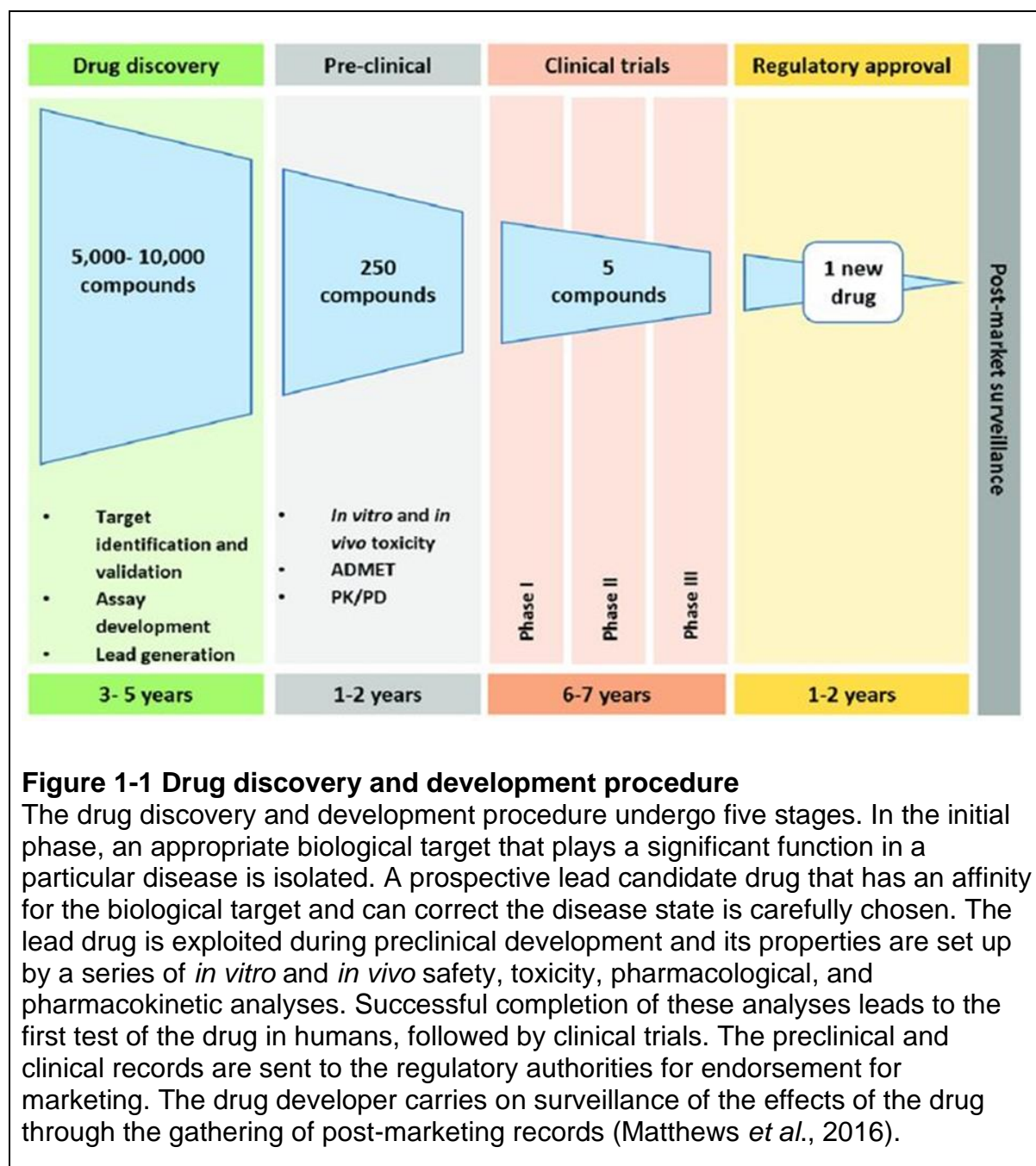
Chapter 1 Introduction

Currently, there are over 60 million chemicals in the world, but only a fraction of them (therapeutic drugs) are approved for the treatment of diseases (Raunio, 2011). The adverse effects and reported cases of idiosyncratic toxicity associated with these products in humans are major limiting factors that reduce the success rate of drug development (Aithal, 2015; 2019; Amacher, 2012; Kaplowitz, 2006; Plant, 2004; Raunio, 2011). In many cases, these liabilities can be identified during drug development, either allowing the early termination of a development programme or the optimisation of alternate candidate drugs. However, some adverse effects are exhibited either only after chronic exposure or in a sensitive subset of the patient population. While clinical trials are used as the gold standard to test drug safety in man, they have several limitations, such as the size of the target population being small, meaning rare events may go unidentified. In addition, clinical trials are time-consuming and expensive, with an estimated cost of over USD 1 billion per drug (Matthews *et al.*, 2016; Morgan *et al.*, 2011). Even following the successful completion of the early stages of clinical trials, the subsequent market withdrawal of drugs due to either idiosyncratic or unpredicted effects not being identified in animal models demonstrates their fallibility (Kola, 2008). The current strategy adopted in modern drug development is the identification of early toxicity through the development of predictive *in vitro* and *in silico* analyses for initial toxicity assessment (Sirenko *et al.*, 2014).

1.1 Toxicity testing in drug discovery and development

Drug discovery and development comprises five stages: identification of the biological target, selection of a lead candidate drug, preclinical safety assessment, toxicity evaluation and pharmacokinetic studies (Figure 1-1). In addition, it is necessary to carry out clinical studies in subjects and acquire regulatory authorisation for marketing (Matthews *et al.*, 2016). Study design in each stage is adapted based on the properties of the drug in question and its physiological target. For instance, in the process of clinical development, researchers generally involve healthy volunteers. However, in the event of inherently toxic anti-cancer agents, special techniques are used in place of healthy volunteers (Gupta *et al.*, 2012).

In silico, *in vitro*, *in vivo*, *ex vivo*, or human clinical research is explored during drug development to establish the effectiveness and safety of the new drug (Gupta *et al.*, 2012; Ward *et al.*, 2011). There can be an overlap between the research used in each stage of drug development and other studies, such as long-term animal reproductive resources as well as phase I clinical trials, that could be undertaken separately.



1.1.1 Drug target classification

Drug discovery methods start with the identification of a potential drug candidate for the correction of pathological conditions or medical syndromes. Traditionally, cellular proteins, for instance, G-protein coupled receptors, ion channels, or nuclear receptors, as well as kinases, have been biological foci for drug discovery pathways. Conversely, improvements in genomic as well as proteomic skills, such as microarrays and genome sequencing, have paved the way for genes, RNA, and novel proteins to become drug discovery targets (Acharya & Garg, 2016; Schenone *et al.*, 2016).

1.1.2 Candidate drug selection

Drug candidates are usually selected with backups (2–3) in case the lead candidate fails at some point. After the selection of a drug target, a potential drug candidate molecule is then identified. It is achieved either by screening compound libraries using high throughput screening or using computational methods such as quantitative structure-activity relationship (QSAR) modelling to identify small molecules with suitable affinity for the biological target (Cumming *et al.*, 2013; Plant, 2015; Yang *et al.*, 2018). However, the difficulty is how to filter through the potential candidates and identify a lead drug candidate, likely to be efficacious and non-toxic in humans. Drug developers use the high throughput screening and the QSAR data to choose a drug candidate for further development as they postulate a few potential drug candidates. Drug attrition rates could be reduced early on by starting toxicology analyses during the lead selection stage to determine which potential drug is the safest and most suitable for venture and expansion. Several *in vitro* and a few *in vivo* studies are conducted in the early stages of drug development to update the properties of the likely drug candidates (Beck *et al.*, 2014). In a situation where the administration of a potential drug candidate is by oral means, the rate of absorption of the compound is evaluated. As uptake of a drug occurs in the small intestine through the trans-epithelial transport routes, the assimilation of drug candidates through the intestinal mucosa is determined by employing computational modelling *in vitro* assays as well as *ex vivo* models utilising intestinal portions of animals. These models help determine whether the drug candidate will cross the

intestinal mucosa through gradient-dependent, passive routes (Annaert *et al.*, 2010; Withington, 2002). Also, the hepatic portal vein transports drugs absorbed through the intestinal mucosa to the liver where they are bio-transformed (Fan *et al.*, 2010).

Drugs and their metabolites undergo systemic circulation and elicit their effects on target and non-target organs. Drug companies use the records from early-stage toxicity research to determine which of the candidate drugs has the highest likelihood of being approved for marketing. The selected lead drug then enters preclinical development where the safety and effectiveness of the drug are assessed.

1.1.3 Preclinical development

Drug developers find the preclinical and clinical drug development phases to be the most time-consuming and costly phases. Throughout these stages, the front-runner drug goes through broad analysis to find out the effectiveness and safety of the drug in humans. However, the toxicity must be assessed using *in vivo* animal studies before the drug can be tested in humans. Early *in vitro* metabolic studies performed by exploiting liver cell lines and primary cells will update the primary metabolites produced when the drug is biotransformed. In the course of preclinical toxicity analysis, the use of animal species allows researchers to establish the primary metabolites that were identified in the early *in vitro* studies (Jia & Liu, 2007; Lennernas, 2007). Acute toxicity is then conducted to determine the LD₅₀ (lethal dose 50%) dose of the drug. These experiments employ both male and female rats; the drug is given once at a high dose through the route of intended exposure, and the animals are observed for two weeks. During the preclinical study, the food and water intake, behaviour, as well as the death of the animals are recorded in two species (one rodent, one non-rodent) to account for species variations. This also adds to drug developers' expenses and ethical challenges (Muralidhara *et al.*, 2001; Stallard *et al.*, 2002).

The sub-chronic study is then undertaken to determine the “no observed adverse effect level” as well as the “lowest observed adverse effect level”. These studies may last for over 80 days and use a single rat and one non-rodent species with more than 20 animals of each gender; the drug is given periodically in toxic doses without causing death. At the final stage of the study, blood samples are collected for

histopathology, haematology, as well as biochemical evaluation. These are carried out to determine the drug's effects on both target and non-target organs (Balls & Clothier, 2010). Toxicity reports generated from preclinical animal experiments are used to support drug development portfolios which might be sent to the regulatory authorities for approval for assessment in humans. Clinical development then follows and, in this process, a tenth of the lowest, utmost tolerated dose seen in the *in vivo* chronic toxicity evaluation becomes the initial dose for human clinical trials (Balls & Clothier, 2010).

1.1.4 Clinical trials

Phase I clinical trials are conducted with a small group of healthy volunteers. They are used to decide the drug dosing routine that is to be administered in imminent trials to ascertain safety or toxicity concerns and to establish the pharmacokinetic outlines of the drug in humans (Yao *et al.*, 2009). Phase I tests are conducted to determine the safety of the drug in humans, and a successful conclusion results from phase II clinical trials (Lim *et al.*, 2018; Newell, 2014). The primary aim of Phase II is to establish the effectiveness of the drug that has undergone phase I trials. Phase III trials are conducted to subject a larger patient population to the drug to validate its safety and scope of therapeutic dose (Sachs *et al.*, 2015). *In vitro*, *in vivo* animal and human toxicity studies carried out throughout drug development phases are designed to advise on the novel drug's possible toxicity.

Before getting approval for marketing, drug developers must prove the safety of the novel drug in test subjects. In this situation, clinical trials are a crucial step in drug development as they elucidate the safety of the drug in subjects. On the other hand, there have been incidents where a drug's ability to cause severe adverse reactions in some individuals only becomes noticeable after quite a few subjects have taken the drug. TGZ is a classic example of such an incident. In a small group of patients, TGZ was found to cause severe liver toxicity and, in some cases, fatality in a small group of patients after it had been prescribed to millions of people living with diabetes (Chojkier, 2005; Ikeda, 2011; Jaeschke, 2007; Julie *et al.*, 2008; Menini *et al.*, 2006). Drug development involves a lengthy and costly process, and the success of the drug is not guaranteed. Many fail either in late-stage clinical trials or in the

market. With more predictive *in vitro* and *in silico* tests, it is unlikely that a drug will fail in the late stage.

1.1.5 The physiological functions of the liver

The liver is the largest second organ in the body that weighs approximately 1.5 kg and accounts for about 2.5% of the human adult body weight (Moore *et al.*, 2010). The liver performs an array of functions in metabolism (drug metabolism, bilirubin via conjugation), immunity (e.g., Kupffer cells remove bacteria, viruses, old and damaged blood cells), digestion (production of bile acid), as well as storage of vitamins (A, D, K, B12, and folate). It comprises several cell types, of which the majority (approximately 80% by number) are hepatocytes, with a lower number of Kupffer cells, stellate cells, or endothelial cells (Kaplowitz, 2006; Tezcan *et al.*, 2019). The liver is a strategically vital organ because of its dual blood supply from the portal vein (about 75%) and the hepatic artery (approximately 25%). The liver has a dual blood supply because the hepatic artery transports oxygenated blood from the general circulation, while the hepatic portal vein transports deoxygenated blood from the small intestine, which may contain nutrients or toxins. It is interlinked with practically every organ system (every organ is interlinked with every other organ); therefore, it is predisposed to a range of diseases. The lobule constitutes the functional unit of the liver. It is hexagonal and consists of a portal triad (portal, vein, hepatic artery, and bile duct) at each corner. The lobule building block is the hepatocytes that possess physiologically distinct apical and basolateral membranes (Figure 1-2) (Adams & Eksteen, 2006; Kaplowitz, 2006).

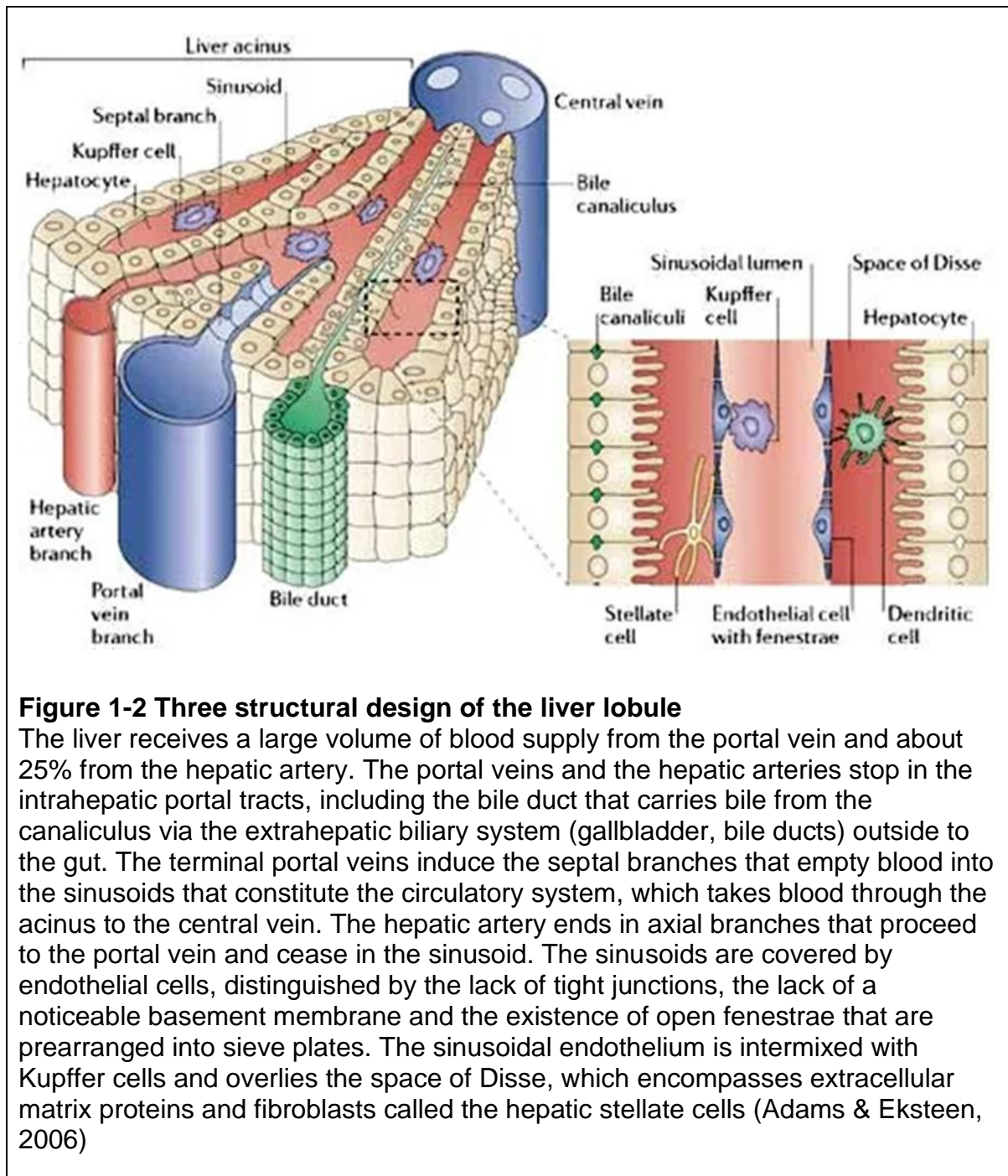


Figure 1-2 Three structural design of the liver lobule

The liver receives a large volume of blood supply from the portal vein and about 25% from the hepatic artery. The portal veins and the hepatic arteries stop in the intrahepatic portal tracts, including the bile duct that carries bile from the canaliculus via the extrahepatic biliary system (gallbladder, bile ducts) outside to the gut. The terminal portal veins induce the septal branches that empty blood into the sinusoids that constitute the circulatory system, which takes blood through the acinus to the central vein. The hepatic artery ends in axial branches that proceed to the portal vein and cease in the sinusoid. The sinusoids are covered by endothelial cells, distinguished by the lack of tight junctions, the lack of a noticeable basement membrane and the existence of open fenestrae that are prearranged into sieve plates. The sinusoidal endothelium is intermixed with Kupffer cells and overlies the space of Disse, which encompasses extracellular matrix proteins and fibroblasts called the hepatic stellate cells (Adams & Eksteen, 2006)

1.1.5.1 Hepatocytes

Hepatocytes are the central parenchymal cells in the liver, forming about 80% of the liver's entire mass. Hepatocytes are enriched in organelles such as the endoplasmic reticulum and the Golgi apparatus. Hepatocytes are abundant in mitochondria (about 1000 per cell); besides, they contain lysosomes and peroxisomes (Malarkey, 2005).

Hepatocytes play critical roles in lipid, carbohydrate, as well as protein metabolism. They are also involved in the production of serum proteins, such as albumin and coagulating factors (Malarkey, 2005). Moreover, hepatocytes produce and secrete bile, detoxify, excrete cholesterol, steroid hormones, xenobiotics, and drugs. Most drugs (over 100s) are metabolised by the mixed functions of monooxidases located in the hepatocytes and support the conversion of both endobiotic and xenobiotic compounds into water-soluble metabolites for elimination by the kidney (Amacher, 2012; Kaplowitz, 2006).

Hepatocytes are grouped into three zones based on perfusion as well as functionality. The hepatocytes' first zone is the periportal zone, which is first-rate perfused and first to redevelop because of its closeness to oxygenated blood and nutrients. Due to its high perfusion, this section of the liver plays a critical role in oxidative metabolism, for instance, the synthesis of glucose from non-carbohydrate sources, bile formation, cholesterol production, and amino acid catabolism. The second zone of the liver, the hepatocytes' pericentral zone, sits between sections one and three. Section three has the lowest perfusion due to its distance from the portal triad (Figure 1-2) (Kaplowitz, 2006).

1.1.5.2 Kupffer cells

Kupffer cells (KC), are the resident macrophages in the liver and contain the prevalent resident tissue macrophage population in the body (Kakinuma *et al.*, 2017). KCs and other cells, for instance, the cells of the innate immune system (natural killer T-cells as well as the dendritic cells) are sited in the sinusoid. The KCs are close to parenchymal and nonparenchymal cells in the liver, which allows KCs to control liver activity in both healthy and disease conditions (Kakinuma *et al.*, 2017). Under healthy conditions, the KCs display a tolerogenic phenotype, which means the tolerance is essential to prevent an unwanted immune response in the case of immunoreactive particles into the liver sinusoid and or antigens present on dead cells as they are discharged from the distribution in the liver. Various toxic mediators can trigger KCs to cause the discharge of cytokines as well as reactive oxygen species (Kakinuma *et al.*, 2017). KCs possess receptors that bind to cells covered with immunoglobins or bind to complement receptors and consequently, phagocyte

cells (Bilzer *et al.*, 2006). However, a change in the functional activity of KCs may be linked with a variety of disease conditions. It implies that, due to the proximity of KCs to parenchymal and nonparenchymal cells in the liver, loss of tolerogenic state can result in hepatocellular injury; that is, KCs transition from tolerogenic to pathologically activated states (chronic inflammatory disorders) (Bilzer *et al.*, 2006). Although KCs can be protective in a few states, such as drug-induced liver injury; impairment in the precise control of inflammatory reactions in KCs can cause chronic liver inflammation (McCuskey & Wisse, 2010).

KCs represent an essential element of innate immunity, the initial, rapid response to potentially dangerous stimuli (Parker & Picut, 2005). Periportal KC has higher lysosomal enzyme activities and a greater phagocytic capacity than midzonal and perivenous KC (Kappas, 2003; Ryter *et al.*, 2006). The rapid clearance of bacteria from the bloodstream has been attributed to fixed tissue macrophages, particularly to KC (Steib & Gerbes, 2009). In brief, most organisms taken up in the liver are bound extracellularly by KC (McCuskey & Wisse, 2010). A previous report has suggested that binding is mediated in part by the interaction of lectins expressed by KC and carbohydrate residues expressed by the bacteria (Steib & Gerbes, 2009). In addition, complementary adhesion molecules (CD11b/ CD18 and CD54) facilitate the adherence of neutrophils to the KC (McCuskey & Wisse, 2010), which subsequently internalise and kill the organisms bound to the KC surface (Hoedemakers *et al.*, 2008). Clearance of infiltrating neutrophils from inflamed tissues is required for the resolution of inflammation. The ingestion of neutrophils by KCs may also have profound implications for developing and expressing adaptive immunity in the liver (Figure 1-2) (Adams & Eksteen, 2006).

It has been suggested that the liver is actively tolerogenic and plays a critical role in preventing generalised inflammation by eliminating circulating CD8+ T cells specific to systemically disseminated antigens (Adams & Eksteen, 2006). Interestingly, recovery from chronically accepted hepatic allografts has a more remarkable ability to induce apoptosis of alloreactive T cells. In contrast, the administration of these cells significantly prolongs the survival of hepatic allografts in an acute rejection model (Sun *et al.*, 2003).

1.1.5.3 Endothelial cells

Endothelial cells (Figure 1-2) are multifunctional cells capable of secreting biologically active mediators (Garbuzova-Davis *et al.*, 2018). Endothelial cells line the liver sinusoid walls and play a role in filtration in the presence of fenestrated (Garbuzova-Davis *et al.*, 2018). These cells exhibit a sizeable endocytic capacity for extracellular matrix components and immune complexes (Garbuzova-Davis *et al.*, 2018; Pate *et al.*, 2010). Endothelial cells play an essential regulatory role as a physical barrier and a source of various chemical substances in circulation. For example, endothelium-derived nitric oxide and prostacyclin induce vascular relaxation and inhibit platelet function in response to physical stimuli, hormones, and platelet-related substances (Barton *et al.*, 2012; Versari *et al.*, 2009).

Some substances can induce smooth muscle cell hyperpolarization. In turn, the endothelial cells can produce several contraction-inducing factors, for instance, endothelin, thromboxane A₂, angiotensin II, and superoxide under some conditions. Endothelial cells can provide a source of growth inhibitors and promoters, including heparin, platelet-derived growth factor, and thrombospondin. Various vasoactive substances, such as nitric oxide (NO), endothelin, and angiotensin II, released from the endothelium may also influence vascular development (Barton *et al.*, 2012; Versari *et al.*, 2009). The endothelial layer can, therefore, control vascular tone and development. Cardiovascular disorders, such as hypertension and atherosclerosis, may play a role in the dysfunction of these endothelium-dependent regulatory systems (Barton *et al.*, 2012). Diabetes patients often display endothelium-dependent vasodilatation disruption. It is mainly because the condition is often associated with other cardiovascular complications, including high blood pressure, obesity, and dyslipidaemia. One of the main adverse effects of these fatty foods is the high levels of circulating free fatty acids that induce ROS development and impair endothelial function (Barton *et al.*, 2012; Versari *et al.*, 2009).

Insulin was shown to induce a concentration-dependent increase in lower limb blood circulation in healthy participants by reducing vascular resistance in skeletal muscles, primarily by vasodilating microcirculation. This observed vasodilatory effect of insulin is mediated at least partly by increased NO output by activating the Insulin

receptor substrate-1/Phosphoinositol 3-Kinase/Akt (Clerk *et al.*, 2004). Free radicals may disturb the balance of NO, destroy the endothelium, and enable toxins to move into the body tissues through excessive permeability (Garbuzova-Davis *et al.*, 2018). In a situation where the endothelium becomes compromised and NO levels are imbalanced, cells that remain in the blood can move into the adjacent body tissue through blood vessels. Many of them involve C-reactive protein, formed by the liver and causing inflammation (Garbuzova-Davis *et al.*, 2018; Michiels, 2003). Endothelial signalling may become impaired when NO action is blocked, culminating in systemic disease since the endothelium consistently retains about 60,000 miles of blood vessels in the human body (Maritim *et al.*, 2003; Tripathy *et al.*, 2003). Various factors, including obesity, smoking, insomnia, a high level of microbial infection, increased glucose consumption, and exposure to metals or air pollutants, can maximise free radicals in the body. If the endothelium acts correctly, it helps maintain blood coagulation, provides an immune response to the body, regulates the fluid volume, the number of electrolytes and other substances flowing through the tissues from the blood, causing dilation or constriction (Garbuzova-Davis *et al.*, 2018; Michiels, 2003).

Also, hepatic ECs in both mice and humans are incredibly varied, forming the second-largest liver cells. Most of them line hepatic sinusoids identified as liver sinusoidal ECs (LSECs) (DeLeve, 2013). They have a sinusoidal architecture, which means that luminal and abluminal plasma membrane fusion occurs in areas called "fenestrae" at locations other than cell junctions. LSECs lose cell markers of continuous endothelial cells during that period, including platelet endothelial adhesion molecule-1, also called the differentiation cluster. Hepatoblasts control this separation of LSECs both through the vascular endothelial growth factor they release and by direct intercellular interactions (DeLeve, 2013). Under physiological conditions, despite significant alterations in hepatic blood flow befalling during digestion, LSECs control hepatic vascular tone, leading to the maintenance of low portal pressure. LSECs preserve hepatic stellate cell quiescence, thereby repressing the production of intrahepatic vasoconstriction and fibrosis. LSECs play a crucial role in the onset and growth of chronic liver diseases under pathological conditions (DeLeve, 2013). They become capillarized and lose their defensive properties, and

they stimulate vasoconstriction and angiogenesis. Following acute liver damage or partial hepatectomy, LSECs are involved in liver regeneration as they renew from LSECs and LSEC progenitors, feel changes under stressful conditions such as surgery, and associate with platelets and inflammatory cells. LSECs also play a part in developing and advancing hepatocellular carcinoma, ageing, inflammation, and infection-related liver lesions (DeLeve, 2013).

1.1.5.4 Stellate cells

The liver also plays a critical role in the uptake of vitamin A and stores over 90% of the retinoids contained in the human body. Stellate cells (Figure1-2) serve as a warehouse to store a large amount of retinol and retinyl palmitate in lipid droplets inside their cytoplasm (Yin *et al.*, 2013). Stellate cells are located between the hepatocytes and the sinusoids and typically extend beyond to connect several sinusoids. Stellate cells regulate the turnover and release of materials into the extracellular space, producing a complex meshwork of proteins and carbohydrates (extracellular matrix) and controlling sinusoidal contractility (Yin *et al.*, 2013). Under stressful conditions, the stellate cells may be stimulated and changed into myofibroblasts, which play a crucial role in provocative fibrotic reactions (Kmieć, 2001; Yin *et al.*, 2013). When triggered, stellate cells may proliferate and create large amounts of extracellular matrix for each cell (Adams & Eksteen, 2006; Kmieć, 2001). Stellate cells' involvement in critical roles in hepatic repair and pathological processes has made it one of the significant spotlights of liver studies (Adams & Eksteen, 2006; Yin *et al.*, 2013). Hepatic fibrosis is a prevalent complication associated with most chronic liver diseases that are potentially life-threatening and thus pose a high medical and economic burden (Weiskirchen & Tacke, 2016).

Furthermore, liver fibrosis is not a simple reaction. Still, it is connected to various soluble factors (cytokines and chemokines) and different cellular subgroups that are liver-resident and infiltrating. The chemical and biological activities of the disease-causing agent are controlled. The pathogenic fibrogenesis series is triggered by the destruction of parenchymal cells resulting from a wide variety of hepatotoxic and injurious agents and mechanisms (Weiskirchen & Tacke, 2016).

In most cases, tissue damage first causes an inflammatory response affecting the local vascular system and the immune system, and the endocrine and neurological mediators are systemically mobilised. Non-parenchymal cells such as endothelium and stellate cells and resident immune cells, such as macrophages, dendritic cells, and mast cells with specialised surface receptors, detect pathogen-associated molecular patterns such as bacterial toxins and molecular patterns associated with damage and mediate this response (Arndtz & Hirschfield, 2016). These contribute to the activation of matrix-producing cell populations, including HSCs transiting to myofibroblasts, portal myofibroblasts, resident fibroblasts, and many other cell types belonging to the myofibroblast pool. Liver fibrosis can be a causative product of various underlying aetiologies, including genetic disorders, chronic viral infection, excessive alcohol intake, or venous obstruction (Arndtz & Hirschfield, 2016; Weiskirchen & Tacke, 2016).

During the last few decades, hepatic stellate cells (HSC) were mainly viewed as "resting cells" that store vitamin A and impact sinusoidal blood flow. HSC facilitates intercellular communication by synthesising and stimulating the production of polypeptide mediators. Erythropoietin and elements of the plasminogen activation system that maintain homeostasis in the hepatic sinusoid microenvironment are also a key function of HSC (Tacke & Weiskirchen, 2012). For instance, HSC can produce a hematopoietic growth factor with potentially beneficial actions during liver regeneration or recovery from injury (Schmeding, 2007). HSC, on the other hand, can act as antigen-presenting cells (APCs) that express pattern recognition receptors (PRRs), respond to damage-associated molecular patterns (DAMPs), and interact with a variety of immune cells to modulate their activity or promote differentiation (Chen *et al.*, 2006; Yu *et al.*, 2004). Moreover, HSC interact with immune cells in a bidirectional manner (Maher, 2001; Kitano & Bloomston, 2016; Wasmuth *et al.*, 2010). They receive a glut of signals from individual immune cells and in turn produce many soluble inflammatory mediators that elaborate on the fact that signals are influencing the biological properties of different immune cells. Key signalling pathways for HSC activation may include nuclear factor kappa B (NF- κ B). This promotes HSC activation upon either lipopolysaccharide (LPS) or TLR4 stimulation or AT induced cytosolic Ca²⁺ influx via purinergic signalling receptors,

including P2Y (Dranoff *et al.*, 2004). During hepatic insult, HSC produces reactive oxygen species (ROS), proinflammatory cytokines, chemokines, and their receptors and can act as non-APCs (Wasmuth *et al.*, 2010). On the other hand, HSC depletion has been linked with high expression of interleukin 10 (IL-10) and interferon-gamma. This might lead to activated HSC and a subsequent response to liver injury (Puche *et al.*, 2013). In summary, HSC significantly contributes to and participates in the liver's immune response.

1.2 Drug-induced liver injury (DILI)

The liver plays a crucial function in xenobiotic metabolism and, as such, it is a critical target organ for the adverse effects of drugs. Almost every given medication may cause liver toxicity (Aithal, 2015; 2019; Alempijevic *et al.*, 2017; Björnsson, 2014; Holt & Ju, 2006; Iryna *et al.*, 2015; Marks & Harbord, 2013; McGill *et al.*, 2014). DILI is one of the vital factors that contribute to a drug's withdrawal from the market (Aithal, 2015; 2019; Uetrecht, 2019), and it represents about 10% of all toxicities uncovered by raised hepatic enzymes and about 50% of acute liver failure (Björnsson, 2014). DILI can be classed into two, thus DILI-1 and DILI-2, based on incidence, animal model predictability, and dose dependency (Alempijevic *et al.*, 2017; Björnsson, 2014). It has been established that DILI-1 produces predictable liver toxicity. It is characterised by a relatively high incidence, is reproducible in at least one animal species, and has a dose-dependent build-up in prevalence and seriousness of the identified injury (Chen *et al.*, 2015). DILI-2, also called an idiosyncratic reaction, is characterised by sudden or unpredictable liver toxicity. It has a relatively low incidence, occurring at therapeutic doses of about 1: 1000 to 1:10000 subjects (Chalasani & Björnsson, 2010, Chen *et al.*, 2015). A wide range of drugs have been implicated in idiosyncratic reactions (discussed further in section 1.2.4). Although the prevalence of idiosyncratic responses is minimal, they can trigger either critical indisposition or result in death (Browning *et al.*, 2004; Chen *et al.*, 2015).

1.2.1 Natural history of DILI

In the American drug-induced liver injury network (DILIN), the presentation of DILI was with jaundice in 70% of cases. After drug withdrawal, the majority recovered;

however, 17% progressed to chronic DILI (defined as abnormal liver tests for more than 6 months) and 10% required a liver transplant and/or died (Fontana & Hayashi, 2014). Mortality increased by 44% in the presence of Stevens-Johnson syndrome. Compared with those with cholestatic DILI, those with hepatocellular DILI were more likely to require a liver transplant (6.2% versus 2.9%, $p < 0.001$) and have a fatal injury (9% versus 4%, $p < 0.001$) (Fontana & Hayashi, 2014). Furthermore, use of non-body-building herbal and dietary supplements was associated with a significantly higher need for liver transplant compared with conventional drugs (13% versus 3%, $p < 0.05$). However, 7% of cases were attributed to herbal and dietary supplements during the first two years of the American DILI registry, compared with 20% 10 years later (Fontana & Hayashi, 2014).

Distinctively, in hepatocellular DILI, a serum bilirubin of ≥ 3 times upper limit of normal (ULN) in the absence of biliary obstruction or Gilbert's syndrome is associated with a mortality of approximately 10% (range 5–50%). The Spanish DILIN developed a composite score to predict ALF: AST ≥ 17.3 times ULN; total bilirubin ≥ 6.6 times ULN; and AST: ALT ≥ 1.5 times ULN. These criteria are able to determine progression to ALF with a specificity of 82% and a sensitivity of 80% (Fontana & Hayashi, 2014). This composite score, however, needs to be validated in additional prospective studies (Fontana & Hayashi, 2014).

According to Ikeda (2011), TGZ caused atypical, liver cell injury-type liver toxicity in humans. Statistically, the double null genotype of glutathione S-transferase isoforms, GSTT1 and GSTM1, has been a risk factor, indicating the low activity of the patients with risk factors in scavenging chemically reactive metabolites (Ikeda, 2011). The metabolic activation was mediated by CYP3A4 and CYP2C8, and CYP3A4 was inducible by repeated exposure to TGZ (Ikeda, 2011). The genotype analysis, on the other hand, revealed that the metabolic idiosyncrasy is in the breakdown rather than the development of TGZ toxic metabolites (Ikeda, 2011). An antibody against hepatic aldolase B was found in the study subjects, implying that an immune reaction was involved in the toxic mechanism. TGZ induced apoptotic cell death in human hepatocytes at high concentrations, and this property may have served as an immunological danger signal, which is thought to play an important role in activating immune reactions. In the case of TGZ, pharmaceutical companies implemented

screening systems for chemically reactive metabolites at an early stage of drug development, taking into account both the amount of covalent binding to the proteins *in vitro* and the assumed clinical dose level (Ikeda, 2011). At the post-marketing stage, gene analyses of study subjects to identify pharmacogenetic biomarkers could be a powerful tool for identifying risky patients (Ikeda, 2011).

1.2.2 The role of immune reactions to DILI

Drug-induced liver injury, as described in the previous section, exhibits clinical features similar to allergic reactions involving adaptive immune system activation, such as a mild lymphocytic infiltrate (Liu *et al.*, 2021). Even in cases of drug-induced hepatotoxicity, inflammatory cell infiltration into the liver is common, implying that the innate immune system plays a role (e.g., neutrophils, macrophages) (Aithal *et al.*, 2004; Björnsson & Aithal, 2020; Liu *et al.*, 2021).

According to existing research, mitochondrial dysfunction, oxidative stress, bile acid disparity, and inflammatory reactions all play a role in the onset and progression of DILI. However, these observations do not fully explain the mechanism of DILI (Aithal *et al.*, 2004; Björnsson & Aithal, 2020; Liu *et al.*, 2021). The liver is a complex immune organ that primarily protects the body by enduring self and foreign antigens (Björnsson & Aithal, 2020; Liu *et al.*, 2021). When tolerance is compromised, activated immune cells may generate pro-inflammatory cytokines and chemokines, causing hepatic injury and inflammation, which defines the extent of the liver injury. Immune checkpoint molecules, regulatory immune cells, and other immune factors may all play a role in the balance of immune activation and tolerance (Björnsson & Aithal, 2020; Liu *et al.*, 2021).

Human Leukocyte Antigen alleles have been implicated in liver injury caused by a wide range of other drugs, including TGZ and flucloxacillin, shedding new light on the DILI puzzle. Besides, in some herbal and dietary supplement-induced liver injuries, antibodies or active T cells that support the immune system have been reported to play a pivotal role in the development of liver injuries (Björnsson & Björnsson, 2021; Liu *et al.*, 2021).

Drugs or their reactive metabolites cause cell stress or apoptosis, which triggers the release of molecules that recruit and stimulate innate immune cells, which results in the generation of pro-inflammatory cytokines (Liu *et al.*, 2021). These mediators stimulate adaptive immune cells, eventually transforming T cells into effector cells and B cells into antibodies released by plasma cells. During the activation of innate and adaptive immunity, host immune tolerance-related immune cells or cytokines may exert immunosuppressive effects (Björnsson & Björnsson, 2021; Liu *et al.*, 2021). However, if the balance is upset, the inflammatory response in the liver is compromised.

DAMPs include high-mobility group box protein 1, heat shock proteins, ATPs, and others, such as mitochondria-derived DAMPs have been shown to induce inflammasomes by binding to Toll-like receptors 2 and 4. Under certain conditions, the recruited immune cells may exacerbate liver injury by releasing a large number of pro-inflammatory factors, resulting in a cytokine storm. Several other immune cells and cytokines associated with the immune reaction, such as Kupffer cells, macrophages, type-1 innate lymphoid cells, NK cells, neutrophils, and others, are implicated in the occurrence of DILI (Liu *et al.*, 2021). These cells stimulate the inflammatory response by producing cytokines, chemokines, and reactive oxygen species (ROS), which attract immune cells to the site of injury to regulate the damage and activate the adaptive immune response (Liu *et al.*, 2021).

NK cells make up about 50% of hepatic lymphocytes in humans and play a role in inspecting transformed or infected cells by releasing granzyme and perforin. NK cells in the liver are involved in physiological and pathophysiological processes such as viral infections and other injuries, such as innate immune responses and cell-mediated cytotoxicity (Björnsson & Aithal, 2020; Liu *et al.*, 2021). These hepatic innate immune cells may play a role in DILI pathogenesis. In the mouse model, a double-stranded RNA viral derivative that caused the accumulation and activation of NK cells increased the halothane-induced hepatotoxicity (Liu *et al.*, 2021). Indeed, NK cells can modulate DILI by producing interferon-gamma, resulting in hepatocyte cytotoxicity, and NK cell cytotoxicity is regulated by a complex network of activating and inhibitory receptors. There is evidence that NK cells play a role in DILI, as they

are frequently involved in DNA damage, making histiocytes vulnerable to NK cell lysis (Björnsson & Aithal, 2020; Liu *et al.*, 2021).

1.2.3 Idiosyncratic drug Induced liver injury (IDILI)

Idiosyncratic drug-induced liver injury (IDILI), as discussed in the previous section, refers to a deleterious liver response that cannot be likened to the drug's normal therapeutic effects and is a result of the individual's reaction to the drug (Dara *et al.*, 2017; Tailor *et al.*, 2015; Watkins, 2019). The mechanisms of IDILI are still unknown, but they are multistep but also multicellular in disposition (Tailor *et al.*, 2015; Watkins, 2019). Because the occurrence of these interactions is relatively low, predicting IDILI during preclinical trials is difficult, if not unlikely. Clinical signs may include hepatic, cholestatic, or mixed injuries, as well as significant elevations in ALT levels (Dara *et al.*, 2017; Tailor *et al.*, 2015; Watkins, 2019). Often, the result is acute liver failure, which leads to morbidity and mortality in the patient. Antibiotics and nonsteroidal anti-inflammatories, including co-amoxiclav, flucloxacillin, diclofenac, and isoniazid, are the most common causes of IDILI (Aithal & Daly, 2010). Considering the mixed clinical manifestations and the various drug classes involved, it appears unlikely that IDILI is caused by a single process. Furthermore, even within the same drug class, similar symptoms may be caused by different mechanisms (Dara *et al.*, 2017; Tailor *et al.*, 2015; Watkins, 2019).

TNF-induced apoptosis, mitochondrial dysfunction, cell stress, genetic polymorphisms, and stimulation of the innate and adaptive immune systems, according to Tailor *et al.*, are among the mechanisms of DILI. Interestingly, danger signals to the immune system can emerge in an environment of cell stress. The cytochrome P450 oxidising system, N-acetyl transferases, and glucuronosyl transferases were among the first associations discovered. Drug transporters and superoxide dismutase are two other proteins that have been linked. Under the metabolism of CYP2C8 and UDP-glucuronosyltransferase-2B7, the nonsteroidal anti-inflammatory drug diclofenac can form highly toxic chemically reactive metabolites (CRMs) (UGT2B7) (Tailor *et al.*, 2015).

Furthermore, polymorphisms in the transporter allele adenosine triphosphate-binding cassette, subfamily C (ABCC2) have been linked to IDILI susceptibility in diclofenac-treated subjects (Tailor *et al.*, 2015).

A significant number of human leukocyte antigen (HLA) associations with drugs that cause IDILI have been discovered, and they are progressively being demonstrated to have a poor outcome in a clinical context (Aithal & Daly, 2010; Tailor *et al.*, 2015). This suggests that the adaptive immune system may play a role in pathophysiology. The discovery of a strong link between the HLA B*57:01 allele and the HIV treatment abacavir has provided new insights into the critical role of T-cells in abacavir hypersensitivity (Tailor *et al.*, 2015). The mechanism underlying abacavir hypersensitivity has now been identified, and this discovery has led to a significant change in clinical practice. Even though abacavir is not the cause of IDILI, it has been linked to flucloxacillin and HLA B*57:01 (Daly *et al.*, 2009; Tailor *et al.*, 2015). The link between IDILI and HLA provides compelling evidence for an immunological mechanism for IDILI (Aithal & Daly, 2010). Recently, multiple gene polymorphisms have been found to coexist and may have a mechanistic link (Aithal & Daly, 2010; Tailor *et al.*, 2015). When the UGT2B7 and ABCC2 polymorphisms were considered together, for instance, they demonstrated a strong connection with diclofenac induced- liver toxicity (Tailor *et al.*, 2015).

CRM generation, covalent binding, as well as genetic polymorphisms all have the potential to contribute to IDILI (Nicoletti *et al.*, 2017). Other considerations, however, may be involved in an immune-stimulated drug response. The presence of T-cells in liver biopsies from subjects with IDILI and the isolation of drug-specific T-cells in subjects with IDILI support an immune response pathophysiology. Immune activation requires two factors: maturation of antigen-presenting cells and presentation of novel antigens to T-cells. CRMs may cause liver cells to release danger signals, triggering the release of antigen-presenting cells (Dara *et al.*, 2017; Tailor *et al.*, 2015; Watkins, 2019).

Damage-associated molecular patterns and pro-inflammatory cytokines are released by stressed or necrotic cells. Both play a role in the maturation of antigen-presenting cells as well as their recruitment to the site of injury. Co-stimulatory molecules are

significantly increased in response to these "danger signals," increasing their ability to trigger T-cells (Nicoletti *et al.*, 2017; Tailor *et al.*, 2015; Watkins, 2019). According to the hapten model, the CRM will bind covalently to endogenous proteins to produce protein adducts. While a drug molecule may be too small to be immunologically significant, a protein adduct may be processed by antigen-presenting cells, presented by major histocompatibility complex (MHC) molecules, and recognised as a foreign antigen by a T-cell (Dara *et al.*, 2017; Tailor *et al.*, 2015; Watkins, 2019).

To investigate the nature of the drug–antigen interaction *in vitro*, naive T-cells from volunteers expressing this allele can be primed with ticlopidine. However, *in vitro* models are incapable of reproducing all the complex regulatory mechanisms in IDILI (Tailor *et al.*, 2015). As a result, there is an urgent need to fully understand the mechanisms involved in IDILI animal models. Recent research with the antimalarial amodiaquine has made significant progress in animal models for IDILI, using PD-1 (*l*) mice to model liver injury (Tailor *et al.*, 2015). However, much larger studies with other drugs are required. A wide range of genetic polymorphisms are linked to IDILI, suggests the involvement of numerous toxicological pathways. Even so, the percentage of HLA associations observed, and current T-cell data suggest that immunological mechanisms play a critical role in the aetiology of IDILI (Dara *et al.*, 2017; Nicoletti *et al.*, 2017; Tailor *et al.*, 2015; Watkins, 2019).

Class I and Class II of the major histocompatibility complex have similar folds. The binding platform is made up of two domains, one of which is derived from a single heavy α -chain (HC) in the case of MHC class I and the other from two chains (α -chain and β -chain) in the case of MHC class II (Tailor *et al.*, 2015; Watkins, 2019). The two domains evolved to form a slightly curved β -sheet as the base and two α -helices on top that are spaced far enough apart to accommodate a peptide chain in between. The peptide-binding unit is aided by two membrane-proximal immunoglobulin (Ig) domains. Each MHC class II chain contains one Ig domain, whereas the non-covalent association of the invariant light chain beta-2 macroglobulin with the heavy γ -chain provides the second Ig-type domain of MHC class I. Transmembrane helices serve as membrane anchors for the HC of MHC class I and both chains of MHC class II (Tailor *et al.*, 2015; Watkins, 2019).

In both human and laboratory studies, it has been shown that MHC variability and selection mechanisms are functionally relevant in the immune system. In contrast to expectations of the MHC hypothesis, the vast bulk of actual evidence has come from human research or laboratory tests up to this point. Hepatitis B virus infections are eliminated more rapidly from the bodies of MHC heterozygotes than from the bodies of MHC homozygotes (Tailor *et al.*, 2015). Comparatively to homozygous mice, MHC-heterozygous animals displayed decreased pathogenicity during bacterial and viral infection, stronger T-cell-mediated immunity after infection with lymphocytic choriomeningitis, and a faster rate of parasitic worm clearance after infection with adenovirus (Tailor *et al.*, 2015). Tumour incidence and remission in heterozygous hens infected with the Rous sarcoma virus were both much lower and occurred considerably more quickly (Dara *et al.*, 2016). Hepacivirus N or the fluke were used to infect captive-raised fish, and the MHC class IIB heterozygotes in captive-raised fish had a greater survival rate than those in wild fish when infected with the virus (*Poeciliopsis o. occidentalis*).

1.2.4 Mechanisms behind the development of idiosyncratic drug reactions

IDRs are not the most common form of adverse drug reaction (ADR) but are unpredictable and sometimes life-threatening. IDRs are complex because they are caused by multi-factorial conditions that may not be explained mechanistically. However, a combination of mechanism (s) cannot explain all the IDRs reported. Nonetheless, multiple theories to clarify the origin of such adverse events have been suggested (Uetrecht & Naisbitt, 2013; Zhang *et al.*, 2011). The "hapten hypothesis": chemical-reactive metabolites or drugs, in theory, form haptens by covalently binding to proteins. The immune system subsequently identifies the altered protein as being non-self, resulting in the surrounding tissue being destroyed due to an immune response (Uetrecht & Naisbitt, 2013; Zhang *et al.*, 2011). The need for simultaneous co-stimulatory "risk" signals later extended this hypothesis. The risk hypothesis suggests that the immune response can only happen if toxic signals are present at the same time, which explains why all drugs that undergo metabolic activation do not cause IDRs. Risk signals may be derived from several stimuli, including cell damage, cellular stress, infection, or disease (Uetrecht & Naisbitt, 2013; Zhang *et al.*, 2011). For instance, the pharmacological interaction hypothesis describes an overt

activation of the immune system by the parent compound, as per the mitochondrial dysfunction hypothesis, which describes the interference of drugs with mitochondrial function. The Inflammagen hypothesis explains the triggering effect of simultaneous inflammation due to environmental stimuli (Boelsterli & Lim, 2007; Shoda *et al.*, 2013; Uetrecht & Naisbitt, 2013).

Several mechanistic findings suggest a crucial role of drug bioactivation to chemically reactive metabolites in the onset of DILI-2. Most of these drugs, linked with DILI-2, produce chemically reactive metabolites in humans (Park *et al.*, 2011; Walgren *et al.*, 2005). The formation of chemically reactive metabolites is often reduced in current drug development by preventing structural warnings or unwanted metabolism soft spots within the drug molecule (Evans *et al.*, 2004). However, consideration of potential intrinsic bioactivation alone is not enough to avoid the risk of ADR. Among over 100 top drugs in the USA, it was shown that although the drugs associated with IDRs are more common, about 50% contain structural alerts for the formation of chemically reactive metabolites. However, most of these drugs are not IDR-related (Stepan *et al.*, 2011; Yang *et al.*, 2017), and these are based on a poor correlation between the risk of IDR and the level of covalent protein binding found *in vitro* (Nakayama *et al.*, 2009; Thompson *et al.*, 2012). The essential existence of the cellular structure of the adducted proteins may be one reason for this weak correlation.

Further insights can be provided by differentiating between modifications of essential protein targets as well as non-essential protein targets (Park *et al.*, 2011; Thompson *et al.*, 2016). Nonetheless, our existing knowledge of the impact of protein alterations on signalling networks and their relationship with IDRs is too small to integrate these data into DILI models (Thompson *et al.*, 2016). The reactive target protein database offers a general idea of target proteins for covalent alteration by reactive chemical metabolites to enhance understanding of the means of causing reactive chemical metabolites in drug toxicity (Judson *et al.*, 2011).

While the formation of DILI chemically reactive metabolites is required in many drugs, it is not enough, and additional methods are required to cause toxicity. When the covalent binding is combined with other factors, a more apparent distinction is

achieved between drugs that generate IDR and safe drugs. These factors may include daily dosage, bioactivation level, the impairment of bile salt export pump (BSEP), cytotoxicity testing with or without a bioactivation propensity, mitochondrial toxicity assessments, and Mrp2 inhibition (Judson *et al.*, 2005; Thompson *et al.*, 2011).

1.2.5 Bioactivation of drugs and the risk for Idiosyncratic drug-mediated hepatic injury

Despite the low toxicity incidence in some populations, drug-related risk factors, other than bioactivation capacity, do not clarify a subject's responsiveness. However, risk factors associated with patients, which affect cellular exposure to chemically reactive metabolites or cause changes following immune reactions, are expected to be pivotal for toxicity consequences (Schehu *et al.*, 2017; Uetrecht *et al.*, 2012). The concept of idiosyncrasy, particular to a subject, suggests a person's vulnerability rather than the presence of unusual drugs (Uetrecht *et al.*, 2012). The risk factors caused by drug properties; for instance, the metabolic stimulation potential and biological and host factors, are the consequence of human vulnerability (Schehu *et al.*, 2017; Uetrecht *et al.*, 2012). Diet, multiple drug use, age, pregnancy, illness, gender, and genetic factors are examples (Schehu *et al.*, 2017; Uetrecht *et al.*, 2012). These observable effects can influence the activity and expression thresholds of liver enzymes implicated in the bioactivation and detoxification of chemically reactive metabolites. To identify potential susceptibility factors, it is critical to have a detailed insight into the metabolic pathways of drugs and variations of the enzymes implicated. The impact of changes to the adaptive immune system in the sense of IDILI risk is less well described (Thompson *et al.*, 2016).

1.3 Hepatic glucose metabolism and diabetes

Chronic liver disease is commonly linked to glucose intolerance and diabetes. Depending on its aetiology, chronic liver pathology has a significant impact on glucose metabolism, and subjects with long-term liver disease exhibit a high prevalence of glucose intolerance and diabetes due to insulin resistance and β -cell impairment (García-Compean *et al.*, 2009).

1.3.1 Hepatic glucose metabolism

Glucose metabolism forms vital metabolic processes that provide energy in the form of adenosine triphosphate (ATP) for cellular functions (Aronoff *et al.*, 2004). The production of ATP from glucose metabolism involves three net-like metabolic pathways. In the first step, glucose is oxidised to two pyruvate molecules via the glycolytic pathway, a mechanism that befalls in the cell's cytosol (Aronoff *et al.*, 2004). The produced pyruvate molecules are transported into the mitochondria and enter the tricarboxylic acid cycle (TCA cycle), also known as the Krebs cycle. Within the TCA cycle, pyruvate undergoes complete oxidation to develop three molecules of carbon dioxide. In this process, hydrogen carriers NAD⁺ (nicotinamide adenine dinucleotide) and FAD (flavin adenine dinucleotide) are reduced to NAD⁺ + H⁺ and FADH₂, respectively. Both NAD⁺ + H⁺ and FADH₂ enter the respiratory chain and pass through the coupled processes of electron transport as well as oxidative phosphorylation to produce water and ATP. The hydrolysis of ATP can then be used to discharge energy needed for a collection of biological functions such as protein synthesis, muscle contraction, and the conduction of nerve impulses (Vander Heiden & DeBerardinis, 2017). Besides this main route of ATP production, glucose metabolism can progress along quite a few other pathways, depending on the conditions within the cell and the body's requirements. In the absence of oxygen (anaerobic condition), pyruvate is altered to lactate rather than going into the TCA cycle.

Although this mechanism results in less efficient energy production, it is imperative to discharge a comparatively smaller amount of usable energy during strenuous exercise when ATP is needed swiftly. Nonetheless, local oxygen provision can be constrictive in muscles that are solely functional (Naifeh & Varacallo, 2018). Lactate produced by this mechanism can disperse from the cells into the systemic circulation, where it is taken up by the liver and oxidised to pyruvate in the presence of oxygen before being converted back to glucose. The muscle cells are the primary sites of anaerobic glycolysis due to high energy requirements and reduced restrictive local oxygen levels during rigorous exercise (Naifeh & Varacallo, 2018). Other tissues, for instance, erythrocytes, also depend on this mechanism of energy production as they lack mitochondria. However, the retina, as well as the kidney

medulla, rely on anaerobic glycolysis for the generation of ATP, yet in the existence of oxygen (Naifeh & Varacallo, 2018; Vander Heiden & DeBerardinis, 2017).

In a situation where there is excess glucose and the demand for energy production is limited, the glucose metabolism is then bound for glycogenesis; excess glucose is converted to glycogen to store high energy precursors (Vander Heiden & DeBerardinis, 2017). Also, when the need for energy production increases, the accumulated glucose concentrations drop. Glycolysis occurs, resulting in the breakdown of glycogen and its conversion back to glucose. However, under these conditions, glucose can be produced from non-carbohydrate precursors such as amino acids or glycerol (Lin & Accili, 2011; Vander Heiden & DeBerardinis, 2017). Furthermore, glucose can enter the pentose phosphate pathway or the phosphogluconate pathway, which is vital for NADPH + H⁺ production. This reducing power is critical for fatty acid and cholesterol synthesis and the reduction of oxidised glutathione (GSSG) to reduced glutathione (GSH). Also, it produces pentose sugar (ribose 5-phosphate) for nucleotide and nucleic acid production (Naifeh & Varacallo, 2018; Prabhu *et al.*, 2002; Vander Heiden & DeBerardinis, 2017). For instance, lipid and protein metabolic pathways (lipid and protein metabolism) can also sustain the reactions that befall during glucose metabolism; for instance, lipogenesis encompasses the pentose phosphate pathways (Figure 1-3).

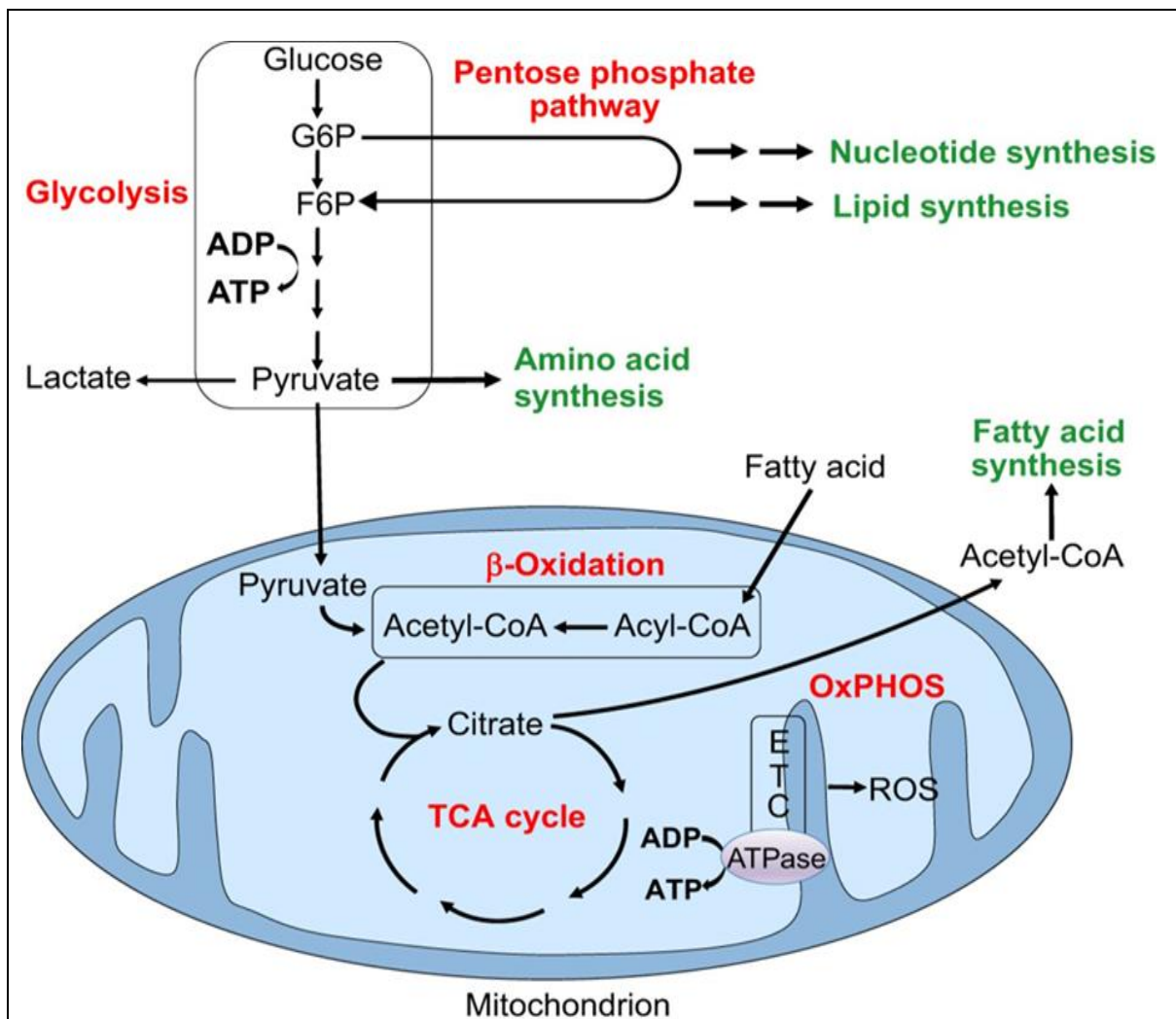


Figure 1-3 Schematic representation of cellular respiration pathways

The key cellular metabolic stages are shown in red, that is, glycolysis, pentose phosphate pathway, β -oxidation and oxidative phosphorylation (OxPHOS). The steps involved in glycolysis and the TCA cycle are defined separately. Each of these pathways produces metabolites that are needed to promote cell growth through energy production (ATP), nucleotides, lipids, amino acids, and fatty acids, which are also shown in green. The most efficient pathway for cellular energy production is OxPHOS, which produces much more ATP than glycolysis, and as such, it is considered the most resourceful pathway for energy production. However, both the glycolysis and the TCA processes produce ATP from substrates, but TCA produces many more ATP molecules than glycolysis. Fructose-6-phosphate is converted to fructose-2,6-bisphosphate, which in turn activates phosphofruktokinase-1 and promotes the rate of glycolysis. Citrate metabolism yields acetyl-CoA which is converted to malonyl-CoAs for fatty acid production (Mathieu & Ruohola-Baker, 2017).

1.3.2 Diabetes mellitus

Diabetes mellitus is a class of metabolic disease characterised by persistent high blood glucose concentration with a disruption to carbohydrate, fat as well as protein metabolism caused by deficiencies in insulin secretion, action, or both (John *et al.*, 2012; Kharroubi, 2015; Roglic, 2016). It is estimated that about 422 million people worldwide have diabetes, and about 2.2 million people died because of hyperglycaemia in 2012. It is estimated that diabetes is the seventh leading cause of death worldwide (Aravinthan *et al.*, 2019; Roglic, 2016). However, there are about 4.7 million people diagnosed with diabetes in the UK, and about 90% of those with type 2 diabetes. Approximately 1 million people live with asymptomatic type 2 diabetes and are unaware because they have not been diagnosed. However, it has been estimated that by the year 2030, the number of people with diabetes in the UK might rise to about 5.5 million (Whicher *et al.*, 2020). The WHO diagnostic criteria for diabetes is fasting blood glucose above 7.0 mmol/L or the 2-hour blood glucose after oral ingestion of 75 g of glucose is above 11.1 mmol/L. As described above, other minor categories of diabetes or related impairments include gestational diabetes, impaired glucose intolerance, as well as impaired fasting glycaemia (John *et al.*, 2012; Kharroubi, 2015). Gestational diabetes is diagnosed in pregnant women in their second or third trimester. In this condition, pregnant women experience the onset of high blood glucose concentration, which some may return to normal after gestation. Impaired glucose tolerance and impaired fasting blood glucose are intermediate conditions between non-diabetes and diabetes, raising the risk of the progressive development of diabetes (Kharroubi, 2015; Whicher *et al.*, 2020).

Diabetes mellitus can be grouped into two types; type 1 and type 2 diabetes, although there are other types (gestational diabetes, diabetes insipidus, brittle diabetes mellitus) (Benbow & Gallagher, 2004; Kharroubi, 2015). Type 1 diabetes mellitus is mainly due to autoimmune destruction of the pancreatic β -cell by T-cell mediated inflammatory reaction and the humoral (B cell reaction) (Devendra *et al.*, 2004). Autoantibodies (islet cell autoantibodies, autoantibodies to insulin, glutamic acid decarboxylase, etc.) opposed to the islet cells are a sign of type 1 diabetes, albeit the role of these antibodies in the development of the disease is poorly understood (Lawrence *et al.*, 2014). These pancreatic autoantibodies could be

isolated in the serum of subjects earlier or later before developing type 1 diabetes (Lawrence *et al.*, 2014). Type 1 diabetes is widely believed to be caused by the degradation of insulin-producing pancreatic β cells by an immune-associated, if not specifically immune-mediated, process. (Craig *et al.*, 2014; Leslie, 2010). Type 1 diabetes usually leads to complete insulin scarcity, and it accounts for about 8% of the diabetes population (Craig *et al.*, 2014). In the past decades, type 1 diabetes has been widely considered a disease in children and teenagers, but this perception has changed in the past few years, so that age at the onset of symptoms is no longer a limiting factor (Leslie, 2010). Apart from genetic susceptibility in type 1 diabetes, several factors, such as viral infection or low levels of vitamin D, have been linked to the pathogenesis of the disease (Matteucci & Giampietro, 2014). Type 1 diabetes progresses suddenly and can produce symptoms such as excessive thirst, an excessively large volume of urine passage, enuresis or blurred vision in subjects affected by the disease (Kahanovitz *et al.*, 2017; Matteucci & Giampietro, 2014).

In type 2 diabetes, there are defects in insulin secretion because of the gradual loss of β -cell insulin secretion recurrently on the background of insulin resistance (DeFronzo *et al.*, 2002; Tobias, 2016; Kharroubi, 2015; Siminerio *et al.*, 2000). Insulin resistance in type 2 diabetes upsurges the requirement for insulin-target tissues. Also, the high demand for insulin may well not be sustained by the β cells due to the deficiencies in the cells' actions (Halban, 2014). In contrast, insulin secretion drops relative to increased demand for insulin over time due to the gradual destruction β -cells and this could transform some type 2 diabetics from being non-reliant on human-made insulin to becoming reliant on artificial insulin (Druet *et al.*, 2006). More than half of the type 2 diabetics whose insulin secretion continues with rare insulin depletion do not rely on artificial insulin to manage the disease. However, they are managed with about six classes of oral antidiabetic drugs, such as biguanides (metformin), sulphonylureas (glimpiride), thiazolidinediones (pioglitazone), dipeptidyl peptidase IV inhibitors (sitagliptin), meglitinides (repaglinide), and α -glucosidase inhibitors (acarbose) (Druet *et al.*, 2006; Moses, 2009).

1.3.3 Treatment and management of diabetes mellitus

Currently, there is no pharmacological intervention that can completely cure type 1 diabetes mellitus; instead, pharmacological interventions such as the use of either oral antidiabetic agents or supplementation with human-made insulin have been the optimal clinical intervention in the treatment of the disease (Pratley, 2013). Also, type 2 diabetes was once considered irreversible and progressive, but it can be reversed by losing weight and avoiding weight gain (Taylor *et al.*, 2021). Oral antidiabetic medications are the main front-line treatments in the management of type 2 diabetes. Also, lifestyle adaptations such as exercise and proper nutrition may help reduce or reverse type 2 diabetes and prolong the lives of diabetes subjects (Balti *et al.*, 2015; Florez *et al.*, 2007; Mathers & Lancor, 2006; Pratley, 2013; Tuso, 2014; Venditti *et al.*, 2008). The target blood glucose regulation proposed by the National Institute of Health and Clinical Excellence (NICE) is in the range of 48 mmol/mol to 58 mmol/mol of glycosylated haemoglobin A1 (HbA1c) (Poole, 2015). Clinicians use HbA1c to determine how well their diabetic patients manage their blood glucose concentration. Glucose moves through the bloodstream and attaches itself to cells. If this occurs, the cell is known to be "glycated." Diabetics and non-diabetics have glycated blood cells. The higher the levels of glucose in the blood, the more it sticks to the cells. But these are irreversible because red blood cells only survive for four months before new ones are made. That is why the HbA1c will only provide average blood glucose for the past three months. (Rathod *et al.*, 2018). Pharmacotherapy may be introduced to type 2 diabetes subjects who have not responded well to lifestyle adaptation to attain safe glycaemic control. As mentioned in the previous section, a wide variety of pharmacological agents have been designed for the treatment of diabetes, and these agents are branded into a few general groups. Primarily, insulin secretion can be promoted by sulphonylureas. Also, biguanides such as metformin reduce hepatic glucose output, enhance liver, and muscle insulin sensitivity. Also, the thiazolidinedione class of compounds increases adipose and muscle insulin sensitivity (Cheng, 2005; Genuth, 2014; Good & Pogach, 2018). If lifestyle and oral antidiabetic agents have failed to control diabetes mellitus, artificial insulin may be used to increase systemic insulin concentrations. However, in type 1

diabetes, pancreatic β -cells transplantation can increase insulin output (Matsumoto, 2011; Takita, 2013).

1.3.3.1 The effect of insulin on glucose homeostasis

Insulin exercises all its known physiological effects in the plasma membrane of target cells by binding to the insulin receptor (INSR) (Haeusler *et al.*, 2017). INSR is a heterotetrameric tyrosine kinase receptor formed by two extracellular α subunits binding insulin and two membrane-spanning β -units each containing a tyrosine kinase domain (Testa, 2014). There are two INSR isoforms, A and B, but B exhibits much more selectivity for insulin. Because it is the predominant isoform expressed in differentiated liver and muscle, it mediates most insulin's metabolic effects (Belfiore *et al.*, 2017). Unlike exon 11, the A isoform is strongly expressed in foetal development as it displays a high affinity for IGF-2 (Belfiore *et al.*, 2017). INSR has two insulin-binding sites but is cooperative with other sites, which means insulin-binding on one site reduces insulin-binding affinity on the other site (De Meyts, 2008).

In years gone by and till date, insulin is the only known β -cell pancreatic hormone that decreases blood glucose concentration (Petersen & Shulman, 2018). Insulin, a small protein containing two polypeptide chains of 51 amino acids, is a vital anabolic molecule for higher blood glucose and amino acid intake. Contrary to other hormones, insulin binds to different receptors in several body cells, especially fat cells, liver cells, and muscle cells. The critical effect of insulin is the suppression of glucose (Petersen & Shulman, 2018; Petunina & Telnova, 2018). Insulin works in three ways to regulate postprandial glucose. Initially, insulin stimulates the cells to maximise insulin-sensitive peripheral tissues, primarily skeletal muscle, to increase glucose uptake (Petersen & Shulman, 2018). Insulin works on the liver to aid glycogenesis (Petersen & Shulman, 2018). Also, insulin concurrently inhibits glucagon production from pancreatic- α cells to signal the liver to decrease glucose production via glycogenesis (Sood *et al.*, 2001).

Insulin can also stimulate fat production, promotion of triglyceride storage in fat cells, promotion of protein synthesis in the liver and muscle, and propagation of cell growth (Sood *et al.*, 2001). The activity of insulin in response to circulating glucose levels is

tightly controlled. Insulin will not be released when the blood glucose concentration in the blood is < 3.3 mmol /L but will be gradually secreted as glucose concentrations increase above this level (Petersen & Shulman, 2018). Glucose concentration is a crucial insulin stimulator. However, other factors may stimulate the secretion of insulin. Increased plasma levels of specific amino acids include arginine, leucine, and lysine, GLP-1 and GIP from the intestine after a meal; as well as the stimulation of the parasympathetic through the vagus nerve (Petersen & Schulman 2018). Glucagon produced from pancreatic alpha cells in Langerhans' islet critically plays a role in retaining glucose homeostasis by triggering hepatic glucose synthesis (Heppner *et al.*, 2010). Therefore, glucagon is a glucose-mobilising hormone, contrary to the glucose-depositing nature of insulin activity. Accordingly, high plasma glucose levels promote insulin release from pancreatic beta cells and inhibit the release of glucagon, whereas low plasma glucose concentrations are one of the potent secretory stimuli. Therefore, normal plasma glucose levels mainly depend on the controlled secretion of the pancreatic beta cells and alpha cells from insulin and glucagon (Heppner *et al.*, 2010; Produit-Zengaffinen *et al.*, 2006). Nuclear receptors are transcription factors that control the metabolism of carbohydrates, lipid metabolism, the immune response, and inflammation. Nuclear receptors have become significant therapeutic targets for treating a variety of diseases because of their complex biological effects. For instance, the increasing prevalence of diabetic nephropathy has led extensive work into the role that function of nuclear hormones receptors in slowing or preventing the progression of renal disease (Qian *et al.*, 2008). The function of nuclear receptors is correlated with metabolism improvements, immune response and inflammation. Nuclear receptors are activated by lipid-soluble signals that cross the plasma membrane, for instance, the steroid hormones. When triggered by various biological processes, the majority act as transcription factors to regulate gene expression. Due to the broad range of nuclear-receptor-controlled techniques, their dysregulation can lead to multiple diseases, such as cancer, diabetes, and infertility (Moutinho *et al.*, 2019). The nuclear receptor is discussed further in section 1.3.4.

1.3.4 Nuclear receptors

Nuclear receptors are a group of ligand-controlled transcription factors that regulate a wide range of biological activities ranging from reproduction, development, or metabolic homeostasis (Kakizaki *et al.*, 2008; Lu & Xie, 2017; Plant & Aouabdi, 2009). The standard way of communicating signals from the environment to the cell is through a complex multi-stage process that starts with receptor activation (Han *et al.*, 2009; King-Jones & Thummel, 2005). The receptor causes a series of cell cytoplasm processes that then regulate the expression of nuclear genes by other transcription factors (King-Jones & Thummel, 2005). The transcription factors of the nuclear superfamily receptor vary in the size, shape, and charges of their stimulating ligands. Almost all nuclear receptor members share a similar structure of cellular domains; thus, another function. Each nuclear receptor promotes the receptor activity, DNA binding, and the effect on the single-molecule of protein (King-Jones and Thummel, 2005).

One of the most significant family transcription factors (superfamilies) forms nuclear receptors (King-Jones & Thummel, 2005). The nuclear receptor consists of a variable NH₂ terminal region called the A/B, a highly conserved DNA-binding domain (DBD), as well as a less conserved carboxyl-terminal ligand-binding domain (LBD). DBDs between various nuclear receptors are actively preserved and have two zinc finger motifs, each with four cysteine residues (Wärnmark *et al.*, 2003). The first zinc finger has a five-residue P-box responsible for specific DNA binding. The second zinc finger shows a relatively weak dimerization ability, which enables DBD to form dimers in the presence of target DNA. To a lesser extent, LBD is kept and maintains the central dimerization region, allowing molecules of various receptors to form dimers, significantly increasing the range of potential DNA targets and regulatory mechanisms. The LBD is composed of 11–13 α -helical regions, one of which contains a hydrophobic ligand-binding pocket. While the AF-2 domain is located at the end of the C region of LBD, it is possible for N-terminal AF-1 to function independently of ligand. Specific structural and molecular studies have shown that ligand-binding causes the LBD to confirmatively transition into a functional state. In essence, α -helix 12 transforms into a position that enables the AF-2 domain to recruit transcriptional coactivators (Figure 1-4) (King-Jones & Thummel, 2005; Kakizaki *et al.*, 2008; Lu, &

Xie, 2017; Wärnmark *et al.*, 2003). Some nuclear receptors also have a highly variable carboxy-terminal tail called the F domain that has unknown roles (Lazar, 2003). When ligands are excluded from the cells, the cytoplasm or nucleus releases free nuclear receptors. Nuclear receptor ligands include a vast number of small lipophilic molecules, including steroids, thyroid hormones, and retinoic acid (Lazar, 2003).

These molecules move through the plasma and nuclear membranes readily and are bound to nuclear receptors. Structural changes resulting from ligand binding in nuclear receptors promote the ligand-receptor complex on unique DNA sequences. These sequences are classified as HREs and serve as enhancers to regulate transcription of regulated genes (Lazar, 2003). The HRE is a short sequence that is close to or represents the AGGTCA consensus. Other nuclear receptors act as homodimers or heterodimers and bind them together into two convergence sequences, forming a functional HRE. In HRE, the nucleotide and structure are arranged as a direct or inverted representation divided by a short variable sequence. The DNA binding domain contains two zinc finger motifs, acting as a clip, which enables chromatin to be bound within the nucleus (King-Jones & Thummel, 2005; Lazar, 2003). Each group has distinct sets of binding DNA recognition, varying from half-sites with inverted repeats, direct repeats, or no repeats in the DNA sequence (King-Jones & Thummel, 2005).

There are many types of nuclear receptors in the superfamily. Type I receptors, which are summarised in table 1-1, include progestin (PR) (ER), androgen (AR), glucocorticoid (GR) and receptors for mineralocorticoid (MR). Receptors of type II include RAR receptors, 9-cis retinoic acid (RXR), and vitamin D3 (VDR), all-trans retinoic acid. Chandra *et al.* describe the type III receptors as having unknown ligands. These are classified as orphan receptors, some of which can act as ligand-independent (King-Jones & Thummel, 2005). There are also functional variations between different receptors. In the absence of a ligand, type I receptors are inactive and occur in a complex cytoplasm with chaperones. These receptors might move into the nucleus when activated and bind to an inverted-reverse sequence of DNA repeats to control the transcription of the target genes as homodimers with a head-to-head configuration. The type II receptors are uniquely connected to direct

repeated HREs, showing various dimerization dynamics such as heterodimerization with RXR. In the absence of a ligand, some of these receptors serve as repressors, making the target gene inactive by recruiting corepressor systems. When the repressors are coupled with their respective hormones, they recruit coactivators and trigger complex corepressors, thus contributing to the expression of the target gene (Lonard & O'Malley, 2007). According to Zhou *et al.*, the type III SF-1 receptor attaches to the HRE as a monomer and functions as a constitutive ligand-independent transcriptional activator. Phosphorylation maintains SF-1 in an active conformation and increases its activation potential significantly. Nuclear receptor coregulators are proteins that interact with the nuclear receptor and facilitate the expression effects of hormonal signals on expression. Several other coregulators stimulate transcription (coactivators); others suppress transcription (corepressors). The mechanism of action of type IV nuclear receptors is similar to that of type II nuclear receptors; however, they bind to DNA as a monomer and recognise extended half-sites in HREs.

Table 1-1 Nuclear receptor subtypes and their signalling mechanisms

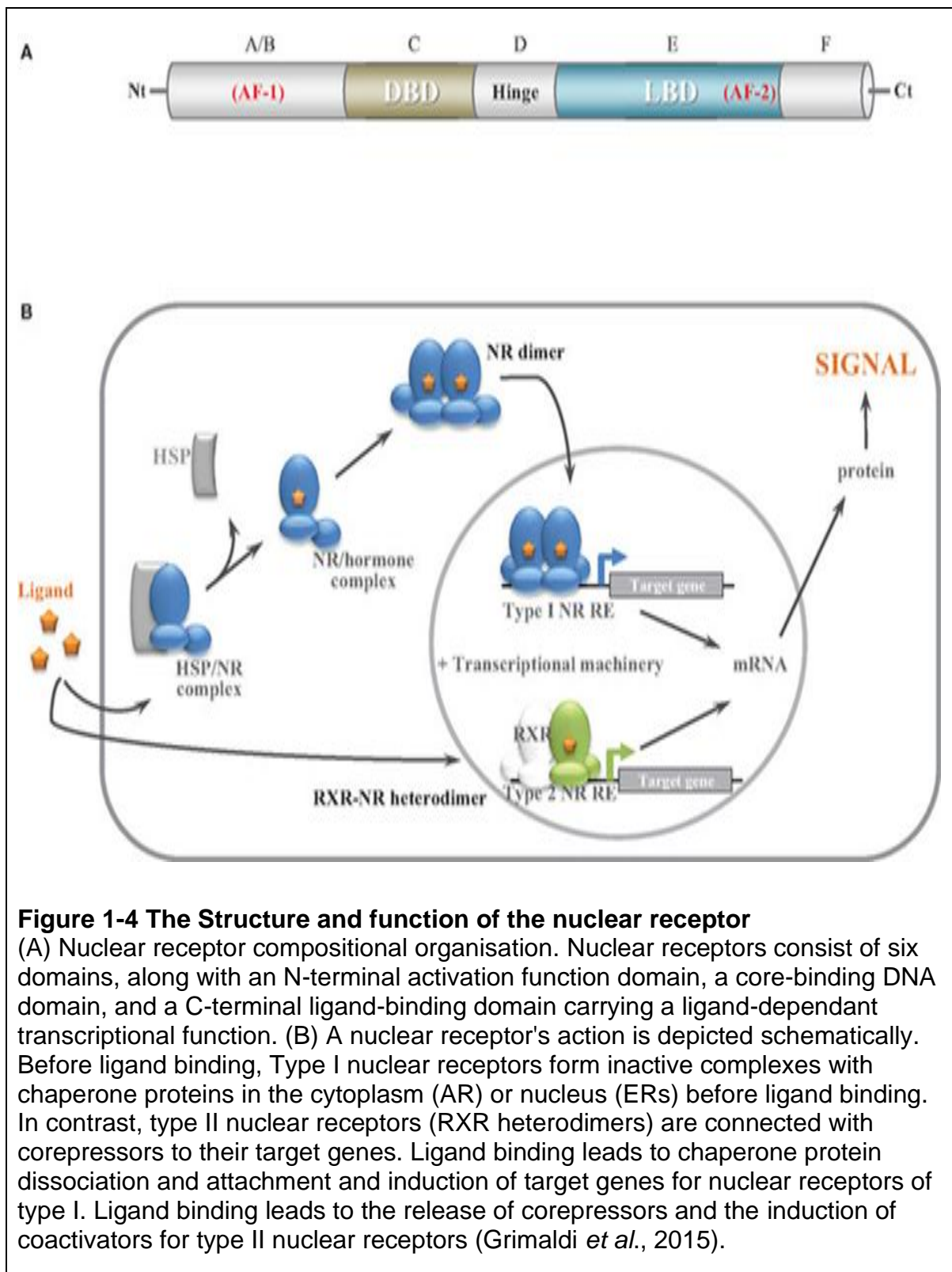
Subtypes of Nuclear receptors	Examples	Signalling mechanisms of subtypes of nuclear receptors
Type I	Estragon receptor, Androgen receptor, Progesterone receptor etc	Resides in the cytoplasm in a complex with chaperone proteins. When stimulated (hexagon), the receptor is discharged from this complex and trafficked into the nucleus. They then bind to palindromic HREs as a homodimer to control transcription.
Type II	Thyroid hormone receptor, Vitamin D receptor, retinoid A receptor etc	These are localised in the nucleus. They interact with co-repressors proteins that occur in an unliganded state, but they are exchanged for co-activators when they bind to a ligand. They generally form heterodimeric complexes with RXR.
Type III	Homodimeric orphan receptors (RevERbA α)	They exist in the nucleus and exchange bound co-repressors and co-activators. They are attached to direct repeat HREs as homodimers. No ligand has been found for their stimulation
Type IV	Monomeric Orphan Receptors (LH-1 and SF-1) (Steroidogenesis factor-1)	These are almost identical to type III except they bind with HREs that are extended half-sites as monomers.

One of the essential functions of a stimulated nuclear receptor is to make the target gene promoter more available to the general transcription machinery or act as a repressor. Therefore, group 1 of the nuclear receptor coactivators comprises ATP-dependent chromatin remodelling factors, including NSD-1 (nuclear receptor-binding SET domain-containing protein 1), TIF1 α and others (Han *et al.*, 2009; Zhou *et al.*, 2006). The Group 2 coactivator of the nuclear receptor comprises acetyltransferases of the SRC family and CBP/p300 (Han *et al.*, 2009; Zhou *et al.*, 2006). Thyroid receptor-associated proteins (TRAP)/DRIP (Vitamin D receptor-interacting proteins) are nuclear receptor coactivators. The TRAP / DRIP factors were established as TR and VDR recruited proteins. More experiments have shown that the TRAP/DRIP

complex acts as a coactivator with other forms of nuclear receptors and probably has a significant role in facilitating nuclear receptor signalling. Molecular studies have shown direct associations between the TRAP complex and general transcription mechanisms (Han *et al.*, 2009; Zhou *et al.*, 2006). Also, coactivators of nuclear receptors include E3 ubiquitin ligases, positive co-factors (PCs), and HMGs (Han *et al.*, 2009; Zhou *et al.*, 2006). Few nuclear receptors interact with general transcription systems specifically. In relation to the coactivator corepressor, ATP-based chromatin (NURD corepressor), histone deacetylation (HDAC1/HDAC-2) or direct interactions with the general transcription apparatus are facilitated to disrupt the preinitiation complex, as well as via phosphorylation, ubiquitination, and protein degradation (Han *et al.*, 2009; Zhou *et al.*, 2006).

Nuclear receptors attached to hormone response elements recruit large numbers of other proteins, called transcription coregulators that promote or repress the synthesis of the related target gene into mRNA (Rosenfeld & Glass, 2001). Structural investigations revealed an amphipathic α -helix with leucine residues on one side of the helix, forming a hydrophobic base. Ligand-dependent conformational changes to the AF-2 α -helix domain, particularly α -helix 12, induce a hydrophobic surface for the interaction with the NR box (López-Velázquez *et al.*, 2012; Zhou *et al.*, 2006). The existence of one hydrophobic surface on one side of an α -helix is always essential. Although certain factors such as CBP, p300, and TRAP220 are critical for individual growth, most coregulators may replace each other in nuclear receptors. They are also tissue-specific and hormone-regulated (Kodera *et al.*, 2014). A nuclear receptor's ability to recruit ligand-specific coregulators is often dependent on the binding of different ligands, which cause various conformational changes in the AF-2 region, ensuring the interactions between proteins. For example, VDR interacts ligand-bound with SRC-1 or TIF2/SRC-2 (Kodera *et al.*, 2014). Nuclear receptors function as active regulators in major biological processes such as homeostasis, detoxification, cell differentiation, embryo formation and development (Figure 1-4) (Grimaldi *et al.*, 2015; Han *et al.*, 2009; Kodera *et al.*, 2013; López-Velázquez *et al.*, 2012; Zhou *et al.*, 2006). Also, apart from the nuclear receptor's direct transcriptional activation of target genes, several nuclear receptors can indirectly influence the transcription of target genes by negatively interfering with the transcription responses

mediated by other groups of transcription factors, particularly those implicated in inflammation, for instance, the nuclear factor- κ B (NF- κ B) (Chinenov *et al.*, 2013). Although recent research conducted in vertebrates has made a considerable contribution to understanding how nuclear receptors regulate the transcript of their target genes, their function in biological development is poorly understood (Han *et al.*, 2009; Koderá *et al.*, 2014; Zhou *et al.*, 2006). Awareness of the location and organisation of genomic regulatory regions that include binding sites for nuclear receptors will promote the evaluation of the molecular predictors and frameworks regulating each receptor in response to physiological signals or therapeutically appropriate drugs (Garza *et al.*, 2011). Previously, gene-by-gene evaluation and the characterisation of the regulatory elements assumed to be targeted by nuclear receptors were primarily conducted, a procedure that was both inefficient and labour intensive (Gao & Zhao, 2017). However, the simultaneous development of chromatin immunoprecipitation (ChIP) assays, DNA microarray-based technologies (gene chip) and whole-genome or high-throughput sequencing has recently led to the development of new methods to classify the positions on a genome-wide scale of bound transcription factors and other proteins associated with chromatin (Gao & Zhao, 2017). These innovative methods have been applied to analyse specific nuclear receptors and explore how these studies' findings have introduced novel paradigms of nuclear receptor action, leading to the realisation that nuclear receptors coordinate extensive transcriptional regulatory networks connecting genetic expression and physiology. These studies were mainly limited to regulated gene proximal promoter regions (Gao & Zhao, 2017; Lee *et al.*, 2006). For instance, the location of the binding sites for ER α (nuclear receptor 3A1) has been extensively investigated using all forms of approaches and array designs based on ChIP (Huss *et al.*, 2007). Most of the findings from these experiments offer not only mechanistic insights into how ER α functions as a transcription factor but also allow for a more explicit comparison of the functional advantages and drawbacks of each method since most studies were carried out with the human breast cancer cell line MCF-7 (Kwon *et al.*, 2007).



1.3.5 Pregnane -X-Receptor in xenobiotic or drug biotransformation and its functions in DILI

Pregnane -X- receptor (PXR) belongs to the nuclear receptor subfamily 1, group I and member 2 (NR1I2). PXR is an essential element of the body's adaptive defence device against toxic substances and xenobiotics (Moore *et al.*, 2003; Wright, 2006). PXR is a part of the NR family of ligand-activated transcription factors that comprises steroid, retinoid, thyroid hormone receptors and various orphan receptors where the physiological ligands are still to be discovered. A considerable variety of endogenous and exogenous chemicals, such as steroids, antibiotics, bile acids, and the herbal antidepressant St. John's wort, could activate PXR (Carnahan & Redinbo, 2005; Teng *et al.*, 2004). Furthermore, accumulated evidence indicates that PXR also plays a vital role in endobiotic metabolism by controlling essential genes implicated in glucose metabolism, lipid and bile acid metabolism. (Ling *et al.*, 2016; Moore *et al.*, 2003). PXR has previously been shown to be a significant regulator of *in vivo* CYP3A expression in a study using transgenic mice (Ling *et al.*, 2016). Studies have also shown that PXR controls a small number of genes involved in various facets of xenobiotic metabolisms, such as oxidation, conjugation, and transportation. The analysis of the PXR ligand-binding domain (LBD) three-dimensional structure recently received interesting insights into the underpinning theory for the promiscuous ligand binding characteristics of this rare NR (Moore *et al.*, 2002).

PXR, also known as the steroid and xenobiotic sensing receptor (SXR), has evolved to protect the body. Its induction across various prescription drugs is the molecular basis for an essential group of harmful drug-drug interactions (Moore *et al.*, 2002). PXR activation regulates and expresses drug-metabolising enzymes and transporters in phases I and II, playing an important role in drug absorption, metabolism, and elimination (Gupta *et al.*, 2008). Also, activation of PXR modulates many cellular processes beyond drug metabolism, such as endobiotic metabolism, oxidative stress response, apoptosis, inflammation, cell proliferation, and regeneration (Gupta *et al.*, 2008; Hakkola *et al.*, 2016; Hu *et al.*, 2010; Moore *et al.*, 2003; Wan *et al.*, 2003). As discussed in the previous section, the liver plays a key function in the metabolism and elimination of xenobiotics. Repeated exposure of the liver to xenobiotics often results in reduced liver function and results in DILI. As PXR

tightly controls gene expression in the hepatic drug clearance system, an aberrant stimulation of PXR will cause drug-induced liver injury DILI (Gupta *et al.*, 2008).

PXR is implicated in both basal and inducible expression of many other CYPs (CYP2B6, CYP2C8, 2C9, 2C19, CYP3A5, CYP3A7, and CYP2A6). CYP3A is the most abundant CYP in the liver by far, accounting for several medically used drugs (Matsumura *et al.*, 2004). Earlier studies have been carried out on ChIP in human hepatocytes exposed to rifampicin to establish new target genes for PXR. Genes, both historically recognised and not proven to be active in drug disposal, have been found with PXR response elements (PXREs) positioned upstream, inside, or downstream of their theoretically related genes (Hariparsad *et al.*, 2009). They reported many different genes with binding PXR sites for the disposition of drugs. As such, the existence of rifampicin shows only improved attachment by CYP4F12. PXR 's role in CYP4F12's basal and inductive responses has been confirmed in hepatocytes where PXR was repressed (Hariparsad *et al.*, 2009). The researchers measured PXR-coactivators and corepressors' interactions with established and newly found PXREs. In the absence of rifampicin, both PXR and the steroid receptor coactivator bind to PXREs, though the binding was more significant after treatment with rifampicin. They also reported a promoter-dependent manner of binding a range of coactivators and corepressors involved in CYP4F12, CYP3A4, CYP2B6, UGT1A1 and P-glycoprotein regulation. They concluded that PXR was involved in the regulation of CYP4F12 and that PXR is bound to a wide range of promoters along with the steroid receptor coactivator but that many of these are not inducible by rifampicin (Hariparsad *et al.*, 2009).

PXR controls CYP3A4 transcription by attaching the xenobiotic response factor in the proximal promoter region near CYP3A4's transcriptional end site (Hariparsad *et al.*, 2009). Induction of CYP3A4 can lead to several PXR ligands in drug-drug interactions (Hariparsad *et al.*, 2009). Biotransformation products are typically non-toxic, more polar and disposable. Some drugs, however, are biotransformed into more toxic electrophiles that can connect cellular constituents and induce liver toxicity or injury (Guengerich, 2001). This gives PXR an essential study target in drug metabolism and drug-drug interactions (DDIs), leading to DILI. Both DILI and DDIs are the most common causes and manifestations of ADRs. DILI is prevalent,

and almost all groups of drugs can trigger liver disease, while DDIs occur via polypharmacy.

Most DILI cases are mild, and recover upon removing the drugs (Gallelli *et al.*, 2016). Polypharmacy raises the difficulty of therapeutic management and hence the possibility of clinically significant drug interactions that can cause the production of ADRs and thus decrease or increase therapeutic efficacy (Glintborg *et al.*, 2005). To prevent the progression of DILI and DDIs to chronic liver disease or liver failure, it is vital to identify and isolate the offending agent as soon as possible. As the acronym implies, DILI only pertained to the liver while DDIs affected other organs, including the liver. DDIs may therefore disrupt, decrease, or improve the absorption of either drug. They can minimise or enhance the activity of any drug, or both, and cause adverse effects (Johnell & Klarin, 2007). For example, both atorvastatin and lovastatin are CYP3A4 substrates, and danazol is a potent CYP3A4 inhibitor. When danazol and statins are administered together, danazol is likely to precipitate statin toxicity because of reduced metabolic clearances. And it would be reasonable for this reason to limit statin choice to pravastatin that is not metabolised by CYP3A4 (Johnell & Klarin, 2007). DILI may result from direct toxicity from the parent drug or its metabolites, or injury may result from immune-mediated mechanisms. Though these mechanisms are different, they can also be interconnected. For instance, the ensuing inflammatory reaction may further enhance the initial destruction of hepatocytes resulting from direct drug toxicity. It is also worth noting that oral drugs with significant hepatic metabolism are much more likely to lead to DILI (Lammert *et al.*, 2009).

CYPs play a crucial role in the formation of reactive metabolites of acetaminophen, with N-acetyl benzoquinone imine binding to liver proteins. And this might result in mitochondrial dysfunction or hepatic necrosis (Jaeschke *et al.*, 2012; Wolf, 2005). Previous studies have reported that activation of PXR up-regulated CYP3A and potentiated acetaminophen hepatotoxicity through CYP3A-mediated bioactivation of acetaminophen (Guo, 2004; Kanno *et al.*, 2015).

The PXR target genes were found to be the Phase II enzymes Uridine 5'-diphosphoglucuronosyltransferase (UGT) and S-transferase Glutathione (GST) (Andrew *et al.*, 2010; Li *et al.*, 2009; Maglich *et al.*, 2002). The enzymes facilitate drug conjugation reactions to improve their hydrophilicity (Cui & Klaassen, 2016). Activation of the phase II gene expression is therefore generally protective as it eliminates reactive metabolites. UGT is a cytosolic enzyme that facilitates glucuronic acid transfers to hydrophobic molecules, which are typically unreactive and easy to eliminate from the body to form more water-soluble glucuronide metabolites (Rowland *et al.*, 2013). Moreover, UGTs can alter the formation of acyl glucuronides in carboxylic acid, some of which are reactive and bind to deoxyribonucleic acid (DNA) or proteins, leading to drug toxicity (Mitsugi *et al.*, 2016; Shipkova *et al.*, 2003). The primary enzyme responsible for biotransformation of trovafloxacin, an antibiotic, that was withdrawn from the market due to its potential to induce idiosyncratic hepatotoxicity, is uridine diphosphate glucuronosyltransferase 1A1 (UGT1A1) (Fujiwara *et al.*, 2015).

Although UGT1A1 is a PXR target gene, PXR ligands can induce this enzyme to increase trovafloxacin's metabolism and eventually the production of reactive acyl glucuronides which might be damaging to the liver (Mitsugi *et al.*, 2016). *In vitro* studies have also shown that activation of PXR as well as knockout leads to hepatic steatosis. PXR knockdown has increased the aldo-etho-reductase 1B10, enhancing acetyl-CoA fatty acid synthesis in HepG2 cells and the primary human liver cells in a fatty acid synthesis that catalyses the conversion of acetyl-CoA to malonyl-CoA. PXR stimulation caused an increase in the sterol regulatory-binding element protein SREBP-1a, a transcription factor that controls lipogenesis (Porstmann *et al.*, 2008; Lewis *et al.*, 2011). In transgenic mice with the hPXR transgene and hPXR, both treated with rifampicin, PXR activation has been shown to promote lipid synthesis and fat accumulation in the liver (Zhou *et al.*, 2006).

Furthermore, the activation of PXR by penicillin in mice resulted in the inhibition of beta-oxygenated fatty acid and ketogenesis by inhibiting the binding by the A2 forkhead box protein to the 1a carnitine palmitoyltransferase promoter and mitochondrial 3-hydroxy-3-HMG-CoA-synthase-2 sequentially (Nakamura *et al.* 2007; Zhou *et al.*, 2006). A reduction in FAO increases the accumulation of fatty

acids and triglycerides in liver cells, contributing to steatosis. PXR activation thus promotes hepatic steatosis through de novo lipogenesis and reduces FAO. Co-administration with drugs stimulating hepatic steatosis of PXR ligands can, therefore, result in a higher risk of DILI (Allard *et al.*, 2019).

1.3.6 Peroxisome proliferator-activated receptors

Peroxisome proliferator-activated receptors (PPARs), which are divided into three subtypes (PPAR, PPAR γ , and PPAR α) (Figure 1-5), are a subfamily of the 48-member nuclear receptor superfamily. They control genes implicated in lipid as well as glucose homeostasis. They form a heterodimer with the co-activator complex and bind to the DNA sequence, the peroxisome proliferator response element (PPREs). In the absence of the ligands, these heterodimers are linked with the co-repressor complex, which inhibits gene transcription (Baran, 2014; Youssef & Badr, 2013). PPAR- α is relatively expressed in liver cells, vascular as well as immune cell types such as monocytes or macrophages endothelial cells, non-neuronal cells such as microglia and astroglia (Moreno *et al.*, 2004). PPAR- α plays a critical role in fatty acid oxidation and lipoprotein metabolism in the hepatocyte, which delivers energy to peripheral tissues. Furthermore, increased mitochondrial and peroxisomal fatty acid oxidation rates in tissues such as the liver, heart muscle, kidney, or brown adipose tissues may play a role in oxidant/antioxidant pathways, demonstrating anti-inflammatory effects (Moreno *et al.*, 2004). PPAR β/δ possesses the broadest tissues expression and is thoughtful of comprehensive biological activities (Youssef & Badr, 2013). PPAR β/δ is expressed in the majority tissues significantly in the skin, brain and adipose tissue and impact on energy homeostasis, cell proliferation, survival, or differentiation as well as wound healing. PPAR γ is localised mainly in the adipose tissue and has attracted significant scientific and clinical interest because of its critical role in adipocyte differentiation (adipogenesis) and energy conservation (lipogenesis) (Youssef & Badr, 2013).

PPAR γ is expressed practically in all tissues, including heart, muscle, colon, kidney, pancreas and spleen, which is expressed in macrophages, large intestine and white adipose tissue (Tyagi *et al.*, 2011). PPARs function as lipid sensors that convert the alterations in lipid concentration into anabolic activity. Various fatty acids serve as

endogenous ligands for PPARs in general, particularly the PPAR γ (Puhl *et al.*, 2012). Both PPAR α and PPAR β/δ are triggered by saturated and unsaturated fatty acids, while PPAR γ has an affinity for polyunsaturated fatty acids. In addition to their large number of endogenous ligands, PPARs are also the crucial targets of several groups of synthetic compounds owing to their enormous metabolic and therapeutic activities (Tyagi *et al.*, 2011). The thiazolidinediones are selective and potent agonists of PPAR γ with affinity values of between 40 and 200 nM (Feige *et al.*, 2006; Sheu *et al.*, 2005).

1.3.7 Mechanism of action of thiazolidinediones

The discovery of thiazolidinediones (TZDs) and a considerable measure of early development research were undertaken in Japan (Ciana *et al.*, 2007). Ciglitazone, the first drug, improved blood glucose regulation in animal models of insulin resistance. However, the exact mechanism of this action is poorly understood, and assessments in humans were stopped due to liver toxicity (Ciana *et al.*, 2007). New compounds with less toxicity in animals were subsequently established, and two significant results contributed to a rapid increase in our understanding of their mode of action (Ciana *et al.*, 2007; Mudaliar & Henry, 2001). TZDs are readily absorbed and, in a matter of hrs, hit peak plasma concentrations. The amount of TGZ being absorbed is equal to the amount of TGZ being cleared from the body when given repeatedly (steady-state). This is typically attained within the first week of administration. In combination with a substantial improvement in fat metabolism, insulin sensitivity increases, including a large decrease in circulating free fatty acids.

Nevertheless, the full impact of TZDs may take 4–12 weeks due to fat deposition; this is because blood flow to fat is much more impaired in obese people. This makes their fat a large compartment for possible lipophilic drug delivery, which eventually fills and becomes a slowly emptying reservoir (Pai, 2012). Rosiglitazone and pioglitazone are mostly protein-bound to albumin in circulation (Ciana *et al.*, 2007; Pai, 2012).

The process by which TZDs stimulate insulin response and the site at which this mechanism happens inside the body were imprecise until it was described that TZDs were high-affinity ligands for PPAR γ a ligand-dependent transcription factor and a

member of the nuclear receptor superfamily (Kubota *et al.*, 2006). TZDs decrease blood glucose concentration through the activation of PPAR γ (Kim *et al.*, 2004; Kubota *et al.*, 2006). However, it has been proposed that the primary site of TZDs action is the skeletal muscle. Still, as PPAR γ is mainly expressed in the adipose tissue, it cannot be disregarded that the insulin-sensitising mechanism could explain the adipocytes' direct effect (Cheng, 2005). PPAR plays a critical role in adipocyte differentiation as well as lipogenesis. Activation of PPAR γ by TZDs, therefore, increases fatty acid uptake and storage in the adipocytes, which causes an increase in adipose tissue mass, including body weight (Heikkinen *et al.*, 2007; Oakes *et al.*, 2001). Previous studies have reported that TZDs therapy boosts the number of small adipocytes as well as the subcutaneous adipose tissue mass through PPARs (Oakes *et al.*, 2001). Decreased circulatory free fatty acid concentrations have been shown to enhance insulin sensitivity of tissues such as the skeletal muscle, liver and pancreatic β -cells (Nakagawa & Medina, 2018; Oakes *et al.*, 2001; Yki-Järvinen, 2004).

On the other hand, high levels of free fatty acids produce toxic effects on these tissues and can lead to insulin resistance (Del Prato, 2009; Kusminski *et al.*, 2009). Improved liver sensitivity by TZDs towards insulin represses liver-glucose production, resulting in hypoglycaemia and hypoinsulinemia (Yki-Järvinen, 2004). Adipokines are specific sub-classes of cytokines that are secreted explicitly from adipose tissue. Altered adipokine release, including adiponectin, TNF α leptin or the 11 β -hydroxysteroid dehydrogenase 1, is another means through which insulin sensitivity is regulated. Low levels of circulatory adiponectin are strongly linked with the progression of insulin resistance. At the same time, the activation of PPAR γ by TZDs has been shown to increase plasma adiponectin concentrations markedly, augmenting insulin sensitivity, which explains the hypoglycaemic effects of the TZDs (Hamasaki, 2012; Parulkar *et al.*, 2001; Weyer *et al.*, 2001; Yamada *et al.*, 2016).

Besides these positive actions of PPAR γ ligands such as TZDs, they have been demonstrated to influence glycaemic regulation through suppressive means of action. The cytokine TNF α has been shown to reduce insulin-stimulated glucose uptake and is found in high levels in obese and insulin-resistant subjects (Hamasaki, 2012; TaheriChadorneshin *et al.*, 2019; Yamada *et al.*, 2016). Also, a few other

molecules have been demonstrated to fuel insulin resistance, including leptin, resistin, as well as 11 β -hydroxysteroid dehydrogenases 1. Inhibition of the expression of these molecules by PPAR γ ligands such as TZDs improves glycaemic regulation. However, it is poorly understood whether this is via an uninterrupted or trans-repressive mechanism (Yki-Järvinen, 2004). Various processes have been reported to support the insulin sensitising description of the TZDs group of PPAR γ agonists. Previous studies have also proposed these consequences for the other tissues (Kahn *et al.*, 2000; Mudaliar & Henry, 2001). The practical physiological implications of these drugs may be owed to a blend of these mechanisms.

However, type 2 diabetes is a complex metabolic condition involving glucose, lipid, and protein metabolism alterations (Kahn *et al.*, 2000; Mudaliar & Henry, 2001; Murphy, 2020). Kahn *et al.* showed that muscle-glucose uptake deficiency is mainly attributable to reactive hyperglycaemia after eating. Fasting glucose increases are attributable to a high hepatic glucose yield, and a mixture of fatty liver defects are due to lipid disturbances (Hamasaki, 2012; Kahn *et al.*, 2000). Recent studies in mice with insulin resistance to conditional gene knockout in individual tissues by Kahn and his group indicate that these classical views may have been excessively simplified (Kahn *et al.*, 2000). Thus, the muscle-specific insulin receptor deleted presented elevated plasma triglycerides and increased FFAs (Kahn *et al.*, 2000). Kahn *et al.* have speculated that adipocytes are a complex cell type that produces a number of signals such as cytokines, hormones, and growth factors that affect not only surrounding cells but also target tissues associated with energy metabolism and affect physiological processes (Kahn *et al.*, 2000).

Interestingly, most of these effects of PPAR γ re-stimulation are not found in visceral adipocytes. However, these cells have a large number of PPAR γ receptors (Kahn *et al.*, 2000). Also, visceral adipocytes are, to some extent, metabolically distinct from peripheral adipocytes; for instance, they are less responsive to insulin and more responsive to catecholamines (Gurnell *et al.*, 2003). Accumulation of fatty acids in subcutaneous adipocytes leads to a lipid steal phenomenon that leads to lower circulating fatty acids and minimal levels of triglycerides in muscle as well as the liver. However, close to 80% of insulin-stimulated glucose reduction takes place in

skeletal muscles in healthy humans, which is a significant source of insulin resistance in type 2 diabetes (Ciana *et al.*, 2007).

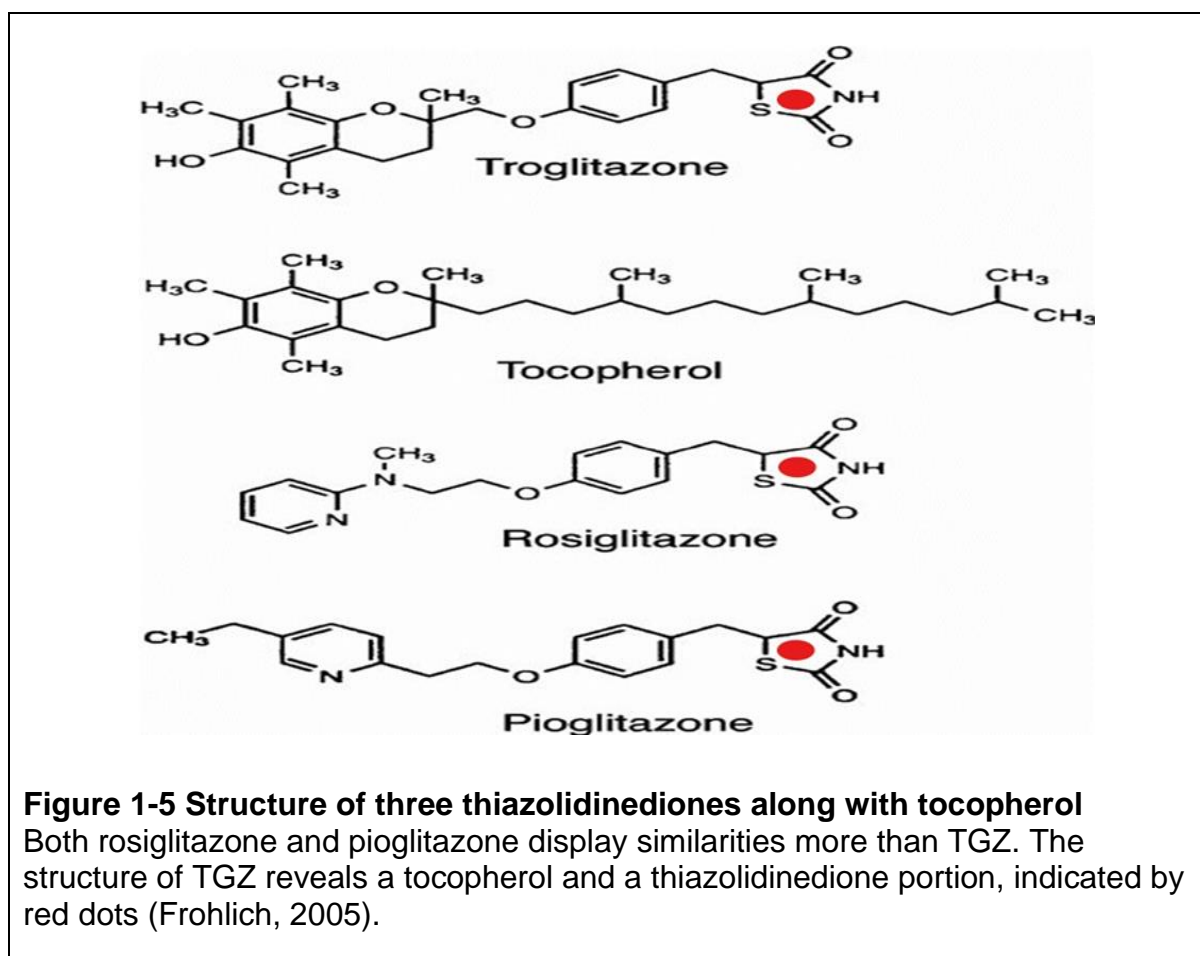
All the members of TZDs possess the thiazolidine-2,4-dione structure, from which the group conveys its name, which is a thiazole containing two keto-oxygen (Figure 1.5). TZDs vary from each other in their side chains, which modify the pharmacodynamics and pharmacokinetic effects of the individual TZDs (Frohlich, 2005). The major TZDs are troglitazone (TGZ), rosiglitazone, and pioglitazone. For this current study, the features, and the mechanism of action of TGZ will be discussed in the next sections (sections 1.3.7.1 and 1.3.7.2). TGZ was withdrawn while pioglitazone and rosiglitazone were not withdrawn as there had been significant pressure on their use. TGZ caused rare but significant liver toxicity and was removed from the market. In all probability, the vitamin E-like constituent of the molecule has been associated with TDZ-induced hepatic toxicity. Hepatotoxicity does not seem to be linked to the other two but requires routine LFT (Mudaliar & Henry, 2001; Ciana *et al.*, 2007).

In general, TZDs are new drugs for the management of type 2 diabetes. TZDs, or glitazones, are a group of oral antidiabetic agents used to treat type 2 diabetes mellitus. They improve blood glucose levels in diabetics via a unique mechanism. Their blood glucose-reducing impact is facilitated by enhancing insulin sensitivity, and for this reason, they are called insulin sensitisers. TZDs exert their blood glucose-lowering effects through a mechanism that involves the activation of PPAR γ and includes the relocation of excess fatty acids to peripheral fat. The other aspect of their action is adipokine secretion modification (Bradley, 2002; Charbonnel, 2007; Kim, 2004; Scheen, 2004).

1.3.7.1 Features of TGZ

TGZ was developed by Daiichi Sankyo (Japan) by the amalgamation of ciglitazone with a substructure of the α -tocopherol molecule with the clinical objective of merging hypoglycaemia effects with the capacity to block lipid peroxidation into a single pharmaceutical molecule (Parker, 2002). TGZ was the first thiazolidinedione that was launched and sold in the USA in the late 1990s. Under the brand name rezulin it was produced by Warner-Lambert Group, and in Europe, it was marketed as

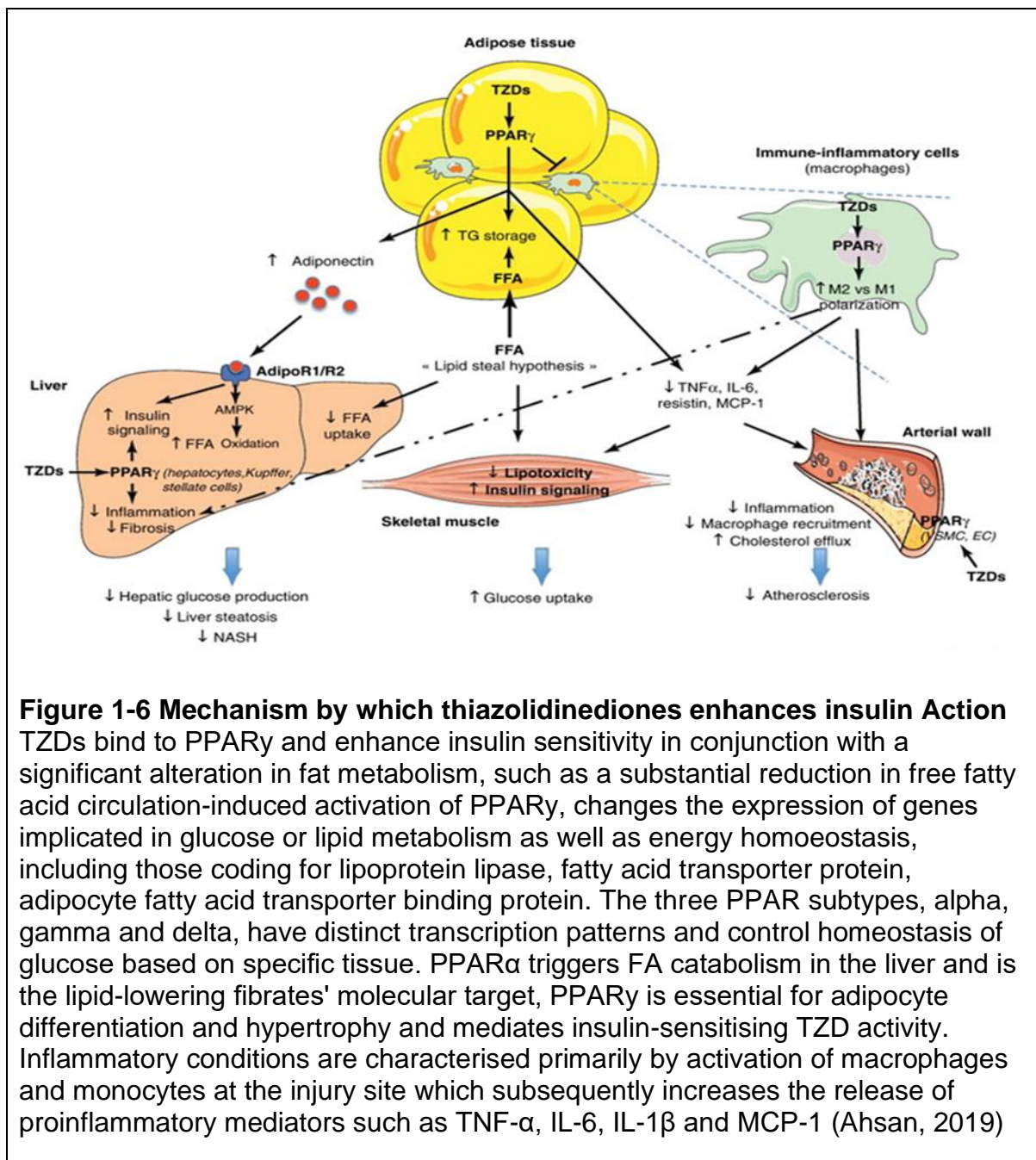
romozin. Clinicians hailed the use of TGZ for the management of type 2 diabetes. The US marketer alone made more than \$2 billion. However, not less than 90 cases of idiosyncratic liver failure resulted in death or liver transplantation. TGZ was withdrawn from the USA market in March 2000, having already been discontinued the sales in the UK three years based on the undesirable consequences (Chojkier, 2005; Wilkinson *et al.*, 2004).



1.3.7.2 Mechanism of action of TGZ

TGZ was the first member of the family of TZDs oral antidiabetic agents. Unlike sulfonylureas, it does not cause insulin secretion, with its mechanism of action reliant on residual insulin. Instead, it promotes insulin sensitivity to the muscle as well as the adipose tissue (Aroda & Ratner, 2012; Kennedy, 2006). TGZ molecules contain a chroman ring moiety like that of vitamin E, exhibiting antioxidant properties

attached to the thiazolidinedione (Smith, 2003). Although understanding its mechanisms of action is marginally developed, TZD is a potent agonist for the nuclear receptor PPAR γ . As discussed in the previous section, PPAR binds to the retinoid X receptor (RXR) to produce a heterodimer. Upon TZD binding, there is a conformational modification in the PPAR γ -RXR complex. As a consequence, a co-repressor is dislocated, which allows for binding to PPAR γ response elements and continuous stimulation of DNA sequences that regulate the expression of genes implicated in lipid metabolism as a consequence of simulating the action of insulin (Bai *et al.*, 2007; Hubbard, 2013; Madsen *et al.*, 2008; Park *et al.*, 2005; Parker, 2002; Rogue *et al.*, 2011; Youn *et al.*, 2008). TZD appeared to have multiple advantages in the control of hyperglycaemia in type 2 diabetes. However, TZD was used together with other antidiabetic agents such as the biguanides or human-made insulin to control hyperglycaemia (Aroda & Ratner, 2012; Kennedy, 2006). Furthermore, TZD was found to play a role in the regulation of plasma triglyceride levels by promoting circulating fatty acid utilisation in the peripheral adipocytes (Park *et al.*, 2005). Okuda *et al.* suggested that this mechanism may lead to a reduction in circulating fatty acids and lipids in the liver or the muscle and may subsequently decrease lipid circulation, leading to a decrease in triglycerides in the skeletal muscles (Figure 1-6).



1.3.7.3 Bioavailability

TGZ was commonly administered orally, with an estimated bioavailability of 40% to 50%, but other factors such as food increased absorption by 35% to 80%. An earlier study reported that the peak plasma concentration in subjects administered TGZ at therapeutic doses of 400 and 600 mg/day was 3.6 μ M and 6.3 μ M, respectively (Ito *et al.*, 2020). A study conducted previously reported that the mean half-life removal ranges from 7.6 to 24 hrs, promoting a once-daily dose routine. The

pharmacokinetics of TGZ are identical between type 2 diabetes patients and nondiabetic individuals (Ito *et al.*, 2020).

1.4 Drug metabolism and metabolic detoxification

Drugs are needed to correct physiological conditions. However, they are alien (xenobiotics) to the body. The human body attempts to remove them earliest because the body detects them as foreign (Coleman, 2010). Drugs must be removed from the body directly after their therapeutic effects are achieved. The longer the drugs stay in the body, the greater their side effects (Coleman, 2010; Omiecinski, 2010). As mentioned in the previous section, drug metabolism promotes this natural tendency to remove xenobiotics from the human body. Drug metabolism may produce pharmacologically active, inactive, or toxic metabolites. For instance, drug metabolism comprises two phases (Phase I and Phase II), the occurrence of which may differ from compound to compound. For instance, the biotransformation of acetaminophen (APA) occurs through both phases (Figure 1-7) as indicated in the previous section and will be discussed in sections (1.4.1.1 and 1.4.1.2). As stated in the previous section, the liver is the primary, but not the only, site for biotransformation of xenobiotics (Coleman, 2010). The smooth endoplasmic reticulum contains many varieties of enzymes, which makes it an ideal site for drug metabolism. Although there are other sites such as the kidney, lungs, epithelial cells of the gastrointestinal tract as well as the skin for drug metabolism, these sites are involved in about 30%, that is, to a limited extent, in drug metabolism as compared to about 70% of most of the drugs that undergo biotransformation in the liver (Coleman, 2010; Omiecinski, 2010). The liver contains enzymes that facilitate chemical reactions such as xenobiotics (phase I). It has other enzymes that bind substances to xenobiotics and produce reactions called conjugations (phase II) (Coleman, 2010; Omiecinski, 2010).

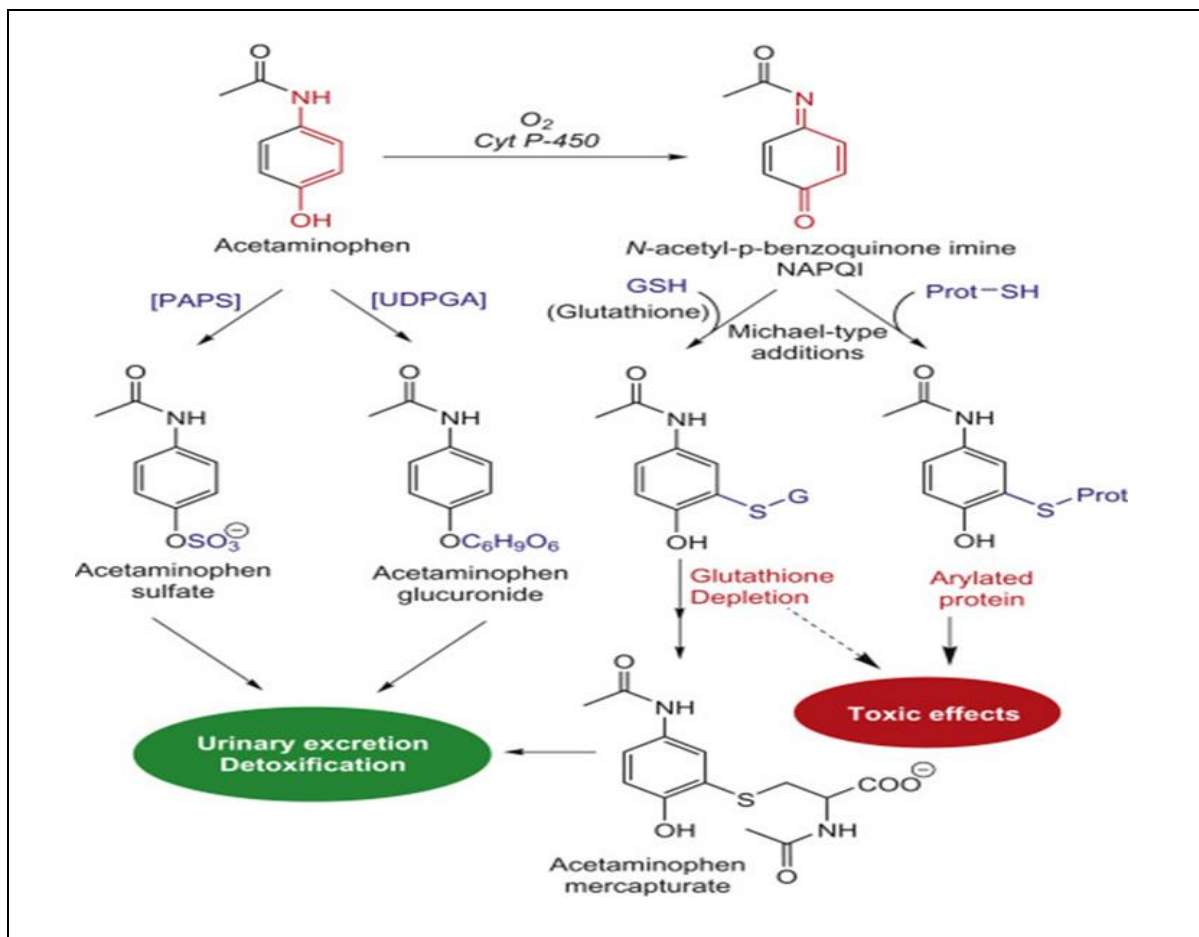


Figure 1-7 Phase I and Phase II metabolism of APA

APAP is commonly metabolised in the liver by the Cytochrome P450 enzyme system into the reactive metabolite called N-acetyl-p-benzo-quinone imine (NAPQI) (phase I). Still, about 80–90% is metabolised by the phase II metabolic route (glucuronidation and sulphation) in which the APAP-reduced glutathione (GSH) conjugate is facilitated by UDP-glucuronosyl transferases (UGT) and sulphotransferase (SULT), into non-toxic compounds: glucuronidated and sulphated metabolites, which are expelled through urine. Accumulation of NAPQI metabolite may result in lipid peroxidation and protein adduct formation, resulting in ATP depletion and necrotic cell death (Macherey & Dansette, 2015).

1.4.1.1 Phase I metabolism

The cytochrome P450 (CYP) enzymes are membrane-bound proteins, located in the smooth endoplasmic reticulum of the liver as well as other tissues. The CYPs are the essential enzymes for the phase I metabolism of xenobiotics (Table 1-2). The CYPs contain a haem group, and the haem group is the iron-porphyrin unit (Gibson & Skett, 2013; Rang *et al.*, 2011). The haem centre is the site for the CYPs and it is

responsible for the reaction of hydrophobic compounds to more polar products for elimination from the body. The iron in the reduced state can attach to carbon monoxide to form a carbon monoxide-bound CYP complex. The complex formed exhibits spectrophotometric absorbance at 450 nm and is thus called CYP450. Drug metabolism is grouped into two phases called Phase I (functionality) and Phase II (conjugation), and these will be discussed in the next sections (Omiecinski, 2010).

Phase I reactions may include oxidation, reduction, and hydrolysis and are carried out in the liver with the involvement of CYP450, Flavin-containing monooxygenase (FMO), mammalian carboxylesterases (CEs), etc. In phase I, biotransformation, a polar group is either introduced or unmasked when present. Most of the products in phase I are not directly excreted and, as such, undergo Phase II reactions (Gibson & Skett, 2013). Examples of drugs that may undergo biotransformation via phase I oxidation are acetanilide (analgesic) and valproic acid (antiepileptic). These reactions may occur at several functional groups, such as carbonyl or hydroxyl. Hydrolysis reactions also fall under phase I metabolism (Gibson & Skett, 2013). These reactions generally involve considerable chemical alteration of the substrate. For instance, upon hydrolysis, esters lead to the formation of carboxylic acids as well as alcohols. In general, esters are ingested as prodrugs but are converted to their active form through hydrolysis, for instance, aspirin (Gibson & Skett, 2013).

1.4.1.2 Phase II metabolism

The phase II reactions follow phase I biotransformation and mostly occur in the products derived from the phase I reactions (Gibson & Skett, 2013). As described in the previous section, phase I reactions act to increase the bioactivation of drugs, which results in an increased potential for toxicity. The addition of hydrophilic groups to the original molecule, a toxic intermediate, or a nontoxic metabolite formed in phase I that necessitates further transformation to optimise its polarity defines phase II reactions. Conjugation, glucuronidation, acetylation, and sulphation (for example, the activation of estragole) are examples of these reactions. (Gibson & Skett, 2013; Rang *et al.*, 2012). Rang *et al.* have reported that transferases are the main enzymes that facilitate phase II metabolism because they speed up the transfer of a moiety from a donor molecule to the drug recipient. Hydroxyl group (-OH) containing

drugs, carboxyl (-COOH), amino (-NH₂), as well as sulfhydryl (-SH) functional groups may undergo glucuronidation reactions with sugar by-products, prevalently, UDP-glucuronic acid. Glucuronidation is catalysed by the enzyme UDP-glucuronosyltransferase (UGTs). In some instances, the biotransformation process may result in the production of a reactive metabolite, which in some instances, may lead to toxicity. Toxicity may vary from genotoxicity to immune-mediated adverse drug reactions. The organ that is commonly affected by adverse drug reactions is the liver, as it is responsible for most of the metabolic reactions (Kalgutkar *et al.*, 2012; Rang *et al.*, 2012). Reactive metabolites are called reactive chemical metabolites because they contain a chemically reactive group that can provoke adverse drug reactions. It has been speculated that TGZ undergoes phase II metabolism to produce reactive metabolites (Table 1-2) (Kalgutkar *et al.*, 2012).

Table 1-2 Reactions categorised as phase I or phase II metabolism

Phase I	Phase II
Non-synthetic or non-conjugative	The synthetic reaction involves conjugation
Oxidation through cytochrome P450, reduction and hydrolysis reactions	Glucuronidation, acetylation and sulphation
Converts a parent drug to more polar active metabolites by unmasking or inserting a polar group (-OH, -SH, -NH ₂)	Converts a parent drug to more polar inactive metabolites via conjugation of subgroups to OH-, -SH, -NH ₂ functional groups on drugs.
Mainly microsomal (endoplasmic reticulum)	Occurs in the mitochondrial and the cytoplasm
The polar metabolites may be directly excreted, usually in the urine, or may be converted further by phase II reactions.	Drugs metabolized via phase II reactions(conjugates) water-soluble and are renally excreted
Produces active metabolites	Produces inactive metabolites

1.4.2 Metabolism of TGZ

TGZ is metabolised in both humans and animals by sulphation and glucuronidation as well as oxidative chromane ring-opening to a quinone metabolite (Figure 1-8) (Kassahun *et al.*, 2001). Sulphation accounts for about 70% of the metabolites detected in human plasma, and this makes the sulphation route the significant metabolic route of TGZ (Kassahun *et al.*, 2001; Smith, 2003). Both sulphates and glucuronide metabolites are excreted into the bile and, as a result, the main route of excretion is faecal (Smith, 2003). TGZ-sulphation is facilitated by a phenol

sulfotransferase (SULT1A3) (Honma, 2002). TGZ-sulphate is circulated from the liver to the bile, enters the small intestine, is absorbed by the enterocytes and transported back to the liver (enterohepatic circulation), leading to a prolonged half-life (Smith, 2003). As described above, the chromane ring in the TGZ molecule can undergo oxidation to form a quinone metabolite, a process metabolised mainly by CYP3A4 (Smith, 2003; Yokoi, 2011). The quinone structure allows it to undergo redox cycling to produce ROS that can cause cellular damage, for instance, lipid peroxidation or protein oxidation. An electron reduction of quinone molecules provides a semi-quinone or hydroquinone which can be oxidised by molecular oxygen to produce the parent quinone, which in turn generates superoxide in the process (Ryter *et al.*, 2007). The parent quinone may cycle again to foster a persistent generation of superoxide and, consequently, secondary ROS in the form of hydrogen peroxide as well as hydroxyl radicals (Bolton & Dunlap, 2016).

Furthermore, TGZ quinone can undergo epoxidation to produce a quinone epoxide or reduce to a hydroquinone form, which is exposed to further breakdown and elimination as sulphate or glucuronide conjugates (Smith, 2003; Yamamoto, 2002). Despite a lack of strong evidence in the literature, this reductive biotransformation is thought to be aided by NAD(P)H, and thus quinone oxidoreductase 1 (NQO1) (Smith, 2003; Yamamoto, 2002). TGZ has been reported to induce CYP3A4 at physiological doses in human and rat liver cells, which led to the suggestion that TGZ exposure could provoke the formation of the quinone metabolites (Lee *et al.*, 2009; Smith, 2003; Yokoi, 2011). However, Yamazaki *et al.* have reported that TGZ is a blocker of cytochrome P450s, for instance, CYP2C8 as well as CYP2C9 and, to a certain level, CYP2C19 and CYP3A4. On the other hand, TGZ does not block any major cytochrome P450 enzymes at therapeutic levels (Kassahun *et al.*, 2001; Yamazaki *et al.*, 2000).

TGZ sulphate and quinone formation form major pathways in contrast to TGZ conjugation to a glucuronide. Plasma levels of TGZ glucuronide are insignificant (Kassahun *et al.*, 2001). Watanabe *et al.* found that the glucuronidation of TGZ in the human intestine is over twofold higher than in the liver, with the reaction in the liver facilitated by UGT1A1. In contrast, in the intestine, it is facilitated by UGT1A8 as well as UGT1A10. TGZ-glucuronide is excreted in the bile and may circulate through the

enterohepatic system (Smith, 2003). Previous studies in normal and diabetic subjects showed insignificant differences in TGZ biotransformation. These indicate that diabetic subjects are not generally metabolically susceptible to TGZ toxicity (Depeint *et al.*, 2006). Nonetheless, Ott *et al.* have reported that subjects with hepatic malfunction recorded high plasma levels of TGZ, TGZ-sulphate, and TGZ-quinone compared with healthy subjects, which was in harmony with the known changes that would occur in a subject with compromised hepatic function.

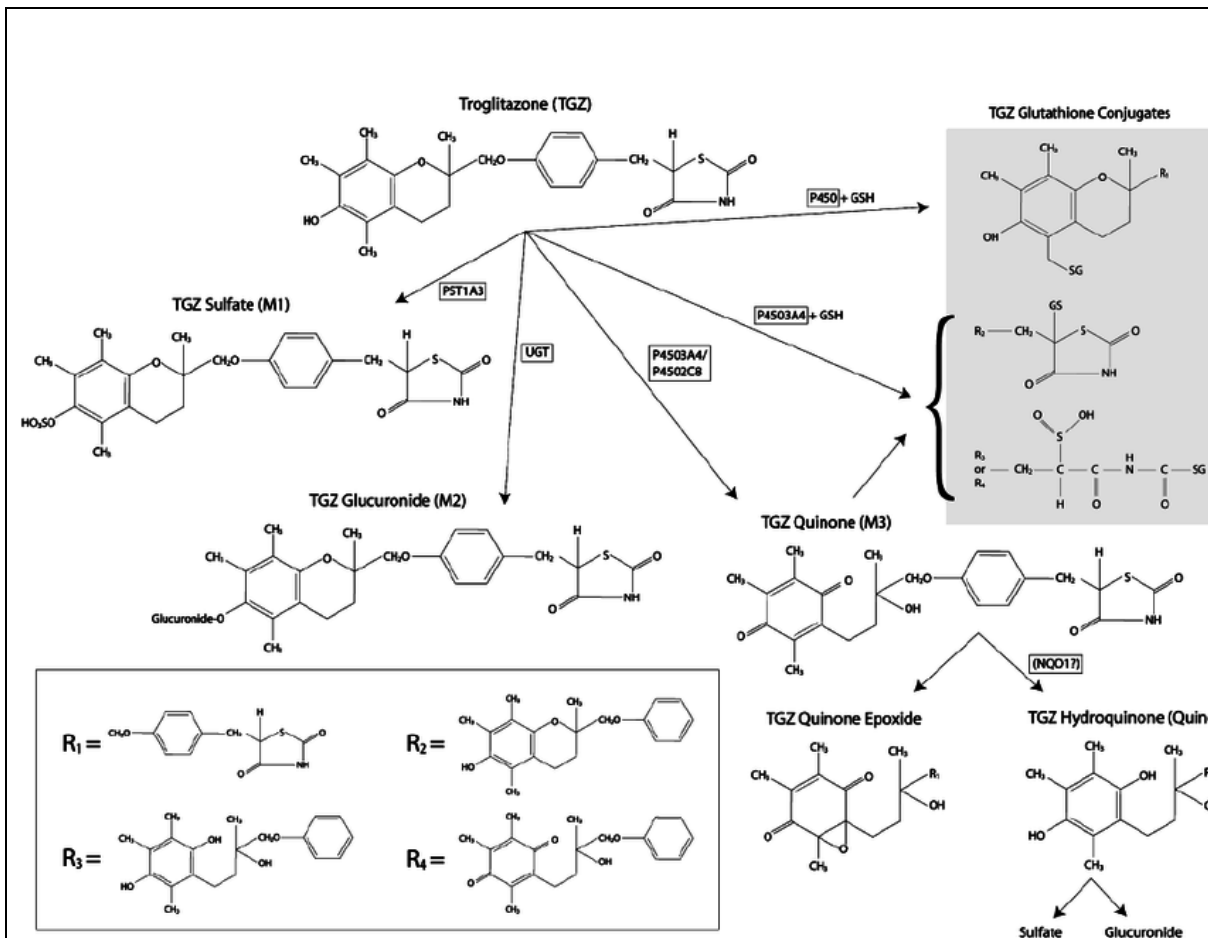


Figure 1-8 Primary metabolic pathways of TGZ

TGZ is metabolised into TGZ-sulphate, TGZ-glucuronide and TGZ-quinone. TGZ-quinone can undergo epoxidation to form troglitazone quinone epoxide or be reduced to TGZ- hydroquinone, which is then sulphated or glucuronidated. The formation of GSH conjugates accounts for the function of metabolic activation pathways for TGZ, which includes oxidation of the substituted chromane ring system to a reactive o-quinone methide derivative. TGZ may covalently alter hepatic proteins and trigger oxidative stress via redox cycling processes, either of which may contribute to DILI. TGZ can also be biotransformed into reactive metabolites, which are then removed through glutathione (GSH) conjugation. Major enzymes: PST1A3: Phenol sulphotransferase 1A3 (SULT1A3); UGT: UDP-glucanoyltransferase; P450: Cytochrome P450; P4503A4: Cytochrome P450 3A4 (CYP3A4); P4502C8: Cytochrome P450 2C8 (CYP2C8); NQO1: NAD(P)H: quinone oxidoreductase 1 (Smith, 2003).

1.4.3 The effect of TGZ on quinone formation and oxidative stress

As discussed in the previous section, TGZ may be oxidised to form a quinone and may undergo a further reaction to form an unstable quinol *in vivo* (He *et al.*, 2001; Smith, 2003). The quinol can be further processed through glucuronidation, as demonstrated by Tettey and his group, who conducted *in vivo* studies in rats treated with TGZ and isolated quinol glucuronide. Previous studies have also reported that CYP2C8 and CYP3A4 are the key enzymes responsible for TGZ-quinone formation (He *et al.*, 2001; Kassahun *et al.*, 2001). However, CYP3A4-mediated TGZ-quinone has been postulated to be the critical metabolic feature underlying TGZ-induced hepatotoxicity (He *et al.*, 2001; Gan *et al.*, 2008; Kassahun *et al.*, 2001; Tettey *et al.*, 2001). Quinones are conventional cytotoxic compounds with a unique structure that enables them to go through redox cycling to produce ROS, which can trigger cellular damage, for instance, lipid peroxidation and protein oxidation (He *et al.*, 2001; Kassahun *et al.*, 2001). The one-electron reduction of a quinone molecule produces a semi-quinone radical species, which then undergoes oxidation by molecular oxygen, redeveloping the parent quinone and creating a superoxide molecule in the course of action. The parent quinone is liberated for recycling, resulting in the constant production of superoxide as well as, subsequently, secondary ROS in the shape of hydrogen peroxide along with hydroxyl radical (Tettey *et al.*, 2001).

In humans, CYP3A4 accounts for the development of quinone metabolites as it facilitates the generation of the quinone component from the chromane ring structure, generating more electrophilic intermediates such as α -ketoisocyanate and sulphenic acid, which can initiate toxicity (Smith, 2003; Yokoi, 2011). TGZ contains a chromane ring of tocopherol moiety, which provides antioxidant properties that can counteract ROS. Therefore, the *in vitro* discovery of ROS makes it challenging to understand the exact properties of TGZ. Nonetheless, it is assumed that the antioxidant activities of TGZ can be consumed, and toxicity is provoked by simple mechanisms related to those of acetaminophen. Also, Yamamoto *et al.* have reported that the parent compound was more toxic than the quinone metabolite in HepG2 cells. Other studies supported their findings and suggested that the parent drug instead of the reactive metabolite causes TGZ-induced cytotoxicity (Tettey *et al.*, 2001; Tirmenstein *et al.*, 2002; Lee *et al.*, 2009). However, other evidence

supports the theory that cytotoxicity occurs due to the direct formation of ROS, implying a limited role of quinone metabolites in toxicity. Okuda *et al.* have suggested that TGZ-induced ROS production could be consequential to mitochondrial permeability pore opening as well as mitochondrial damage, not by a direct mechanism of injury but by after-effect. Although other studies have reported that the formation of TGZ-reactive metabolites plays a role in TGZ-mediated toxicity, it remains divisive. Studies in NIS1 rat liver cells treated with 5 μM TGZ and above could provoke oxidative stress (Narayanan *et al.*, 2003). A build-up of superoxide concentration was associated with modifications to mitochondrial membrane potential and membrane peroxidation. And it is understood that this is caused by the formation of quinone moieties. However, there is a possible mechanism postulated that explains the development of oxidative stress. Besides, Hewitt *et al.* reported that there was no link between phase I (CYP1A2, 2A6, 2C9, 3A4) and phase II sulphation and glucuronidation (SULT and UGT) metabolising enzyme concentrations with TGZ cytotoxicity in human liver cells. However, they recorded a negative association between TGZ cytotoxicity and the entirety of CYP3A4 and UGT reactions regarding phenol SULT activities. Their observations led to the postulation that TGZ and TGZ-sulphate are direct toxicants of TGZ. Simultaneously, oxidation through CYP3A4 and glucuronidation form part of the detoxification pathway (Hewitt *et al.*, 2002).

In contrast, oxidation through CYP3A4 as well as glucuronidation form part of the detoxification pathway (Hewitt *et al.*, 2002). Also, Depeint *et al.* investigated the effects of TGZ on human and porcine liver cells. Porcine liver cells lack sulphation capacity and are more resilient to TGZ toxicity than human liver cells. It has been reported that after two hrs of treatment with 25 μM of TGZ, they recorded a permanent inhibition of protein synthesis, whereas 50 μM TGZ caused cell death in human liver cells. On the contrary, at 50 μM TGZ treatment, protein synthesis was reversible in porcine liver cells, but 100 μM TGZ caused cytotoxicity. The resistance to toxicity exhibited by the porcine liver cells was attributed to the compensation of sulphation with glucuronidation (Depeint *et al.*, 2006).

Conversely, they reported that human liver cells treated with both TGZ and sulphation blockers such as 2,4-nitrophenol, did not reduce the cytotoxicity. Still, the

formation of TGZ-sulphate was decreased by over 80%, but they did not record any effects on the quinone metabolite production. However, they did observe a 4-fold increase in unmetabolised TGZ. HepG2 and rat liver cells exposed to TGZ-sulphate had a negligible cytotoxic effect; similarly, HepG2 cells exposed to glucuronide had no cytotoxic effect (Yamamoto *et al.*, 2001; Haskin *et al.*, 2001). However, treatment with TGZ-quinone did cause significant cell death in both HepG2 and rat liver cells, but it was less cytotoxic than the parent TGZ (Chojkier, 2005; Tettey *et al.*, 2001; Yamamoto *et al.*, 2002). All previous studies support the idea that TGZ is more cytotoxic than its primary metabolites (TGZ, TGZ-sulphate, TGZ-quinone, and TGZ-quinone glucuronide) but do not support any specific toxicity mechanism directly. This has resulted in speculation that toxicity induced by TGZ may account for other biotransformation pathways. Yamamoto *et al.* again noted that inhibitors of the main drug-metabolising enzymes responsible for TGZ metabolism, ketoconazole, a CYP3A4 inhibitor and a CYP2C8 inhibitor, quercetin, did not rescue HepG2 cells from TGZ-induced cell death, suggesting that cytochrome P450 metabolism is not imperative for TGZ toxicity (Yamamoto *et al.*, 2002). Conversely, the HepG2 cell line expresses low levels of drug-metabolising enzymes. Hence, a careful interpretation of cytotoxicity data should be carried out so as not to make positive or negative false inferences (Yokoi, 2011). Contrary to the reports by Yokoi (2011), HepG2 cells transfected with CYP3A4 and co-treated with ketoconazole, a CYP3A4 inhibitor, rescued the cells from TGZ toxicity, indicating that enhanced toxicity is facilitated by CYP3A4-dependent reactive metabolites (Vignati *et al.*, 2005). However, Masubachi (2006) suggested that the discrepancy in metabolism-related toxicity may result from the other cytotoxic metabolites produced by CYP3A4 but not those resulting from TGZ-quinone. The involvement of these metabolites in the general toxicity is relatively low because they will not cause a build-up in the cells and become inadequate to apply their toxic effects.

1.4.4 From authorization to the removal of TGZ from the market

TGZ was developed by Daiichi Sankyo (Japan) by the amalgamation of ciglitazone with a substructure of the α -tocopherol molecule with the clinical objective of merging hypoglycaemic effects with the capacity to block lipid peroxidation into a single pharmaceutical molecule (Parker, 2002; Jaeschke, 2007). TGZ was the first

thiazolidinedione launched and sold in the USA in the late 1990s, under the brand name Rezulin, produced by Warner-Lambert group and in Europe. Clinicians hailed the use of TGZ for the management of type 2 diabetes. The USA marketer alone made more than \$2 billion. During clinical trials, it was shown that TGZ caused a 3-fold increase in serum ALT levels in about 1.9% of the 2510 subjects put on TGZ (Bailey, 2000). Aside from this indication of liver toxicity, TGZ was approved in 1997.

ALT levels were detected in early clinical trials of TGZ. During the combined TGZ trials in the United States, 2 510 patients were given the drug, with 1 134 receiving it for at least six months and 475 receiving a placebo. In 50 of the TGZ-treated patients, serum ALT levels were three times higher than the upper limit of normal, compared to 0.6% in the placebo group (Jaeschke, 2007; Scheen, 2001). Treatment was discontinued in 0.8% of TGZ-treated patients but not in any placebo-treated patients due to increased ALT. Twelve of the 20 patients had peak serum ALT concentrations that were more than ten times the upper limit of normal, and five had concentrations that were more than 20 times the upper limit of normal (Scheen, 2001). Researchers found significant hepatocellular injury in 18 of these patients. A liver biopsy performed on two of these patients revealed evidence of a hepatocellular drug reaction, and two other patients had additional cholestatic symptoms (Chojkier, 2005; Ikeda, 2011; Jaeschke, 2007; Scheen, 2001). The majority of patients with ALT levels greater than three times the upper limit of normal did not exhibit symptoms of liver dysfunction and were thus observed only through monitoring during clinical trials. The peak values occurred between the third and seventh months in many patients, and serum ALT concentrations were restored to baseline in the 20 patients whose treatment was halted. ALT values also returned to baseline, indicating that in some patients, the liver can adapt to injury caused by TGZ without experiencing symptoms of liver dysfunction, which were only observed through monitoring during the clinical trials (Graham *et al.*, 2003; Jaeschke, 2007; Scheen, 2001). Also, the FDA received 560 reports of TGZ-related hepatotoxicity in 1998, as well as 43 cases of acute liver failure. Nine of these patients received liver transplants, and the remaining 28 died. Jaundice was prevalent in 498 patients at the time of assessment, and it was the first symptom in 62% of cases. Histological profiles from several of the patients revealed a repeated pattern of hepatocellular

necrosis with bridging necrosis, then fibrosis, or collapse. Elevation of ALT was common in Japan within 2 to 5 months of beginning troglitazone therapy. When the drug was stopped, ALT levels dropped quickly, usually to less than half of the peak level in 4 weeks. Surprisingly, total bilirubin levels at the time of TGZ discontinuation may be a prognostic factor. An investigation into the side effects of troglitazone by Japan's Ministry of Health and Welfare revealed 110 cases of liver damage (Jaeschke, 2007; Scheen, 2001).

1.4.5 Proposed mechanism of TGZ-induced liver toxicity

As the mechanism of TGZ liver toxicity is marginally understood, several different possible mechanisms have been postulated. It was initially proposed that TGZ is mainly metabolised into sulphate and glucuronide conjugates (Narayanan *et al.*, 2003; Smith, 2003). The oxidative reaction TGZ undergoes phase I reaction via oxidation by cytochrome P450 (CYP) enzymes, especially CYP3A4 and CYP2C8 enzymes, to generate a reactive electrophilic open ring intermediate. The reactive intermediate is fused with GSH in a reaction facilitated by the enzyme GST, producing a non-toxic metabolite that can easily be excreted.

Nonetheless, it has been postulated that the build-up of the electrophilic open ring intermediate could deplete cellular GSH levels, allowing reactive metabolites to covalently bind with cellular macromolecules, causing toxicity (Narayanan *et al.*, 2003; Smith, 2003). There are other possible mechanisms of TGZ-induced liver toxicity. Another theory associates the transformations that occur during the clearance of TGZ from hepatocytes via a metabolic conjugation as a possible mechanism of TGZ-induced hepatotoxicity (Julie *et al.*, 2008).

Previous studies have reported that TGZ could trigger liver toxicity via inhibition of the bile salt export pump, leading to cholestasis, mitochondrial dysfunction leading to cell death as well as genetic susceptibility such as single nucleotide polymorphism in genes involved in the metabolism and transport of TGZ (Fong & Contreras, 2009; Graham *et al.*, 2003; Jaeschke, 2007; Kassahun *et al.*, 2001; Madsen *et al.*, 2008; Meechan *et al.*, 2006). An alternative mechanism involves TGZ-mediated damage to the mitochondria, either directly or through the action of the aforementioned reactive species (Masubuchi *et al.*, 2006). It should also be noted that TGZ toxicity is affected

by several individual factors that lead to the accumulation of the drug in the liver. The above mechanism can occur due to reduced clearance in subjects with impaired liver function, or polymorphisms of SULT1A3 are seen in the human population, which affect the level of enzymatic reactions in liver cells. Variation in SULT1A3 would lead to variation in the conversion rate of TGZ to TGZ-sulphate between subjects, which may result in a build-up of either the parent compound or its primary metabolite in the body (Funk *et al.*, 2001; Snow & Mosley, 2007).

As the mechanism of TGZ liver toxicity is marginally understood, several different possible mechanisms have been postulated. It was initially proposed that TGZ is mainly metabolised into sulphate and glucuronide conjugates (Narayanan *et al.*, 2003; Smith, 2003). The oxidative reaction TGZ undergoes phase I reaction via oxidation by cytochrome P450 (CYP) enzymes, especially CYP3A4 and CYP2C8 enzymes, to generate a reactive electrophilic open ring intermediate. The reactive intermediate is fused with GSH in a reaction facilitated by the enzyme GST, producing a non-toxic metabolite that can easily be excreted.

Nonetheless, a lymphocyte transformation test that measures the proliferation of T cells to a drug *in vitro* of drug-specific T-cells has been demonstrated to contribute to IDILI in some subjects. Immune reactions occur in many different types of cells in many different locations, and they develop over time (Underhill & Khetani, 2018). A probable chain of events leading to idiosyncratic drug-induced liver injury (IDILI), for instance, begins with the development of reactive metabolites in hepatocytes, which results in drug-modified proteins and the discharge of danger-associated molecular pattern molecules (DAMPs) from hepatocytes (Underhill & Khetani, 2018). DAMPs activate antigen-presenting cells that have absorbed drug-modified proteins (Underhill & Khetani, 2018).

DAMPs activate antigen-presenting cells that have ingested drug-modified proteins. The antigen-presenting cells move to lymph nodes and the spleen, which are specifically designed to provide optimal conditions for communication between the antigen-presenting cells and the few T cells that recognise specific drug-modified hepatic proteins (Underhill & Khetani, 2018). Under the impact of chemokines discharged by hepatocytes and activated macrophages, activated T cells, both

helper T cells and cytotoxic T cells, return to the liver and mediate liver injury (Underhill & Khetani, 2018). These events also activate other cells, such as T regulatory cells, which normally protect the liver from severe damage. The mechanism is most likely more challenging. Although this sequence of events cannot be replicated *in vitro*, some aspects of the IDILI mechanism may be able to be replicated *in vitro*. However, deducing the mechanism of IDILI from *in vitro* studies would be inappropriate unless the predictions from the *in vitro* studies were consistent with the characteristics of IDILI in patients (Underhill & Khetani, 2018).

A positive lymphocyte transformation test is frequently linked to IDILI. This is not always the case, and it appears to be drug-related (Whritenour *et al.*, 2017). Antidrug antibodies and/or autoantibodies are another possibility. Because such studies are difficult to conduct, they have been avoided in most cases. These characteristics strongly suggest that the majority of IDILI is immune-mediated. As a result, mechanistic research should focus on testing the immune hypothesis, with additional studies to elucidate the steps leading to the induction and resolution of immune responses to the drugs involved (Whritenour *et al.*, 2017).

1.4.5.1 The mitochondria as the primary organelle target of TGZ toxicity

Mitochondria are located in every cell of the human body except the red blood cell. Most mammalian cells provide much of the energy required for homeostasis, particularly during fasting (Labbe *et al.*, 2008; Maianski *et al.*, 2003; Masubuchi *et al.*, 2006). Mitochondria play crucial roles in the various biosynthetic pathways, most notably ATP production for cellular activities through the oxidative degradation of endogenous substrates like pyruvate (generated from glycolysis), fatty acids, and amino acids (Masubuchi *et al.*, 2006). In this process, the oxidation of pyruvate occurs in the tricarboxylic acid cycle (TCA), while the degradation of fatty acids in the mitochondria is regulated by β -oxidation. Fatty acids may cross the mitochondrial membranes to enter the β -oxidation process. Whereas short and medium-chain fatty acids enter easily into mitochondria, long-chain fatty acids may only cross the mitochondrial membranes with the aid of a multi-enzymatic network that includes coenzyme and L-carnitine. Carnitine palmitoyltransferase 1 facilitates the rate-limiting step of the oxidation of long-chain fatty acids because malonyl CoA, an

endogenous product synthesised during de novo lipogenesis, can be strongly inhibited by this enzyme (Wallace & Fan, 2010). Within these mitochondria, short and medium-chain fatty acids are activated by unique acyl-CoA synthesis in acyl-CoA molecules. In contrast, long-chain fatty acyl-carnitine intermediates are converted to their corresponding acyl-CoA thioesters (Wallace & Fan, 2010). These acetyl CoA moieties may be used to synthesise ketone bodies, primarily acetoacetate and -hydroxybutyrate, which are then released into the bloodstream by extra-hepatic tissues such as the kidneys or muscles. Because β -oxidation and ketogenesis are central to energy homeostasis (Derks *et al.*, 2008; Labbe *et al.*, 2008), some organ failure can result in a critical deficiency of fatty acid oxidation (FAO), and ultimately death (Derks *et al.*, 2008; Labbe *et al.*, 2008). FAO deficiency is related to reduced plasma ketone bodies, the build-up of acyl-carnitine and dicarboxylic acid derivatives in the plasma (or urine) and extreme hypoglycaemia (Labbe *et al.*, 2008). Hyperglycaemia may be caused by decreased hepatic glucose production and increased extra-hepatic use (Derks *et al.*, 2008). While hypoketonaemia is commonly seen in mitochondrial FAO disorders, hyperketonaemia can occur during therapeutic changes in mitochondrial-oxidation (Labbe *et al.*, 2008). The plausible mechanism is that drug-induced TCA cycle impairment happens in extra-hepatic tissues that consume a high quantity of ketone bodies (Labbe *et al.*, 2008). Acetyl-CoA molecules and reduced cofactors cause pyruvate and fatty acid oxidative depletion (Labbe *et al.*, 2008; Wallace & Fan, 2010). NAD⁺ and FAD are used to produce NADH and FADH₂ by multiple dehydrogenases implicated in the TCA cycle and β oxidation, which supply the mitochondrial respiratory chain (MRC) with electrons and protons (Chen, 2018; Wallace & Fan, 2010). In the presence of protons, electrons are sequentially passed into the various multi-protein complexes of the MRC and eventually into cytochrome oxidase such as IV. The movement of electrons from the matrix to the intermembrane of the mitochondria inside the MRC produces significant membrane potential space (Chen, 2018; Wallace & Fan, 2010). The ATP synthase consists of a molecular motor comprised of two parts: F₁ and F_o. The F₁ region includes the ATP synthesis catalytic sites and extends into the mitochondrial matrix. An F_o is a proton turbine which is built into the internal membrane and attached to the F₁ motor.

The movement of protons downstream determines the potential gradient strength of the rotor revolving around the ATP synthesis. The movement of protons by F_0 is thus associated with ATP synthesis (Artika, 2019). As cells consume energy, protons re-enter the matrix via the F_0 portion of the ATP or complex V synthase, releasing some of the potential energy. This energy is then used for the phosphorylation of ADP into ATP by the F_1 component of the ATP synthase. Through MRC operation, the development of ROS is a crucial feature of mitochondria (Artika, 2019; Gülden *et al.*, 2010; Wallace & Fan, 2010). The mitochondrial superoxide dismutase (MnSOD) dismutates the superoxide anion radical into hydrogen peroxide (H_2O_2), which is detoxified into water by the mitochondrial glutathione peroxidase (GPx), which acts as a cofactor and incorporates reduced glutathione (GSH). Therefore, much of the MRC-generated ROS is detoxified by mitochondrial antioxidant defences in the usual (non-diseased) state. The excess ROS diffuses from the mitochondria and serves as the second messenger to initiate cell processes, such as mitogenesis (Wallace & Fan, 2010). This detoxification process will, however, overcome indifferent pathophysiological conditions. This happens when the liver mitochondria have GSH depletion, which significantly reduces their capacity to detoxify H_2O_2 because they have no catalase (Marí *et al.*, 2009). A drop in mitochondrial GSH below a critical threshold thus facilitates the accumulation of H_2O_2 through its detoxification. In effect, this triggers mitochondrial dysfunction, MPTP opening, c-Jun-N-terminal kinase activation (JNK) and cell death (Jones *et al.*, 2010). Chronic pathological conditions such as fasting and malnutrition are diseased states, especially in the mitochondria, favouring GSH depletion. Mitochondrial antioxidant enzymes may be compromised even when chronic dysfunction of the MRC occurs. The likelihood of a single electron reduction of oxygen and superoxide anion formation in complexes I and III increases considerably (Brookes, 2005; Cardoso *et al.*, 2010). High stable levels of ROS damage OXPHOS and mtDNA (Mansouri *et al.*, 2010). Such oxidative damage exacerbates mitochondrial dysfunction, increasing electron leakage and ROS production further, contributing to a chain reaction.

Any injury to the mitochondria may produce severe toxicity in cells and lead to the induction of apoptosis or necrosis depending on the level of mitochondrial damage. One of the suggested mechanisms of TGZ-induced liver injury is through

mitochondrial-mediated cytotoxicity (Masubuchi *et al.*, 2006; Okuda *et al.*, 2010). Mitochondrial malfunction is repeatedly detected in conjunction with TGZ cytotoxicity, proposing a role for mitochondria in the mechanism of TGZ-induced toxicity (Masubuchi *et al.*, 2006; Tirmenstein *et al.*, 2002). An earlier study by Tirmenstein *et al.* who treated HepaRG cells with TGZ for 48 hrs. reported substantially minimal levels of basal mitochondrial respiration compared to the untreated cells; the oxygen consumed for ATP production was virtually terminated. Contrastingly, the levels of ATP, although reduced, were not entirely blocked (Masubuchi *et al.*, 2006; Tirmenstein *et al.*, 2002). However, they suggested that the cells might have switched to glycolysis as a compensatory mechanism for ATP production. Besides, they observed a subsequent decline in mitochondrial membrane potential as well as the activation of pro-apoptotic caspase-3. However, TGZ at 30 μ M caused a 20-fold increase in ROS cellular levels; nonetheless, this was regarded as a secondary effect of primary mitochondrial injury. Increased ROS levels can cause structural modifications in mitochondria, and Hu *et al.* proposed that increased ROS levels initiate a vicious circle of toxic effects, including mtDNA injury. Also, Masubuchi *et al.* found that TGZ induced the MPT pore and suggested that the toxic effects resulted from the direct impact of TGZ on the ETC or MPT pore. In common, a previous study reported that the significant mtDNA injury was related to a reduction in ATP levels and a complete drop in cell viability (Rachek *et al.*, 2009). On the contrary, HepG2 cells treated with TGZ at 100 μ M did not affect ATP levels, although they recorded a significantly decreased membrane potential, suggestive of toxicity (Bova *et al.*, 2005).

1.4.5.2 The effect of TGZ on metabolome

Many other drugs are metabolised once they reach the body. Based on the pharmacological and toxicological properties of drug metabolites, they can be grouped into active metabolites, inactive metabolites, as well as reactive metabolites (Krämer & Testa, 2008; Wang *et al.*, 2017; Wishart *et al.*, 2017). Reactive metabolites can attach to cellular macromolecules, for instance, proteins and DNA, impair normal cellular activities and result in toxicity (Boysen *et al.*, 2011; Park *et al.*, 2011). Nakayama *et al.* have reported that the early stages of drug development require screening for reactive metabolites. Because reactive metabolites are

unstable and often unpredictable, they are challenging to identify and classify. Metabolomics is a valuable method for profiling the metabolism of drugs and bioactivation, in particular, the reactive and unknown metabolites.

Metabolomics focused on mass spectrometry has become a promising research method for diverse biological systems, such as bacteria, plants, mammalian cells, and body fluids (Ferne *et al.*, 2004). Genetic and other physiological or environmental alterations may lead to metabolite changes that can be demonstrated by metabolomics. In blood plasma, cancer patients' urine, and cancer cell lines, alterations of metabolites have been identified, offering exciting biomarker discovery possibilities (Davis & Kramer, 2006).

Metabolomics also helps explain cellular pathways by showing the metabolic status of drug-treated or nontreated cancer cells (Pan *et al.*, 2016; Russmann *et al.*, 2009). As the relationship between genotype and phenotype is illustrated in metabolomics (Veling *et al.*, 2017), we have profiled over 100 strains of yeast with various individual gene knockouts to elucidate the activity of the mitochondrial protein. Nonetheless, whole cells were limited to profiling, which was unable to reveal the metabolic signature of the compartments (Van Vranken & Rutter, 2016). In comparison, an appreciated metabolic profile in subcellular compartments by creating the expression "the entire (cell) is more cramped than the sum of its components" (Van Vranken & Rutter, 2016). Though mitochondrial metabolomics with modern mass spectrometer equipment has been identified and optimised for many research teams, it has not been widely used due to technical glitches (Marco-Lázaro *et al.*, 2011; Swayne *et al.*, 2009). Also, previous studies have demonstrated that the mitochondrial metabolic signature can discriminate against phenotypes. While only a portion of the features detected could be noted as metabolites based on retention period, the other features suggested that mitochondria contained significant amounts of unspecified or unknown metabolites (Go *et al.*, 2014; Roede *et al.*, 2012).

Pfizenmaier *et al.* also carried out comparison-specific metabolomics analysis via the filtration of Chinese hamster ovary cells and found a minimal mitochondrial ATP supply. Chen *et al.* evaluated absolute concentrations for over 100 mitochondrial

matrix metabolites compared to whole cells using mitochondrial immunopurification with an artificial epitopal label fixed to an outer membrane anchor (Chen *et al.*, 2016). The researchers then reported that, in comparison with mitochondria, a higher level was seen for most metabolites in whole cells. Moreover, the metabolic response to the respiratory chain was higher in mitochondria than in entire cells. They then postulated that it is understandable to expect compartment-specific metabolic alterations. Also, they found metabolic signatures distinctive to the compartment that may be associated with metabolic changes in mitochondrial mutants (Chen *et al.*, 2016).

The diffusion of pyruvate through the mitochondria's inner membrane forms a core branch of the cell-energy metabolism (Divakaruni & Murphy, 2012). Friday *et al.* have reported that TGZ blocks pyruvate supply into mitochondria, thus decreasing pyruvate supply to the TCA cycle. Given the limited supply of intramitochondrial pyruvate, the TCA cycle may be unbalanced. To compensate for the discrepancy, it may reduce malate concentrations or increase glutamate conversion to α -ketoglutarate.

A previous study reported that TGZ did not influence other amino acid concentrations, specifically methionine, leucine, phenylalanine, tryptophan, and valine (Oliver III *et al.*, 2010). Other researchers have suggested that anaplerotic substrates were not employed to account for the intermediate TCA deficit. While it has been established in recent decades that a mitochondrial pyruvate carrier exists, it has only recently been identified on a molecular level (Diers *et al.*, 2012; Friday *et al.*, 2010; Oliver III *et al.*, 2010). Two small transmembrane proteins in the inner membrane, mitochondrial pyruvate carrier 1 (MPC1) and 2 (MPC2), are essential components of a seemingly complex process that facilitates inhibitor sensitive pyruvate transport (Bricker *et al.*, 2012; Diers *et al.*, 2012). This established complex can be a rational therapeutic target for the regulation of energy balance and, what is more, the metabolic profile.

TZDs are the most effective antidiabetic agents for averting the progression from high blood plasma glucose levels to type 2 diabetes. The reported association between dysregulated glucose biotransformation and the physiological defect has

initiated the remodelling of pioglitazone to manage pathological conditions such as neurodegenerative conditions and other cancers (Colmers *et al.*, 2012; DeFronzo & Abdul-Ghani, 2011; Miller *et al.*, 2011). Nevertheless, serious side effects of TZDs, such as volume expansion, osteoporosis, elevated adiposity, and heart disease risk, have limited more extensive clinical application (He *et al.*, 2001; Graham *et al.*, 2010). TZD activity is attributable to PPAR γ , a nuclear receptor controlling gene expression related to lipid accumulation, cell differentiation, as well as inflammation (Cho *et al.*, 2005). Furthermore, the finding that low-micromolar concentrations of TZDs bind to membranes representing the circulating concentrations of treated patients indicates that some of the metabolic effects of the TZDs may be triggered by direct modulation of mitochondrial function. Findings from previous studies have reported a unique inhibition of MPC activity by TZDs (Belcher & Matthews, 2000; Cho *et al.*, 2005). Also, depleted intracellular glutamate levels may interfere indirectly with the TCA cycle as glutamate is an anaplerotic substrate (Birney, 2002), which would lead to reduced intermediates of the TCA cycle such as malate and the production of ATP. Besides, lowered levels of glutamate may also influence the biosynthesis of GSH, as GSH is produced from cysteine, glutamic acid, and glycine (Birney, 2002; Yang *et al.*, 2014). Cells more vulnerable to toxicity are protected from oxidative stress via termination of oxidants and combined oxidation to GSSG, making the cell more vulnerable to toxicity. GSH/GSSG is considered the cell's primary redox buffer due to high levels of GSH, and the GSH/GSSG ratio is regarded as the main predictor of cell redox status (Agledal *et al.*, 2010; Zhao *et al.*, 2009). GSH can also be produced through a decrease in GSSG attributable to the glutathione reductase enzyme (Zhao *et al.*, 2009; Yang *et al.*, 2014).

Reduced nicotinamide adenine dinucleotide phosphate (NADPH) is produced through the pentose phosphate system, and cytosolic malate conversion into pyruvate also produces substantial NADPH levels (Agledal *et al.*, 2010; Yang *et al.*, 2014). Reduced concentrations of intracellular nicotinamide, an NADPH precursor, can also reduce NADPH's supply and eventually reduce the levels of GSH in cells (Bradshaw, 2019; Yang & Sauve, 2016). Previous research on metabolite profiling has been correlated with many of these findings, lending support to the hypothesis that TGZ influences both energy production in cells and GSH concentrations (Intapa

& Jabra Rizk, 2014; Kuo *et al.*, 2014; Phimister *et al.*, 2005). There are three enzymes in mammals that can address the thermodynamic challenges of ammonia assimilation: carbamoyl phosphate synthetase I (CPS1), the ATP-dependent, rate-limiting step of the urea cycle; GDH, an NAD(P)H-dependent enzyme that facilitates the reductive introduction of an amine group to an organic molecule (amination) - ketoglutarate; and GS, which facilitates the ATP production.

Previous researchers found that TGZ increased deamination at the expense of transamination by redirecting glutamate from the transamination pathway into the mitochondrion, where the deamination pathway, GDH, is located. If the transamination pathway is mainly cytosolic, this response would result in a glutamate shift from the cytosol to the mitochondrial compartment. Glutamine carbons enter the TCA cycle after being deamidated to glutamate and then converted to α -ketoglutarate (Friday *et al.*, 2010; Oliver III *et al.*, 2010; Reynolds & Clem, 2014). Their observation may be due to the restricted intramitochondrial pyruvate distribution because the ALT pathway is a transamination process that requires pyruvate. Still, no intramitochondrial pyruvate means that glutamate is converted into alpha-ketoglutarate by the GDH catalysed deamination method. When highly permeable pyruvate methyl ester was used to restore intramitochondrial pyruvate availability, glutamate metabolism was reduced via GDH and glutamate metabolism was increased via ALT (Oliver III *et al.*, 2010; Spinelli *et al.*, 2017).

1.4.5.3 The effects of TGZ on Cell death

Apoptosis (programmed cell death) is a series of controlled biochemical events that result in morphological alterations such as cell shrinkage, blebbing, condensation of chromatin and DNA fragmentation (Figure 1-9) (Kroemer *et al.*, 2007; Renehan, 2001). Apoptosis plays a critical role in biological activities ranging from embryogenesis to ageing and impacts upon biological homeostasis. Deregulation of apoptosis has been associated with several adverse physiological conditions, including disease and chemical toxicity (Kroemer *et al.*, 2007; McIlwain *et al.*, 2013; Taylor *et al.*, 2008). Two distinct pathways exist for the activation of apoptosis (Kalkavan & Green, 2017). The intrinsic mechanism pathway is associated with permeabilisation of the mitochondria and the release of cytochrome c into the

cytoplasm. The cytochrome c released from the mitochondria binds the apoptotic protease activating factor-1 (Apaf-1), inducing its conformational alteration and oligomerisation, creating a caspase activation platform called the apoptosome. This multi-protein complex formation with the cytochrome c sets off the caspase cascade's stimulation via caspase -9 (Figure1-9) (Hüttemann *et al.*, 2011; Kalkavan & Green, 2017; Kroemer *et al.*, 2007; Taylor *et al.*, 2008). Apoptosis may also be triggered by DNA damage or severe cellular stress (Taylor *et al.*, 2008). The Fas ligand binding may induce the extrinsic pathways to a death receptor which, together with the adaptor protein (FADD/TRADD), recruits, dimerises, and stimulates caspase-8. The activated caspase-8 may then initiate apoptosis directly through DNA cleavage and, by this means, activate executioner caspase-3/7. It may also trigger the intrinsic apoptotic pathway through the breakup of BID to induce programmed cell death (Harper *et al.*, 2003; McIlwain *et al.*, 2013). Akasaki and his group have reported that tumour necrosis factor-related apoptosis-inducing ligand (TRAIL) is one of the promising anti-neoplastic products capable of selectively killing cancer cells with an insignificant effect on healthy cells. TRAIL can activate caspase cascades by interacting with TRAIL-responsive receptors (DR), such as DR4 and DR5, which cause caspase-8 cleavage in the Fas-related death domain protein-dependent procedure. The cleaved caspase-8 may act as an initiator capable of processing other groups, for instance, caspase-3 in a caspase cascade. Cleaved caspase-8 may cause Bid cleavage, which may upregulate mitochondrial cytochrome c (Cyt-c) discharge (Harper *et al.*, 2003; Kalkavan & Green, 2017). Cytochrome c may subsequently interact with Apaf-1 to trigger caspase-9 activation. Caspase-8 and caspase-9 may then stimulate caspase-3, which forms the critical activator of apoptotic DNA fragmentation (McIlwain *et al.*, 2013). It has been previously reported that TGZ causes dose-dependent depletion of ATP, the opening of the MPT pore and reduced membrane potential, which in turn causes the discharge of pro-apoptotic proteins and the consequent instigation of apoptosis or necrosis (unprogrammed cell death). Studies in HepG2 cells demonstrated the involvement of TGZ in the induction of apoptosis through the classical c-Jun N-terminal protein kinase (JNK) pathway, which will be discussed further in the next section (Bae & Song, 2003).

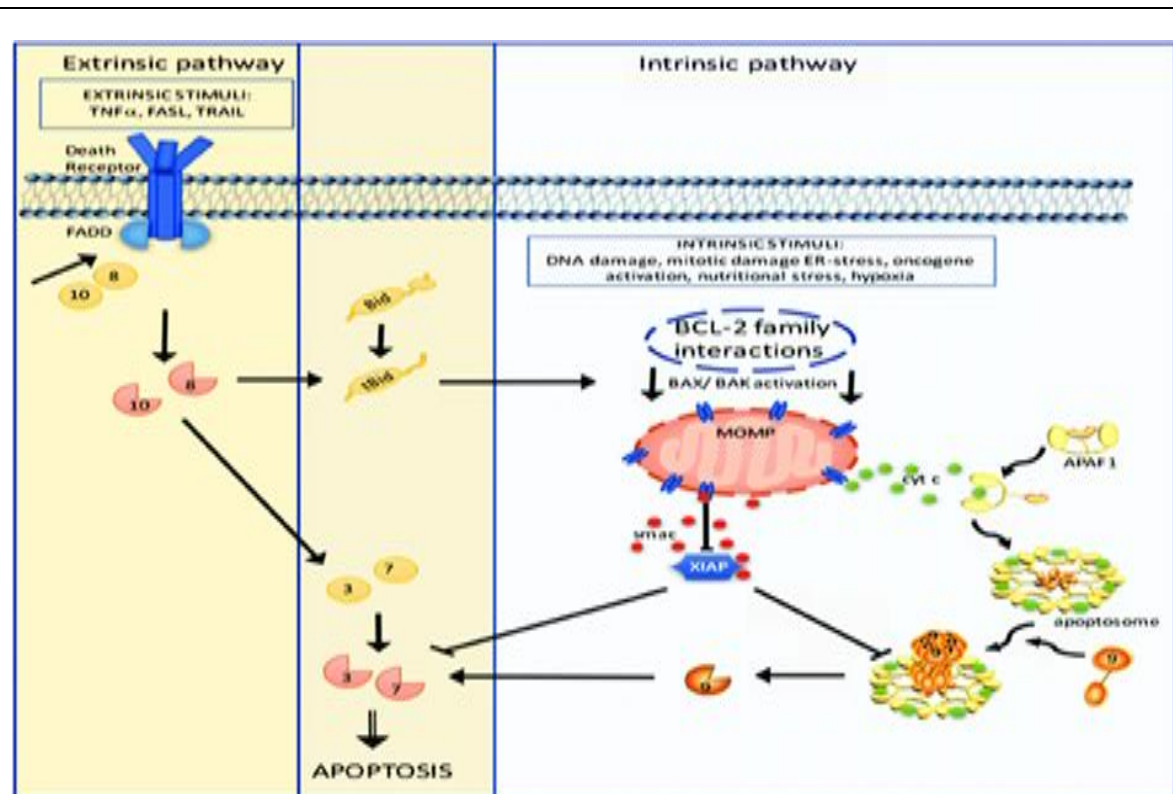


Figure 1-9 Schematic representation of the intrinsic and extrinsic apoptotic pathways

Apoptosis operates via two main, different pathways: death receptor-mediated (or extrinsic) and mitochondria-dependent (or intrinsic). Together with the adaptor Fas-associated death-domain (FADD) protein and the initiator procaspase-8 or 10, they form the death-inducing signalling complex (DISC). This association eases the dimerisation and self-activation of the initiator caspases, consequently cleaving and activating the executioner caspases-3 and -7, eventually causing apoptosis. However, the intrinsic pathways can be triggered via diverse intracellular stress that modulate Bcl-2 family protein interactions that control the activation of the Bcl-2 effector proteins such as Bax and Bak. Upon stimulation, Bax and Bak initiate MOMP, which then discharges proapoptotic proteins. Cytochrome c connects APAF1 and stimulates oligomerisation, leading to the formation of an apoptosome which then recruits and activates the initiator procaspase 9. Active caspase -9 cleaves and activates the executioner caspase-3 and -7. Simultaneously with cytochrome c, Smac is released from the intermembrane space and inhibits XIAP. Both pathways are linked where caspase-8 can cleave the BH3-only protein BH3-interacting domain agonist, making it an active, truncated to form tBID, which stimulates Bax/Bak. The numbers in the circles denote the corresponding pro- and active caspases, while the broken-up circles symbolise active caspases (Kalkavan & Green (2017)).

1.4.5.4 TGZ-induced JNK activation on apoptosis

JNK forms part of the mitogen-activated protein kinase (MAPK) family that controls various biological activities involved in some physiological disorders, such as neurodegenerative abnormalities. JNK has ten isoforms, which are encoded by three genes: JNK1 (four isoforms), JNK2 (four isoforms), and JNK3 (two isoforms) (Gourmaud *et al.*, 2015). JNK1 and JNK2 are found in all cells and tissues, whereas JNK3 is found primarily in the heart, brain, and testicles (Gourmaud *et al.*, 2015). JNK3 has been identified as a degenerative signal transducer, and it appears to be the isoform involved in JNK over-activation following harmful stress stimuli in the adult brain, such as ischemia, hypoxia, and epilepsies. The information on reduced apoptosis of hippocampal neurons and reduced seizures generated by kainic acid in JNK3 knockout mice, as well as the idea that JNK3 mice are also protected against ischemia, explains this principle (Davies & Tournier, 2012; Javadov *et al.*, 2014).

Previous research has shown that JNKs play an important role in the regulation of inflammation, apoptosis and necrosis signalling pathways and several transcriptional and non-transcriptional processes involved in neuron and cardiomyocyte injury during ischemia-reperfusion (Javadov *et al.*, 2014).

As a result, JNK migrates to the nucleus and modifies the function of the AP-1 transcription factor, causing a change in gene expression and, as a result, biological responses such as inflammation and/or apoptosis. Activation of JNK worsens brain injury in stroke, causing inflammation and leading to ischemic cell death. Therefore, it seems logical that JNK signalling pathways could be explored as a potential target for pharmacological interventions to address some physiological abnormalities or hepatotoxicity (Davies & Tournier, 2012). Bae and Song (2003) reported that treatment of HepG2 cells with TGZ did cause 5-fold activation of JNK and P38 kinase. They supported their findings by pre-treating HepG2 cells with a JNK inhibitor (anthral), which resulted in a significant decrease in the rate of TGZ-mediated apoptosis. TGZ may exert its toxicity by directly activating the JNK-related apoptotic pathway, followed by up-regulation of the proapoptotic proteins such as Bad and Bax with cleavage of Bid protein and decreased levels of anti-apoptotic proteins such as Bcl-2 (Bae & Song, 2003; Kalkavan & Green, 2017; Wang *et al.*,

2007; Westphal *et al.*, 2014). JNK may also cause apoptosis by provoking the release of cytochrome c from the mitochondria through the stimulation of Bid cleavage and Bax translocation into the mitochondria (Dhanasekaran & Reddy, 2008; Szabo *et al.*, 2013; Yu *et al.*, 2004). For that reason, if ATP is highly depleted or the compensatory mechanisms of glycolysis cannot generate extra ATP, the cells can undergo necrosis as a means of cell death as an alternative to apoptosis. Therefore, it is possible that TGZ causes apoptosis and necrosis reliant on the availability of ATP (Dhanasekaran & Reddy, 2008; Smith, 2003; Yu *et al.*, 2004). Although there are several possible means of TGZ toxicity, there is mounting evidence suggesting that TGZ is a hepatotoxin that elicits cytotoxicity by triggering mitochondrial injury because of respirational abnormalities. Defective respiration results in decreased cellular ATP and, as a result, energy deprivation in the mitochondria as well as loss of membrane potential, which can trigger cell death mechanisms such as apoptosis and necrosis. There is speculation that there is a secondary production of ROS that exerts a general intracellular detrimental effect, such as mtDNA binding, which then damages the generation of a healthy ETC, leading to oxidative stress due to the flux of superoxide. Another argument is that the injury could be latent and can, therefore, remain undetected for long periods as apoptosis does not cause elevation of the serum liver enzymes (Smith, 2003).

1.4.5.5 The role of TGZ on necrotic cell death

In contrast with apoptosis, necrosis can be described as an unprogrammed or non-controlled cell or tissue death (Figure 1-10). Necrosis is an ATP reduction in membrane injury upon toxic exposure or physical damage to the cell (Dara & Kaplowitz, 2017; Yuan & Kaplowitz, 2013). For instance, TGZ causes necrosis through a deficiency of metabolic activities, resulting in a substantial reduction of ATP as well as the integrity of the cell membrane (Ong *et al.*, 2007). As a result, cells undergoing necrosis stop their production of proteins coupled with ATP.

Organisationally, the cell organelles swell and become inactive during the early phases of necrosis. The cell membrane forms blebs (Figure 1-10) (Jog *et al.*, 2014; Krysko *et al.*, 2006). These blebs, which hold no organelles, merge, enlarge in size, and eventually the cell membrane ruptures, causing the discharge of the cell's constituents into the surrounding tissue. For instance, the discharged content

successively produces an inflammatory response in the affected tissue, for instance, the liver (Jog *et al.*, 2014; Krysko *et al.*, 2006). The inflammatory response is facilitated by individual cells of the immune system that are attracted to the liver; cytokines that are involved in cell communication or ROS. The inflammatory response, which is commonly considered an essential part of necrosis, further injures the liver tissue (Jog *et al.*, 2014; Krysko *et al.*, 2006). Krysko *et al.* have reported that, similar to the less regulated plasma membrane modifications, cells undergoing necrosis do not present clean chromatin condensation and DNA fragmentation as observed in apoptosis.

.

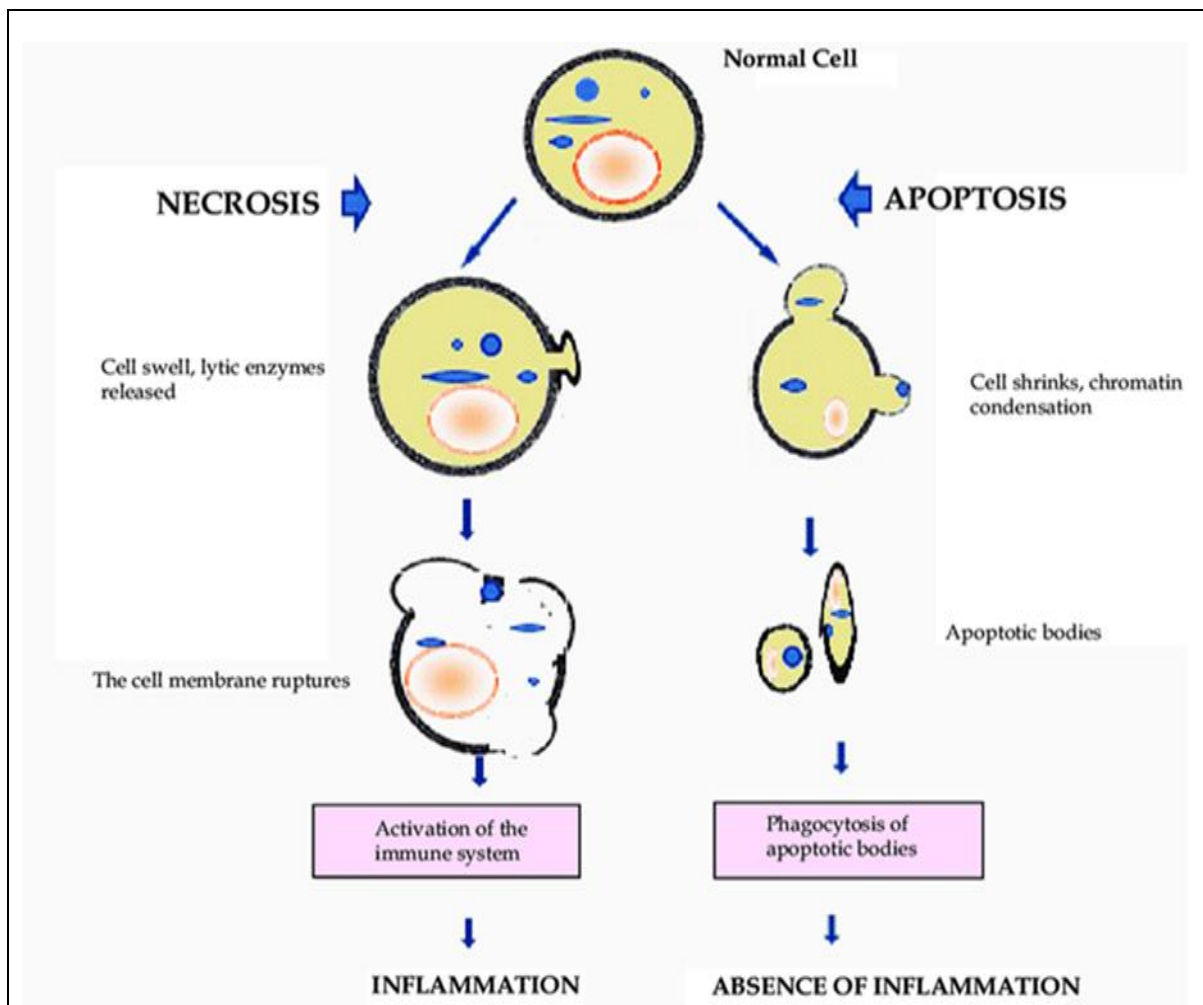


Figure 1-10 Morphological features of necrotic and apoptotic cell death

Apoptosis involves cell shrinkage, chromatin condensation, and blebbing of the cell membrane at the nuclear periphery. The eventual development of apoptotic membrane-bound bodies containing organelles, cytosol and nuclear fragments is phagocytosed without activated inflammatory processes. The necrotic cell swells up until the cell membrane becomes leaky due to acute cellular damage and eventually disrupts and spills its contents into the surrounding tissue, resulting in inflammation. Necrosis occurs as a result of traumatic cell death. The cell swells up due to acute cellular injury until the cell membrane disrupts and releases all cellular contents into the extracellular space (Budak & Akdog, 2011).

1.4.5.6 Inhibition of bile transport by TGZ and its effects on hepatocytes

As described in section 1.2, DILI is one of the main grounds for the removal of approved drugs from the market (Aithal, 2015; 2019; Kaplowitz, 2013); nonetheless, the competence to correctly forecast a drug's tendency for DILI is inadequate due to a lack of understanding of the underlying mechanisms (Aithal, 2015; 2019). One of

the essential projected means of DILI is the inhibition of bile salt export pump (BSEP)-facilitated excretion of bile acids, which may upsurge liver exposure to bile acids, eventually causing apoptosis or necrotic cell death (Byrne *et al.*, 2002; Deng, 2018; Morgan *et al.*, 2010; Whitebread *et al.*, 2017; Woodhead *et al.*, 2014). Bile belongs to the steroid acids and is composed of approximately 80% organic compounds, with phospholipids and cholesterol as other constituents (Monte *et al.*, 2009; Snow & Mosley, 2007). Increased production of bile acid or impaired bile removal (cholestasis) may lead to a build-up of bile salts and other toxic biliary solutes within the liver. Although the role of TGZ in cholestasis is unclear, the bile salt export pump (BSEP) encoded by the ABCB11 gene is suggested to be the potential target for TGZ-induced liver toxicity. One of the critical functions of BSEP is to export bile acids and xenobiotic conjugates from liver cells into the canaliculus (Funk *et al.*, 2001; Snow & Mosley, 2007). Sodium-taurocholate cotransporting polypeptide (NTCP), organic anion transporting polypeptides (OATPs), organic solute transporters (OST α /OST β) as well as the multidrug resistance-associated protein 4 (MRP4), are other transporters implicated in bile salt transporters. The NTCP and OATPs facilitate the uptake of bile salts from the blood into the liver cells, whereas both OST α /OST and MRP4 discharge bile salts from the liver cells and transport them into the blood (Kubitz *et al.*, 2012; Kullak-ublick *et al.*, 2004; Suga *et al.*, 2017). Funk *et al.* reported that after treating an isolated perfused rat liver with 10 μ M TGZ, a reduction in bile flow was observed within an hour; this led to a dose-dependent increase in the plasma bile acid concentration. Furthermore, Funk *et al.* postulated that the formation of TGZ-sulphate in an isolated canalicular rat liver might have contributed to their observation; that is, TGZ-sulphate significantly reduced ATP-dependent taurocholate transport controlled by the canalicular bile salt export pump (Bsep) in an isolated canalicular rat liver plasma membrane. The researchers further showed that TGZ-sulphate did block an ATP-dependent taurocholate transport which was facilitated by the canalicular bile salt export pump. Snow & Mosley (2007) suggested that TGZ-sulphate might cause a significant inhibition of BSEP, which could cause high intracellular bile salts and then cause hepatotoxicity through either mitochondrial malfunction or apoptosis (Figure 1-11) (Funk *et al.*, 2001; Yang *et al.*, 2014). High intracellular bile salts can induce cell death via mitochondrial malfunction and apoptosis, a process that is reported in

TGZ-facilitated cell death, described by Smith (2003). As BSEP-mediated excretion of bile salts is dependent on ATP, the impaired ability of mitochondria to produce ATP will eventually disrupt the activity of BSEP (Masubuchi, 2006). Also, mitochondria facilitate death receptor signalling and mitochondrial malfunction can instigate apoptosis and cause oxidative injury (Carrã *et al.*, 2015; Zhu *et al.*, 2012). However, FAS receptor-mediated apoptosis appears to be the primary pathway. Jaeschke *et al.* have reported that bile salts promote cytoplasmic translocation of Fas to the plasma membrane where the receptors self-combine and cause apoptosis. This mechanism supports the idea that the accumulation of bile salts from impaired BSEP will result in cell death through apoptosis. For this reason, effective transport coordination in the liver is essential to guarantee the efficient excretion of bile salts.

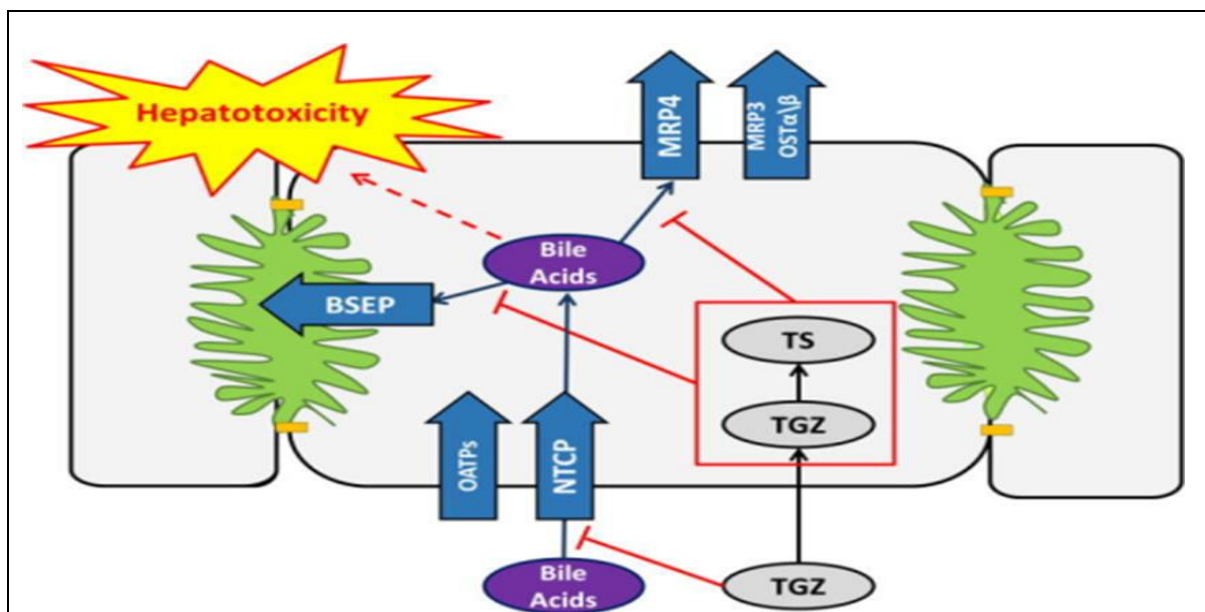


Figure 1-11 Proposed mechanism of TGZ-mediated liver toxicity

Bile acids are transported into the liver cells via sodium-taurocholate co-transporting polypeptide (NTCP) and organic anion transporting polypeptides (OATPs). Hepatocellular bile acids are expelled into the bile via the bile salt export pump (BSEP). Bile acids can, what is more, be carried through the basolateral membrane to sinusoidal blood by basolateral efflux transporters, for instance, multidrug resistance-associated protein (MRP) 4, MRP3, or organic solute transporter (OST)α/β. TGZ and its major metabolite, TGZ sulphate (TS), are potent blockers of liver bile acid transporters, which might result in a build-up of bile acid in the liver and consequent toxicity (Yang *et al.*, 2014).

1.4.5.7 The effect of TGZ on cholesterol synthesis

Cholesterol is a crucial constituent of cellular membranes and functions as a precursor of steroid hormones, bile acids, or vitamin D in other tissues. Nonetheless, excess or deficient physiological levels of cholesterol can be detrimental to the cells. As such, cholesterol synthesis is tightly controlled via a feedback mechanism to maintain cholesterol homeostasis in animals. Cholesterol synthesis is facilitated by a class of microsomal enzymes such as HMG-CoA reductase. They are the rate-limiting enzymes, and they are transcriptionally regulated by sterol regulatory element-binding protein (SREBP-2) (Horton *et al.*, 2002). SREBPs belong to a large group of transcription factors that control the expression of a range of enzymes needed for endogenous cholesterol, fatty acid triacylglycerol and phospholipid production. There are three isoforms of SREBPs: SREBP-1a, SREBP-1c, and SREBP-2, which have different functions in synthesising lipids (Horton *et al.*, 2002). SREBP-1c is predominantly contained in the liver, and it is implicated in the activation of genes implicated in fatty acid synthesis. Also, SREBP-2 is involved in the activation of LDL receptor genes as well as different genes implicated in cholesterol synthesis, for instance, the HMG-CoA reductase.

The SREBP1-a isoform is involved in both cholesterol and fatty acid synthetic pathways (Horton *et al.*, 2002). SREBP transcription factors are produced as inactive precursors attached to the endoplasmic reticulum (ER) membranes and form a complex with SREBP-cleavage activating protein (SCAP). For this reason, when the sterol level is depleted, SCAP escorts the SREBPs from the ER to the Golgi where they are processed by two occupant proteases (site1 protease and site2 proteases) that sequentially cleave the SREBPs and release the NH (2)-terminal active domains from the membrane, allowing them to translocate to the nucleus and activate transcription of their target genes (Gong *et al.*, 2006; Horton *et al.*, 2002). Insulin-induced genes, (Insig)-1 and -2 are membrane proteins in the ER and play a crucial role in the control of SREBP cleavage (Bridges *et al.*, 2014; McPherson & Gauthier, 2004). In a situation whereby the intracellular sterol levels are increased, SCAP binds to Insigs. This action inhibits the translocation of the SREBP-SCAP complex

from ER to Golgi as well as proteolytic activation of SREBP (Bridges *et al.*, 2014; Horton *et al.*, 2002; McPherson & Gauthier, 2004).

Consequently, cholesterol and fatty acid synthesis decrease (Brown *et al.*, 2002; Gong *et al.*, 2006). Yang *et al.* have reported that Insig-1 is an ER protein which binds to SCAP and promotes the sterol-facilitated maintenance of the SCAP/SREBP complex in the ER. Insig-1 gene expression is positively regulated by transcriptionally active SREBP, resulting in a feedback mechanism which controls lipid balance, whereas Insig-2 insulin negatively controls Insig-2 expression (Yang *et al.*, 2008). An earlier study by Engelking *et al.* has reported that mice with Insig-1 and Insig-2 gene disturbances showed overexpression of genes implicated in the synthesis of cholesterol and fatty acids as well as an excessive build-up of cholesterol and triglycerides in the liver. It has been reported recently that PPAR γ activation by rosiglitazone induces the expression of Insig-1 in the white adipose tissue of diabetic rats and blocks the processing of SREBPs and lipogenesis. The researchers postulated that it is a feedback mechanism to regulate lipogenesis in the adipose tissue (Kast-Woelbern *et al.*, 2004). However, an experiment conducted by treating macrophages with TGZ and pioglitazone increased the expression of SREBP-2 target genes, HMG-CoA synthase and HMG-CoA reductase (Iida *et al.*, 2002). Their findings led to the assumption that PPAR γ activation increased gene expression of SREBP-2. As a result, the effects of PPAR γ stimulation on the processing of SREBPs and their target gene expression could be tissue-specific. Klopotek *et al.* having treated HepG2 and Caco-2 cells with various concentrations of TGZ, reported that TGZ decreased cholesterol production in both cell types through the activation of PPAR γ which then reduced the levels of SREBP-2 and a continuous reduction of its target genes implicated in cholesterol synthesis (Klopotek *et al.*, 2006).

On the other hand, Klopotek *et al.* have reported that TGZ dose-dependently blocked cholesterol synthesis in CHO and HepG2 cells, which led to the postulation that there is a common pathway for TGZ action (Klopotek *et al.*, 2006). They further noted that the exclusion of TGZ from the culture medium resulted in the loss of sterol build-up and was followed by restored cholesterol production. Also, they reported that actinomycin D and cycloheximide inhibited the activation of PPAR γ induced by

TGZ. However, in the compounds mentioned above, the blocking of cholesterol production by TGZ was unaffected, suggesting that the inhibitory mechanism of cholesterol production is not reliant on PPAR γ activation. For these reasons, the exact mechanisms (pathways) of TGZ in cholesterol synthesis are still questionable (Klopotek *et al.*, 2006).

To summarize, the mechanism of TGZ-induced liver injury is complicated, which is why researchers have yet to find an answer/s. However, the allergic and immune response signs and symptoms are sporadic, and a metabolic flaw in its metabolism is suspected of playing a pivotal role in TGZ-induced hepatotoxicity. TGZ is a potent inducer of CYP 3A4 (Yamamoto *et al.*, 2002). It has a unique alpha-tocopherol (vitamin E-like) side chain which can be biotransformed into a highly active quinolone-like metabolite, which may account for its occasional deviant biotransformation and liver toxicity (Yamamoto *et al.*, 2002; Vignati *et al.*, 2005). The developing tendency is that a defect in cellular defence mechanisms against oxidative stress and reactive metabolites appears to promote TGZ-induced hepatotoxicity without any doubt. Also, transporter inhibition (BSEP), leading to bile acid accumulation. ROS production and oxidative stress resulting from TGZ-induced dysfunction of oxidative phosphorylation (OXPHOS) and impaired electron transport through the respiratory chain may also be some of the probable pathways of TGZ-induced hepatotoxicity.

With many agents or disorders that adversely affect mitochondria, one of the above categories may outweigh the other, but there is frequently significant overlapping, and one set of injuries may lead to another. The common argument is that these agents and conditions all congregate on pathways that lead to substantial disturbance of mitochondrial structure or activity. After the withdrawal of TGZ, a lot of research about the potential mechanisms of its hepatotoxicity has been conducted. There is rapidly accumulating experimental evidence confirming that mitochondrial dysfunction plays a key role (Graham *et al.*, 2003). The homeostasis of cholesterol emerges from the complex mechanism that occurs primarily in the liver. A deficiency of one of the factors involved in cholesterol metabolism can cause profound changes and, in effect, liver disease. For instance, most of the cholesterol that enters the

hepatocyte in the LDL particles is distributed through the cell and reproduced within VLDL particles without reaching equilibrium with the regulatory pool.

1.4.6 The necessity to study a drug that has been withdrawn from the market

TGZ was removed from the market based on reported cases of hepatotoxicity and some fatalities. However, there has been a burgeoning of interest in the compound as some studies have speculated that the PPAR γ mediated effects could be harnessed in anti-cancer treatments to halt the progression of tumour cells (Rubin, 2002). The involvement of PPAR γ in cell proliferation could be used to explain the above notion. The binding of diverse ligands to PPAR γ can provoke various downstream effects depending on their inhibitory or stimulatory effects. In several types of cancer, TZDs have been shown to inhibit proliferation while also promoting apoptosis and differentiation. Zhong and his group studied the anti-cancer effects of lovastatin and TGZ in anaplastic thyroid cancer cells and discovered that a sub-lethal concentration of both lovastatin and TGZ has a tumour-specific anti-proliferation effect *in vitro* and *in vivo*. They suggested that this combination treatment inhibitory effect was due in part to cell cycle arrest at the G0/G1 phase (Zhong *et al.*, 2018). TGZ is an ideal drug to explore the interaction of many different, interconnected biological pathways. A better understanding of the mechanism of TGZ-mediated toxicity may enable drug developers to redesign or redefine it to correct other pathological conditions.

1.5 *In silico* and metabolomics tools in modern toxicity studies

Advances in laboratory-based studies, as well as the availability of high input data, make it easy for current researchers to assess metabolic and transport data. However, when researchers obtain these data, they place them into large databases, and in some cases, nothing is done with them (Colquitt *et al.*, 2011; Yang *et al.*, 2019; Wishart *et al.*, 2017). Most of these data are collected through experiments focusing on small sets of individual reactions. The novel approach of *in silico* modelling offers the ability to examine the mechanisms of these reactions and how they influence each other, allowing the analysis of large amounts of data and the investigation of the amount of control exerted by individual reactions on the cell, organ, or whole system (Colquitt *et al.*, 2011).

In silico studies, will help speed up toxicity studies by countenancing the integration of data in a manner that allows the emergence of biological phenotypes from disparate experimental data. For example, computational modelling may incorporate mathematical approaches such as flux balance analysis (FBA) to analyse the flow of metabolites via a metabolic network or to predict the steady-state flux distribution of the metabolic system (Orth *et al.*, 2010). This steady-state implies that metabolic fluxes (reaction rates), as well as intracellular metabolite concentrations, are both constant over time (Orth *et al.*, 2010). For instance, FBA can be used to predict, for instance, the growth rate of single-celled organisms such as bacteria or the standard of production of other relevant biological metabolites (Orth *et al.*, 2010; Venkatapathy & Wang, 2012). The use of software for producing molecular descriptors, simulation tools, modelling systems for toxicity predictions as well as visualisation tools are also some of the critical factors that need to be considered in model development (Venkatapathy & Wang, 2012).

In silico systems have the distinct advantage of being able to evaluate early chemical toxicities before they are produced. However, a small error in a single reaction, such as an incorrect metabolite name, could affect the entire stimulation process (Madan *et al.*, 2012; Orth *et al.*, 2010). Another limitation in using FBA (steady-state) is that it cannot predict dynamic changes in metabolic fluxes with time (Orth *et al.*, 2010). However, this drawback could be improved by integrating it with other computationally intensive extensions of FBA, such as minimisation of metabolic adjustment (MoMA) and regulatory on/off minimisation (ROOM). The MoMA may be used to search for the flux distribution in the mutant flux space that is closest to the optimal flux distribution in the wild type. In contrast, ROOM could predict the metabolic study state after gene knockouts by minimising the number of significant flux changes concerning the wild type (Shlomi *et al.*, 2005).

1.6 Hypothesis and aims

This current study is motivated by the fact that TGZ appeared to be a promising anti-diabetic agent after going through the mill of clinical trials, till the issue of specific liver toxicity was identified after the drug was marketed (Rhodes, 2009). Why was this not detected earlier by animal models? In pre-clinical studies, TGZ toxicity was not reported in whole animal studies. It has been proposed that normal rats were employed and that the human subjects who experienced liver toxicity had impaired liver function due to their diabetic condition and, as such, compromised the ability to metabolise TGZ (Tirmenstein *et al.*, 2002). Animal models have been used in the past decades for toxicity studies. However, *in vivo* animal studies are confined by time, ethical consideration, as well as a financial burden. These limitations may have a negative impact on their effectiveness. Therefore, it seems logical to explore the suitability of computational approaches for assessing chemical toxicity as an added measure. *In silico* toxicology could be used to supplement existing toxicity analysis to predict toxicity, analyse, simulate, visualise, guide toxicity assessments and reduce late-stage failures in drug development.

It is hypothesised that TGZ could cause liver toxicity through mitochondrial dysfunction, which initially causes the release of pro-apoptotic signals, leading to cellular apoptosis.

And to test this hypothesis as the prime objective, a combination of *in silico* and *in vitro* approaches will be used to explore TGZ toxicity mechanisms. The project's initial aims were to validate the model systems to be used within the project; the first aim was to validate a cell culture system to explore TGZ toxicity *in vitro*. Several cellular assays were undertaken to replicate the previously reported effects of TGZ hepatotoxicity.

The secondary objective was to build a computational model incorporating all the known effects of TGZ on hepatocyte biology. This model was parameterised using data from the literature and validated against the *in vitro* data generated by the prime objective.

Chapter 2 Materials and general methods

2.1 Materials

2.1.1 Materials for *in vitro* studies

The hepatoma cell line Huh7 is a well-differentiated liver cell derived from a human carcinoma cell line, donated by a 57-year-old Japanese man in 1982 (Krelle *et al.*, 2013). The cell line was developed by Nakabayashi and Sato (Krelle *et al.*, 2013). Cells were routinely grown in Dulbecco's modified eagle medium (DMEM) containing phenol red, 4.5 g/L D-glucose and 4 mM L-glutamine, supplemented with 10% (v/v) heat-inactivated foetal bovine serum (FBS), 100 U/ml Penicillin and 100 U/ml Streptomycin. Cells were kept at 37 °C in a humidified incubator with 5% CO₂. The materials used for this study are in table 2-1.

Table 2-1 Materials and reagents

Materials	Sources
0.4% v/v trypan blue solution	Sigma-Aldrich, UK
3-(4, 5-dimethylthiazolyl-2)-2, 5-diphenyltetrazolium bromide (MTT), Hybri-Max™ dimethyl sulphoxide (DMSO),	Sigma-Aldrich, UK
Antibiotic (penicillin/streptomycin)	Sigma-Aldrich, UK
Automated cell counter™	Fisher Scientific -UK
Caspase 3/7, Caspase -8, and Caspase-9 Glo kits	Promega, Southampton, UK
Cell counting chamber slides (Countess)	Sigma Aldrich, UK
Fas Ligand human (FasL)	Sigma Aldrich, Poole, UK

Foetal Bovine Serum (FBS)	Sigma Aldrich, Poole, UK
Huh7 cell lines	European Collection of Authenticated Cell Cultures (ECACC)
Hybrid-Max™ dimethyl sulphoxide (DMSO),	Sigma Aldrich, UK
Inactivated foetal bovine serum (FBS)	Sigma-Aldrich, UK
Microtiter plate reader (FLUOstar Omega)	BMG LABTECH, UK
Multi-channel pipette	Sarstedt, Numbrecht, Germany
Nunc™ 96 Well Plate Polystyrene	Thermo Scientific, IL, USA
Nunc™ F96 Microwell™ White Polystyrene Plate	Thermo Scientific, IL, USA
Phosphate –buffer saline (PBS) powder,	Sigma-Aldrich, UK
Staurosporine	Sigma-Aldrich, UK
Sterile pipettes (5,10,25 and 50 ml)	Sarstedt, Numbrecht, Germany
T25, T75 culture flask	Sigma-Aldrich, UK
Troglitazone (TGZ)	Sigma Aldrich. UK
Trypsin-EDTA solution	Sigma-Aldrich, UK

2.1.2 Materials for *in silico* studies

2.1.2.1 Software

In this study, Snoopy software is used to model and animate or simulate hierarchical charts and Petri nets. There are three main classes of Petri net: standard Petri nets (PN), extended Petri nets (xPN) and extended stochastic Petri nets (xSPN) (Rohr *et al.*, 2010). Snoopy is adaptable as its basic design enables the execution of new graph styles. It is adaptive by supporting the simultaneous use of several graphical techniques while the GUI adapts animatedly to the graph type in the active window (Rohr *et al.*, 2010). Snoopy is platform-independent and can run on Mac OS X, Windows, and Linux. Another essential software for this study is the Multi Formalism Interaction Network Simulator (MUFINS) (Wu *et al.*, 2016). It consists of a suite of 24 tools that enable the execution of a wide range of analysis systems, and it is bundled with JyMet, a Graphical User Interface (GUI), allowing MUFINS to be used by both technical experts and non-specialists (Wu *et al.*, 2016). The tools within MUFINS can be grouped as follows: Flux balance analysis (FBA), phenotypic phase plane (PhPP), dynamic FBA (dFBA), flux variability analysis (FVA), differential producibility analysis (DPA), fermentation equation (FBA precursor) Gene/Reaction Perturbation: Gene Deletion Analysis, Gene Interactions, Omic Constraints: Gene inactivity is moderated by metabolism and expression (GIMME).

Regulation: Regulatory FBA (rFBA), linear inhibitor and activator constraints, integrated FBA (id FBA), integrated FBA (idFBA), integrated FBA (iFBA), quasi-steady-state Petri nets (QSSPN) make it possible to construct constraint-based model (Wu *et al.*, 2016).

2.1.2.2 File setups

Petri nets could be designed with Snoopy, saved and uploaded in a Snoopy-specific file format using XML technology (Rohr *et al.*, 2010). However, the file formats diverge to some extent for each Petri net group and are classically denoted by distinct extensions, such as spped (PN), spt (xPN). Snoopy offers built-in animation as well as random variable simulation, and these are used in this study. As listed in the previous section (Rohr *et al.*, 2010), Snoopy provides a constant

simulation of continuous Petri nets and exports them for various analyses, as listed in the previous section (Rohr *et al.*, 2010). The Petri net, as well as simulation plots, can be saved in an encapsulated postscript (eps) set-up.

2.1.2.3 Sample file

The Petri net used can be downloaded freely for non-profit academic research purposes at <http://www.informatik.tu-cottbus.de/software/snoopy.html> (Rohr *et al.*, 2010). The MUFIN version of SFBA can be found at: <http://sysbio3.fhms.surrey.ac.uk/mufins>. The computational experiment discussed in this study could be repeated by downloading Snoopy to open model files and following the stages defined in the subsequent section.

2.2 Methods

2.2.1 Systems biology

Having identified the possible TGZ metabolic and non-metabolic pathways, a Petri net was used to represent these pathways graphically. The model was constructed using SNOOPY (a tool used to animate and simulate a hierarchical graph-based system). A Petri net is a controlled two-part graph with nodes that symbolise transitions and places (Heiner *et al.*, 2012). The Petri net operates on a graphical notation where circles represent places, rectangles represent transitions, edges are illustrated as arrows, and tokens are denoted as dots or numbers drawn within place symbols. Directed edges link places to transitions and transitions to places. Each place in the Petri net may contain a non-negative integer number of tokens connected to it (Figure 2-1) (Heiner *et al.*, 2012).

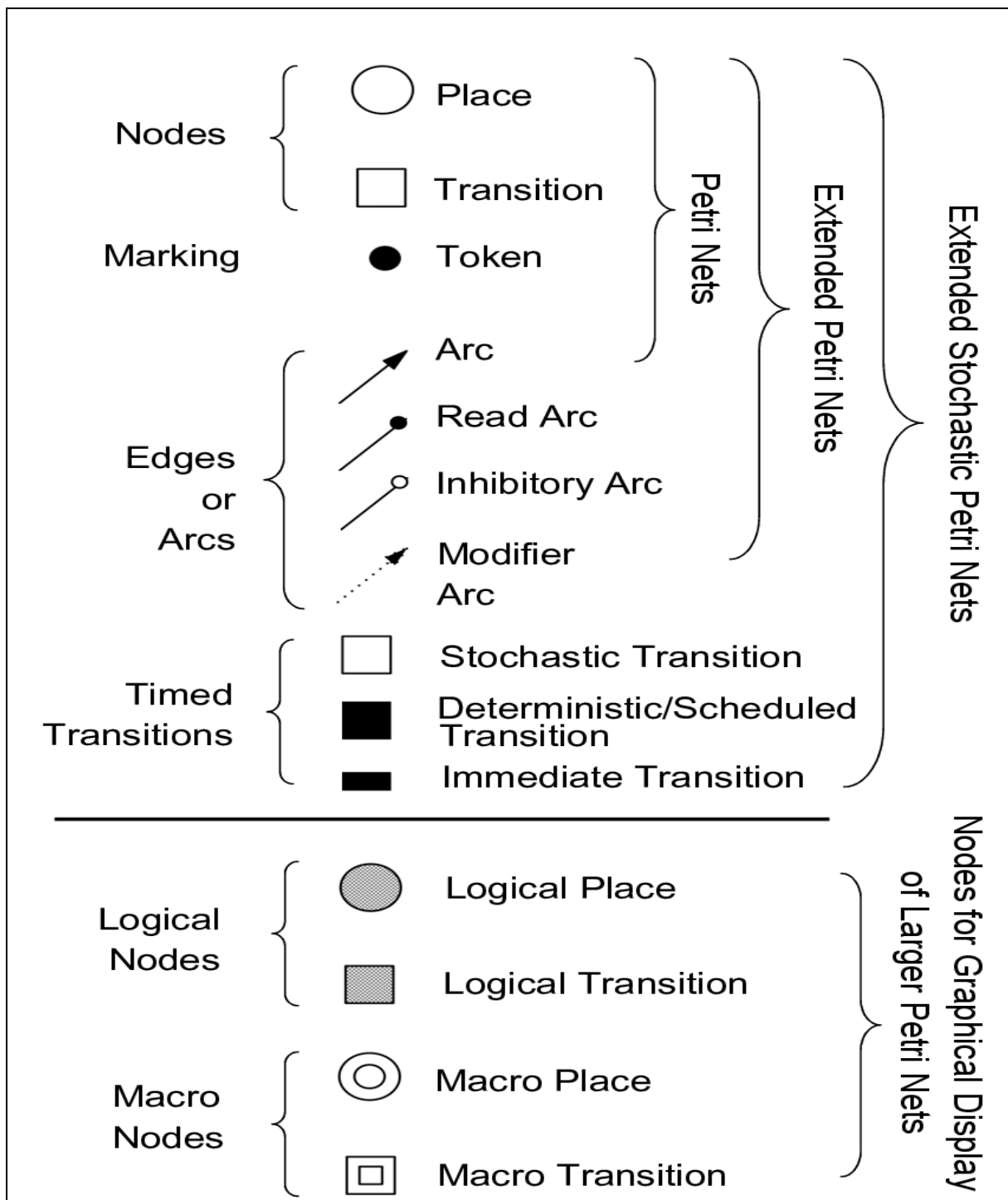
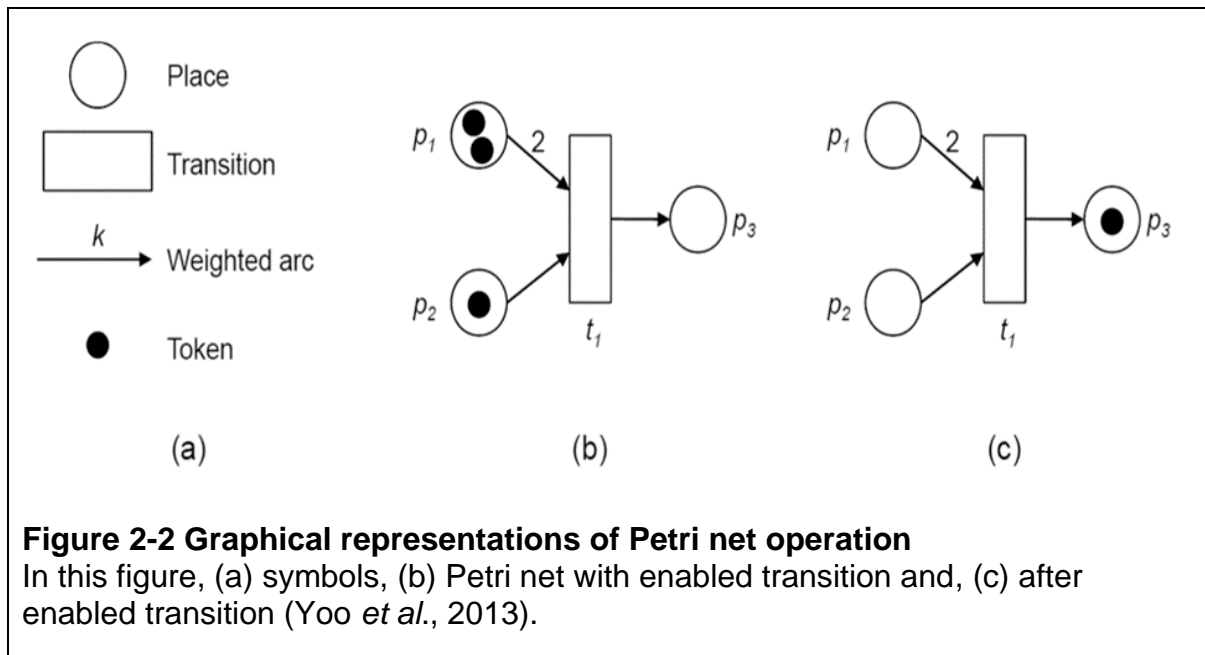


Figure 2-1 Petri net elements and their graphical representation

Petri nets are weighted, fixed-two-part graphs made up of nodes and arcs. Arcs join the nodes, the places as well as the transitions. An arc links a place with a transition or in reverse; however, two transitions or "places" cannot connect. Places can hold tokens while "transitions" cannot contain any tokens. Standard Petri net arcs are made of places, transitions, and standard arcs, adapted (Heiner *et al.*, 20012).

Tokens may be propagated across all places in the Petri net (marking) and represent the system's condition. Upon firing, transitions alter the state of the system by delivering tokens from pre-places to post-places. The number of tokens consumed from the given pre-places is shown by the weight of an edge connecting with the transition, while the number of tokens delivered to the post-place is indicated by the weight of the edge connecting the "transition" and post-places (Figure 2-2). The "transition" may fire when all the pre-places hold enough tokens (Yoo *et al.*, 2013).



2.2.1.1 The read arcs

The read arcs are also called test arcs. They are graphically symbolised by black dots as arch heads, requesting tokens in a place demonstrating progressive side-conditions, for instance, the conformation of a protein complex that may regulate whether a reaction is feasible or a specific physiological state of a cell that may predict if a cell is responsive to particular triggers. The test place requires no fewer than many tokens as provided by the read arc's collection to facilitate a transition. Animating the "transition" may not alter the number of tokens in a tested place (Heiner *et al.*, 2012). Two different arcs may simulate a read arch. Although a read arc and two different arcs have the same total effect, there is an indirect semantic variation that renders it suitable to represent molecular mechanisms within a

biochemical network. For instance, enzyme A catalyses the reaction of substrates K to produce M (Heiner *et al.*, 2012). Then A is transiently consumed by forming the enzyme-substrate complex and reformed as the enzyme-product complex decays to form M. Such an enzymatic reaction is represented in a mechanism-oriented design by two reverse arcs if the development and decay of the enzyme-substrate complex are not overtly exhibited (Heiner *et al.*, 2012).

Conversely, read arcs are suitable for conditions where an unphosphorylated receptor (M) autophosphorylates (M-P) because of a conformational change to M (Heiner *et al.*, 2012). The token in M represents the active conformation of the receptor, which is not rapidly utilised. Therefore, the token remains in M (Heiner *et al.*, 2012).

2.2.1.2 Inhibitory arcs

A hollow dot graphically represents inhibitory arcs as arc heads and indicates negative side-conditions in an abstract concentration level, such as when the presence of a specific protein, such as a distinct inhibitory component or a protein complex, constrains a specific reaction or process (Heiner *et al.*, 2012). To enable transition, the inhibiting place would contain fewer tokens than provided by the diversity of the inhibitory arc. The transition's activation would have no effect on the number of tokens on the inhibiting place. Standard Petri nets can only simulate inhibitory arcs if the inhibiting places are bounded, that is, the number of tokens does not exceed a given finite number. In this instance, it strictly enhances precision (Heiner *et al.*, 2012).

2.2.1.3 Animation of qualitative Petri nets in snoopy

After creating the Petri net, the incorporated animation of the movement of tokens may present initial insight into the dynamic behaviour and the interconnection of the model. Snoopy visualises the activity of tokens, allowing for any easy command. The animation may be initiated by hand or set automatically with altered firing strategies such as a single step, where a single transition is arbitrarily selected, an intermediate step, and this forms an arbitrary subgroup of synchronised transitions, or a maximal step, where a maximal set of synchronised transitions is arbitrarily selected (Figure

2-3) (Heiner *et al.*, 2012; Rohr *et al.*, 2010). The panel menu on the left allows selecting the type of graph element to be created. The drawing window in the middle shows the Petri net under construction. The window on the right belongs to the place selected in the drawing window and allows for editing the properties in place.

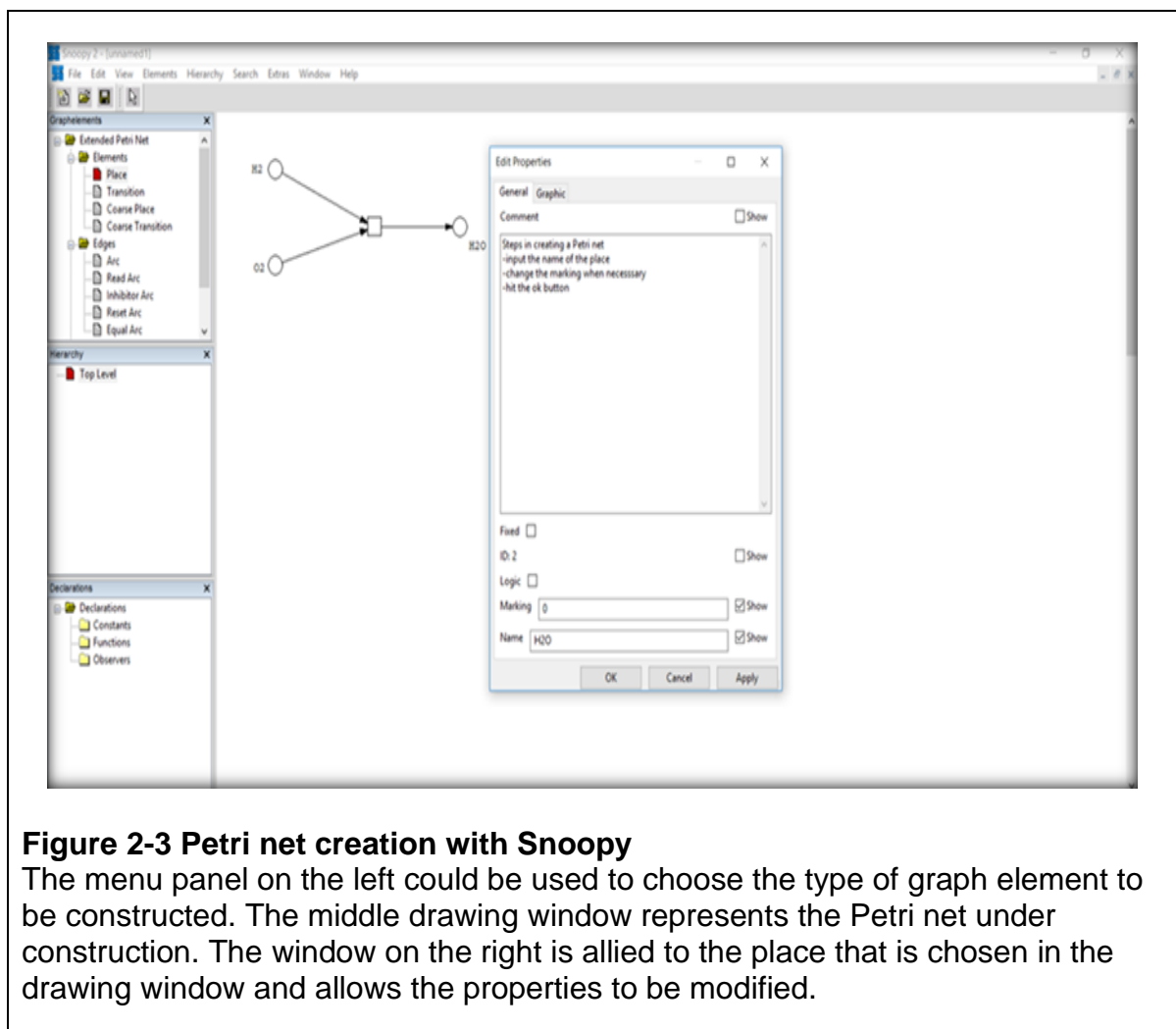


Figure 2-3 Petri net creation with Snoopy

The menu panel on the left could be used to choose the type of graph element to be constructed. The middle drawing window represents the Petri net under construction. The window on the right is allied to the place that is chosen in the drawing window and allows the properties to be modified.

2.2.2 The non-metabolic pathways of TGZ-induced hepatotoxicity

The non-metabolic pathway is also a complex function of drug-protein interactions in the liver. For instance, TGZ activates PXR. The activated PXR forms a heterodimer with the retinol x-receptor and binds to the hormone response element on the DNA of PXR target genes (Brewer & Chen, 2016). This, in turn, upregulates phase II conjugation enzymes as well as the induction of phase I oxidative enzymes and subsequent degradation of PXR target genes, as shown in a screenshot (Figure 2-

4). As discussed in the previous section, various theoretical systems have obtained significant results in modelling mechanistically various levels of cellular organisation, such as metabolic, signalling, and gene regulatory networks.

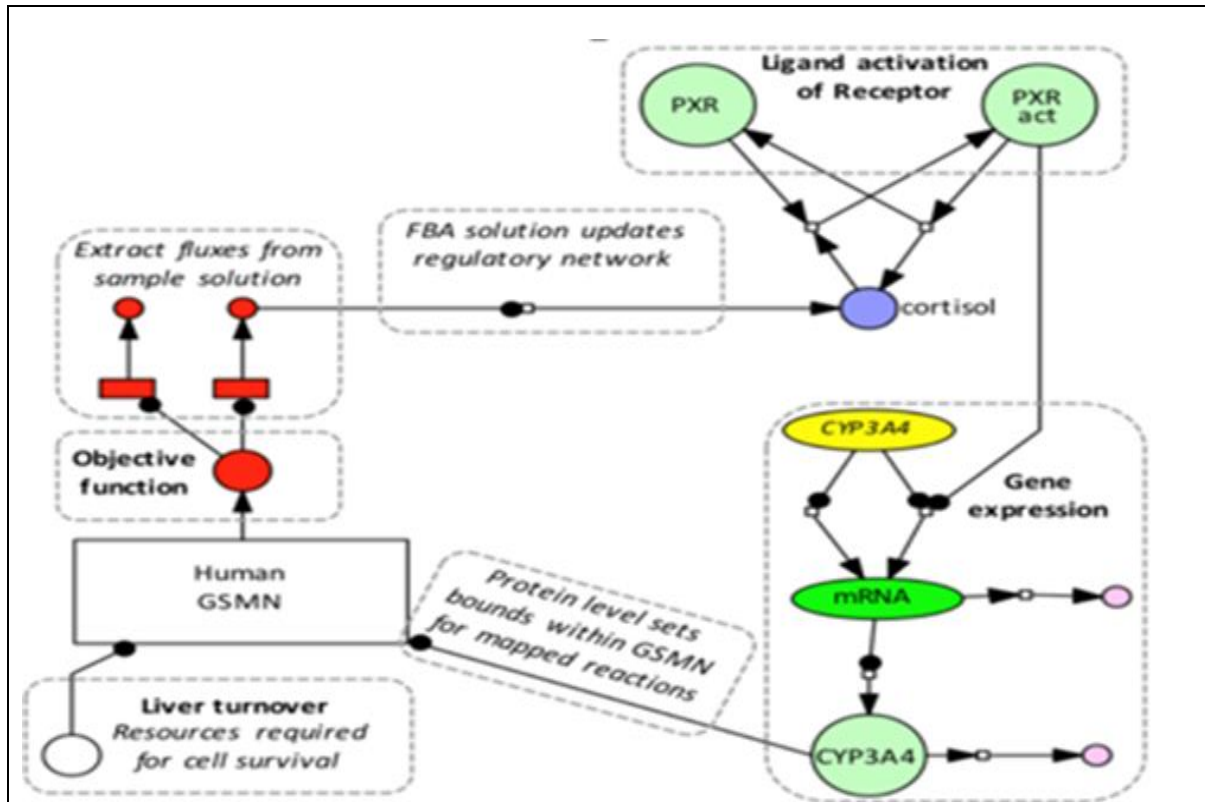


Figure 2-4 Overview of the Quasi-State Petri net approach

QSSPN incorporates a genome-scale metabolic network (e.g., recon2 human GSMN) incorporates a dynamic regulatory system represented in a Petri net. Flux balance analysis is used to explore the solution space for a given objective function, reverting to an optimal solution. In this case, the solution space is further constrained by the need to meet a biomass constraint, representing cellular resources required for survival (e.g., amino acids). Stimulation of the system by a ligand (cortisol) leads to the activation of its cognate receptor (PXR) and a gene regulatory cascade. This results in alterations in the encoded protein level (CYP3A4), which in turn informs the upper and lower bounds within the GSMN for any reactions catalysed by that protein. Fluxes are extracted from FBA sample solution and employed to update the status of the regulatory network, effecting the cycle of stimulus -response-return to baseline (Wu *et al.*, 2016).

2.2.2.1 Using SurreyFBA for metabolic analysis

As discussed in the previous section, a variety of theoretical techniques have obtained significant results in mechanistically modelling various levels of cellular systems, such as metabolic signalling, including gene regulatory networks (Wu *et al.*, 2016). In a real cell, all these methods progress concurrently, and without multi-scale simulation, the awareness and predictive strength delivered by models will be restricted (Wu *et al.*, 2016). For example, the Petri net was described as a model for systems that exhibit simultaneous asynchronous activities. More specifically, the limitation on Petri net modelling is less modelling and predictive power. Also, Petri net cannot be used to test for a specific marking in an unbounded place, as well as an inability to determine a zero marking in a place.

Interestingly, whereas Petri net is limited in this application, MUFINS is the first application to answer this problem of multi-formalism simulation. Unique algorithms accessible in MUFINS, present answers to significant technical challenges such as integrating CBM and hybrid deterministic dynamic simulation, integrated signalling, or metabolic models (Wu *et al.*, 2016). It allows the study of broad clinical transcriptome analyses in the GSMN framework (Wu *et al.*, 2016).

Having created the model in the Petri net, it was saved and determined the Surrey FBA reaction. The reaction table lists the following: reaction description, reaction formula comprising abbreviated names of metabolites, lower flux bound, upper flux limits, and the regulations linked to genes. The Comments section contains any free reaction text description displayed in a screenshot (Table 2-2). Comments were used to categorise reactions of interest. The reaction queries were found in the "Edit->search" simulation results tables.

Table 2-2 SurreyFBA analysis displaying metabolic reactions

ID	Equation	LB	UB	Rule	Comment
R_TGZ_ext	M_TGZ_c = M_TGZ_it	-1000.0	1000.0		#TGZ exchange reaction
R_TGZshuffle	M_TGZ_c = M_TGZ_r	-1000.0	1000.0		#TGZ transport between cytosol and ER
R_TGZquinone_ext	M_TGZquinone_r = M_TGZquinone_it	0.0	1000.0		#TGZ quinone exchange reaction
R_TGZquinone	M_TGZ_r = M_TGZquinone_r + M_h_r	0.0	1000.0		#TGZ quinone formation by CYP3A4
R_10FTHF5GLUit	M_10thf5glu_c = M_10thf5glu_l	0.0	1000.0		#5-glutamyl-10FTHF transport, lysosomal: M_10thf5glu
R_10FTHF5GLUtm	M_10thf5glu_m = M_10thf5glu_c	0.0	1000.0		#5-glutamyl-10FTHF transport, mitochondrial: M_10thf5glu
R_TGZglc	M_TGZ_r + M_udpgluc_r = M_TGZglc_r + M_udp_r	0.0	1000.0		#TGZ glucuronidation by GST1A
R_TGZglc_ext	M_TGZglc_r = M_TGZglc_it	0.0	1000.0		#TGZ glucuronide exchange reaction
R_10FTHF6GLUit	M_10thf6glu_c = M_10thf6glu_l	0.0	1000.0		#6-glutamyl-10FTHF transport, lysosomal: M_10thf6glu
R_10FTHF6GLUtm	M_10thf6glu_m = M_10thf6glu_c	0.0	1000.0		#6-glutamyl-10FTHF transport, mitochondrial: M_10thf6glu
R_10FTHF7GLUit	M_10thf7glu_c = M_10thf7glu_l	0.0	1000.0		#7-glutamyl-10FTHF transport, lysosomal: M_10thf7glu
R_10FTHF7GLUtm	M_10thf7glu_m = M_10thf7glu_c	0.0	1000.0		#7-glutamyl-10FTHF transport, mitochondrial: M_10thf7glu
R_10FTHfI	M_10thf_c = M_10thf_l	-1000.0	1000.0		#10-Formyltetrahydrofolate lysosomal transport via diff
R_10FTHfM	M_10thf_c = M_10thf_m	-1000.0	1000.0		#10-Formyltetrahydrofolate mitochondrial transport via diff
R_11DOCRTSLtm	M_11doctsl_c = M_11doctsl_m	-1000.0	1000.0		#11-deoxycortisol intracellular transport: M_11doctsl_c =
R_11DOCRTSLr	M_11doctsl_c = M_11doctsl_r	-1000.0	1000.0		#11-deoxycortisol intracellular transport: M_11doctsl_c =
R_11DOCRTSTRNtm	M_11doctslm_c = M_11doctslm_m	-1000.0	1000.0		#11-deoxycorticosterone intracellular transport: M_11doct
R_11DOCRTSTRNr	M_11doctslm_c = M_11doctslm_r	-1000.0	1000.0		#11-deoxycorticosterone intracellular transport: M_11doct
R_13DAMPPOX	M_13damp_c + M_h2o_c + M_o2_c = M_bampald_c + M_h2	0.0	1000.0	(8639.1) OR (26.1) OR (31.	#1.3-Diaminopropane oxygen oxidoreductase (deaminati
R_1MNCAMi	M_1mncam_c + M_atp_c + M_h2o_c + 2.0 M_h_c = M_1mnc	0.0	1000.0		#N1-Methylnicotinamide transport: M_1mncam_c + M_atp
R_1PPDCRp	M_1ppdn2c_x + M_h_x + M_nadh_x = M_Lpipecol_x + M_nad_x	0.0	1000.0		#delta1-piperidine-2-carboxylate reductase, peritosoma
R_1a25DHVTD3TRn	M_1a25dhvtd3_c = M_1a25dhvtd3_n	0.0	1000.0		#translocation of 1-alpha,25-Dihydroxyvitamin D3 to nuclei
R_1a_24_25VITD2Hm	M_2425dhvtd2_m + M_h_m + M_nadph_m + M_o2_m = M_1a	0.0	1000.0		#1-alpha-Vitamin D-24,25-hydroxylase (D2): M_2425dhvit
R_1a_24_25VITD3Hm	M_2425dhvtd3_m + M_h_m + M_nadph_m + M_o2_m = M_1a	0.0	1000.0		#1-alpha-Vitamin D-24,25-hydroxylase (D3): M_2425dhvit
R_1a_25VITD2Hm	M_1a25dhvtd2_m + M_h_m + M_nadph_m + M_o2_m = M_1a	0.0	1000.0		#1-alpha,24R,25-Vitamin D-hydroxylase (D2): M_1a25dhv
R_1a_25VITD3Hm	M_1a25dhvtd3_m + M_h_m + M_nadph_m + M_o2_m = M_1a	0.0	1000.0		#1-alpha,24R,25-Vitamin D-hydroxylase (D3): M_1a25dhv
R_24NPHte	M_24nph_e = M_24nph_c	-1000.0	1000.0		#entibiotic transport: M_24nph_e = M_24nph_c
R_24_25DHVITD2i	M_2425dhvtd2_c = M_2425dhvtd2_e	0.0	1000.0		#24,25-Dihydroxyvitamin D2 transport from cytoplasm: M
R_24_25DHVITD2tm	M_2425dhvtd2_m = M_2425dhvtd2_c	0.0	1000.0		#24,25-Dihydroxyvitamin D2 transport from mitochondria:
R_24_25DHVITD3i	M_2425dhvtd3_c = M_2425dhvtd3_e	0.0	1000.0		#24,25-Dihydroxyvitamin D3 transport from cytoplasm: M
R_24_25DHVITD3tm	M_2425dhvtd3_m = M_2425dhvtd3_c	0.0	1000.0		#24,25-Dihydroxyvitamin D3 transport from mitochondria:
R_24_25VITD2Hm	M_25hvitd2_m + M_h_m + M_nadph_m + M_o2_m = M_2425d	0.0	1000.0	(1591.1)	#24R-Vitamin D-25-hydroxylase (D2): M_25hvitd2_m + M
R_24_25VITD3Hm	M_25hvitd3_m + M_h_m + M_nadph_m + M_o2_m = M_2425d	0.0	1000.0	(1591.1)	#24R-Vitamin D-25-hydroxylase (D3): M_25hvitd3_m + M
R_25HVITD2i	M_25hvitd2_c = M_25hvitd2_e	0.0	1000.0		#25-hydroxyvitamin D2 transport from cytoplasm: M_25hvit
R_25HVITD2tm	M_25hvitd2_m = M_25hvitd2_c	0.0	1000.0		#25-hydroxyvitamin D2 transport from mitochondria: M_25hvit

The external metabolites that reflect metabolic flow sources and drops were identified. Excluding external metabolites, the FBA model cannot determine any value apart from 0, since there will be no metabolic flux source. In this case, "_b" was used as a tag at the end of the metabolite name to indicate an external metabolite. In SurreyFBA, this tag was used to define external metabolites by clicking "Solve->Externality tag" in the JyMet menu and typing "_b" in the dialogue box displayed in the screenshot (Table 2-3).

Table 2-3 Table showing external metabolite tag dialogue box

The screenshot shows the jMet2.34 software interface. At the top, there is a menu bar (File, Edit, View, Analyse, Solve, QSSPN, Help) and a toolbar with options for Direction (max), Objective, Solver (Simplex), Reduce matrix, and Comments. Below this is a summary bar showing 2169 genes, 0 enzymes, 7451 reactions, and 5775 metabolites. The main window displays a table of reactions with columns for ID, Equation, LB, UB, Rule, and Comment. An 'Input' dialog box is open in the center, with the text 'Enter the tag indicating external metabolites' and a text input field containing the number '0'. The dialog has 'OK' and 'Cancel' buttons.

ID	Equation	LB	UB	Rule	Comment
R_TGZ_ext	M_TGZ_c = M_TGZ_xt	-1000.0	1000.0		# TGZ exchange reaction
R_TGZshutte	M_TGZ_c = M_TGZ_r	-1000.0	1000.0		# TGZ transport between cytosol and ER
R_TGZquinone_ext	M_TGZquinone_r = M_TGZquinone_xt	0.0	1000.0		# TGZ quinone exchange reaction
R_TGZquinone	M_TGZ_r = M_TGZquinone_r + M_h_r	0.0	1000.0		# TGZ quinone formation by CYP3A4
R_10FTHF5GLUj	M_10thf5glu_c = M_10thf5glu_j	0.0	1000.0		#5-glutamyl-10FTHF transport, lysosomal: M_10thf5glu
R_10FTHF5GLUm	M_10thf5glu_m = M_10thf5glu_c	0.0	1000.0		#5-glutamyl-10FTHF transport, mitochondrial: M_10thf5glu
R_TGZglc	M_TGZ_r + M_udpgluc_r = M_TGZglc_r + M_udp_r	0.0	1000.0		# TGZ glucuronidation by GST1A
R_TGZglc_ext	M_TGZglc_r = M_TGZglc_xt	0.0	1000.0		# TGZ glucuronide exchange reaction
R_10FTHF6GLUj	M_10thf6glu_c = M_10thf6glu_j	0.0	1000.0		#6-glutamyl-10FTHF transport, lysosomal: M_10thf6glu
R_10FTHF6GLUm	M_10thf6glu_m = M_10thf6glu_c	0.0	1000.0		#6-glutamyl-10FTHF transport, mitochondrial: M_10thf6glu
R_10FTHF7GLUj	M_10thf7glu_c = M_10thf7glu_j	0.0	1000.0		#7-glutamyl-10FTHF transport, lysosomal: M_10thf7glu
R_10FTHF7GLUm	M_10thf7glu_m = M_10thf7glu_c	0.0	1000.0		#7-glutamyl-10FTHF transport, mitochondrial: M_10thf7glu
R_10FTHFj	M_10thf_c = M_10thf_j	0.0	1000.0		#10-Formyltetrahydrofolate lysosomal transport via diffus
R_10FTHFm	M_10thf_c = M_10thf_m	0.0	1000.0		#10-Formyltetrahydrofolate mitochondrial transport via dif
R_11DOCRSLtm	M_11doctsl_c = M_11doctsl_m	0.0	1000.0		#11-deoxycofisol intracellular transport: M_11doctsl_c =
R_11DOCRSLr	M_11doctsl_c = M_11doctsl_r	0.0	1000.0		#11-deoxycofisol intracellular transport: M_11doctsl_c =
R_11DOCRSTRNm	M_11doctsl_m = M_11doctsl_r	0.0	1000.0		#11-deoxycofisol intracellular transport: M_11doctsl_m =
R_11DOCRSTRNr	M_11doctsl_r = M_11doctsl_m	0.0	1000.0		#11-deoxycofisol intracellular transport: M_11doctsl_r =
R_13DAMPPOX	M_13damp_c = M_h2o_c + M_o2_c = M_bampald_c + M_h2	0.0	1000.0	(8639.1) OR (26.1) OR (31.	#1.3-Diaminopropane oxygen oxidoreductase (deaminat
R_1MNCAMb	M_1mncam_c = M_atp_c + M_h2o_c + 2.0.M_h_c = M_1mnc	0.0	1000.0		#11-Methylnicotinamide transport: M_1mncam_c = M_atp
R_1PPDCRp	M_1ppidr2c_x + M_h_x + M_nadh_x = M_lpipecol_x + M_nad_x	0.0	1000.0		#delta1-piperidine-2-carboxylate reductase, peroxosoma
R_1a25DHVTD3Trn	M_1a25dhvtd3_c = M_1a25dhvtd3_n	0.0	1000.0		#translocation of 1-alpha-25-Dihydroxyvitamin D3 to nucle
R_1a_24_25VTD2Hm	M_2425dhvtd2_m + M_h_m = M_nadh_m + M_o2_m = M_1a	0.0	1000.0		#1-alpha-Vitamin D-24,25-hydroxylase (D2): M_2425dhvtd
R_1a_24_25VTD3Hm	M_2425dhvtd3_m + M_h_m = M_nadh_m + M_o2_m = M_1a	0.0	1000.0		#1-alpha-Vitamin D-24,25-hydroxylase (D3): M_2425dhvtd
R_1a_25VTD2Hm	M_1a25dhvtd2_m + M_h_m = M_nadh_m + M_o2_m = M_1a	0.0	1000.0		#1-alpha,24R,25-Vitamin D-hydroxylase (D2): M_1a25dhv
R_1a_25VTD3Hm	M_1a25dhvtd3_m + M_h_m = M_nadh_m + M_o2_m = M_1a	0.0	1000.0		#1-alpha,24R,25-Vitamin D-hydroxylase (D3): M_1a25dhv
R_24HPhle	M_24nph_e = M_24nph_c	-1000.0	1000.0		#xenobiotic transport: M_24nph_e = M_24nph_c
R_24_25DHVTD2i	M_2425dhvtd2_c = M_2425dhvtd2_e	0.0	1000.0		#24,25-Dihydroxyvitamin D2 transport from cytoplasm: M_
R_24_25DHVTD2m	M_2425dhvtd2_m = M_2425dhvtd2_c	0.0	1000.0		#24,25-Dihydroxyvitamin D2 transport from mitochondria
R_24_25DHVTD3i	M_2425dhvtd3_c = M_2425dhvtd3_e	0.0	1000.0		#24,25-Dihydroxyvitamin D3 transport from cytoplasm: M_
R_24_25DHVTD3m	M_2425dhvtd3_m = M_2425dhvtd3_c	0.0	1000.0		#24,25-Dihydroxyvitamin D3 transport from mitochondria
R_24_25VTD2Hm	M_25hvt2_m + M_h_m = M_nadh_m + M_o2_m = M_2425d	0.0	1000.0	(1591.1)	#24R-Vitamin D-25-hydroxylase (D2): M_25hvt2_m + M_
R_24_25VTD3Hm	M_25hvt3_m + M_h_m = M_nadh_m + M_o2_m = M_2425d	0.0	1000.0	(1591.1)	#24R-Vitamin D-25-hydroxylase (D3): M_25hvt3_m + M_
R_25HVTD2i	M_25hvt2_c = M_25hvt2_e	0.0	1000.0		#25-hydroxyvitamin D2 transport from cytoplasm: M_25hvt
R_25HVTD2m	M_25hvt2_m = M_25hvt2_c	0.0	1000.0		#25-hydroxyvitamin D2 transport from mitochondria: M_25hvt

The "Essential Reactions" method of SurreyFBA checks the essentiality of every reaction in the system. For each reaction, the programme controls the flux through this reaction to 0 and calculates the maximal value of the objective function. If inactivation of a defined reaction results in the objective function flux equalling 0, the reaction is reported as essential. In other words, the software reports reactions that must be active to achieve a specific metabolic objective, for instance, growth that is chemically feasible.

2.2.2.2 General description of the SurreyFBA software

The software could be used to run the essentiality scan reaction by clicking "Analyse->Essential" reactions. The calculations will take about 10 minutes. You will see the following screen: The results are saved to a file using "File->Save table.". "xls" and the extension would open in Excel. Flux balance analysis could be

performed by selecting "Analyse->FBA" and then "Solve->solve". This could be filtered and sorted by regulatory network fluxes. "Edit->search" could be used to filter all reactions tagged with the "@regnet" string. Subsequently, clicking the "Transition rate" header could categorise these reactions by flux to identify all regulatory network reactions with non-zero flux in an organism. In this case, all non-zero reaction names and fluxes could be selected in a reaction to a given solution (Wu *et al.*, 2016). "View->Layout->hierarchical" is clicked to visualise these fluxes with the automatic, hierarchical layout. The network could be visualised in a Petri net (two-part graph) representation, with rectangles representing transitions and circles representing places. Flux values could be written within the reaction rectangle; line thickness could be used to visualise fluxes. The layout could be adjusted manually, and the configuration saved with the "File->Save graph" function. The graph would then be used to visualise results with "Visualise->Layout->custom". The graph layout also acts as a reaction name filter. This visualisation mode is ideal for visualising effective pathways emerging in genome-scale networks under certain conditions (Wu *et al.*, 2016).

2.2.3 *In vitro* assay

2.2.3.1 Cell culturing

Cells were subcultured when they reached a confluent of 70–90%. The routine culture was carried out in T75 culture flasks with a surface area of 75 cm² and the volumes reflected the surface area of the flask. The culture medium was aspirated from the cells. Cells were washed with 10 ml of sterile phosphate-buffered saline (PBS) to remove traces of media as Huh7 cells were adherent, and then with 2 ml of 0.05% trypsin-EDTA. The cells were incubated at 37 °C for 3-6 minutes for detachment. After the cells were detached, fresh culture medium (8 ml) was added to prevent trypsin action. The suspended cells were transferred to a 15 ml falcon tube and centrifuged at 600 x g for 5 minutes. The supernatant was removed, and the cell pellet was re-suspended in the fresh culture medium. Soft pipetting action was employed to expedite the dispersal and dissociation of small cell clumps into separate cells. Cells were split as required, either into a fresh T75 culture flask to preserve stock or an experiment (Freshney, 2010).

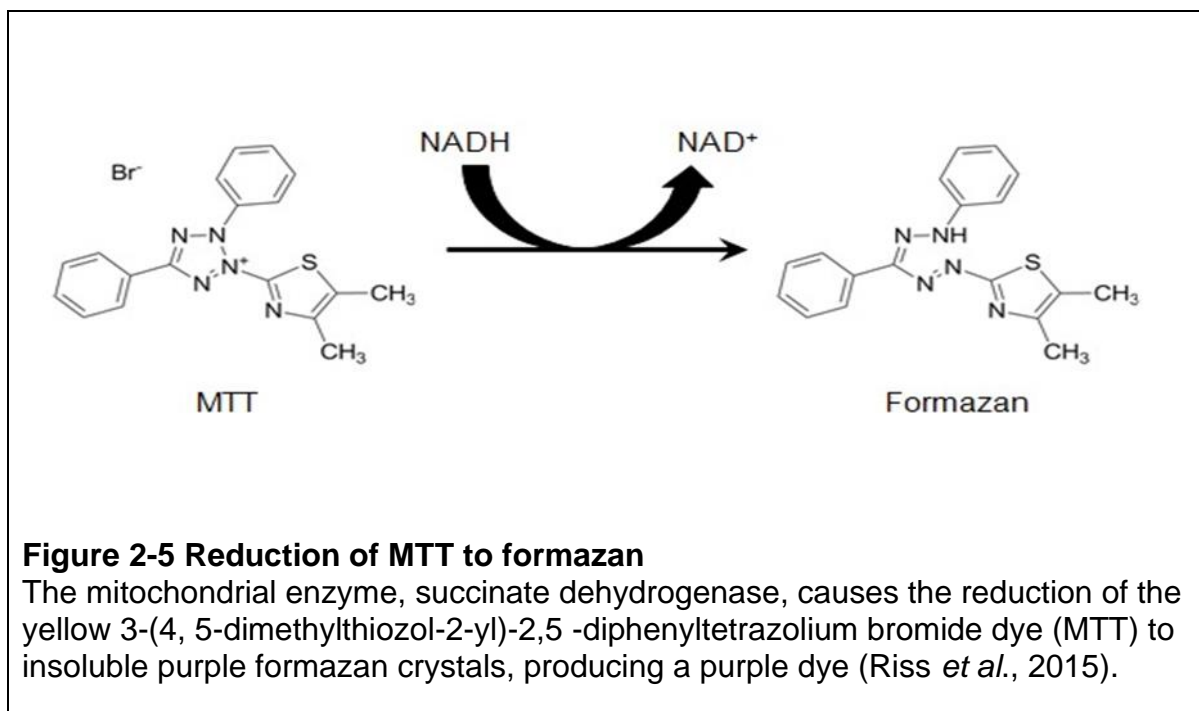
2.2.3.2 Cryopreservation and thawing of cells

Cells were preserved in liquid nitrogen to keep stock availability. Cells can be stored in liquid nitrogen for several years without any loss in viability. Cells reaching a log phase (70-80% confluent) were detached with the trypsin described in the previous section. The cell pellet was resuspended to 1×10^6 cells/ml in a freezing medium made of 10% DMSO and 90% FBS, v/v, and transferred into cryovials (1 ml/vial). The cryovials were placed on ice for 30 minutes before being transferred to a Nalgene® Cryo 1 °C Freezing container with alcohol and kept in a -80 °C freezer for 24 hrs. to gently freeze the cells before being transferred to liquid nitrogen. To recover frozen cells, they were removed from liquid nitrogen and placed in a 37 °C pre-warmed water bath. When thawed, the contents were transferred to a 15 ml centrifuge tube containing a pre-warmed medium. The cell suspension was centrifuged at 300 x g for 5 minutes. The supernatant was removed, and the pellet was resuspended in 10 ml of complete culture medium and transferred to a T25 culture flask and incubated. The culture medium was replaced after 24 hrs. (Freshney, 2010).

2.2.4 Determination of TGZ on cell viability using MTT assay

Huh7 cells were seeded at 25000 per well in 96-well plates, plus 200 µL of the cell media. The cells were incubated at 37 °C, 5%, CO₂ / 95% air for 24 and 48 hrs to allow adherence to the plates. Cells were observed under the microscope to check growth and considered ready for treatment when they were 70- 80% confluent. Cells were treated with various concentrations of TGZ, including very low physiological concentrations (0.1-50µM) and incubated for 24 hrs. For the last two hrs of the incubation period, the yellow 3-(4, 5-dimethylthiazol-2-yl)-2,5 -diphenyltetrazolium bromide dye (MTT) reagent was dissolved in sterile PBS to a concentration of 5 mg/ml and filtered. It was kept at 4 °C protected from the light because it is photosensitive (Riss *et al.*, 2015; Sliwka *et al.*, 2016; Stockert *et al.*, 2012; Yin *et al.*, 2005). Comparing the number of control cells to the quantity produced by cells exposed to a specific agent can measure the effectiveness of the agent in the induction of cytotoxicity and was determined by the creation of a dose-response curve. Absorbance was read with a spectrophotometer (plate reader) at a

wavelength of 540 nm. Wells containing 10 μ L DMSO were read as a background reading and its absorbance was deducted from all values. Absorbance was expressed as a percentage of vehicle control. Mean absorbance values of each TGZ concentration were calculated from each independent experiment. Results were expressed as viability percentage compared to the control. All experiments were conducted at least three independent repeats.



2.2.5 Determination of doubling time of Huh7 cells under various conditions

Having determined the Huh7 cells were seeded in 12-well plates at 25,000 per well with 1000 μ L of the medium. The cells were incubated at 37 $^{\circ}$ C with 5% CO₂ /95% air for 24 hrs to allow adherence to the plates. Cells were then incubated in complete medium (medium containing 10% FBS), serum-free medium, or serum-free medium containing 15 μ M TGZ. Cell counting was carried out every six hrs until 60 hrs using an Invitrogen automated cell counter (countess). Three independent repeats were carried out, using four wells for each condition. The mean values were determined and plotted as a log (log number of cells).

2.2.6 Determination of Vitamin C cytoprotective concentration in Huh7 cells.

The procedure in section 2.2.4 was followed to determine the cytoprotective dose of vitamin C in Huh7 cells. Cells were treated with various concentrations of vitamin C (5 to 1000 μM). Negative controls consisting of 50 μM TGZ and 1000 μM H_2O_2 were used. Cell viability was normalised between the range of 100% viable (untreated cells) and 0% viable. All experiments were undertaken in six technical repeats to account for technical variation, and three independent repeats were carried out to account for biological inconsistency. The data was represented as the mean (+SEM) of the three independent experiments, with each experimental treatment being the mean of the technical repeats ($n = 9$). Having determined the cytoprotective dose of vitamin C on Huh7 cells, the combined effect of TGZ (5-50 μM) and the cytoprotective dose of vitamin C (100 μM) on Huh7 cell viability using the method described above was explored.

2.2.7 Assessment of apoptosis by caspase assay

Caspase-Glo 3/7, 8 and 9 are luminescent assays and are used to detect the activity of caspase 3/7, 8 and 9, respectively. The caspase assays provide a luminogenic caspase substrate that contains the tetrapeptide DEVD, LETD, and LEHD for caspase-3/7, caspase-8, and caspase-9, respectively. The aminoluciferin is released upon substrate cleavage by individual active caspases and generates light in a luminescence reaction, which is measured by a luminometer (Mack *et al.*, 2000). Caspase activity was determined following the manufacturer's instructions. In a white 96-well plate, 100 μL medium of Huh7 cells at a density of 1×10^4 cells/well were seeded in a white 96-well plate. The plates were incubated overnight for the cells to adhere. The cells were treated with experimental compounds for 24 hrs. In addition, 1 μM Staurosporine was used as a positive control for both Caspase-3/7 and Caspase-9, whereas 10 μM Fas ligand was used as a positive control for caspase-8 activity.

Before the experiment, the Caspase-Glo reagent was prepared and allowed to equilibrate at room temperature. The 96-well plate was allowed to equilibrate to room temperature, and 100 μL of reagent was added to each well. The plate was gently mixed at 300 rpm for 30 seconds on an orbital shaker and kept at room temperature

for one hour. Luminescence was read by a BMG LABTECHFLUOstar Omega plate reader (Ortenberg, Germany). After 24-hrs of incubation, 100 μ L of caspase-3/7, caspase-8, or caspase-9 probe solution was added to each well and kept at constant room temperature for three hrs. Caspase activity was then measured using a luminometer.

2.2.8 Measurement of CYP3A4 induction

The P450-Glo™ Assay presents a luminescent approach to measure cytochrome P450 (CYP) activity according to the manufacturer's description. The substrates are CYP enzyme substrates that are proluciferins, a by-product of beetle luciferin [(4S)-4,5-dihydro-2-(6'-hydroxy-2'-benzothiazolyl)-4-thiazolecarboxylic acid]. The derivatives are transformed through CYP enzymes into luciferin products. D-luciferin is produced and detected in a subsequent reaction with the luciferin detection reagent. The quantity of light generated in the second reaction is relative to CYP activity. Huh7 cells were plated on white-walled. At a density of 1×10^4 cells per well, 100 μ L of culture medium was added, and the cells were incubated overnight at 37°C for attachment to the plate. Cells were treated with various concentrations of TGZ (5 μ M, 10 μ M, 20 μ M, 30 μ M, 40 μ M and 50 μ M for 48 hrs. Control (untreated cells), CYP3A4 inhibitor (20 μ M clotrimazole) and inducer (20 μ M rifampicin) were included. The luminogenic substrate was added to the medium only to contain a background luminescence. The rest of the experiment was carried out according to the manufacturer's protocol. CYP3A4 induction was measured using a luminometer.

2.2.9 Quantification of ROS by 2',7'- dichlorofluorescein diacetate dye

Huh7 cells were plated in a black 96-well plate at a density of 1×10^4 cells per well with 100 μ L culture medium and incubated overnight at 37 °C for attachment to the plate. Cells were treated with various concentrations of TGZ for 24 hrs. In the last 4 hrs of the incubation period, 1 mM of H₂O₂ was added as a positive control. An hour before the end of the treatment period, 10 μ M of dichlorofluorescein diacetate (DCF-DA) dye was prepared in a phenol red-free culture medium. 100 μ L of DCF-DA was added to each well and incubated for 45 minutes. The fluorescence was read using a SpectraMax Gemini XPS Microplate reader (CA, USA) at 485 and 535 excitation and emission, respectively. The fluorescence intensity of the phenol-free medium (blank)

was subtracted from all the readings. This study determined the cytoprotective dose of vitamin C and then the combined effects of TGZ and vitamin C on ROS production in Huh7 cells. Huh7 cells were exposed to the various concentrations of TGZ (5 to 50 μM), 100 μM vitamin C and 1 mM of H_2O_2 as a positive control.

2.2.10 Quantification of intracellular H_2O_2 in Huh7 cells

A range of ROS, such as superoxide anion, hydrogen peroxide, as well as hydroxyl radical, are produced by the mitochondrial metabolism when oxidative stress occurs. Among diverse ROS, hydrogen peroxide (H_2O_2) is more stable and has a longer half-life, making it ideal for cell culture studies (Kelts *et al.*, 2015). Huh7 cells were seeded in a 96-well plate at a density of 1×10^4 cells per well in a complete medium and incubated overnight to allow the cells to adhere to the plate. After overnight incubation, the cells were treated with various concentrations of TGZ for 24 hrs. The H_2O_2 substrate was thawed and placed on ice. Prior to the final six hrs of the incubation period, 20 μL of H_2O_2 was added to the cells and harmonised. The total volume in each well was 100 μL and the final concentration of H_2O_2 was 25 μM . The plate was incubated for the final six hrs of treatment. The ROS-Glo Detection solution was formulated by adding 1 ml of Luciferin detection reagent to 10 ml of D-Cysteine and 10 ml of signal enhancer solution. The volumes were adjusted proportionally based on the required number of wells. After 20 minutes at room temperature, luminescence was measured with a BMG LABTECH FLUOstar Omega plate reader (Ortengberg, Germany). The H_2O_2 substrate responds to the H_2O_2 present in the system by producing the luciferin precursor that D-cysteine converts to generate a luminescent signal. The amount of signal generated is directly proportional to the quantity of H_2O_2 contained in the cell culture system.

2.2.11 ATP quantification

Intracellular ATP was quantified using an ATP detection kit (Abcam, Cambridge). The assay's mechanism is centred on the phosphorylation of glycerol to produce a product that can easily be quantified colourimetrically (OD 570 nm) or fluorometrically (Ex/Em =535/597). Huh7 cells were harvested at a density of 1×10^6 in a six-well plate and incubated overnight for attachment. Cells were treated with TGZ and incubated for a further 24 hrs. Cells were washed with PBS and

resuspended in 100 μ L ATP assay buffer, homogenised using a sonicator and centrifuged at 13,000 xg for 15 minutes at 4 °C to remove any insoluble particles. The supernatant was then collected in a clean Eppendorf tube, labelled appropriately and kept on ice. The rest of the assay was undertaken following the manufacturer's instructions and measurements were taken using a plate reader at 535 nm / 587nm (Ex/Em).

2.2.12 Urea quantification assay

The Urea Assay Kit (Colourimetric) provides a rapid, simple, precise, and consistent quantification of urea content in various samples, for instance, serum, plasma, urine, or the supernatant of cell culture medium. The assay works through urea, which reacts as a substrate with the compound in the presence of enzymes to produce a product that in turn reacts with the probe to produce colour, which is then measured at an optical density of 570 nm. The optical density of the coloured solution is directly proportional to the amount of urea contained in the solution. Huh7 cells were harvested at a density of 1×10^6 in a six-well plate and incubated overnight for attachment. The cells were treated with TGZ and incubated for a further 24 hrs. Cells were washed with PBS and resuspended in 100 μ L assay buffer solution. Cells were homogenised using a sonicator and centrifuged at top speed for 5 minutes at 4 °C to eliminate any insoluble particles. The supernatant was then collected in a clean Eppendorf tube, labelled appropriately, and kept on ice; the rest of the assay was undertaken following the manufacturer's instructions. Finally, cholesterol output was measured using a BMG LABTECH FLUOstar Omega plate reader (Ortengberg, Germany) at OD 570 nm. Sample background control was deducted from sample values. The mean absorbance value of the blank from each standard and sample values (corrected absorbance) was calculated. The corrected absorbance values for individual standards were plotted as the act of the final concentration of urea. The sample readings were deduced from the standard curve to determine the concentration of urea in various concentrations of TGZ-treated Huh7 cells.

2.2.13 Glutamate dehydrogenase activity assay

Glutamate dehydrogenase (GDH) catalyses the reversible inter-conversion of glutamate to α -ketoglutarate and ammonia. Higher concentrations of GDH are found

in the liver, kidney, and pancreas. Still, GDH activities appear to be balanced in the liver, providing the appropriate ratio of ammonia and amino acids for urea synthesis in periportal hepatocytes. Since GDH is at the intersection of several critical metabolic pathways, a firm regulation of its activity is thought to be essential for cellular survival. Therefore, the effects of TGZ on GDH activity in response to ammonia or urea production were evaluated. Cells that undergo necrotic death may exhibit high levels of GDH activity. To evaluate the effect of TGZ on GDH activity in Huh7 cells, the GDH activity assay kit (Sigma, Poole, UK) was used. The GDH activity assay is based on a coupled enzyme assay. GDH consumes glutamate as a specific substrate and produces NADH stoichiometrically, leading to the proportional colour generation, which is equal to the GDH levels in a sample. Cells were seeded at 1×10^6 in a six-well plate and incubated overnight for attachment to the plate. Cells were treated with various concentrations of TGZ and 10 μ M simvastatin as a positive control for 24 hrs. After the treatment period, the cells were collected in Eppendorf tubes and labelled. The NADH standard curve was prepared, and the rest of the assay was carried out according to the manufacturer's protocol. The initial reading (T_{initial}) was taken at 450 nm absorbance at the initial time (A_{450}) initial until the (A_{450}) initial was within the linear range of the standard curve. Readings were taken until the value of the most active sample was near or exceeded the end of the linear range of the standard curve. The background was corrected by subtracting the final readings [$(A_{450})_{\text{final}}$] obtained for the blank NADH standard from the final readings of the standards as well as the samples, and a new standard curve was set up in each of the three repeats. The GDH activity in each sample was calculated and plotted.

2.2.14 Pyruvate quantification assay

Pyruvate is a bedrock molecule essential for various phases of human metabolism. Pyruvate is the product of glycolysis obtained from supplementary supplies in the cellular cytoplasm and fated to be carried into the mitochondria. It forms the power source input underpinning the citric acid cycle carbon flux. Interruption of mitochondrial pyruvate flux may interrupt carbon flux via any of the pathways traversing the citric cycle (Herzig *et al.*, 2012). The Pyruvate Assay Kit (Sigma-Aldrich, Poole) was used to determine the concentration of pyruvate. Huh7 cells

were seeded at 1×10^6 in a six-well plate and incubated overnight for attachment to the plate. Cells were treated with various concentrations of TGZ for 24 hrs. Cells were then washed with cold PBS, resuspended in pyruvate assay buffer, homogenised and centrifuged at $15000 \times g$ for 5 minutes at $4 \text{ }^\circ\text{C}$. The supernatant was collected in a clean Eppendorf tube and kept on ice. The rest of the assay was conducted according to the manufacturer's directions, and absorbance was measured at 570 nm using a microplate reader. Readings for each standard and samples were averaged and the mean absorbance reading of the blank was subtracted from the standard and the sample readings (corrected absorbance). The corrected absorbance readings for each standard were used to construct standard curves in each of the three independent assays. Sample readings were inferred from the standard curve to determine the concentration of pyruvate in each sample.

2.2.15 Ammonia quantification assay

Ammonia is an essential source of nitrogen for living organisms, but it is toxic when present at high concentrations. It is an integral derivative of amino acid metabolism. Homeostasis of ammonia is firmly controlled to a low plasma level, thus within the normal range ($10\text{--}40 \text{ } \mu\text{mol/L}$) (Oliver III *et al.*, 2008; Slivac *et al.*, 2010). The liver is the critical organ for ammonia metabolism. However, other tissues, such as the muscle and the kidney, also play a vital role in the inter-organ exchange and final clearance of ammonia molecules. Huh7 cells were seeded in a six-well plate at a density of 2×10^6 and incubated overnight for attachment. Ammonia concentration was determined using the Ammonia Assay Kit (Sigma- Aldrich, Poole). Cells were treated with various concentrations of TGZ ($5\text{--}50 \text{ } \mu\text{M}$) and incubated for 24 hrs. Cells were then washed with cold PBS, resuspended in $100 \text{ } \mu\text{L}$ of Assay Buffer, homogenised, and centrifuged in a cold microcentrifuge for 10 minutes at $4 \text{ }^\circ\text{C}$ at $13000 \times g$. The supernatant was transferred into clean Eppendorf tubes and kept on ice; the rest of the assay was undertaken following the manufacturer's directions. Absorbance was measured using a microplate reader. The readings for each standard, control, and TGZ-treated samples were averaged. The average values for the blank were deducted from the controls and the TGZ-treated samples (corrected absorbance). The corrected values for each standard were used to construct a standard curve for each independent repeat. The corrected sample OD values from

the standard curve were applied to determine the ammonia concentration in each sample.

2.2.16 Glutathione depletion assay

Glutathione (GSH) is a three-amino-acid peptide that acts as an antioxidant in eukaryotic cells. Xenobiotics or reactive chemical species may cause a reduction in GSH levels either through oxidation or reaction with the thiol group. A reduction in GSH levels may be used as a tool to assess toxicological responses relative to oxidative stress (Franco & Cidlowski, 2012). This assay was performed to evaluate if TGZ would cause GSH depletion in Huh7 cells. Huh7 cells were seeded at a density of 1×10^4 cells per well in a 96-well plate and incubated overnight for adherence to the plate. The cells were treated with various concentrations of TGZ and incubated for 48 hrs. The rest of the assay was carried out according to the manufacturer's instructions. 100 μ L of freshly prepared 1X GSH-Glo™ reagent was added to each well, mixed on a plate shaker and kept at room temperature for 30 minutes. 100 μ L of reconstituted luciferin detection reagent was added to each well, mixed briefly on a plate shaker, and incubated for 15 minutes. Luminescence was quantified using a luminometer. The net-GSH-dependent luminescence was calculated by deducting the average luminescence of the negative control reactions from the GSH-containing reactions. The gained signal from GSH reactions in untreated samples (control) denotes the total GSH activity, whereas changes from the average net signal for total GSH activity to the net signals for reactions with TGZ-treated samples suggest the effect of the compound on GSH concentrations in Huh7 cells.

2.2.17 Determination of cholesterol levels in Huh7 cells

Cholesterol forms a fundamental constituent of cell layers and is a primary transition in hormone or bile acid production. Cholesterol does not circulate evenly within cellular membranes. Nonetheless, relatively, there are fundamentally and kinetically discrete cholesterol-rich and deprived areas. Under normal physiological states, about 90% of the total cellular cholesterol remains at the plasma membrane, whereas a negligible, limited amount of cholesterol is present in the endoplasmic reticulum as well as the mitochondrial inner membranes. Inside the cells, intracellular cholesterol may be relocated to several compartments through either vesicular or

non-vesicular routes. Flaws in these carriage paths can change cellular cholesterol homeostasis, which may eventually lead to clinical conditions such as steatosis. The Cholesterol Quantitation kit (Sigma- Aldrich, Poole) was employed to measure the total cholesterol levels in Huh7 cells treated with TGZ. The kit measures total cholesterol concentration based on enzymatic assays that produce a colourimetric (570 nm) or fluorometric (Ex 535/Em 587) product relative to the cholesterol contained in a sample. Cells were seeded at 1×10^6 in a six-well plate and incubated overnight for attachment to the plate. Cells were treated with various concentrations of TGZ and 10 μ M simvastatin as a positive control for 24 hrs. After the treatment period, the cells were collected in Eppendorf tubes and labelled.

200 μ L of chloroform: isopropanol: IGEPAL (7:11:01) was placed in a micro homogeniser and centrifuged at 1300 x for 15 minutes to remove the insoluble material. The organic phase was transferred into new, labelled Eppendorf tubes and airdried at 50 °C to eliminate the chloroform. The pellet was then discarded, and the samples were vacuumed for 30 minutes to remove any remaining organic solvent. The dried lipids were dissolved with 200 μ L of the cholesterol assay buffer and vortexed until evenly mixed. The rest of the assay was carried out following the manufacturer's instructions, and absorbance was measured at 570 nm using a BMG LABTECH FLUOstar Omega plate reader (Ortengberg, Germany). Therefore, the blank values have been deducted from all the readings and plotted against the cholesterol standard curve using the cholesterol standard values. The concentration of cholesterol contained in each sample from the standard curve was determined, and a new standard curve for each of the three independent experiments has been generated.

2.2.18 Determination of bile acid in HEK293 cells

Bile is a complex mixture of lipids, proteins, carbohydrates, vitamins, and other traces of elements. However, bile acids form a significant constituent of the total composition and consist of twelve different subgroups (Li & Apte, 2015). Bile acids are synthesised from excess cholesterol, secreted from the liver, taken up into the small intestines, and transported back to the liver via the portal blood (Li & Apte, 2015). Bile acid production plays a crucial role in cholesterol haemostasis. It is

needed for the complete uptake of dietary lipids and fat-soluble vitamins as well as other vital nutrients into the small intestines. Under normal conditions, newly produced bile acids are conjugated with glycine or taurine to produce bile salts. Detecting circulatory levels of bile acids can be employed to identify liver pathophysiology. Besides, elevated serum bile concentrations may be a result of intrahepatic cholestasis. Therefore, the Total Bile Acid Assay Kit (Sigma-Aldrich, Poole) was used to determine bile acid levels in TGZ-treated NTCP-transfected HEK293 cells. The Human Embryonic Kidney 293 cell line (HEK293) cell was chosen for this assay because Huh7 cells do not inherently express the sodium taurocholate co-transporting polypeptide (NTCP), a primary bile acid uptake transporter (Zhao *et al.*, 2015). HEK293 is a common tool for researchers to overexpress proteins of interest and study their function and molecular regulation because it lends itself easily to genetic manipulation. The assay is based on the fluorometric process to determine bile acids in biological samples. The assay is based on the principle that the presence of 3 α -hydroxysteroid dehydrogenase reacts with all the twelve bile acids and converts NAD to NADH.

The diaphorase then uses NADH to reduce resazurin to resorufin, which is then detected fluorometrically. HEK293 cells were seeded at 1×10^6 in a six-well plate and incubated overnight for attachment to the plate. Cells were treated with various concentrations of TGZ for 48 hrs. Cells were washed three times with PBS, lysed through homogenisation in cold PBS and centrifuged at 15000 x g for 10 minutes at 4 °C. The rest of the assay was conducted according to the manufacturer's directions, and fluorescence was measured at 530nm/ 585 nm (Ex/Em). The bile acid concentration of each sample was calculated using the manufacturer's formula.

2.2.19 Statistical analysis

Unless otherwise stated, all experimental data were expressed as mean, with the standard error of the mean used to indicate experimental variability. The statistical analysis was designed to compare the differences between treatments at various test drug concentrations relative to the control treatment (no drug). The mean \pm SEM of response at each test drug concentration was used for linear regression. A four-parameter logistic equation was used to fit the graphs with 0% and 100% as the

lowest and highest responses exhibited by the cells in media and the test drugs, respectively. The half-maximal (50%) inhibitory concentration (IC_{50}) and half-maximal effective concentration (EC_{50}) values and the 95% confidence limits were calculated from the fitted curves. An F test was used to calculate the significance of differences between the IC_{50} values. GraphPad Prism v7 was used to perform these analyses.

Analysis of variance (ANOVA) was used for the MTT and the Caspase Assays based on the assumption that:

(i) The population of the sample data are normally distributed

Dunnett's multiple comparisons test was used to compare:

The difference between each test drug concentration and the control treatment (with no drug) at 24 hrs drug exposure.

- The differences between each treatment at 0 hour and each time interval of exposure.

The level of statistical significance was set *a priori* at $p < 0.05$.

Chapter 3 *In vitro* assessment of TGZ-induced Toxicity

3.1 The Effects TGZ in Huh7 cells viability

Cytotoxicity is initiated by the adverse actions of compounds as well as physical agents on cells. Currently, various methods are used to determine cellular activity and cell integrity in control cells or cells exposed to a toxicant, stress, or pathology (Cummings *et al.*, 2012). The measurement of cellular activity relies on a cell type, the kind of toxicant used, and the type of cell death being investigated. The classification and description of modes of cell death are essential in toxicology research. Cell death in every cell type is mediated by multiple signalling pathways, which serve as potential cell cytotoxicity targets. Awareness of how toxicants or physical agents trigger the different trails of cell death is critical for determining the acute, subacute, or chronic effects of drugs and chemical agents. Cummings *et al.* have reported that systemic evaluation of the initiation of cell death allows the design and testing of nontoxic and more effective drugs.

Although TGZ improved high blood glucose levels through the attenuation of peripheral insulin in non-insulin diabetic subjects, reported cases of liver injury contributed to the removal of TGZ from the market (Jaeschke, 2007; Yamamoto *et al.*, 2001). Yamamoto *et al.* have reported that the liver toxicity caused by TGZ was reversible; however, few incidents of liver injury causing death have been recorded. The data on TGZ-induced liver injury is limited and, as such, the mechanism of TGZ-induced liver toxicity is poorly understood. It is, therefore, imperative to expound on the mechanism of TGZ toxicity in animal hepatic cells. There have been suggestions that PPAR γ activation by TGZ reduces cell growth and provokes cell death in human gastric cancer cells (Nagamine *et al.*, 2003; Yamamoto *et al.*, 2001).

The means by which TGZ-induced hepatotoxicity may conceivably be due to the initiation of cell death. This study, therefore, explored whether TGZ would cause toxicity in Huh7 cells. The stability between cell proliferation as well as cell death is firmly regulated to sustain the cell population in a tissue. Various human diseases, such as cancer, have been linked to impairment of programmed cell death (Fulda, 2009; Liu, 2004). Apoptosis is a vital physiological mechanism that selectively removes cells that are involved in various biological processes. The Bcl-2 family,

which consists of ant-apoptotic and pro-apoptotic proteins, has been reported to play a critical role in the regulation of apoptosis. Bcl-2 and Bcl-XL, for example, inhibit apoptosis through direct binding and sequestering of pro-apoptotic BH3-only proteins that can directly or indirectly activate Bax or Bak, or by preventing the release of mitochondrial apoptogenic elements into the cytoplasm, such as cytochrome c and apoptosis-inducing factor. However, the overexpression of Bcl-2 anti-apoptotic proteins inhibits cytochrome c discharge, disrupting apoptosis, and this mechanism may be linked with various types of tumours (Ding & Yin, 2009; Edlich, 2018; Guo *et al.*, 2009).

Apoptosis is characterised by intrinsic and extrinsic pathways described in the previous section 1.4.6.6 of this thesis. The extrinsic trail is controlled by the induction of death receptors such as FAS. They recruit the death domain, creating a death-inducing signalling complex that is when they bind to their ligands. This complex further activates the cell death protease caspase 8 and results in apoptotic cell death (Fulda & Debatin, 2006; López-Hernández *et al.*, 2006).

In contrast, the death signals regulate the Bcl-2 family of proteins and disrupt the mitochondrial potential. The release of pro-apoptotic Bcl-2 family members promotes the opening of mitochondrial pores, causing the discharge of cytochrome c as well as caspase-9. Caspase-9, together with apaf-1 and cytochrome c, recruits the executioner caspase cascade, leading to programmed cell death (Kumar, 2006; Nancy & Troy, 2013).

3.1.1 *In vitro* models to study the effects of liver toxicity

Isolated organs, liver slices, and cells are the three major *in vitro* models for current toxicity research. Among them, the isolated perfused liver is closest to the *in vivo* system, maintaining the 3-dimensional organ structure as well as cell-to-cell communications. For this reason, isolated liver cells are most often employed to study the effects of drugs on the cellular level in comparison to other *in vitro* models (Dias-da-Silva *et al.*, 2015). However, the lack of organ-specific cell-to-cell interactions may be one of the setbacks of employing isolated liver cells. Still, 3D-liver culture models have become accessible to represent the *in vivo* system (Pridgeon *et al.*, 2017). Also, the use of stem cells in toxicity studies has gained

popularity among researchers due to their undifferentiated features that can develop into more specialised cells (Hu & Li, 2015; Kegel *et al.*, 2016; Pridgeon *et al.*, 2017). Primary human liver cells are the gold standard of cultured hepatocytes.

They keep most of the metabolic competence of the liver, which is crucial for toxicity research. In spite of this, it should be defined that the activity of specific systems such as cytochrome P450 is usually minimal compared to the *in vivo* approach. As mentioned in the previous section, a more restraining issue is that healthy primary liver cells are scarce and not accessible to all researchers (Crespi *et al.*, 2017). Also, samples from different volunteers exhibit vast disparities in expression and functions of drug-metabolising enzymes, which is based on the reason that different volunteers may possess different genetic makeup, which can make data evaluation very difficult (Crespi *et al.*, 2017; Gomez-Lechon *et al.*, 2008; Stampella *et al.*, 2017). Primary liver cell culture exhibits a short lifecycle, lasting only about a week in culture. But immortalised liver cell lines exhibit undefined proliferative competence and can be cultured easily *in vitro*. Even though these cells typically demonstrate substantially decreased liver cell activities, for example, low levels of liver-specific drug-metabolising enzymes as well as transcription factors, they could, notwithstanding, in theory, serve as the source of a more practical alternate investigational method (Crespi *et al.*, 2017; Gomez-Lechon *et al.*, 2008; Stampella *et al.*, 2017).

Hepatocellular carcinoma cell lines such as HepG2 and Hep3B have been widely used in the study of liver physiology (Donato *et al.*, 2013). Because it can take several cell passages before the limit of toxic effect is attained, HepG2 and Hep3B cell lines are primarily useful for studying the toxicity of chemicals that impact DNA replication and cell cycling (Donato *et al.*, 2013). However, in comparison to Huh7, the expression levels of various liver-specific drug-metabolising enzymes, such as CYP450 enzyme expression in HepG2 and Hep3B cells, are significantly lower. Their basal CYP3A4 levels are lower than Huh7, and transcription factors are also low (Donato *et al.*, 2013). Previous research has reported that Huh7 cells express Phase I and II enzymes at levels like human hepatocytes (Donato *et al.*, 2013). Huh7 was identified as a potential alternative hepatocyte model for drug metabolism studies (Donato *et al.*, 2013). For this current study, Huh7 cells as a model system

were used to study the mechanism of TGZ-induced liver toxicity for the reasons mentioned in the previous section.

TGZ was selected for this study based on the reasons given in the introduction section that it is more toxic than the other thiazolidinediones and that it can be repurposed or prevent similar compounds from causing toxicity in potential drug developments. Therefore, the following objectives were set to determine the effects of TGZ on Huh7 cells:

- Determine the effect of TGZ on cell (Huh7) viability under two different time points
- Determine the IC₅₀ values of TGZ by the MTT method
- Determine the doubling time of Huh7 under different condition media
- Determine the lethal doses of TGZ by the MTT method
- Determine the lower and higher doses of TGZ on Huh7 cell viability
- Determine the effect of TGZ on apoptosis in Huh7 through caspase activation

3.2 Results

3.2.1 The effects of TGZ on cell viability at different time points

The effect of TGZ on cell viability was determined using Huh7 cells. The MTT assay, which measures cellular metabolic activity, was used as a predictor of cell viability. To determine the effect of TGZ on cell viability, Huh7 cells were seeded in a 96-well plate and treated with varying concentrations of TGZ ranging from (0–50 μ M). Cell viability was assessed at 24 and 48 hrs using the MTT assay and expressed as the percentage of the control (cells in a culture medium). The Huh7 cells treated with TGZ show a dose-dependent decrease in cell viability with significant cell toxicity at 50 μ M when compared to the control. The results show that incubation time is important; after 48 hours, there was a significant decrease in cell viability when compared to a 24-hr exposure time. Therefore, 24 hrs incubation time was chosen for toxicity assessment.

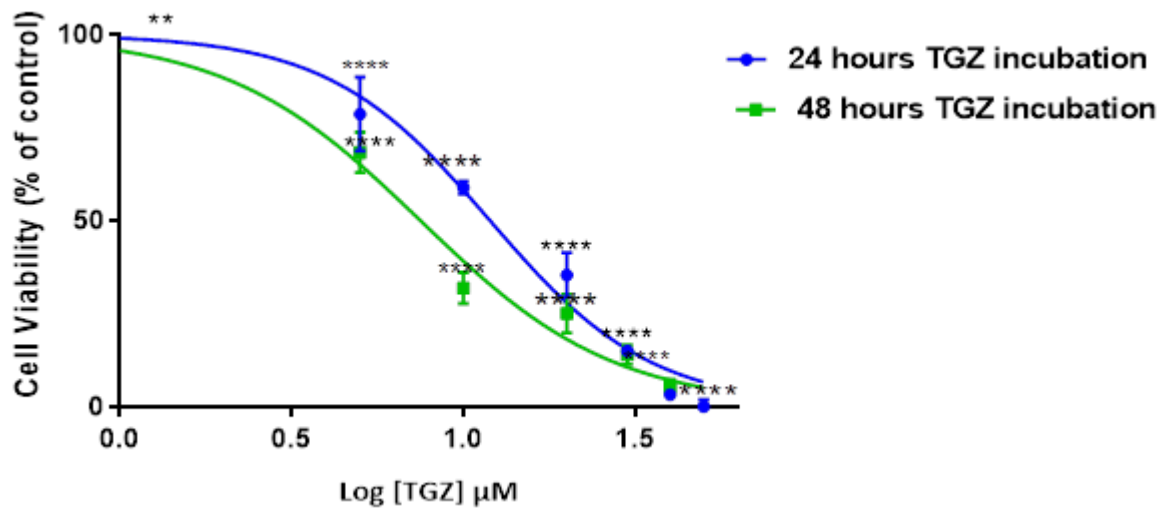


Figure 3-1 The effects of TGZ on Huh7 viability at both 24 and 48 hrs exposure

Huh7 cells were incubated with media (cells + cells). The cells were treated with TGZ (5 to 50 μM) for 24 hrs. Three independent repeats ($n = 9$) were carried out using six replicate wells in each treatment. The mean values were determined and plotted as a percentage of the viability of the control (defined as 100%). Error bars represent the mean \pm SEM of six replicates. Data were analysed using two-way ANOVA, followed by Dunnett's multiple comparisons test, and P values are shown where the difference between responses of different treatments was shown to be statistically significant ($P < 0.0001$) for both time sets (24 and 48 hrs).

3.2.2 The effects of TGZ on Huh7 cell viability by MTT method

Huh7 cells were seeded in 96 well plates and treated with varying concentrations of TGZ, ranging from (2-50 μM). Cell viability was assessed at 24 hrs and expressed as the percentage of the control (cells in a culture medium without TGZ). The dose-relationship between TGZ and Huh7 cells after 24 hrs of exposure was determined. Huh7 cells treated with TGZ showed dose-dependent cell death (Figure 3-1). Based on the dose-response curve, the IC_{50} value of TGZ was determined by non-linear regression and calculated as 15 μM . The Huh7 cells treated with TGZ showed a

significant dose-dependent decrease in cell viability compared to the control. The TGZ concentration at 50 μM was the most toxic (killed about 90% of the cells). The lethal doses (LD_{10} , LD_{25} , LD_{50} , LD_{75} , and LD_{90}) of TGZ were determined from (Figure 3-2) as 3.7 μM and 6.7, 12.2 μM , 22.3 μM and 40 μM , respectively.

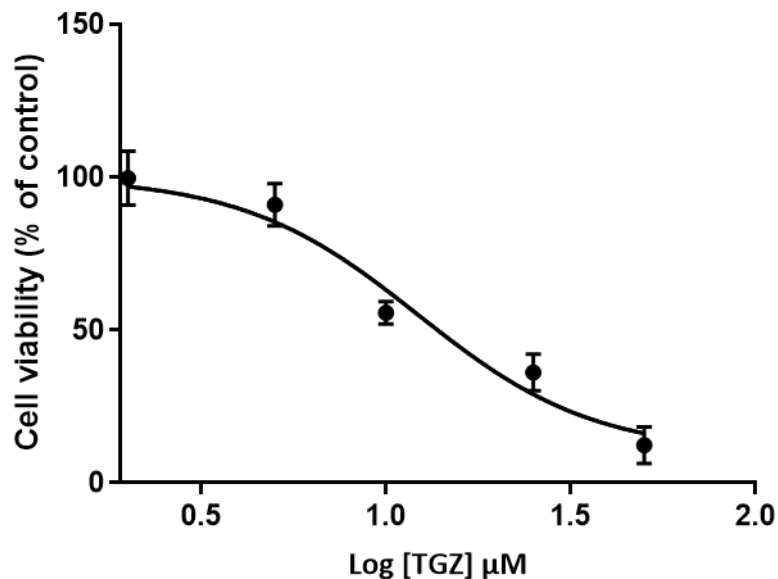


Figure 3-2 The effects of TGZ on Huh7 viability at 24 hrs exposure

Huh7 cells were exposed to media alone (cells + media) as a control. The cells were exposed to TGZ (2 to 50 μM) (treated samples) for 24 hrs. Three independent repeats were carried out using six replicate wells in each treatment. The mean values were determined and plotted as the percentage viability of the control (defined as 100%). Non-linear regression was used to fit the data. The data is presented as the mean SEM. of viability was determined relative to the untreated cells (control). A Two-way Analysis of Variance (ANOVA) was used to analyse the data. Dunnett's multiple comparisons test and P values showed that 2 μM treatment was statistically insignificant. However, cells treated with 10 to 50 μM TGZ were determined to be statistically significant (ns = not significant), *** $P < 0.0002$ **** $P < 0.0001$.

3.2.3 Determination of doubling time in Huh7 cell growth

In order to maintain viability, genetic stability, and phenotypic stability, cell lines need to be cultured when confluent. In this case, they need to be subcultured regularly

before they enter the stationary phase and until a monolayer becomes over 90% confluent. Producing a growth curve for a cell line is useful for determining the cell line's growth characteristics under different conditions. Therefore, the effects of other environmental conditions on the growth rate of Huh7 cells were determined. Three different conditions that, in theory, may influence the growth rate of cell lines were used. Huh7 cells were incubated in complete media (containing 10% foetal bovine serum (FBS), serum-free media (media without FBS) and 15 μ M (IC_{50}) of TGZ obtained from section (3.2.1), in either complete media or serum-free media. Cell counting of each treated condition was carried out every four hrs up to 60 hrs. The rate of cell growth and the doubling time were calculated using GraphPad Prism. Cells exposed to complete media had a doubling time of 21 hrs, followed by cells incubated in serum-free media at 28 hrs, and cells treated with 15 μ M TGZ in complete media and serum-free media had 49 and 50 hrs, respectively. The 15 μ M treatment data between 49 and 60 hrs was excluded because the cell number declined (cell death). The doubling time for Huh7 cells incubated in complete media, serum-free media, and TGZ 15 μ M in complete and serum-free media was determined to be 21, 28, 48, and 49 hrs, respectively. The growth of Huh7 cells in complete media, serum-free media, TGZ treatment in complete media and serum-free media were also determined to be 0.03, 0.02, 0.1441 and 0.040, respectively (Figure 3-3). The data was analysed using two-way ANOVA, followed by Dunnett's multiple comparison test. P values are shown where the differences between the responses of different conditions were determined to be statistically significant. $P < 0.0001$. However, the differences in the responses of the different conditions between 0 and 6 hrs were determined to be statistically insignificant. $P < 0.8265$. Between 6 to 60 hrs and 12 to 60 hrs, the difference between the complete media and serum free media responses was determined to be statistically significant. $P < 0.0001$. The 15 μ M TGZ treatments were shown to be statistically insignificant between 0 and 18 hrs. $P < 0.99$, but a significant difference between 18 to 48 hrs at 15 μ M TGZ was recorded.

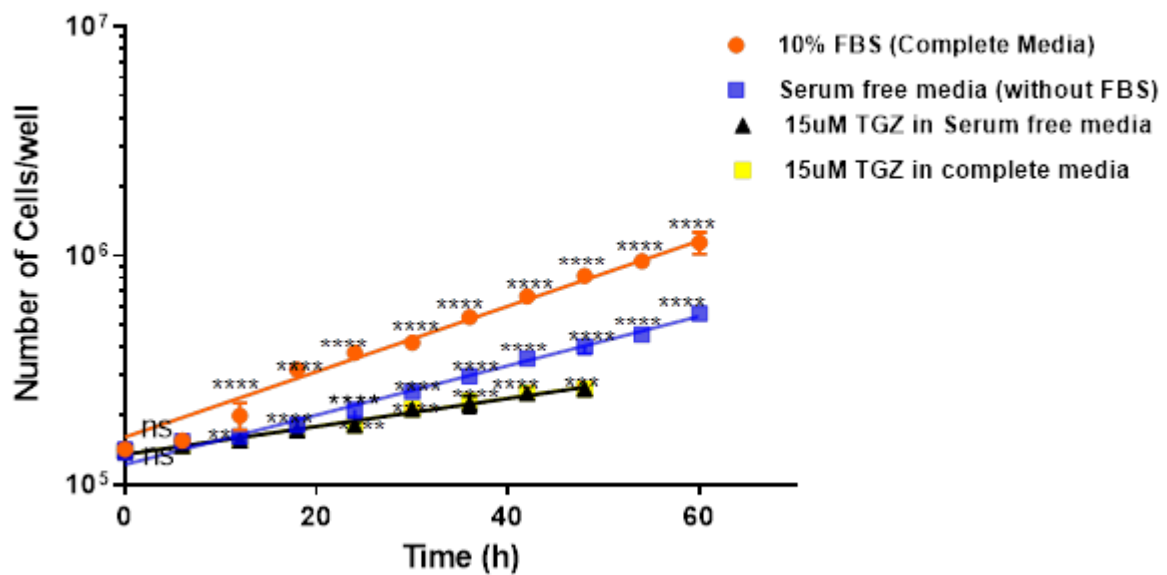
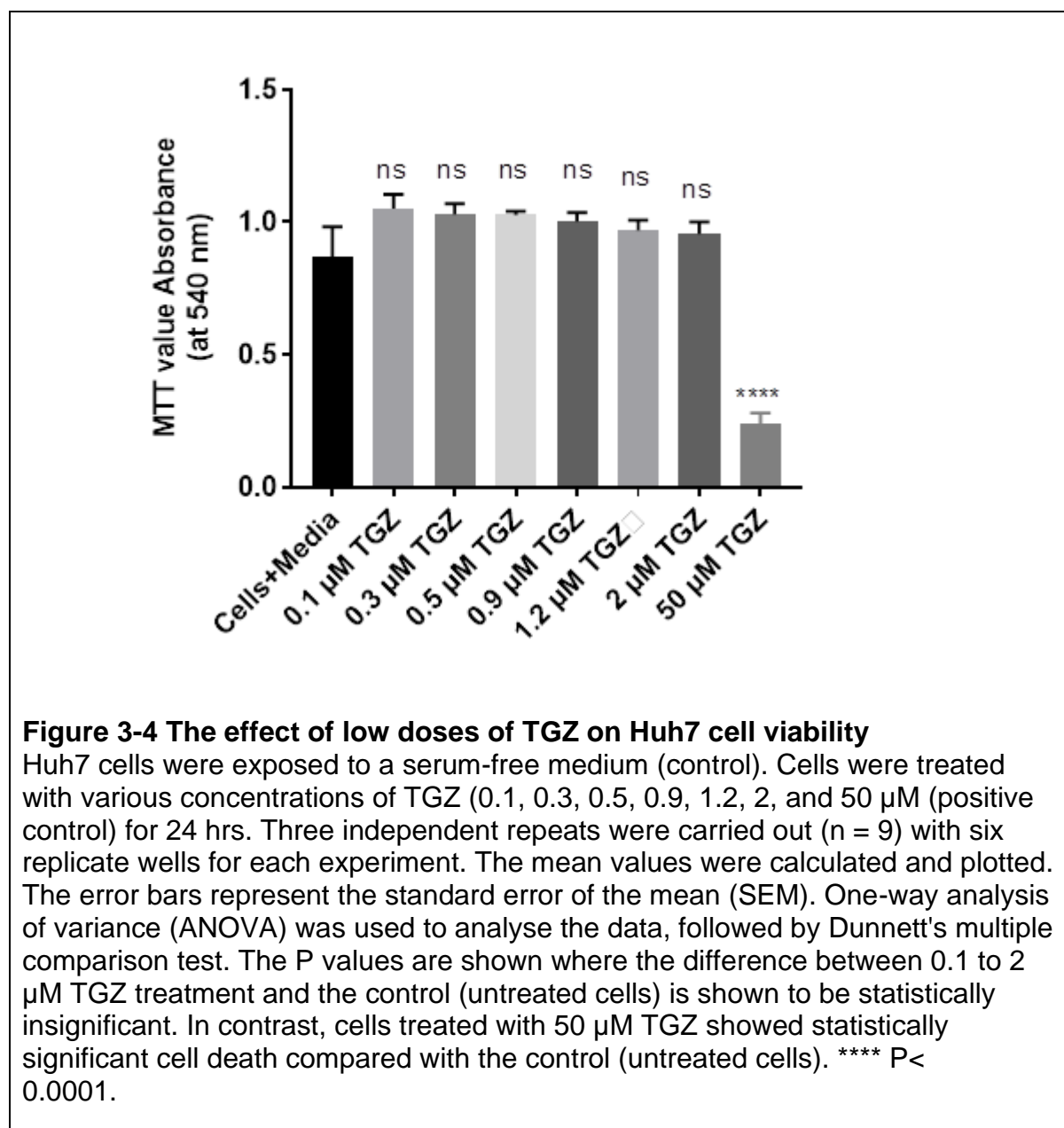


Figure 3-3 Exponential growth curve of Huh7 cell line between 0-60 hrs
 Huh7 cells were incubated with media containing 10% FBS (complete media) and media without FBS (serum-free media). The cells were then treated with 15 μ M TGZ (IC_{50} value of TGZ determined from figure 3-2 in either complete or serum free media for 60 hrs. Three independent repeats ($n = 9$) were carried out using four replicate wells for each condition. The mean values were determined and plotted as a log (log number of cells). Error bars represent the mean \pm SEM of six replicates.

3.2.4 Effect of low doses of TGZ on Huh7 cell viability

Toxicological hormesis describes a biphasic dose-response to xenobiotics or environmental agents, illustrated by a low dose stimulation or beneficial effect and an inhibitory or toxic effect of the high dose of chemicals. Hormesis can also be described as an adaptive response to moderate stimulation of cells and organisms (Calabrese, 2009; Jagota *et al.*, 2019). Huh7 cells were exposed to low doses and high doses of TGZ to determine the impact of these doses on Huh7 cell viability. The MTT assay described in section 2.2.4 was followed to complete the task in this section. Cells exposed to low doses of TGZ (0.1 μ M and 0.3 μ M) did not exhibit a decline in viability compared to the control (untreated cells); however, cells treated with 50 μ M TGZ significantly decreased Huh7 cell viability. Also, a significant

difference in cell viability between cells treated with the lower doses of TGZ and those exposed to 50 μM was recorded. Cells exposed to the lower doses did not show a reduction in cell viability, but cells exposed to 50 μM TGZ showed a significant decrease in cell viability (Figure 3-4).



3.2.5 Effects of TGZ on caspase activities in Huh7 cells

Apoptosis is a physiological, highly organised and genetically programmed cell death that plays a critical role in removing damaged or aged cells. Besides, it serves as the

core defence machinery against some damaging factors such as carcinogens or viral infections (Daisy & Saipriya, 2012; Díaz *et al.*, 2005; Ding & Yin, 2009; Hotchkiss *et al.*, 2009; Jorgensen *et al.*, 2017). Apoptosis is characterised by distinct cellular architecture changes, which leads to self-execution (Diaz *et al.*, 2005). Apoptosis is, therefore, an integral part of normal tissue homeostasis that regulates cell populations in an organ. The inception of apoptosis is exemplified by a sequence of morphological changes, including chromatin condensation and nuclear fragmentation, plasma membrane blebbing, cell and nucleus shrinkage. Eventually, the cells break up into small membrane-surrounded fragments, which results in the formation of apoptotic bodies that are taken up and degraded by neighbouring phagocytic cells without stimulating an inflammatory reaction (McIlwain *et al.*, 2013; Taylor *et al.*, 2008). Therefore, apoptosis happens due to the cascade of caspase activation (McIlwain *et al.*, 2013; Taylor *et al.*, 2008). Previous studies have identified two apoptotic signalling pathways that can trigger activation of caspases: the first is receptor-mediated death signalling pathways stimulated by extrinsic signals such as the attachment of Fas to its receptors. The second signalling pathway is activated by the intrinsic stress signals and is described by apoptotic events in mitochondria (Parrish *et al.*, 2013). A previous study on substrate specificity and biological activity has also demonstrated that in the event of apoptosis, caspases are activated by a self-augmenting cascade (Julien & Wells, 2017). Activation of the upstream caspases (caspase-2, -8, -9, and -10) by pro-apoptotic signals leads to proteolytic activation of the downstream or effector caspases (-3, -6, and-7) (McIlwain *et al.*, 2013). The effector caspases cleave a set of vital proteins, initiating and executing the apoptotic degradation phase, including DNA degradation and production of the typical morphologic features (McIlwain *et al.*, 2013).

Apoptosis not only plays a critical function in maintaining tissue homeostasis; the regulation of apoptosis also plays a crucial role in pathological development. For instance, changes in normal levels of apoptosis or unprogrammed (necrotic) cell death are critical mechanisms that may contribute to the progression of several liver diseases (Krstic *et al.*, 2018; Donato *et al.*, 2010). On the other hand, the failure of apoptosis has been considered a key determinant in the development of

hepatocellular carcinoma (Kim & Kim, 2012). Feldstein *et al.* have suggested that hepatocyte apoptosis may play a key role in liver injury.

Previous studies have reported that apoptosis is the fate of cell death or necrosis (Iorga & Dara, 2019; Wang & Yang, 2018). Therefore, this chapter aims to determine the effect of TGZ-induced apoptosis through the activation of caspases. This was achieved by treating Huh7 cells with TGZ and measuring apoptosis via Caspase-3/7, -8, and -9. TGZ downregulates anti-apoptotic proteins of the Bcl-2 family and the Bcl-xL and upregulates pro-apoptotic proteins such as Bax and Bad.

This section aimed to investigate the effects of TGZ on the activation of the apoptotic trails in Huh7 cells through the activation of caspases. Huh7 cells were exposed to the various doses of TGZ, and apoptosis was determined through caspase-3/7, caspase-8, and caspase-9. Staurosporine was used as a positive control because previous research has shown that it induces apoptosis in Huh7 cells (Belmokhtar *et al.*, 2001; Malsy *et al.*, 2019).

3.2.5.1 Results

3.2.5.2 The effect of TGZ on caspase 3/7 activity in Huh7 cells

Caspases are the basic executioners of apoptotic cell death (McIlwain *et al.*, 2013). Therefore, the activation of the effector caspase-3/7 was determined by using the luminescence-based Caspase-Glo 3/7 assay (section 2.2.8). Huh7 cells were treated with TGZ concentrations of 5 μ M to 50 μ M for 24 hrs, and 1 μ M staurosporine was used as a positive control. A dose-dependent activation of caspase 3/7 activity was significantly ($P < 0.0001$) recorded in this study (Figure 3-5).

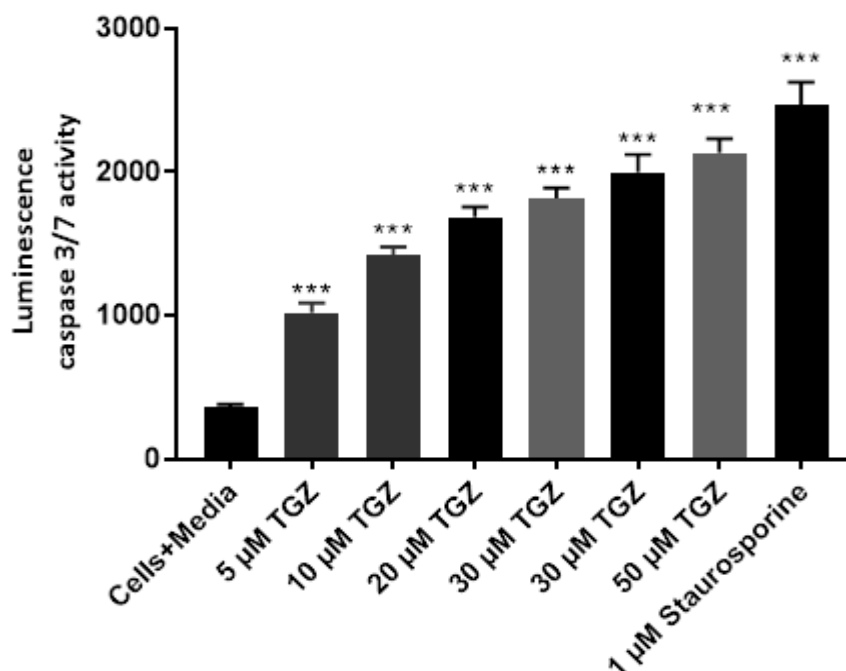


Figure 3-5 The effects of TGZ on caspase 3/7 activity in Huh7 cell

Huh7 cells were incubated in a serum-free medium (cells) as a negative control. Cells were then treated with 1 μM Staurosporine (positive control). Cells were treated with TGZ (5 to 50 μM) for 24 hrs. Caspase-3/7 activity was determined using a luminescent Caspase-Glo 3/7 assay. Luminescence was determined using a BMG LABTECH Omega FLUOstar Omega plate reader. Three independent repeats were carried out (n = 9). The mean values were calculated and plotted. The error bars represent the standard error of the mean (SEM). One-way analysis of variance (ANOVA) was used to analyse the data, followed by Dunnett's multiple comparison tests. The P values were shown where the difference between different treatments' responses was shown to be statistically significant, with **P < 0.0024 **** P < 0.0001 for all three sets of tests. TGZ dose-dependently induced caspase-3/7 activation in Huh7 cells.

3.2.5.3 The effect of TGZ on initiator caspase-9 activity in Huh7 cells

Of the caspases implicated in apoptosis signal transduction, the initiator caspases-8 and caspase-9 are activated at multiple-protein activation platforms, and activation is thought to involve homo-dimerisation of the monomeric zymogens. Caspase-9, which is a crucial initiator caspase that requires apoptosis signalling through the

mitochondrial pathways, is activated in the apoptosome complex and failure to activate caspase-9 has extreme pathophysiological effects (Li *et al.*, 2017). To determine the effect of TGZ activation of the above cysteine proteases of the caspase family, Huh7 cells were exposed to various concentrations of TGZ (5 μM to 50 μM) for 24 hrs. Caspase-9 activity was measured using luminescence-based Caspase-Glo 9 assays. Luminescence was determined using a BMG LABTECH FLUOstar Omega plate reader. Our results show a dose-dependent induction of caspase-9 (Figure 3-6).

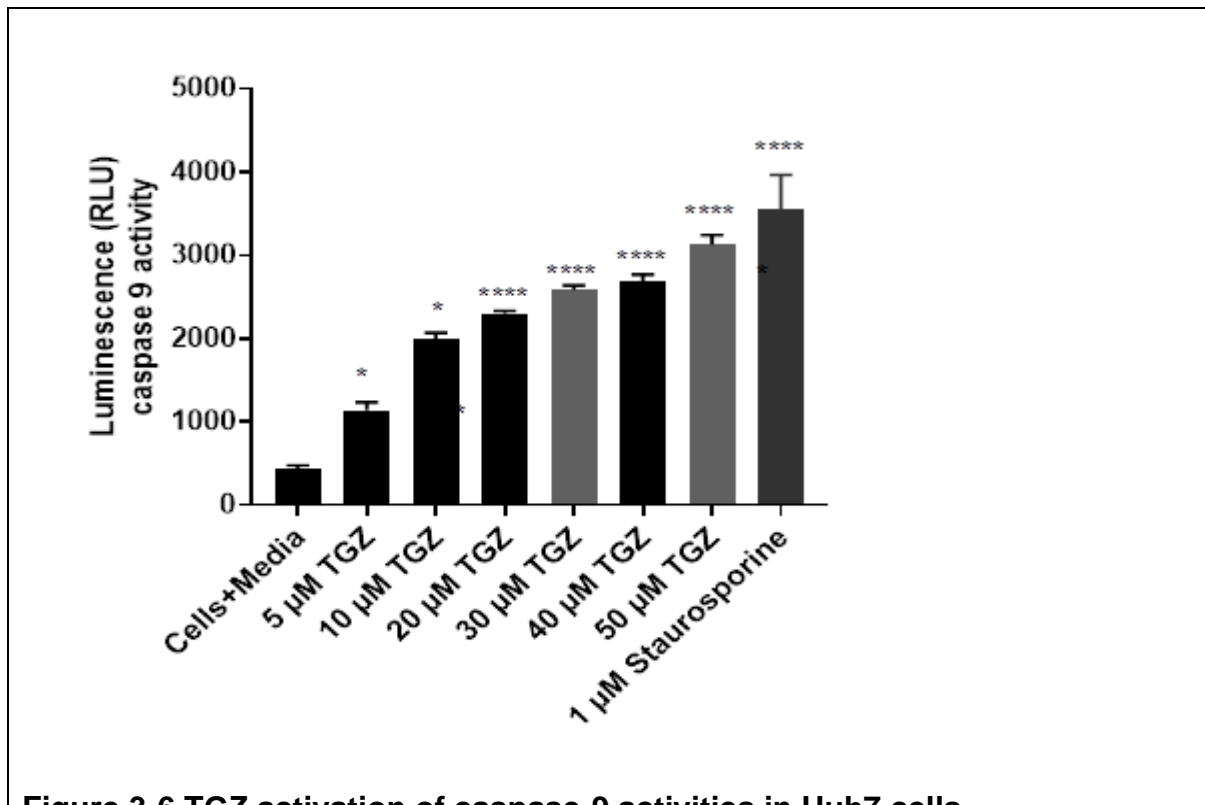


Figure 3-6 TGZ activation of caspase-9 activities in Huh7 cells

Huh7 cells were incubated in a serum-free medium (cells+media) as a control. Cells were then treated with 1 μM Staurosporine and used as a positive control. Cells were treated with TGZ (5 to 50 μM) for 24 hrs. Caspase-9 was determined using the luminescence Caspase-Glo 9 assay. Luminescence was determined using a BMG LABTECH Omega FLUOstar plate reader. Three independent repeats were carried out ($n = 9$) with three wells for each experiment. The mean values were calculated and plotted. The error bars represent the standard error of the mean (SEM). One-way analysis of variance (ANOVA) was used to analyse the data, followed by Dunnett's multiple comparison test. The P values are shown where the difference between the responses of different treatments was statistically significant. * $P < 0.0402$, *** $P < 0.0008$, **** $P < 0.0001$.

3.2.5.4 The effect of TGZ on initiator caspase-8 activity in Huh7 cells

Caspase-8, a part of the cysteine proteases, is involved in apoptosis as well as cytokine handling (Fritsch *et al.*, 2019). Caspase-8 is delivered as an inert polypeptide chain zymogen procaspase and is invigorated through proteolytic cleavage by either autoactivation after enlistment into a multimeric complex or trans-cleavage by other caspases (Fritsch *et al.*, 2019). In this way, ligand binding-induced trimerization of death receptors leads to the recruitment of the receptor-specific adaptor protein Fas-associated death domain, which at that point, initiates caspase-8 (Fritsch *et al.*, 2019). Activated caspase has been reported to propagate signal by directly cleaving and activating downstream caspases or cleaving the BH3 Bcl2-interacting protein and eventually results in cytochrome c discharge from the mitochondria, triggering activation of caspase-9 in a complex with dATP as well as Apaf-1. Activated caspase-9 then stimulates further downstream caspases (Fritsch *et al.*, 2019). The effect of TGZ on caspase-8 activation in Huh7 cells using the luminescence-based caspase-Glo 8 assay by following the procedure in section 2.2.8 was determined. Huh7 cells were exposed to various concentrations of TGZ (5 μ M to 50 μ M) for 24 hrs. 1 μ M staurosporine was used as a positive control. This study did not record caspase-8 activation in Huh7 cells, compared to the control (cells+media); cells treated with 1 μ M staurosporine did not induce caspase-8 activation. In contrast, Huh7 cells treated with 10 μ M Fas ligand significantly induced caspase-8 activation in Huh7 cells (Figure 3-7).

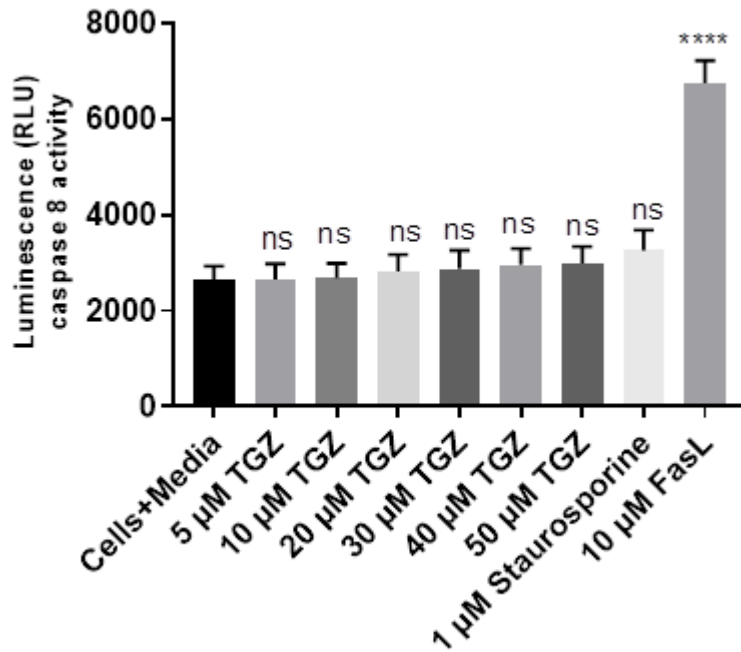


Figure 3-7 TGZ activation of caspase-8 activities in Huh7 cells

Huh7 cells were incubated in serum-free medium (cells+media) as a control. Cells were then treated with 10 µM Fas Ligand as a positive control. Cells were treated with TGZ (5 to 50 µM) for 24 hrs. Caspase-8 activation was determined using the luminescent Caspase-Glo 8 assay. Luminescence was determined using a BMG LABTECH FLUOstar Omega plate reader. Three independent repeats were carried out (n = 9). The mean values were calculated and plotted. The error bars represent the standard error of the mean (SEM). Data were analysed by one-way analysis of variance (ANOVA) followed by Dunnett's multiple comparisons test, and the P values are shown where the difference between TGZ concentration of 5 to 50 µM and 1 µM Staurosporine treatments were shown to be statistically insignificant; however, cells incubated with 10 µM Fas Ligand were determined to be statistically significant between the control (cells), NS (not significant) and ****P < 0.0001

3.3 Discussion

Cell viability or proliferation rates of cells are good indicators of cell health.

Environmental chemicals such as xenobiotics can affect cell quality and morphology (Domura *et al.*, 2017; Miller & Zachary, 2017). For example, TGZ can cause cellular toxicity through various means, such as cell membrane destruction, protein synthesis prevention, irreversible receptor activation, or enzymatic reactions (Domura *et al.*, 2017; Miller & Zachary, 2017). And to assess cell death induced by these processes, simple, consistent, and replicable short-term cellular toxicity and viability assays are needed. Viability and cytotoxicity assays using cultured cells are commonly used for chemical cytotoxicity studies or drug toxicity evaluation. Cell viability and cytotoxicity assays focus on various cell functions, including cell membrane permeability, enzyme activity, cell adherence, ATP production, or co-enzyme development (Domura *et al.*, 2017). *In vitro* cytotoxicity or cell viability assays have positives, such as efficiency, relatively low cost, and optimisation capacity. However, they have some drawbacks because they are not technically developed enough, and for these reasons, they cannot replace animal experiments entirely (Aslantürk, 2018; Méry *et al.*, 2017).

The fundamental aim of this chapter is to determine the toxicity of TGZ using cell-based assays. As a result, the IC₅₀ value of TGZ after a 24-hour treatment period was determined to be 15 µM. This value was similar to the previous report by Yamamoto *et al.*, who recorded an IC₅₀ value of 16 µM TGZ in Huh7 cells after 24 hr exposure. However, an earlier study by Tettey *et al.* demonstrated that 24 hrs of treatment with TGZ in rat liver cells produced 35 µM and 20 µM in HepG2 cells that share similar characteristics with the Huh7 cells. Other researchers using different cell lines and various treatment time points have reported IC₅₀ values of between 10 and 50 µM (Fujita *et al.*, 2017; (Sliwka *et al.*, 2016; Yamamoto *et al.*, 2002).

Having determined the IC₅₀ value of TGZ, the various concentrations of TGZ were explored to determine the doses that would kill 10, and 90% of the cell population. Huh7 cells were exposed to various concentrations of TGZ, and it was recorded that 3.7 µM TGZ would kill 10% of the Huh7 cell population. However, a TGZ concentration of 40 µM would be required to kill approximately 90% of the cells.

In the past decades, acute toxicity testing methods have been programmed to provide a robust dose-response curve characterisation with multiple animals at 3-5 doses to evaluate the tolerance to potentially lethal chemical doses in the laboratory animal study population. A group of animals received single dosing with doses chosen to support the anticipated LD₅₀ dose, at which 50% of the animals or a population are expected to die (Rang *et al.*, 2012). Animals were observed for over 10 days following the early stages, nature, magnitude, and reversibility of toxic effects and the duration of lethality following acute exposure to chemical substances (Rang *et al.*, 2012). To ensure the best data, doses close to the LD₁₀ and LD₂₅ would have been included in the study. The increasing concentration would at least have been seen to have a declining proportion of survivors and two or more doses would have provided partial responses (Rang *et al.*, 2012).

After determining the IC₅₀ value of TGZ, the effect of different conditions on the growth (doubling time) of the Huh7 cell was determined. As described in the method section, Huh7 cells were exposed to serum-free medium, complete medium, and a 15 µM TGZ concentration. A slower growth rate of cells exposed to serum-free and TGZ-containing media was recorded. However, at 60 hrs, the maximum number of cells exposed to complete media was about half of the cell population in comparison with other condition media. The recordings are similar to previous studies that reported that the various concentrations of TGZ inhibited cell proliferation (Zhou *et al.*, 2008).

Cellular growth curves begin with a lag phase ranging from a few hrs to about 48 hrs, dependent on the particular cell line (Assanga, 2013; Vermeulen *et al.*, 2003). The lag phase, also called the recovery stage, is the period needed for the cell to recuperate from trypsinisation to restore its cytoskeleton. At this point, the cell releases an external matrix that aids the linkage between the cell and its proliferation, along with the compounds or chemicals on the cell, which could be elucidated at the log phase (Assanga, 2013), substrate. The cell may then enter the log phase, where the cell number doubles (DT), as in the case of Huh7 cells exposed to complete media (Figure 3-3). Huh7 cells exposed to 15 µM TGZ showed a slower growth rate as well as a decrease in cell population between 50 and 60 hours, indicating cell death. In this case, it could be suggested that TGZ inhibited cell

growth and caused cell death after 50 hrs. This also confirms the cell growth inhibition reported in this study. Previous studies that exposed cells to the various concentrations of TGZ have also reported inhibition of cell proliferation even in cells exposed to 5 μ M TGZ in either serum-free or complete media (Akinyeke & Stewart, 2011; Zhou *et al.*, 2008). The cell population and growth rate of cells treated with complete media were about half the numbers of cells treated with serum-free media. However, cells treated with TGZ in serum-free media exhibited a slower growth rate and the least number of cells. An explanation of our observation, in this case, could be attributed to the fact that the cells lacked the necessary growth factors to proliferate. Cells may grow at a steady rate while remodelling their metabolites as well as gene expression. DT is a useful approach for other experiments to model the population level of TGZ on cell viability.

As per the findings, it can be deduced that the Huh7 cell could be cultivated within four days in complete media for any experimental procedure. Cell cycle or doubling time, as denoted by growth curves, are useful tools for defining the characteristics, growth rate, and optimal development of a specific cell line. Cellular culture doubling time may allow researchers to predict the best time range for evaluating the effects of either biological or chemical products in *in vitro* experiments (Assanga, 2013).

Liver cells have a range of drug-metabolising enzymes. This is because the liver is the critical site of drug detoxification and receives blood directly from the gut after ingestion. Thus, the liver acts as the primary barrier. This subsequently means that liver cells are more susceptible to the by-products or reactive intermediates of drug biotransformation. Comparing our data to previous reports (Rachek *et al.*, 2009; Yang *et al.*, 2014), it can be argued that TGZ-induced cytotoxicity is cell type-dependent. Thus, researchers can also suggest that exposure to the parent drug itself is not predictive of an adverse event on its own; however, it might be dependent upon other latent factors, such as a change in the metabolic profile of the cells. While it is unclear whether cytotoxicity is caused by TGZ or a metabolite, the data presented here suggest that a combination of effects may be at work, as toxicity was observed in Huh7 cells with a maximum loss of viable population of approximately 80% at 50 M TGZ concentration.

Although it remains controversial, Funk *et al.* have suggested that TGZ-sulphate might be a contributor. In line with *in vitro* studies, Narayanan *et al.* who treated cells with TGZ also reported biotransformation of TGZ to a quinone by-product. Quinone is implicated in redox cycling leading to ROS production. Furthermore, inhibition of sulphation by 2,6-dichloro-nitrophenol, a major biotransformation pathway of TGZ, increased the levels of unmetabolised TGZ but did not induce any significant increase in the production of TGZ-quinone. The inhibition of sulphation produced cytotoxicity, indicating that the toxicity may result from the accumulation of the parent drug, TGZ, and not the formation of a reactive metabolite (Wang & Lin, 2013; Yamamoto *et al.*, 2002). Based on our data recorded in cytotoxicity, it could be suggested that the enhanced cytotoxicity observed after TGZ-treated Huh7 cells may be due to activation of other apoptotic pathways, therefore producing apoptosis-dependent cell death. Thus, one of the objectives of this chapter was to evaluate the mode of cell death in Huh7 cells exposed to TGZ and determine the impact of TGZ on apoptosis through caspase activation. Recent studies have reported that TGZ inhibited growth in colon cancer, breast cancer, and prostate cancer (Youn *et al.*, 2008). However, Toyoda *et al.* investigated the effect of TGZ on the growth and apoptosis of liver cancer cells *in vitro*. They reported that TGZ dose-dependently inhibited the growth of the liver cancer cell line, Huh7. In this current study, Huh7 cells were chosen to assess TGZ for almost all our experiments because a previous report by Toyoda *et al.* demonstrated that HepG2, which expressed the same PPAR γ mRNA level as Huh7, was relatively insensitive to the growth inhibitory effect of TGZ. Consistent with previous studies (Hashimoto *et al.*, 2007), a TGZ dose-dependent inhibition of the growth of the Huh7 cell has been recorded in this study. As a result, these findings support the use of Huh7 cells as an excellent model for an *in vitro* system to investigate TGZ-induced hepatotoxicity.

To determine the underlying mechanisms of the inhibition of cell viability by TGZ, they investigated whether TGZ acts by inducing apoptosis in liver cancer cells (Hashimoto *et al.*, 2007). The researchers performed a DNA fragmentation assay and Hoechst staining. And in both studies, TGZ induced apoptosis in a dose-dependent manner. This agrees with findings by Chinetti *et al.*, who have also reported TGZ-induced apoptosis in human monocyte-derived macrophages.

However, other reports have shown that apoptosis was not an essential mechanism by which TGZ induced cell growth inhibition (Hashimoto *et al.*, 2007; Nagamine *et al.*, 2003). An *in vitro* study by Akasaki *et al.*, reported that exposure of human glioma cells to TGZ decreased Bcl-2 protein to nearly untraceable concentrations. Other past studies have also examined the relationship between activation of PPAR γ and nuclear factor kappa B (NF κ B). NF κ B, a DNA binding protein that enhances the expression of several genes implicated in cell proliferation and plays an essential role in cell development, survival, and oncogenesis, and it was suggested that PPAR γ induced cellular apoptosis by inhibiting the antiapoptotic NF κ B signalling pathway (Elrod & Sun, 2008; Toyoda, 2002).

In this current study, it is noted that Huh7 cells exposed to the various concentrations of TGZ dose-dependently activated the executioner caspases-3/7 and the initiator caspase-9 effectively. However, TGZ did not induce the activation of caspase-8. Caspases-3 or caspase-7 play a crucial role in executing cellular apoptosis (McDonnell *et al.*, 2003; Walsh *et al.*, 2008). Caspase-3 activation is considered vital. The executioner caspase-3 has been shown to play a role in cleaving a wide range of cellular substrates and promoting DNA fragmentation, both of which lead to cell death. This is consistent with a previous study by Toyoda (2002), who reported that TGZ inhibited cellular growth activities and subsequent cell death through caspase-3 activation. Toyoda (2002) further noted that there were no observable effects on caspase-8 activation by TGZ, consistent with our findings in (Figure 3-7), where the impact on caspase-8 activity was only recorded in cells exposed to Fas Ligand. Activation of caspase-9 was also observed in this study, with activity increasing in a concentration-dependent manner. Because caspase-8 activation indicates an extrinsic apoptotic cascade and caspase-9 activation indicates an intrinsic apoptotic cascade, the data presented here are consistent with the activation of intrinsic apoptosis. Apoptosis can also happen when cells receive an apoptotic signal and the mitochondria release cytochrome c, which binds to Apaf-1 and Ced-4 and forms a complex with dATP. This complex formation may trigger the recruitment of caspase-9, causing its stimulation (McDonnell *et al.*, 2003). The stimulated caspase-9 may cleave downstream caspases, for instance, caspase- 3/7, initiating the caspase cascade. It was unclear whether the TGZ-induced cytotoxicity observed in this

current study was due to expression levels of Bcl-2 or the other apoptotic repressor genes; for instance, Bcl-xL resulted in TGZ-induced cell death. Furthermore, activation of caspase-3 via multiple pathways may cause apoptosis in a time and dose-dependent manner, as reported in this and previous studies (Vermeulen *et al.*, 2003). Therefore, it is possible to propose that blocking apoptosis through caspase activation would allow researchers to better understand TGZ-induced liver toxicity.

The results in this chapter indicate that TGZ-causes apoptosis through various mechanisms, for instance, activation of caspase-3/7 that can trigger cell death (Vermeulen *et al.*, 2003; Walsh *et al.*, 2008). Also, apoptotic signalling by way of the intrinsic pathways mainly includes activation of the proapoptotic Bcl-2 family members Bax and Bak, which aids the discharge of cytochrome c from the mitochondria, caspase-9 cleavage, or activation (Trécherel *et al.*, 2012; Zhang *et al.*, 2004). The stimulated caspase-9 will, in the end, cleave or activate the downstream effector caspases such as caspase-3 and -7, resulting in apoptosis (Chai *et al.*, 2001; Chao *et al.*, 2005). This pathway is negatively controlled by quite a few antiapoptotic Bcl-2 family members, such as Bcl-2 and Bcl- β (Tsujimoto, 2003). Apoptotic signalling via the extrinsic pathway involves ligand binding to death receptors or the induction of trimerisation of death receptors. The death receptors are members of the tumour necrosis factor receptor superfamily, such as Fas (Franco & Cidlowski, 2006). Upon activation and trimerisation of death receptors, the intracellular death domain of the death receptors recruits adapter proteins such as the Fas-associated death domain, forming a death-inducing signalling complex (DISC), which promotes the recruitment of procaspase-8 to the DISC (Kim *et al.*, 2000). Caspase-8 is then stimulated, causing the triggering of the downstream effector caspases, for instance, caspase-3 and -7. The effector caspases can also be stimulated by death receptors, consequentially through caspase-8-mediated cleavage of Bid, which eases Bax stimulation and successive release of cytochrome c from the mitochondria (Westphal *et al.*, 2013). As a result, the Bid cleavage links up both apoptotic pathways. Cellular FLICE inhibitory protein (c-FLIP), an inactive homolog of caspase-8, functions as an inhibitor of the extrinsic apoptotic pathway by blocking caspase-8 activation (Chao *et al.*, 2005).

Also, the effect of low and higher concentrations of TGZ was assessed, and it was observed that cells treated with low doses (1 to 3 μ M) of TGZ showed an increase in cell growth and declined after 3 μ M to 50 μ M TGZ concentration. Cells treated with a high dose of TGZ at 50 μ M inhibited cell growth by 80%. It can be argued, therefore, that TGZ can act as both an antioxidant and induce oxidative stress. However, TGZ has been reported to exhibit antioxidant activity. A possible explanation might be due to hormesis, which is a mechanism by which a lower dose of a drug or an agent causes beneficial effects through cellular adaptation. In contrast, at higher concentrations, toxic effects are produced. Hormesis appears to be influenced by a variety of physiological cellular means that congregate on increased stress endurance as well as prolonged existence (Sarup *et al.*, 2014); for example, mild heat stress in flies results in increased levels of stress response proteins (Demirovic *et al.*, 2014).

There is currently no dose-response modification that has a substantial inference for toxicity evaluation related to dose-response relationships and adaptive responses. The theory of hormesis can also be considered within a preventive context; for instance, other studies have linked beneficial responses from low to moderate activity levels with hermetic mechanisms (Abete *et al.*, 2008). And in line with our finding, a lower dose of TGZ promoted cell viability. Hormesis could play a key role in pharmacological interventions; for example, the concept of hermetic-biphasic dose-response is already an essential feature in pharmacology, especially in drug discovery. The hormesis concept is also important in clinical pharmacology areas in which high doses are integral to killing harmful organisms or tumour cells. The hormesis concept is additionally critical in clinical pharmacology, in which high concentrations are critical for destroying tumour cells. The minimal dosage stimulatory reaction has not been suggested as a hormetic dose-response. However, it is debatable whether such cases demonstrate the hormetic dose-response, reflecting its significance in biomedical research. It can be used in a variety of biological models, gender and age groups, endpoints, chemical classes, and the constraints it imposes on the quantitative highlights of the dose-response as a marker of biological plasticity. Hormetic dose-response may be integrated into current biological studies to enhance drug design as well as discovery (Abete *et al.*,

2008; Calabrese *et al.*, 2007). To the best of our knowledge, data on effect of the low doses of TGZ on cell proliferation is minimal. Our study adds volume to the very few studies on the low doses of TGZ on cell proliferation.

3.4 Other probable factors that might contribute to TGZ-induced liver hepatotoxicity

The liver is responsible for total body cholesterol excretion via biliary excretion of bile acids and free cholesterol. Hepatic cholesterol production, controlled by a type of homeostatic control, is affected by the hepatic level of free cholesterol or glycogen, or both. Here it was assumed that besides statin, TGZ is one of the pharmacological agents that affect cholesterol's hepatic biosynthesis. The main metabolic end products in cholesterol degradation are bile acids (Chiang, 2017), although cholesterol may also be transformed into sex hormones and adrenocortical hormones. Since cholesterol degradation relies on the concentrations of bile salts in the liver, any factor that will increase bile acid output will also stimulate the synthesis of cholesterol and may, subsequently, lower the serum cholesterol content (Chiang, 2017).

Also, Glutamate dehydrogenase (GDH) is a metabolic enzyme that facilitates the reversible reaction of L-glutamate to α -ketoglutarate with concomitant reduction of NAD(P)⁺ to NAD(P)H or inversely (Grimaldi *et al.*, 2017; Plaitakis *et al.*, 2017; Takeuchi *et al.*, 2018). GDH is mainly expressed in the mitochondria, although recently, it was shown that GDH is present in the cytoplasm, endoplasmic reticulum, and nucleus (Grimaldi *et al.*, 2017). However, its activities outside the mitochondria are poorly understood. GDH is a critical enzyme in mitochondrial carbohydrate biotransformation and facilitates the final stage in glutaminolysis after the conversion of glutamine to glutamate through phosphate-activated glutamine (Grimaldi *et al.*, 2017). In this pathway, α -ketoglutarate can be transported into the tricarboxylic acid (TCA) cycle, a process (anaplerosis) that can produce ATP via oxidation of α -ketoglutarate and increase the ATP: ADP ratio to trigger insulin discharge (Grimaldi *et al.*, 2017; Plaitakis *et al.*, 2017). Glutamate can also be altered into malate by the TCA cycle or into pyruvate via malic enzyme to generate NADPH, needed for cellular stress protection as well as for lipid and cholesterol biotransformation (Grimaldi *et*

al., 2017). Sanki *et al.* have reported that GDH was engaged with ureagenesis as the change of glutamate into α -ketoglutarate likewise delivers NH_3^+ , which can be utilised to make carbamoyl phosphate for the urea cycle. Cell growth, as well as proliferation, is highly dependent on nutrient availability. Nitrogen is an essential element for protein and nucleotide synthesis.

Although the liver can convert ammonia to nontoxic urea in the urea cycle, the urea synthesis capacity is reduced in subjects with liver impairment, resulting in a reduced capacity to detoxify ammonia in the liver (Adeva *et al.*, 2012). Besides, high production of ammonia is also produced in urea cycle disorders and other conditions that lead to either defective ammonia removal or overproduction of ammonia beyond liver clearance capacity (Adeva *et al.*, 2012). Therefore, it was suggested that high levels of ammonia might cause liver injury through another process.

The urea cycle begins in the mitochondria of liver cells and ends in the cytoplasm. The urea cycle converts excess ammonia into urea in the mitochondria of liver cells, as ammonia originates from protein catabolism. Glutamine is then exported from muscles and the peripheral tissues and utilised by the liver. Glutaminase converts glutamine to glutamate and ammonia. Glutamate also yields additional urea via the enzyme glutaminase hydrogenase (Adeva *et al.*, 2012; Sokal *et al.*, 2013; Watford, 2018). From here, ammonia is primarily integrated into mitochondria and eventually leads to urea production. Urea then exits the hepatocyte cytoplasm and is ultimately expelled in urine. Urea is the primary circulating pool of nitrogen, and its generation changes are similar to the degradation of dietary and endogenous proteins (Adeva *et al.*, 2012; Sokal *et al.*, 2013). This is an energy-driven process that happens only within the liver's mitochondria and cytoplasm. When this process is not functioning efficiently, toxic ammonia builds up within the body and, in turn, causes hepatotoxicity (Adeva *et al.*, 2012; Jia *et al.*, 2013; Koppe *et al.*, 2016; Sokal *et al.*, 2013).

Therefore, the following objectives were set in this chapter to determine the possible TGZ toxicity pathways:

- Determine the effect of TGZ on glutamate dehydrogenase activity in Huh7 cells

- Determine the effect of TGZ on ammonia and urea production in Huh7 cells
- Determine the effect of TGZ on Cholesterol homeostasis
- Determine the effect of TGZ on extracellular bile acid concentration

3.4.1 The effect of TGZ on glutamate dehydrogenase activity in Huh7 cells

GDH activity in serum can be used to distinguish between inflammation of the liver, which does not exhibit increased serum GDH activity, and diseases that lead to hepatocyte necrosis, which develops in raised serum GDH. This is because its presence in the liver is much greater than in other organs (Plaitakis *et al.*, 2017). Besides, GDH overactivity in pancreatic β -cells also leads to high insulin secretion via steadily increasing ATP synthesis (Li *et al.*, 2013).

ATP quantification assays were undertaken to determine the impact of TGZ on GDH activity in Huh7 cells. As demonstrated (Figure 3-8), cells treated with TGZ showed a dose-dependent increase in GDH activity within the TGZ-treated cells. TGZ concentrations of 5 to 20 μ M did not cause an increase in GDH activity. However, a significant rise in GDH was recorded in cells treated with TGZ concentrations of 30 to 50 μ M relative to the control cells (untreated cells) (Figure 3-8).

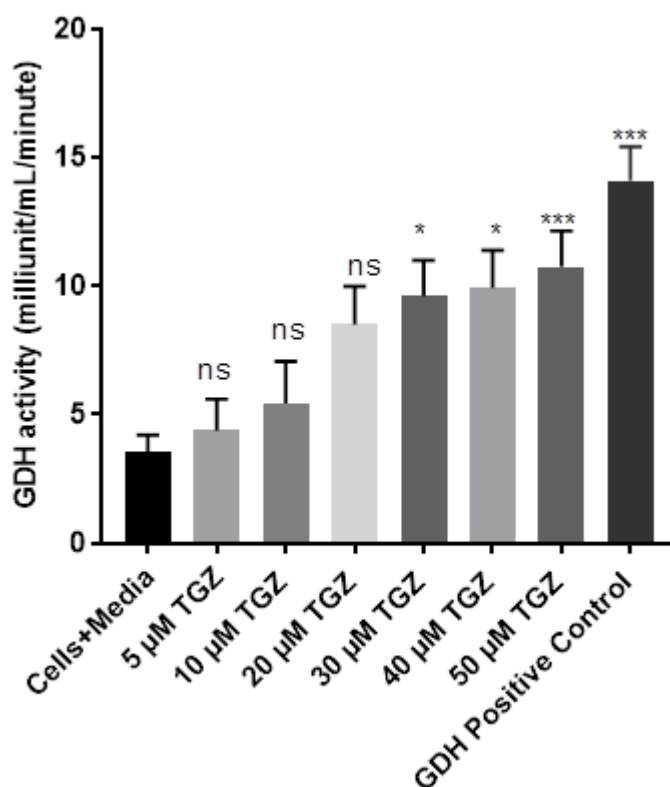


Figure 3-8 Effect of TGZ on GDH activity in Huh7 cells

Cells were exposed to TGZ (5 to 50 µM) for 48 hrs. Treated samples and control samples were collected and put in a 96-well plate. Absorbance was measured at 450 nm using a BMG LABTECH Omega FLUOstar plate reader. Three independent repeats were carried out (n = 9). The mean values were calculated and plotted. The error bars represent the standard error of the mean (SEM). One-way analysis of variance (ANOVA) was used to analyse the data, followed by Dunnett's multiple comparison test. The P values are shown where the difference between responses of 5 µM to 20 µM treatments and the control (Cells) were shown to be statistically insignificant, whereas 30 µM to 50 µM were determined to be significant relative to the control, ns (not significant). * P < 0.0284, ** P < 0.0086, *** P < 0.0003.

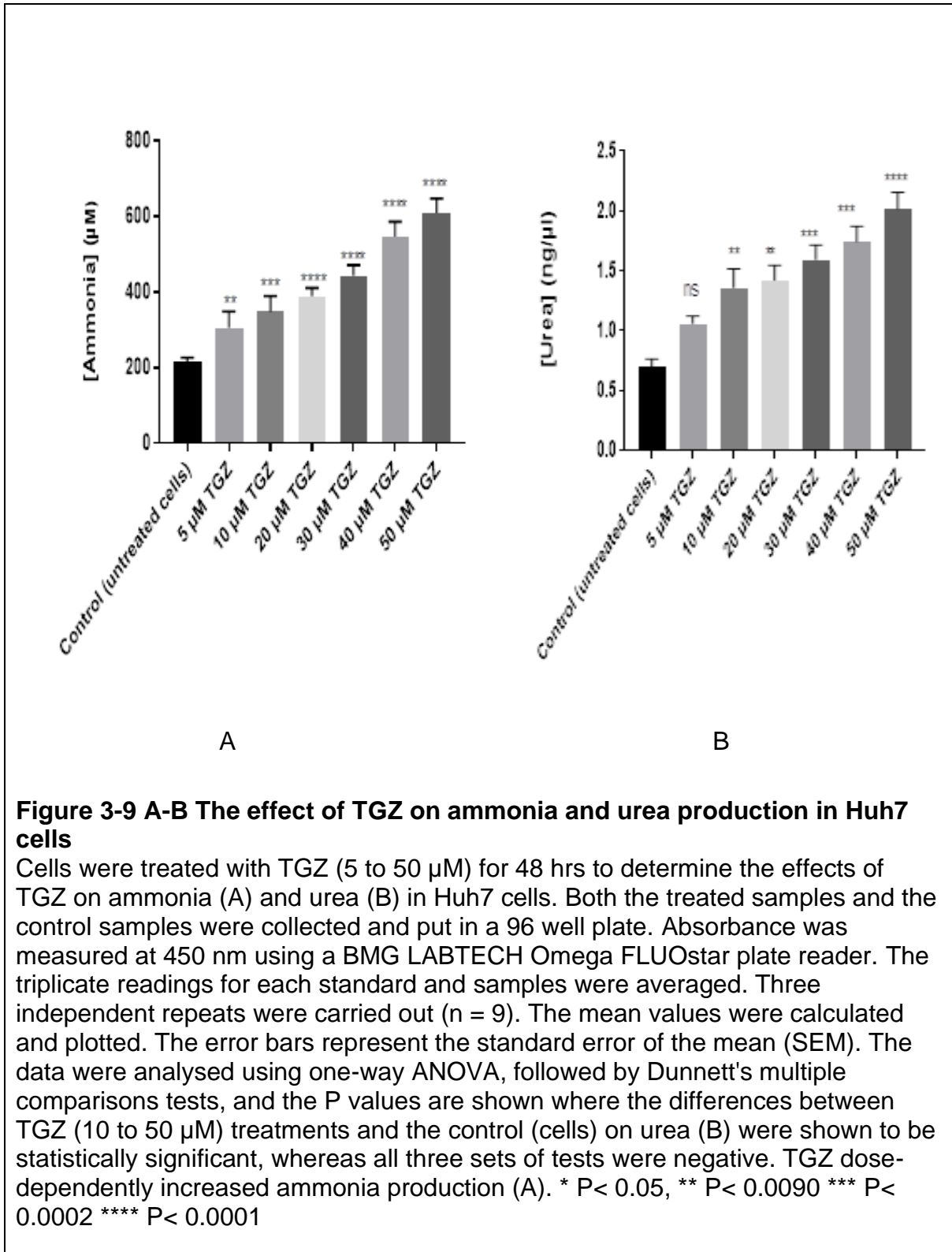
3.4.2 The effect of TGZ on ammonia production and urea formation in Huh7 cells

Ammonia is a key source of nitrogen for living systems. It is synthesised via amino acid biotransformation, and it is toxic when present at a high level (Chastre *et al.*, 2010). To determine if TGZ has any effect on ammonia production in cells, Huh7

cells were exposed to the various concentrations of TGZ and ammonia concentration directly by using NH_3 and NH_4^+ . In this assay, NADH is converted to NAD^+ in NH_3 , ketoglutarate, and glutamate dehydrogenase, and the decrease in optical density is proportional to the NH_3 levels in the samples. The readings for each standard and sample were averaged. The mean value at 450 nm absorbance value of the blank was subtracted from all standard and sample readings (Appendix B). As demonstrated (Figure 3-9A), cells treated with TGZ showed a dose-dependent increase in ammonia levels in Huh7 cells in a significant manner when compared to the control cells.

Having determined that TGZ causes elevation of ammonia in hepatocytes and that ammonia is a by-product of protein nitrogen biotransformation, which then serves as the essential vehicle for ammonia excretion from the body, The impact of TGZ on urea production in Huh7 was determined by treating Huh7 cells with various concentrations of TGZ. The urea levels in both the treated and control samples were determined. For 10 minutes, samples and standards were exposed to urease, an enzyme that hydrolysis urea to ammonia and CO_2 . The ammonia reacts further with a chromogen in an alkali solution to form a blue-green coloured product. After 30 minutes, the plate was read in a standard 96-well spectrophotometric microplate reader at an optical density of 450 nm. The readings for each standard and sample were averaged. The mean value absorbance value of the blank was subtracted from all standard and sample readings (Appendix C). Urea concentrations in both the TGZ-treated and control groups were determined by comparing them with urea known standards. A dose-dependent increase in urea production from TGZ concentrations from 10 to 50 μM in a significant manner. However, urea production in Huh7 cells treated with 5 μM TGZ was very low (Figure 3-9B). In this study, TGZ was seen to increase urea production in Huh7 cells. The loss of viable cells would be expected to decrease the overall urea production, and therefore, care must be taken to avoid exaggerated interpretations. Based on the MTT assay, cells exposed to 5 μM of TGZ were still 90% viable, and thus, the increase in urea at low concentrations of TGZ treatment can be considered independent of cell death. Similarly, the changes in other metabolite levels must also be interpreted in the same manner, in which the decreased levels observed could be attributed to a smaller number of

viable cells. But this is not the case in urea production in TGZ-treated cells. The urea production time course assay in TGZ-treated Huh7 cells would have helped to explain whether TGZ stimulated urea production before cell death in this current study.



3.4.3 The effect of TGZ on cholesterol homeostasis

Cholesterol is a lipid sterol generated and transported throughout the cell's plasma membrane, regulating fluidity and concentrating in specialised sphingolipid-rich domains (rafts and caveolae). Cholesterol plays a critical physiological function in the human body through more than a few structural and metabolic functions (Schindler & Pasqualini, 2005). Cholesterol is a precursor for steroid hormones, sex hormones, estrogens, testosterone, vitamin D, as well as bile acids (Schindler & Pasqualini, 2005). However, too much cholesterol can lead to pathological conditions such as atherosclerosis. Cholesterol homeostasis relies on intricate cellular processes whose deregulation can lead to several life-threatening diseases, such as familial and age-related hypercholesterolemia. Cholesterol is transported throughout the human body within the lipoproteins, which have cell-specific signals that direct the lipids they transport to certain tissues. Therefore, lipoproteins are in different forms in the blood depending on their density (low-density lipoproteins and high-density lipoproteins). Cholesterol remains within a lipoprotein as free cholesterol and a free fatty cholesterol ester, which is the primary form of cholesterol transport and storage (Yuan & Hegele, 2007). However, higher cellular levels of cholesterol can lead to disease conditions like cells of the artery wall, where the build-up of cholesterol triggers atherosclerosis. However, lower levels (hypocholesterolaemia) may be linked to cancer or respiratory diseases (Yuan & Hegele, 2007). The liver plays an essential role in lipid metabolism, serving as the centre for lipoprotein uptake, formation, and export to the circulation. Alterations in liver lipid metabolism can contribute to the development of chronic liver diseases such as nonalcoholic fatty liver disease and add to other chronic liver diseases (Adams, 2005).

Moreover, chronic liver disease can impact hepatic lipid metabolism, leading to alterations in circulating lipid concentrations, contributing to dyslipidaemia. Therefore, determining the circulatory concentration of lipoprotein is essential to the diagnosis of lipid transport disorders. An effort was made to assess the impact of TGZ on cholesterol levels in Huh7 cells. Therefore, a commercially available cholesterol quantitation kit from Sigma-Aldrich was used to quantify the total cholesterol in Huh7 cells exposed to TGZ. The kit is used to determine the levels of free cholesterol, cholesteryl esters, or both present in a sample. Total cholesterol

was determined by a coupled enzyme assay, which results in a colourimetric (570 nm) product proportional to the cholesterol present in a sample. Huh7 cells were treated with various concentrations of TGZ (5 μ M to 50 μ M), 10 μ M simvastatin (negative control) and 20 μ g of cholesterol (positive control). Untreated cells (cells + medium only) were included as a control. Cells were exposed to the above conditions for 48 hrs, as outlined in section 2.2.18. Therefore, the total cholesterol in the various samples was determined. Absorbance was read at 570 nm using a BMG FLUOstar Omega plate reader. Blank standard readings were subtracted from all readings (corrected absorbance readings). The cholesterol standard curve was plotted (Appendix E), and the corrected absorbance of the sample was applied to the cholesterol standard curve to determine the cholesterol content in the sample well. Total cholesterol was calculated according to the manufacturer's instructions. A significant reduction in cholesterol concentration was observed in cells treated with TGZ and Simvastatin, whereas cholesterol concentration increased in cells treated with 10 μ g of cholesterol (Figure 3-10).

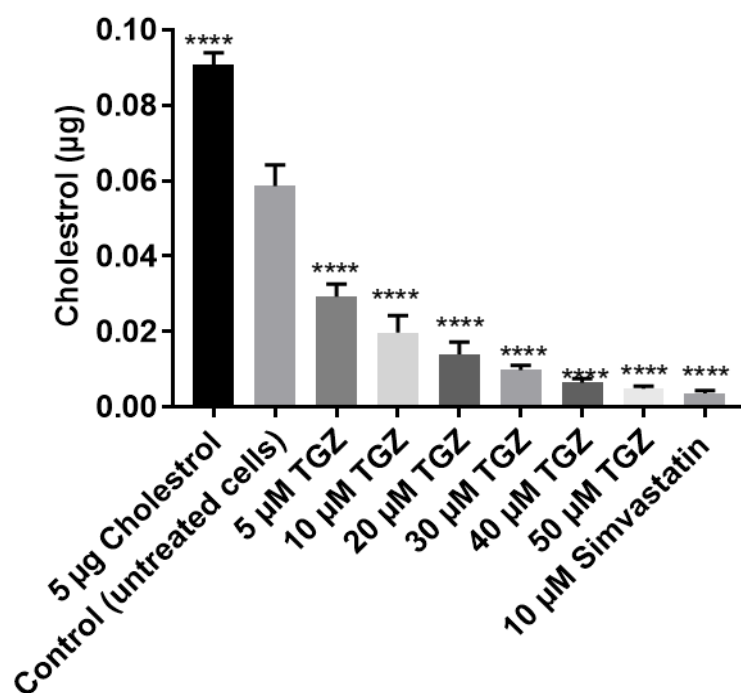


Figure 3-10 The effect of TGZ on cholesterol levels in Huh7 cells

Huh7 cells were incubated with media (cells + media). The cells were treated with TGZ (5 to 50 µM), 10 µM and 5 µg cholesterol for 48 hrs. Three independent repetitions (n = 9) were performed. The mean values were determined and plotted. Error bars represent the mean ± SEM of three replicates. The data was analysed using one-way ANOVA, followed by Dunnett's multiple comparison test. P values are shown where the various treatments are determined to be statistically significant. **** P < 0.000.

3.4.4 TGZ-induced cholestasis as a contributing factor to liver toxicity

Bile acids are produced in the hepatocyte by cholesterol oxidation and biotransformed via glycine or taurine conjugation and then secreted into bile. Bile acids are further biotransformed by bacterial enzymes in the intestine and undergo enterohepatic circulation (Chiang, 2009; Hofmann & Hagey, 2008). As a detergent molecule, bile acids play essential roles in cholesterol homeostasis as well as the absorption of vitamins and lipids. Bile acids form about 67% of the total composition of bile. The average composition in healthy individuals is the conjugates of cholic, chenodeoxycholic, and lithocholic acids (Chiang, 2009). Bile acids are essential for

lipid solubilisation as they form micelles with cholesterol as well as fatty acids. Bile acid synthesis is crucial for the removal of cholesterol from the body and the uptake of dietary lipids into the small intestine. BSEP is located on the liver cells' canalicular plasma membrane and plays a critical role in the biliary clearance of bile acids. Therefore, any drug or agent that blocks BSEP can cause cholestasis and possibly hepatic injury. TGZ and its sulphate metabolite are potent blockers of bile (BSEP). TGZ-induced bile acid retention has been theorised to be one of the underlying mechanisms of liver injury. Thus, it was proposed that inhibition of BSEP by TGZ may cause cholestasis (accumulation of bile acids) and therefore, it was exposed to HEK293 cells (overexpressing human organic anion-transporting polypeptides (OATP) 1B1 and OATP1B3), which contribute to hepatic uptake of bile acids such as taurocholic acid (Cui *et al.*, 2000) to the various concentrations of TGZ for 48 hrs, and, using a commercially available kit from Sigma Aldrich, extracellular (the level of bile acids released into the culture media) was determined.

The kit used for this assay provides a convenient fluorometric means to determine extracellular bile acid in a sample. The assay is based on the principle that 3 α -hydroxysteroid dehydrogenase acts in response to bile acids and alters NAD to NADH, which decreases the probe to a highly fluorescent artefact. The subsequent fluorescence intensity represents the bile acid level in the sample. A dose-dependent decrease in extracellular bile acids in TGZ-treated cells in a significant manner was recorded (Figure 3-11).

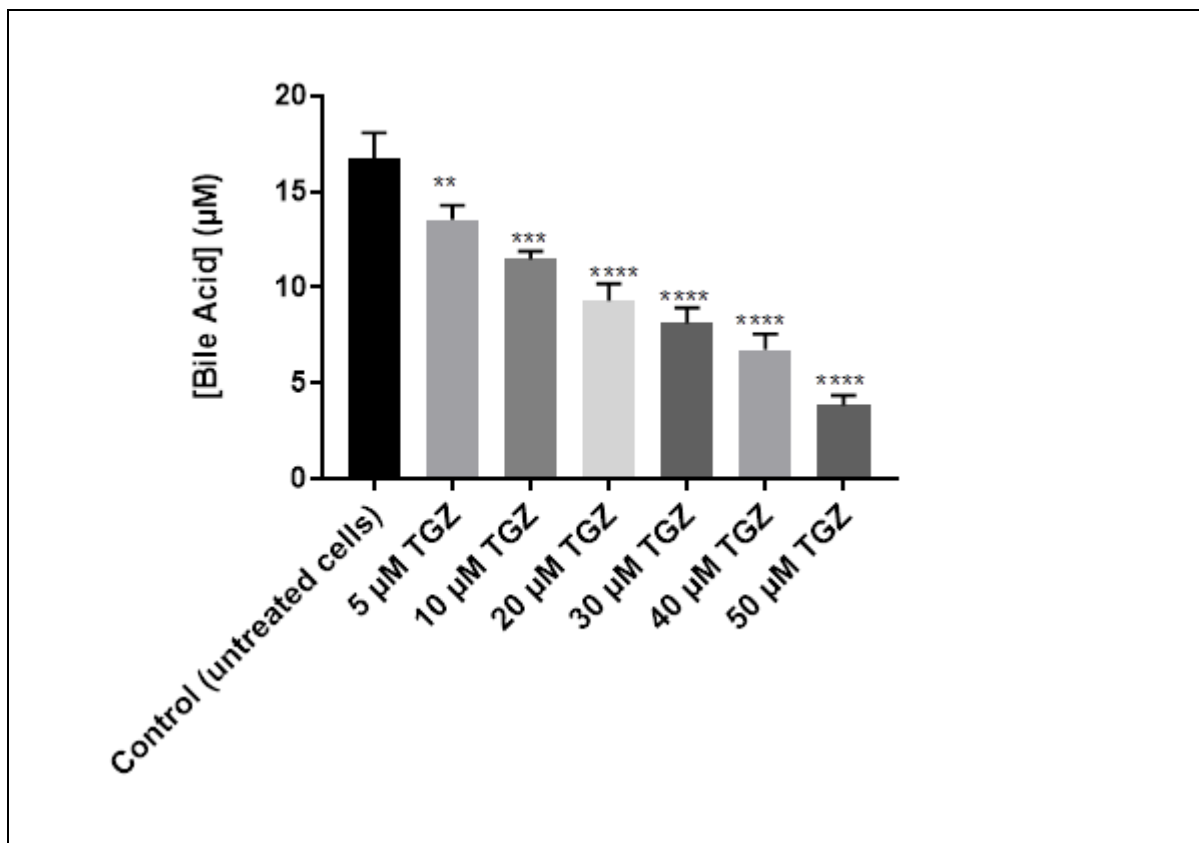


Figure 3-11 The effect of TGZ on extracellular bile acid concentration in HEK293 cells.

HEK293 cells were incubated in a serum-free medium (cells+media). Cells were treated with TGZ (5 to 50 µM) for 48 hrs. Cells were lysed, the supernatant was collected, and absorbance was measured at 570 nm using a BMG LABTECH Omega FLUOstar plate reader. Three independent repeats were carried out (n = 9). The mean values were determined and plotted. The error bars represent the standard error of the mean (SEM). One-way analysis of variance (ANOVA) was used to analyse the data, followed by Dunnett's multiple comparison test. The P values show the difference between the responses of different treatments and the control (cells) were statistically significant, ** P < 0.0026, **** P < 0.0001.

3.5 Discussion

In this study, the effect of TGZ on GDH activity in Huh7 cells was evaluated. A dose-dependent increase in GDH activity in the cells exposed to the various concentrations of TGZ was recorded. Although Botman *et al.* have previously reported that the liver expresses high levels of GDH, an indication of NAD⁺ dependence, our results indicate that the rise in GDH activity was because of the influence of TGZ. GDH, as a hexameric enzyme in mitochondrial carbohydrate metabolism, facilitates the reversible conversion of glutamate to α-ketoglutarate as

well as ammonia while reducing NAD(P)⁺ to NAD(P)H (Botman *et al.*, 2014). Consistent with a previous study by Friday *et al.*, TGZ did induce an accelerated flux of GDH as well as ammonia production in cancer cells. However, they did note that TGZ inhibited transport into the TCA cycle, decreasing α -ketoglutarate and stimulating GDH flux through a pull mechanism. Also, they reported a simultaneous inhibition of the sodium-proton exchanger by TGZ and driving GDH through the push mechanism. However, the glutaminase flux remained unchanged while the ammonia production increased due to the increase in deamination flux. Friday *et al.* further co-treated cancer cells with TGZ and pioglitazone and recorded an additive effect on GDH flux. Also, they reported a simultaneous inhibition of the sodium-proton exchanger by TGZ and driving GDH through the push mechanism. However, the glutaminase flux remained unchanged while the ammonia production increased due to the increase in deamination flux. Friday *et al.* further co-treated cancer cells with TGZ and pioglitazone and recorded an additive effect on GDH flux. They, therefore, suggested that it might be due to PPAR γ -mediated downregulation of NHE gene expression. Inhibition of GDH may be most effective in causing drastic cell death. A dose-dependent increase in ammonia production in Huh7 cells was recorded in this study. However, the increase in ammonia production by TGZ might not be associated with an increase in GDH activity, which indicates that intracellular pH may be reduced (Welbourne *et al.*, 2001). One potential pathway for TGZ to reduce the intracellular pH would be to decrease protein kinase C activity, which subsequently represses the action of sodium/hydrogen ion exchange (Isshiki *et al.*, 2000; Welbourne *et al.*, 2001).

Despite extensive study of GDH over the past decades, its role in cell biology has still not been adequately explained. Extensive kinetic research has demonstrated many aspects of GDH catalysis, but unanswered questions remain (Engel, 2013). It is understood that mammalian GDH's thermodynamic equilibrium promotes glutamate synthesis, but it is currently unclear whether the enzyme functions *in vivo* via reductive amination or an oxidation-deamination route. As the GDH-catalysed reaction is reversible, its pathway is predicted to rely on substrate concentration and enzyme specificity (K_m value) for such substrates (Masclaux-Daubresse *et al.*, 2006; Plaitakis *et al.*, 2013). Furthermore, substrate concentrations, pH, ionic strength, and

buffer composition all have an impact on GDH catalysis (Engel, 2013; Zaganas & Plaitakis, 2002). A study on GDH, isolated from mammalian tissue or recombinant hGDH1, has shown that the enzyme functions optimally at a basic pH (7.75 to 8.00). ADP stimulation decreases significantly at lower pH (Kanavouras *et al.*, 2007). On the other hand, the maximum pH for hGDH2 is 7.50, allowing the enzyme to operate efficiently at even lower pH levels (7.25-7.0). In triethanolamine buffer pH 8.0 at 1.0 mM ADP, hGDH1 and hGDH2 have similar catalytic properties (maximum rate of reaction (V_{max}) and Michaelis-Menten constant (K_m) for α -ketoglutarate, ammonia, and glutamate) (Kanavouras *et al.*, 2007). GDH might operate in an oxidative deamination direction due to the relatively high K_m for ammonia, particularly in tissues with typically reduced ammonia concentrations. There is evidence that ammonia K_m is influenced by cellular pH. Previous research that used hGDH1 has reported a reduction of buffer pH from 8.00 to 7.5 or 7.0 elevated ammonia K_m from 12.8 mM to 35.0 mM and 57.5 mM, respectively (Zaganas *et al.*, 2013). The corresponding ammonia K_m for recombinant hGDH2 ranged from 14.7 mM to 33.0 mM and 62.2 mM (Zaganas *et al.*, 2013). They proposed that intracellular acidification might have developed in astrocytes preceding glutamate absorption or in epithelial cells of the kidney's proximal convoluted tubules during systemic acidosis, eventually impeding α -ketoglutarate reduction amination (Azarias *et al.*, 2011; Van de Poll, 2004; Dimovasili, 2015).

In mammalian tissues, GDH contributes to Krebs cycle anaplerosis as well as energy generation. GDH in the liver cells contributes to ammonia production, with NH_3 being removed through the urea cycle. Although GDH represents about 1% of total proteins, its enzymatic activity is approximately five-fold higher than in other tissues (Botman *et al.*, 2014; Spanaki *et al.*, 2014).

Nonetheless, previous studies have recorded a substantial increase in ammonium production at a 5 μ M TGZ concentration, which approximately estimates the decrease in alanine formation. According to the researchers, this was a representation of an accelerated flow of glutamate through the deamination pathway (Botman *et al.*, 2014; Spanaki *et al.*, 2014). Research by Welbourne *et al.* also showed higher levels of glutamate; TGZ prevented the use of glutamine but not the production of ammonium. They subsequently indicated that the flow via GDH was

retained, given the decreased total usage of glutamine. They also reported that TGZ increases glutamate flow through the GDH pathway and increases ammonium production (Welbourne *et al.*, 2001).

Ammonia derived from the diet or produced by the skeletal muscles, the kidney, and the brain is mostly detoxified in the liver cells (Spanaki & Plaitakis, 2011). The amino acid may be discharged from the muscles through the blood in the form of alanine and glutamine and taken up by the liver for neoglucogenesis. This pathway produces ammonia via glutamine deamination. By glutamate deamination, the later reaction being facilitated by GDH generates α -ketoglutarate, a Krebs cycle intermediate and ammonia, consequently providing the total body ammonia pool.

Having determined the impact of GDH activity in Huh7 cells, the effect of TGZ on ammonia production in Huh7 cells was also determined. Then the effect of TGZ on ammonia production was estimated to ascertain whether the significant GDH activity observed in Huh7 cells treated with TGZ would impact ammonia production.

Interestingly, there was a dose-dependent increase in ammonia levels in Huh7 cells. Metabolic mechanisms generate ammonia in cells, and it is a substance in all phylogenetic concentrations. Despite its continuous existence in living organisms, ammonia can cause toxicity. These harmful effects may arise from the action of ammonia at intracellular sites and may also manifest as a result of an impairment in ammonia detoxification processes (Lange *et al.*, 2009; Taub, 2004).

Relatively few articles have been published about the exact mechanism of the toxic or inhibitory action of ammonia on cells, and the exact mechanism remains unclear. Ammonia can perturb the intracellular pH as well as electrochemical gradients. In aqueous solution, ammonia and ammonium are linked in pH-dependent equilibrium. At physiological pH of 7.1-7.5, which is also the pH at which most of the mammalian cell cultures are carried out, only about 1% of the total ammonia levels are present as NH_3 , with the rest being NH_4^+ . Ammonia is a small, uncharged, lipophilic molecule that readily diffuses across cellular membranes. The diffusion will follow the gradient of the chemical potential of ammonia, which can be approximated by the gradient of the partial pressure of NH_3 (Guha *et al.*, 2019). The small amount of NH_3

in the extracellular and intracellular aqueous phases will diffuse across the membranes, quickly equilibrating any transmembrane gradient (Guha *et al.*, 2019).

As protonation is extremely fast, the pH equilibrium will be rebuilt instantaneously. In a compartment with a low pH, the partial pressure of NH₃ is more moderate, leading to a constant flow of NH₃ across the membrane into this compartment until equilibrium is attained, that is, the pH increases (Chaudhry, 2001; Guha *et al.*, 2019). In this way, ammonia can negatively affect the activities of the organelles with low pH, such as the lysosomes. In contrast, the diffusion of NH₄⁺ across cellular membranes is extremely slow. However, it can be transported actively across the cell membrane via specific transport proteins such as the Na⁺ K⁺-ATPase, by facilitated diffusion through the Na⁺ K⁺ 2CL-cotransporter, or via the Na⁺/H⁺-exchanger. NH₄⁺ may interact with the binding site for K⁺ due to hydrated NH₄⁺ possessing the same ionic radius as K⁺, which can perturb the transmembrane transport of the Na⁺/H⁺-exchanger (Chaudhry, 2001).

This may further lead to critical constraints on ion gradients across the cell membrane. Previous research discovered that when cells were cultured in 10 mM glucose and 2 mM glutamine, the maximum capacity for inward K⁺ transport was significantly higher than when cells were cultured in glutamine alone, with metabolic energy derived from glutamine oxidation (Tildón *et al.*, 2018; Zaganas *et al.*, 2013). Ammonia production increased due to increased glutamine turnover in the glutamine-containing medium, and ammonium will compete with K⁺. Active transport through the Na⁺/K⁺-ATPase can occur against the concentration gradient. And this will cause high energy demand since the K⁺ gradients have to be maintained.

The diffusion of ammonia into mitochondria as well as other organelles will cause an increase in the pH within these compartments. Under a physiological condition where extracellular ammonia becomes higher, it induces an expansion of the mitochondrial matrix. In contrast, higher intracellular ammonia levels will result in a drop in the pH of the mitochondrial matrix. The primary source of the ammonia accumulated in cell cultures is glutamine, which plays an essential role in the metabolism of rapidly growing cells. Gras *et al.* also documented TGZ glutamine metabolism inhibition, while its un-insulin-like improvement in blood glucose

utilisation *in vitro* has been reported. Because glucose utilisation may be linked to increased glutamine use, glucose absorption can primarily inhibit glutamine use and, as a result, reduce transamination pathway flux (Tildón *et al.*, 2018). However, toxic ammonia accumulation could be overcome by substituting glutamine with glutamate or other amino acids for nutrient control. That is, the addition of glutamine at low concentrations or the removal of ammonia or ammonium from the culture medium through ion-exchange resins or ion exchange membranes (Zaganas *et al.*, 2013).

In summary, based on the liver cell damage model resulting from ammonia, the present study has revealed that increased ammonia production in Huh7 cells by TGZ might be one of the mechanisms of TGZ-induced liver toxicity. This may involve mitochondrial damage by activating an intrinsic Ca²⁺-independent apoptosis pathway (Kim *et al.*, 2006). It appears that therapeutic approaches to inhibit the absorption of ammonia and rebalance apoptosis might be efficient in preventing TGZ-induced liver damage.

Having demonstrated the impact of TGZ on ammonia production, the assessment of TGZ on urea production in Huh7 cells was conducted. The results recorded in the present study show a dose-dependent increase in urea production. Urea exerts its toxic action through ROS production (D'Apolito *et al.*, 2015). High levels of urea have been defined to elevate intracellular ROS production in various cells, such as vascular endothelial cells. Moderate levels of urea have been shown to control the phenotype of aortic smooth muscle cells (Madsen *et al.*, 2017). Also, Trecherel *et al.* showed that urea was able to induce the expression of a pro-apoptotic member of the Bcl2 family, the Bcl-xL/Bcl-2 protein, in VSMC, urea-provoked Bad overexpression may be responsible for the increased apoptosis recorded in the arterial wall of patients with uraemia. Bad can stimulate the cells to the pro-apoptotic effect of oxidative stress, therefore, suggesting high levels of urea production might be one of the contributing factors in TGZ-induced hepatotoxicity.

The liver, as well as the small intestine, are the significant organs implicated in cholesterol synthesis in humans. This chapter aimed to determine whether TGZ influences cholesterol synthesis in Huh7 cells. Even at 5 µM TGZ, a significant dose-dependent decrease in cholesterol level was observed; however, Huh7 cells

exposed to 50 M TGZ concentration reduced total cholesterol by approximately 90%. It can be argued that a substantial decrease in cell viability at 50 μ M TGZ (Figure 3-2) might have contributed to the drastic reduction of cholesterol concentration in cells exposed to 50 μ M recorded in section 3.4.3 (Figure 3-10). However, previous studies treated HepG2 cells with lower TGZ concentrations using slightly reduced cell viability to determine whether the TGZ-induced cholesterol reduction was not entirely due to the cell population (Klopotek *et al.*, 2006). They reported that cells treated with low doses of TGZ still recorded lower protein levels of SREBP-2 in the nucleus and a subsequent decrease in mRNA levels of its target genes, HMG-CoA reductase, as well as low-density lipoprotein (Klopotek *et al.*, 2006). Therefore, it was presumed that downregulation of HMG-CoA reductase expression was linked to a reduced protein concentration of the enzyme. As such, a subsequent reduction in cholesterol synthesis was recorded in Huh7 cells treated with TGZ. Also, the reduced levels of the mature SREBP-2 within the nucleus of the cells exposed to TGZ could have two distinct explanations. TGZ might either inhibit the processing of the mature SREBP-2 in the Golgi or inhibit gene expression of SREBP and thus biosynthesis of the immature SREBP-2. Insig-1 and -2 play a crucial role in the proteolytic procession of the immature SREBP-2 (Janowski, 2002; Klopotek *et al.*, 2006). Both Insig-1 and -2 can inhibit the translocation of the SREBP-SCAP complex from the endoplasmic reticulum. Other studies by Kast-Woelbern *et al.* using rosiglitazone also recorded a reduction of mature SREBP in white adipose tissue through Insig-1 upregulation. Although previous studies did not detect Insig-1 mRNA and did not record but observe an increase in Insig-2 expression in TGZ treated cells, they did not demonstrate whether the increase in expression levels of Insig-1 or -2 (Janowski, 2002; Klopotek *et al.*, 2006).

The researchers suggested that because they only determined the mRNA levels of Insigs after 4 hrs of exposure, Insigs might have been expressed previously, which could have inhibited the proteolytic process of the immature SREBP-2. However, they recorded a reduced effect of TGZ on the gene expression of SREBP-2. They suggested that the decreased nuclear levels of the mature SREBP-2 might be due to the reduced formation of the immature SREBP-2. A reduction in extracellular cholesterol levels in cells is a marker of decreased cholesterol synthesis (Klopotek *et*

et al., 2006). HepG2 cells exposed to low TGZ concentrations for 24 hrs increased gene expression activity as well as low-density lipoprotein receptor activity. Their findings could be explained by the longer exposure time of cells to TGZ in that exposure of cells to TGZ initially produced cellular cholesterol depletion (Klopotek *et al.*, 2006). Depletion of intracellular cholesterol might cause an upregulation of SREBP-2 processing as well as LDL receptor expression via downregulation of Insig-1. However, other studies have reported that the activation of PPAR γ in THP-1 macrophages exposed to TGZ as well as caused an upregulation of HMG-CoA reductase mRNA expression (Iida *et al.*, 2002; Schmitz & Torzewski, 2002). The difference between these studies might also be due to the different cell types employed, as macrophages can excrete cholesterol through ABC1 onto apoA1 and the efflux is triggered by PPAR γ (Chawla *et al.*, 2001).

Our data suggest that TGZ decreases cholesterol levels in Huh7 cells and that this might result from TGZ's down-regulation of cholesterol synthesis in the cells through a reduced level of nuclear SREBP-2 or dose-dependent cell death. Physiologically, cholesterol biosynthesis in the hepatic and the intestine is vital. It is closely related to the cholesterol levels in plasma and the low-density lipoprotein, which might strongly be linked to the risk of heart disease. Also, earlier research that used tumour cells of MA-10 Leydig reported a reduction in cholesterol esters and a rise in free cholesterol, which restored the plasma membrane cholesterol pool impervious to cholesterol oxidase. The authors argued that their results were the consequence of PPAR γ induction as well as the retention or repression of cholesterol transfer into the cell and are attributable to TGZ on cholesterol ester (Freeman & Romero, 2003). Any effects on homeostasis, either through the inhibition of cholesterol synthesis or overproduction of cholesterol, can cause a deleterious effect when not controlled to maintain normal physiological levels (Begrache *et al.*, 2011; Luo *et al.*, 2019; Wong *et al.*, 2018). Again, it could be stated that TGZ might cause liver toxicity through cholesterol imbalances tilting to the lowest physiological levels.

Bile acid (BA) disruption has been implicated in liver and DILI diseases. Therefore, BA is becoming a more and more popular screening tool in DILI evaluation. This study also aimed to assess the impact of TGZ-induced BA accumulation in liver cells. This current study shows a dose-dependent reduction of extracellular bile acid

in HEK293 cells exposed to TGZ. And an explanation for our recordings might be due to TGZ 's ability to inhibit BSEP in that BSEP inhibition might lead to a build-up of BAs in the cells. It could be argued that under a condition where there was no inhibition of BSEP, the levels of extracellular discharge of bile acids would not be affected.

Previous work by other researchers has focused on the connection between BSEP inhibition and cholestasis (Garzel *et al.*, 2013; Jackson *et al.*, 2018; Rodrigues *et al.*, 2013). However, *in vitro* BSEP inhibition studies do not accurately predict *in vivo* DILI incidence (Garzel *et al.*, 2013; Jackson *et al.*, 2018; Rodrigues *et al.*, 2013). BAs function as signalling molecules to inhibit hepatic insult by stimulating the compensatory process, for example, FXR. The significant difference in clinical liver injury occurrence between these two potent BSEP inhibitors shows that other mechanisms might be involved in BSEP inhibition. FXR stimulation will also improve the expression of BSEP, but it does not matter if there is an inhibitor of BSEP. Previous studies have also demonstrated BSEP inhibition in sandwich-cultivated cells and they concluded that all the toxicity recorded was due to BSEP inhibition (Ogimura *et al.*, 2011; Rodrigues *et al.*, 2013; Susukida *et al.*, 2015). Besides, FFAs have been reported to sensitise liver cells to cytotoxicity (Pusl *et al.*, 2008). Accumulation of lipids or retention of hepatic bile acids has been reported to cause similar cytotoxicity pathways (Perez & Briz, 2009; Pusl *et al.*, 2008). BA toxicity capacity was significantly increased more than 20 times in both donors after TGZ exposure. However, CsA treatment in the absence and presence of FFAs was affected and only marginally decreased. They suggested that TGZ but not CsA caused cell death in a BA-dependent manner, and FFAs increased the hepatocyte susceptibility to TGZ-induced BA-dependent toxicity (Pusl *et al.*, 2008).

Again, ER stress resulting in cell death has been reported to be a possible mechanism for BA-induced cholestatic hepatotoxicity (Perez & Briz, 2009; Tamaki *et al.*, 2008). Blocking the BA homeostatic mechanism through inhibition of BSEP and FXR antagonism could increase ER stress, initiating the apoptotic cascades. Still, CsA treatment significantly induced C/EBP homologous protein mRNA content, a key marker of ER stress and the initial architect of cell death (Perez & Briz, 2009; Tamaki *et al.*, 2008). A blockade of the BA homeostatic mechanism would eventually

cause an increase in BA and later cell death (Perez & Briz, 2009). These findings may add to the weight of evidence that TGZ is a potent BSEP inhibitor.

.

Chapter 4 Effects of TGZ on mitochondrial impairment

4.1 Introduction

Organisms may be exposed to free radicals, or ROS (Balaban *et al.*, 2005; Nogueira & Hay, 2013). ROS is generated continuously by an aerobic organism during cellular metabolism or in response to different environmental stimuli, mainly in the mitochondria (Balaban *et al.*, 2005; Nogueira & Hay, 2013).

Mitochondria are a vital source of ROS within mammalian cells as a by-product of respiration. However, exposure to exogenous drugs can trigger ROS production either directly or via metabolism. Generally, ROS has been classified as a toxic product that must be neutralised to prevent cell death (Nogueira & Hay, 2013). However, a recent study has shown that low levels of ROS generation are implicated in cell signalling, cell fate, and cell proliferation (Nogueira & Hay, 2013). Therefore, understanding the mechanism of ROS generation in normal as well as in pathological conditions could lead to successful treatment of various diseases that have been speculated to occur because of ROS production.

Mitochondrial ROS generation has been explained in several cell signalling pathways (Murphy, 2008; Nogueira & Hay, 2013; Turrens, 2007). Cellular respiration is diminished in a situation where the tissue becomes deficient in oxygen. It results in hypoxia and mitochondrial ROS generation can trigger signalling pathways that decrease cellular oxygen utilisation and decrease cellular oxygen consumption (Krause, 2018; Murphy, 2008; Nogueira & Hay, 2013).

Poor coupling of the cytochrome P450 catalytic cycle will cause ROS generation to metabolise both endogenous and exogenous biotransformation. P450 enzymes are heme thiazole enzymes involved in the monooxygenation of lipophilic compounds in the preparation of phase II biotransformation and elimination. In monooxygenation reactions, two electrons are transferred to the P450 enzyme, facilitated by NADPH P450 reductase. The input of electrons is a requisite to trigger oxygen and introduce an oxygen atom into the substrate molecule (Hata *et al.*, 2001). On the other hand, the pairing efficiency of electron transfer diverges based on the P450 isoform; on the other hand, it is not more than 50%. At a critical point, the inept pairing can result in

high ROS levels enough to instigate oxidative stress (Samoilova *et al.*, 2011; Schieber & Chandel, 2014). TGZ is an excellent example of the means through which an exogenous compound can produce ROS via different routes. In the presence of the electron carrier, NADH, TGZ can undergo a similar quinone cycling to that previously stated (He *et al.*, 2001).

While there is an entire scope of ROS that can instigate harm and induce oxidative stress, there have been reports that have implicated oxidative stress in drug-induced liver injury. Drug-induced oxidative stress is regarded as a mechanism of toxicity in various tissues or organs, most commonly the liver (Narayanan *et al.*, 2003; Samoilova *et al.*, 2011). Based on the data recorded in the previous chapter and in perspective on contemplations, raised ROS levels have been linked with several of the drug-induced injuries. With TGZ, this presented itself as a possible means by which apoptosis might be stimulated. It was postulated that treatment of cells with TGZ induces oxidative stress that ultimately activates apoptotic cellular death. However, oxidative stress could be blocked within the liver by creating a continuous balance between the intrahepatic antioxidants (glutathione, vitamin E, β -carotene, and vitamin C) as well as ROS. Therefore, this study aimed to determine whether treatment of Huh7 cells with various concentrations of TGZ would cause ROS production.

In addition, Huh7 cells were co-treated with TGZ and vitamin C to see if vitamin C could help reduce ROS production. Also, an essential role of the mitochondria within the cell is to produce energy in response to demand, in ATP. The role of mitochondrial has been explored in other study settings in previous years (Hu & Ren, 2016; Manivannan *et al.*, 2017; Shehu *et al.*, 2017; Starkov, 2008). Currently, there are *in vitro* studies that could be utilised to uncover mitochondrial DILI in a pre-clinical setting, including but not limited to: oxygen consumption rates during mitochondrial respiration, ETC complex activity, mitochondrial transmembrane potential, as well as the assessment of mtDNA integrity. Mitochondrial impairment is often latent until the number of mitochondria affected reaches a maximum, beyond which damage can diversely reveal itself. Slight disruptions in respiration can cause cell dysfunction, but severe damage can result in cell necrosis and, in theory, fibrosis (Wasmuth *et al.*, 2010). β -oxidation occurs when fatty acid molecules are broken

down and produce acetyl CoA for the Krebs cycle. However, if this is inhibited, fatty acids may accumulate, become esterified, and converted to triglycerides, eventually accumulating and eventually leading to steatosis. Drugs can either directly inhibit β -oxidation through interaction with FAO enzymes or indirectly by inhibiting β -oxidation impairing the ETC (Poirier *et al.*, 2006).

TGZ has been shown to inhibit acyl-CoA synthase, preventing long-chain acyl-CoA formation (Jove *et al.*, 2003; Tirmenstein, 2002). Severe inhibition of mitochondrial β -oxidation causes an increase in free fatty acids in the cytoplasm. In a situation whereby the fatty acids cannot be wholly oxidised, they become esterified into triglycerides. Triglycerides accumulated in the cells can form a fatty deposit in the cells (steatosis). In acute and severe liver toxicity, lipid deposits in the form of small vesicles accumulate in the liver cells (micro steatosis), and the lesion is linked with succeeding hepatic failure (Ong *et al.*, 2007).

Cells deprived of ATP experience reduced gluconeogenesis, which can cause hypoglycaemia (Cui *et al.*, 2017). Furthermore, obstructed energy generation in the cell can trigger hepatic cytolysis (large scale cell death in the form of apoptosis or necrosis) depending on the severity of ATP depletion (Cui *et al.*, 2017). Apoptotic cells are eliminated by macrophage-based phagocytosis. However, when apoptosis is sustained over a prolonged period, inflammatory cells can experience the knock-on effect of producing a state of cytolytic liver inflammation, which in its mildest early phases can lead to higher levels of hepatic enzymes AST and ALT (Massart *et al.*, 2018). In more severe cases, it can result in liver failure, which would require a liver transplant as the only clinical intervention (Massart *et al.*, 2018; Schmeding *et al.*, 2010). The presence of lactate may also be used to uncover impaired mitochondrial activity in cells. When ETC is damaged and the flow of electrons is inhibited, it can result in an accumulation of electrons in the chain, which can cause oxidative stress because of the generation of peroxide from the damaged chain (Sousa *et al.*, 2018). Also, there is a secondary result of inhibited electron flow that leads to a switch in energy generation from oxidative phosphorylation to glycolysis. Reduction in electron flow decreases the level of re-oxidation of the electron carrier NADH to NAD⁺ (Phypers & Pierce, 2006). Under normal physiological aerobic conditions, pyruvate is oxidised to acetyl CoA for the Krebs' cycle using NAD⁺ and producing NADH

(Phypers & Pierce, 2006). NADH is then transported within the mitochondrial membrane to maintain low levels; in the mitochondrial inner membrane, it can donate electrons to oxidative phosphorylation (Phypers & Pierce, 2006). NADH levels in mitochondrial dysfunction remain low. Due to a high NADH/NAD⁺ ratio, the oxidation of pyruvate dehydrogenase decreases and instead becomes reduced to lactate. This may accumulate to cause lactic acidosis (Pessayre *et al.*, 2012; Phypers & Pierce, 2006).

Therefore, the following objectives were set in this chapter to determine the possible TGZ toxicity pathways:

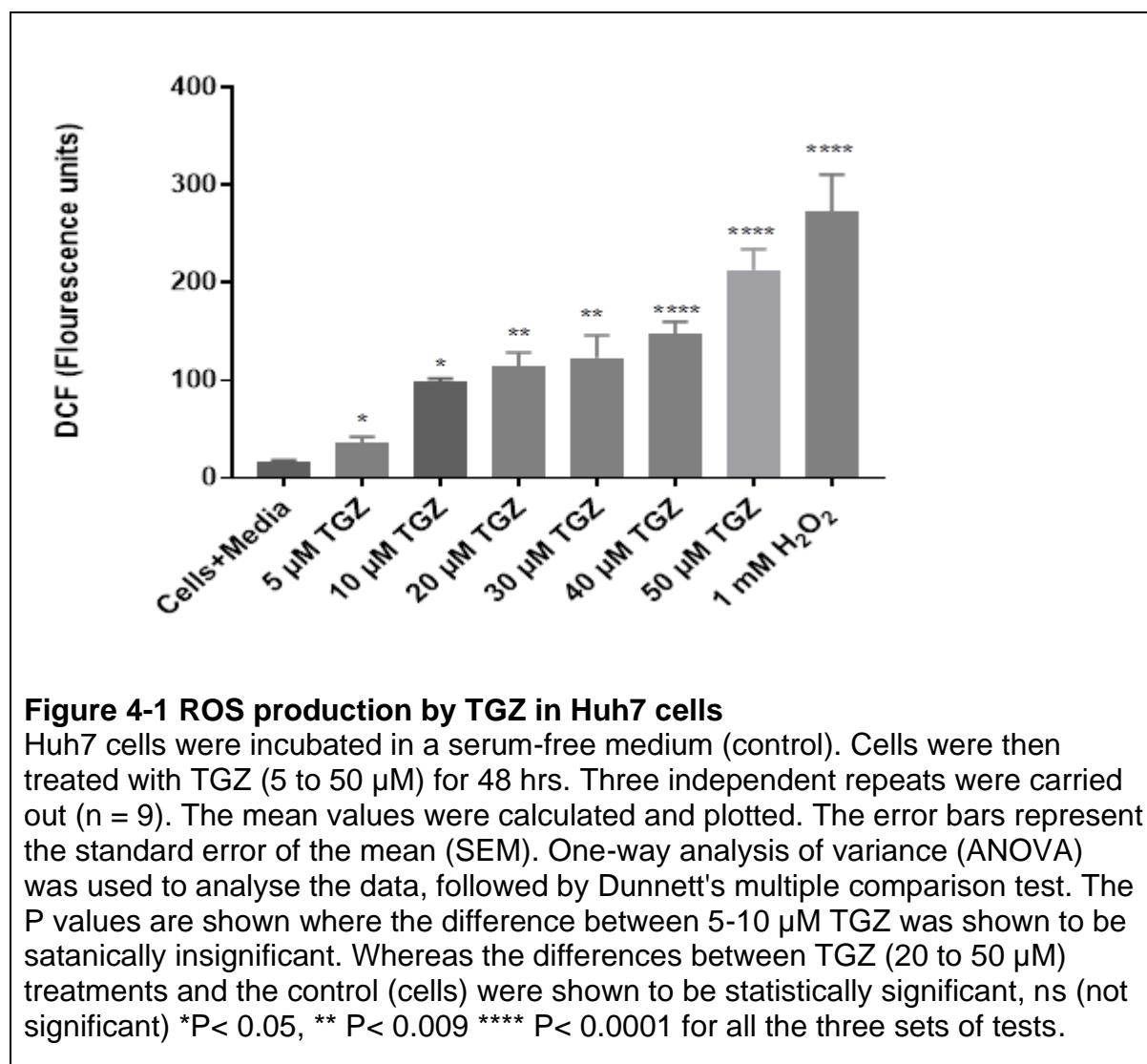
- Determine the effect of TGZ on ROS production in Huh7 cells
- Determine the effect of co-treatment of TGZ and vitamin C on ROS levels in Huh7
- Determine the effect of TGZ on H₂O₂ levels in Huh7 cells
- Determine the effect of TGZ on glutathione homeostasis in Huh7 cells
- Determine the effect of TGZ on cellular ATP levels in Huh7 cells
- Determine the effects of TGZ on intracellular pyruvate levels in Huh7 cells
- Determine the effect of TGZ on Glutamate dehydrogenase activity in Huh7 cells

4.2 Results

4.2.1 Quantification of ROS levels in Huh7 cells treated with TGZ

To determine mitochondrial related pathways in apoptosis induced by TGZ and ROS production after exposure to TGZ, Huh7 cells were treated with various concentrations of TGZ for 48 hrs. Using DCFH-DA as a fluorescent probe and following the method described in section 2.2.10, the results show a dose-dependent increase in ROS production in TGZ-treated cells, with higher ROS levels observed between 20 μ M and 50 μ M. However, the most increased ROS production was recorded in Huh7 cells treated with 1 mM H₂O₂ (a positive control). However, a significant increase in ROS production in cells exposed to TGZ concentrations of 20 μ M, 30 μ M, 40 μ M, and 50 μ M was recorded in this study (Figure 4-1). However, H₂O₂, in theory, can be broken down by Fenton's reaction to produce a hydroxyl free

radical (OH), which is very toxic and generally reactive (Enami *et al.*, 2013). The results were further confirmed in the next section (section 4.2.2) by using the ROS-Glo™ H₂O₂. The kit is designed for a luminescent assay that determines the levels of H₂O₂ directly in cell culture. It is convenient to assay because it has a longer half-life than all ROS in cultured cells; various ROS are also converted to H₂O₂ within cells (Johnson, 2016; Santo *et al.*, 2016).



4.2.2 Quantification of hydrogen peroxide levels in Huh7 cells

As discussed in the preceding section, hydrogen peroxide (H₂O₂) is a reactive metabolic derivative that functions as a key regulator of a few oxidative stress-related conditions. To determine the levels of H₂O₂ in Huh7 cells treated with various

concentrations of TGZ, Huh7 cells were treated with the different concentrations of TGZ for 48 hrs. A fluorometric hydrogen peroxide assay kit to quantify the levels of hydrogen peroxide in Huh7 cells was used. The kit detects H₂O₂ discharged from the cells. In the presence of horseradish peroxidase (HRP), the oxiRed probe reacts with H₂O₂ to generate a colour, which was measured at a wavelength of 570 nm. A standard curve (Appendix D) was created, and each standard, control, and sample were averaged. The mean value of the blank (standard) was subtracted from all standards, controls, and sample readings (corrected absorbance). The corrected values for each standard as a function of the final concentration of H₂O₂. A dose-dependent increase in H₂O₂ production in Huh7 cells in a significant manner was recorded (Figure 4-2).

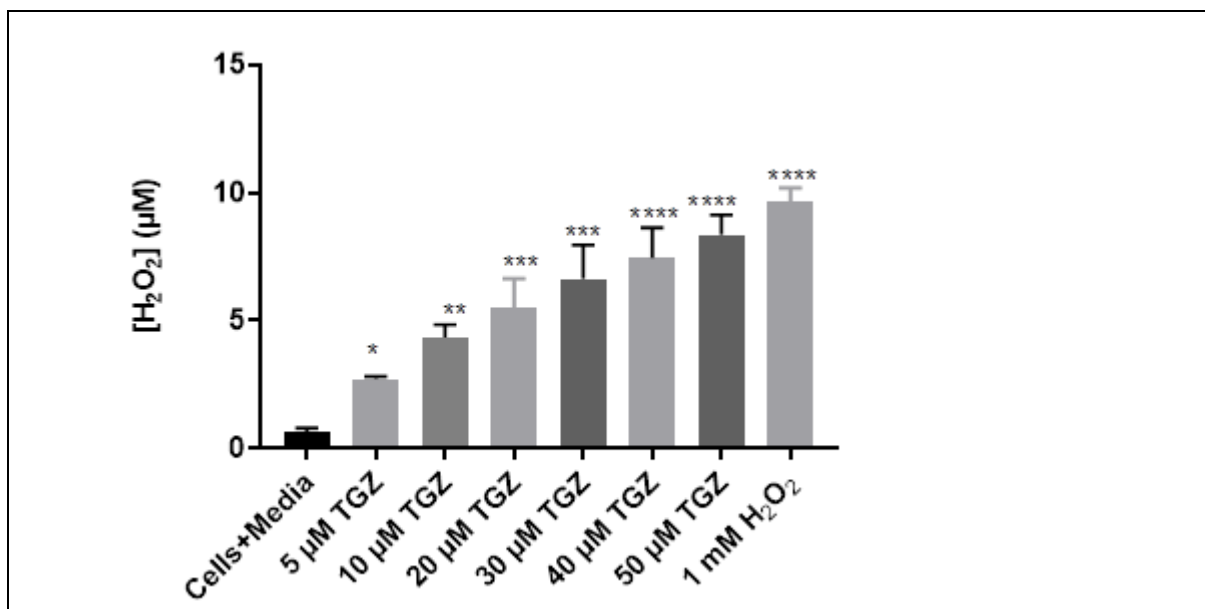


Figure 4-2 The effects of TGZ on H₂O₂ production in Huh7 cells

The effects of TGZ on H₂O₂ production in Huh7 viability. Huh7 cells were incubated with media (cells + cells). The cells were treated with TGZ (5 to 50 µM) for 48 hrs. Three independent repeats (n = 9) were carried out. The mean values were determined and plotted. Error bars represent the mean ± SEM of three replicates. The data was analysed using one-way ANOVA, followed by Dunnett's multiple comparison test. P values are shown where the various treatments were determined to be statistically significant compared with the control. However, we recorded no significant difference between cells treated with 5 µM and the control, ns (not significant), * P< 0.0335. ** P< 0.0048 *** P< 0.0002 **** P< 0.0001.

4.2.3 Effects of ascorbic acid on Huh7 cells viability

Ascorbic acid (vitamin C) is a commonly used dietary antioxidant (Herbert *et al.*, 2005). Its antioxidant properties are well-established *in vitro* since it can be readily demonstrated to prevent oxidation of lipids, DNA, and other biological molecules. However, vitamin C is also possible to act as a pro-oxidant, thus promoting the Fenton reaction, which, acting on peroxides, produces highly reactive hydroxyl radicals (Abasht *et al.*, 2016; Herbert *et al.*, 2005). Despite the promotion of vitamin C as a treatment for different syndromes in prophylaxis and therapy, most medical formulations are poorly supported by evidence with certain inconsistencies (Paulsen *et al.*, 2014). The reports that vitamin C supplementation averts liver toxicity, however, are still not fully understood. Therefore, the beneficial effects of vitamin C in TGZ-induced Huh7 cells were explored. Although vitamin C has been reported to be cytoprotective at certain concentrations and deleterious at individual doses, a preliminary selection of a dose that might be cytoprotective was selected. Therefore, Huh7 cells were treated with various doses of vitamin C (5 μ M to 1000 μ M) for 24 hrs, and cell viability was determined by following the MTT assay method in section 2.2.4. The results showed no significant decrease or increase in cell viability in Huh7 cells treated with 5 μ M to 100 μ M. However, the highest viability in Huh7 cells treated with 100 μ M was recorded.

Therefore, 100 μ M vitamin C as a cytoprotective dose was chosen for our subsequent cytoprotective studies by vitamin C. Cell treated with 150 μ M to 1000 μ M showed a significant reduction in cell viability (Figure 4-3).

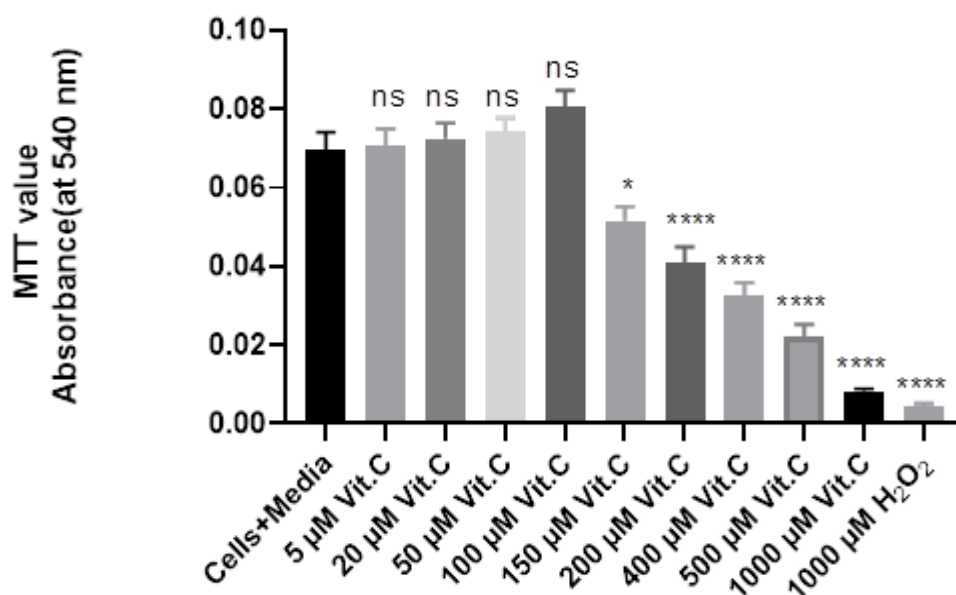


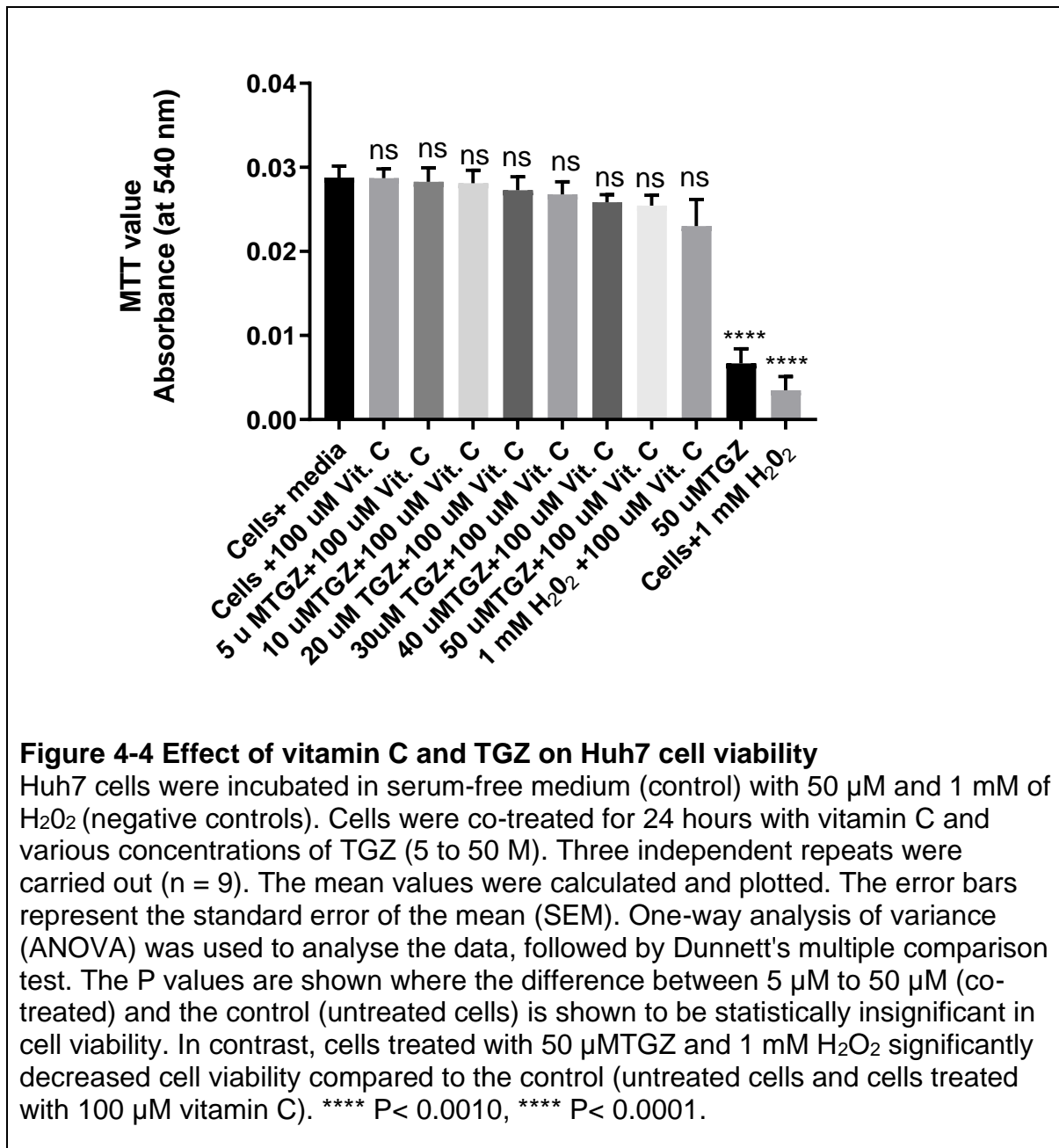
Figure 4-3 The effect of vitamin C in Huh7 cells viability

Huh7 cells were incubated in a serum-free medium (control) and 1 mM H₂O₂ (positive control). Cells were exposed to vitamin C (5 to 1000 µM) for 24 hrs. Three independent repeats were carried out (n = 9). The mean values were calculated and plotted. The error bars represent the standard error of the mean (SEM). One-way analysis of variance (ANOVA) was used to analyse the data, followed by Dunnett's multiple comparison test. The P values are shown where the difference between 5 to 100 µM, and the control (untreated cells) is shown to be statistically insignificant. In contrast, cells treated with 150 µM to 1000 µM as well as the 1 mM H₂O₂ treatment were statistically significant compared with the control (untreated cells). **** P < 0.0001.

4.2.4 The effect of co-treatment of vitamin C and TGZ on Huh7 cells viability

Having determined the cytoprotective concentration of vitamin C, Huh7 cells were exposed to co-treatment of vitamin C and TGZ, with 100 µM of vitamin C as a positive control. As negative controls, 50 µM TGZ and 1 mM H₂O₂ were included as negative controls. Then cell viability was determined using the MTT assay method described in section 2.2.3. Huh7 cells co-treated with vitamin C and TGZ concentrations (5 µM to 40 µM) did not reduce cell viability. However, cells co-treated with vitamin C and 50 µM TGZ did significantly reduce cell viability. Also, the

positive controls (50 μ M TGZ and 1 mM H₂O₂) did decrease cell viability relative to the control (untreated cells) ** P < 0.0010 **** P < 0.0001 (Figure 4-4).



4.2.5 Quantification of ROS levels in Huh7 cells co-treatment treated with TGZ and vitamin C

We first determined that TGZ causes an increase in ROS levels in Huh7 cells, and then we determined whether the rescue effect of vitamin C on TGZ-induced cell death (Figure 4-4). This study then explored whether co-treatment with vitamin C and TGZ affected ROS production in Huh7 cells. To determine this effect, cells were co-treated with various concentrations of TGZ and vitamin C for 48 hrs. Using DCFA-DA as a fluorescent probe, ROS production was determined. ROS production in cells cotreated with vitamin C and the various concentrations of TGZ was negligible (Figure 4-5). However, a significant production of ROS was recorded in Huh7 cells exposed to 1 mM H₂O₂ (a positive control).

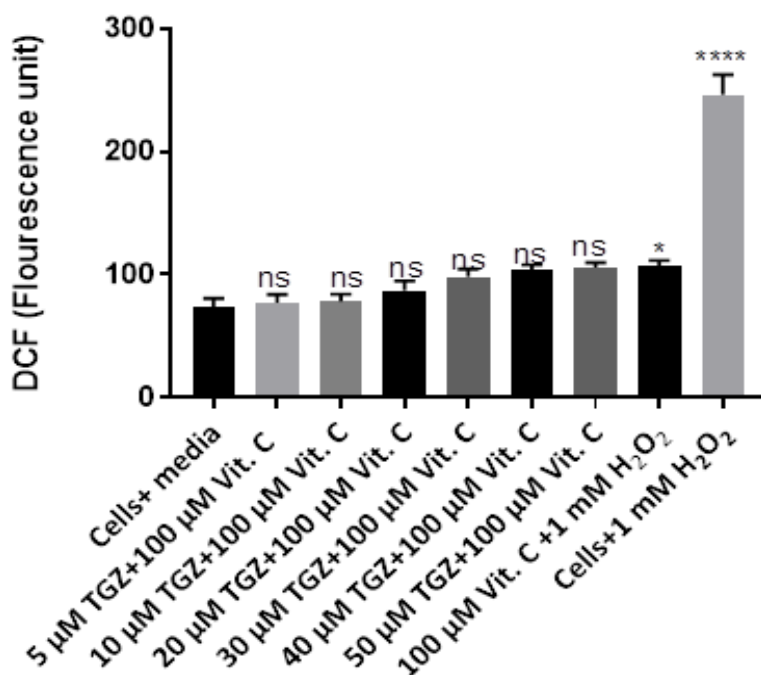


Figure 4-5 Effect of co-treatment of Vitamin C and TGZ on ROS production in Huh7 cells.

Huh7 cells were exposed to serum-free medium (control) and 1 mM H₂O₂ (positive control). Cells were treated with 100 µM of vitamin C and TGZ (5 to 50 µM) for 48 hrs. Three independent repeats were carried out (n = 9). The mean values were calculated and plotted where the error bars represent the mean (SEM) standard error. One-way analysis of variance (ANOVA) was used to determine the data, which was then followed by Dunnett's multiple comparison tests. The P values are shown where the difference between different treatments and the control (cells) is shown to be statistically insignificant, ns (not significant). In contrast, the difference between the control and the positive control was shown to be statistically significant, **** P < 0.0001.

4.2.6 Effect of TGZ on glutathione homeostasis in Huh7 cells

Glutathione (GSH) is a three-amino-acid peptide found in mammalian cells, acting as a significant reducing agent and antioxidant defence through tight regulation of the redox status. Redox signalling actions play an important role in monitoring cell death pathways (Circu & Aw, 2010). Although oxidative stress as well as ROS formation have been implicated in regulating cell death, other redox-dependent signalling

mechanisms have also been identified as critical factors in the activation of the cell death mechanism. Depletion of GSH is a typical feature of apoptotic cell death caused by a wide range of factors, including death receptor activation, stress, environmental agents, and cytotoxic drugs (Franco & Cidlowski, 2006; Troyano *et al.*, 2003). An alteration in GSH levels is vital for determining toxicological response and may cause oxidative stress and subsequently lead to apoptosis (Circu & Aw, 2010).

Therefore, the effects of low doses and a higher dose (1 μ M, 1.5 μ M, 3 μ M, 5 μ M, 6 μ M, 7 μ M and 50 μ M) of TGZ were determined on GSH levels in Huh7 cells. Different TGZ doses were used in this experiment because the LD₁₀, LD₂₅, LD₅₀, LD₇₅, and LD₉₀ (3.7, 6.7, 12.2, 22.3, and 40 μ M, respectively) were calculated in section 3.2.1 (Figure 3-1). And in section 3.2.3 (Figure 3-3), it was recorded that lower doses of TGZ did not cause cell death. The above TGZ concentrations were used to determine glutathione level in the Huh7 cell population with 10%, 25%, 75%, 90%, and 100% viability because this study wanted to elucidate whether the outcome would not be false positive or negative. For example, as demonstrated earlier, a higher concentration could kill about 90% of the Huh7 cell population and could produce a misleading result on the effect of TGZ on GSH levels. Using the GHS-GLO™ Glutathione Assay kit by Promega, glutathione levels in Huh7 cells were determined. The assay is a luminescence-based assay for detecting and quantifying GSH levels in mammalian cells. The assay is based on the change of luciferin derivative into luciferin in glutathione, which is catalysed by glutathione s-transferase (GST). The signal produced in a coupled reaction with firefly luciferase is proportional to the amount of glutathione present in the sample. Huh7 cells (Figure 4-6): 50 μ M TGZ caused a significant reduction in GSH levels in Huh7 cells.

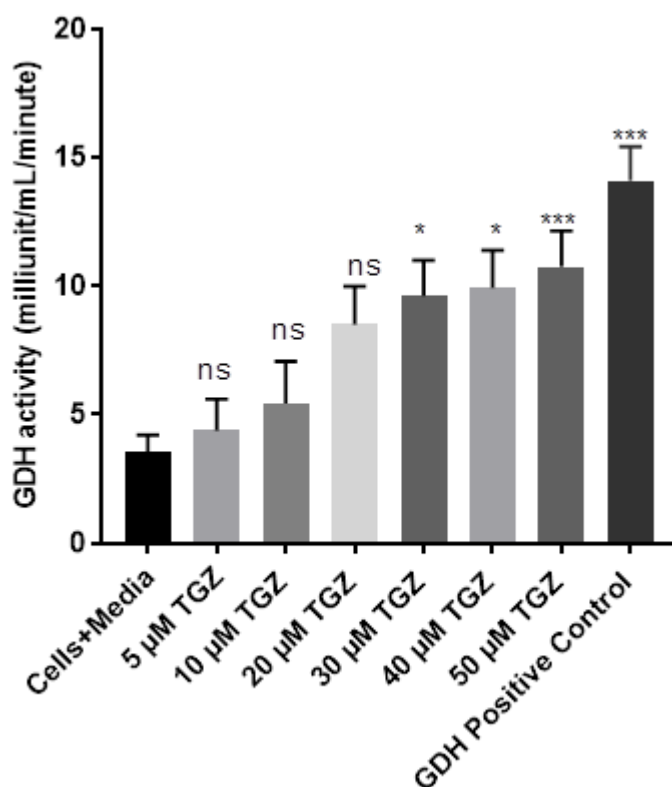


Figure 4-6 The effect of TGZ on GSH levels in Huh7 cells

Huh7 cells were incubated in media (control). The cells were treated with 2 µM rotenone and TGZ (1 to 50 µM) for 48 hrs. Three independent repeats (n = 9) were carried out. The mean values were determined and plotted. Error bars represent the mean ± SEM of three replicates. The data was analysed using one-way ANOVA, followed by Dunnett's multiple comparison test. P values are shown where the cells treated with TGZ concentrations (1 µM to 7 µM) relative to the control were determined to be statistically insignificant. However, cells treated with 50 µM TGZ were shown to be statistically significant * P < 0.0495.

4.2.7 Determination of CYP3A4 induction in TGZ-treated Huh7 cells

As described in section 1.4 of this thesis, drug metabolism takes place in the liver by mainly the Cytochrome P450 enzymes (Fahmi *et al.*, 2008). Several adverse drug reactions ensuing from multiple drug treatments have been linked with drug-drug interactions, encompassing inhibition and induction of drug-metabolising enzymes (Fahmi *et al.*, 2008). Thus, during drug discovery and lead optimisation, it is

imperative to assess the potential CYP inducibility of drug candidates, increasing the possibility of making drugs that are free of CYP-inducing properties (Fahmi *et al.*, 2008). Given that CYP3A4 metabolism produces a reactive epoxide that could be removed safely through GSH conjugation, CYP3A4 induction using the luminescence assay method described in chapter two was determined. This study explored the induction of CYP isoenzyme (3A4) by exposing Huh7 cells to various concentrations of TGZ, 20 μ M rifampicin (positive inducer of CYP3A4), and 20 μ M clotrimazole (negative control). This was included to confirm whether the induced activity was a result of the CYP3A4 enzyme. A dose-dependent induction of CYP3A4 was recorded. The CYP3A4 activity was 5-fold greater after 50 μ M TGZ treatment. A 6-fold increase was observed in cells exposed to 20 M rifampicin. There was no CYP3A4 induction in cells treated with 20 μ M clotrimazole was recorded (Figure 4-7).

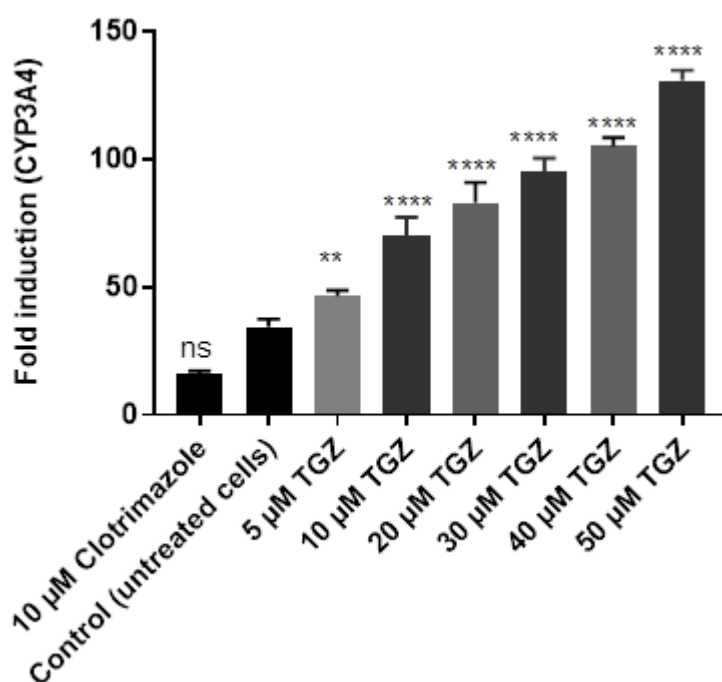


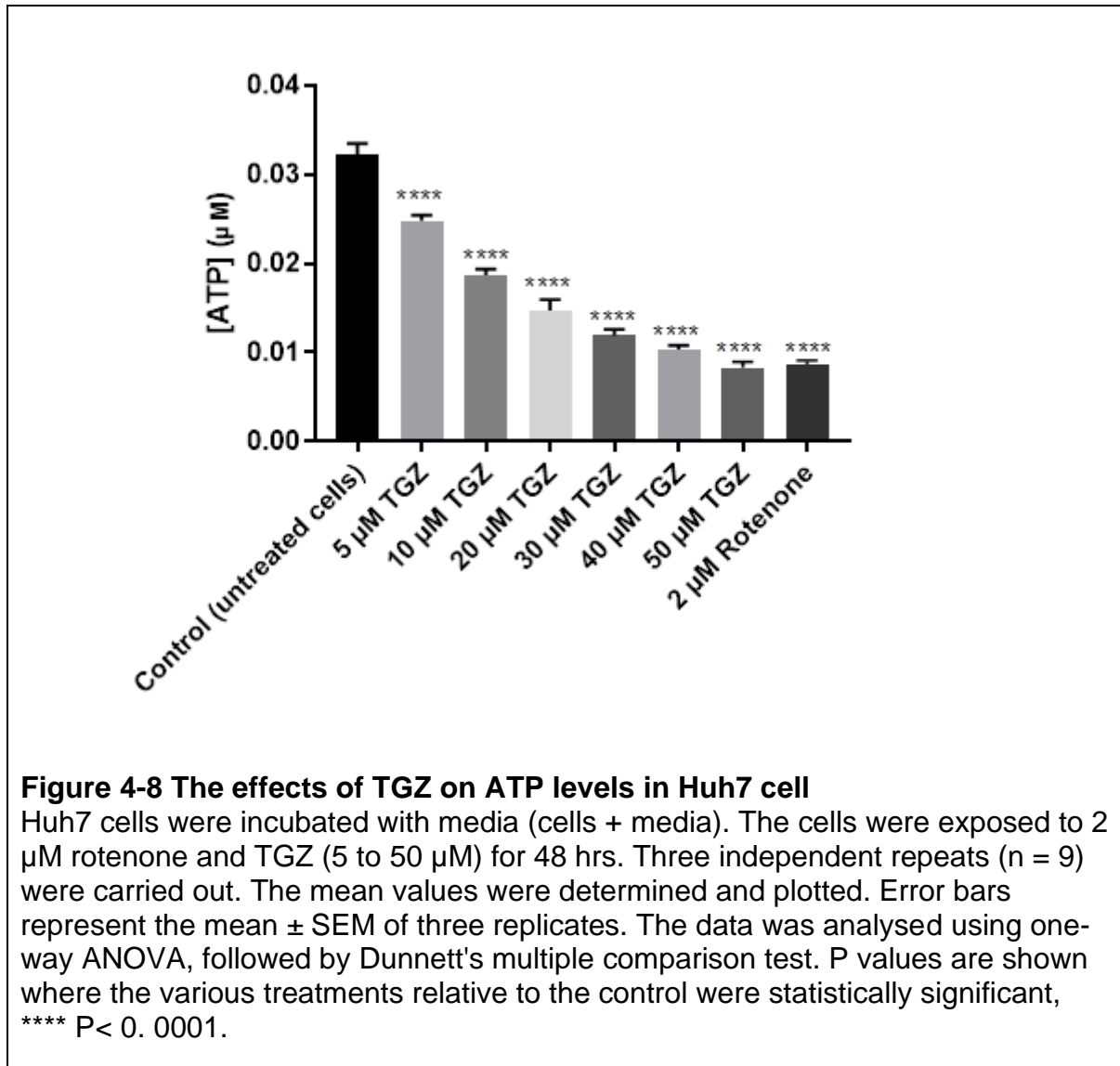
Figure 4-7 The effect of TGZ on CYP3A4 induction in Huh7 cells

Huh7 cells were incubated in a serum-free medium (cells+media). Cells were then treated with 20 µM Rifampicin (positive control) and 20 µM Clotrimazole as a negative control. Cells were treated with TGZ (5 to 50 µM) for 48 hrs. Luminescence was measured using the BMG LABTECH Omega FLUOstar plate reader. Three independent repeats were carried out (n = 9). The mean values were calculated and plotted. The error bars represent the standard error of the mean (SEM). Data were analysed using one-way ANOVA, followed by Dunnett's multiple comparisons tests, and P values are shown where the difference between responses of different treatments and the control (Cells) was shown to be statistically significant, * P 0.05, **** P 0.0001.

4.2.8 Effect of TGZ on cellular ATP levels in Huh7 cells

As discussed in the introduction chapter, TGZ can cause a significant increase in mtDNA damage, which causes a subsequent reduction in ATP levels and ultimately leads to a loss of cellular viability. Therefore, the effect of TGZ on ATP levels in Huh7 cells was evaluated. And to determine the impact of TGZ on cellular ATP levels, a commercially available kit was used to quantify ATP levels in TGZ-treated Huh7 cells. We also treated cells with 2 µM rotenone, a mitochondrial respiratory chain complex I inhibitor (positive control) (Li *et al.*, 2002). The rest of the assay was

carried out according to the method described in section (2.2.14). As demonstrated (Figure 4-8), cells treated with TGZ showed a dose-dependent reduction of APT levels within the TGZ-treated cells. All the TGZ concentrations elicited a decrease in ATP levels that was significantly lower than the control cells (untreated cells).



4.2.9 Effects of TGZ on intracellular pyruvate levels in Huh7 cells

Pyruvate, a product of glycolysis, is an essential cellular component for activities such as mitochondrial respiration. It is also necessary for fermentation; for example, without fermentation, cells may be unable to regenerate the critical NAD⁺ supply because all NAD⁺ would be converted to NADH. Essentially, pyruvate enables the

cell to regenerate its NAD⁺ supply to maintain glycolysis (Divakaruni & Murphy, 2012; Herzig *et al.*, 2012; McCommis & Finck, 2015).

Increasing levels of data indicate that PPAR γ -independent processes, some of which are too quick to be attributed to transcriptional activities, may be relevant to effects on metabolism (Chen *et al.*, 2012; Choi *et al.*, 2010). Besides, it has been demonstrated that TGZ binds to mitochondrial membranes at low micromolar sensitivity, indicating the distributing levels in subjects exposed to TGZ suggest that some of their metabolic consequences may be generated by completely modifying mitochondrial activity (Eckland & Danhof, 2000; Chen *et al.*, 2012; Choi *et al.*, 2010; Kirchheimer *et al.*, 2006; Norris *et al.*, 2003). In this current study, the impact of TGZ on pyruvate levels in Huh7 cells was assessed by following the methods described in section 2.2.15. Media levels of pyruvate were measured using a commercially available kit (Sigma-Aldrich, Poole). A dose-dependent decrease in pyruvate levels in Huh7 cells was recorded (Figure 4-9).

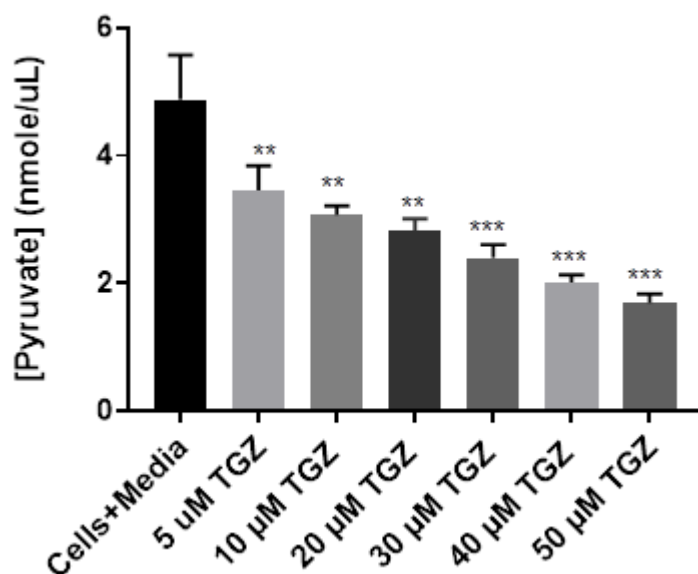


Figure 4-9 The effects of TGZ on pyruvate levels in Huh7 cells

Huh7 cells were incubated with media (cells + media). The cells were exposed to TGZ concentrations of (5 to 50 μ M) for 48 hrs. Three independent repeats (n = 9) were carried out. The mean values were determined and plotted. Error bars represent the mean \pm SEM of three replicates. The data was analysed using one-way ANOVA, followed by Dunnett's multiple comparison test. TGZ dose-dependently decreased pyruvate levels in Huh7 cells. The P values are shown where the various treatments compared to the control were determined to be statistically significant. * P < 0.0407 ** P < 0.0085 *** P < 0.0002 **** P < 0.0001

4.3 Discussion

There is mounting evidence of mitochondrial impairment in the aetiology of DILI. Several drugs that were withdrawn from the market exhibited mitochondrial liabilities that provoked toxicities (Aithal, 2015; 2019; Pessayre *et al.*, 2020). Then an evaluation of the effects of TGZ on mitochondrial activity was made. Having exposed Huh7 cells to the various concentrations of TGZ, a dose-dependent ROS production in the Huh7 cells was recorded. ROS production could be attributed to the ability of TGZ to inhibit mitochondrial respiratory chain complex I, which will then lead to increased ubisemiquinone formation, the primary electron donor in mitochondrial superoxide production. Inhibition of complex V by TGZ was predicted by the model, but other *in vitro* studies have demonstrated that TGZ inhibits the mitochondrial

respiratory chain complexes (I-V) (Hu *et al.*, 2015; Nadanaciva *et al.*, 2007). Besides, all the TGZ concentrations (5 μ M to 50 μ M) decreased the cellular ATP level compared to the control. Rotenone, a complex I inhibitor, caused a significant ATP reduction (Verrax *et al.*, 2011). A potential mechanism may be that rotenone inhibits the respiratory mitochondrial chain at the complex I site, and this may lead to a reduction in the cellular level of ATP. However, the involvement of pyruvate/malate supports the speculation that ATP differs in different types of cells (Verrax *et al.*, 2011). A decreased cellular level of ATP of about 30% has been found to block apoptosis (Verrax *et al.*, 2011). This mechanism relies on pyruvate/malate stimulated-ATP development, which might alter cell death from apoptotic to necrotic. And in this current study, a significant decrease in cellular ATP levels in cells exposed to TGZ was recorded. Also, previous studies have reported a disruption of mitochondrial activity followed by increased membrane permeability, calcium flux, as well as nuclear condensation (Haskin *et al.*, 2001; Liao *et al.*, 2010; Ong *et al.*, 2007). In line with other studies, 10 μ M TGZ caused a rapid reduction in mitochondrial membrane potential and Ca⁺ in CD-1 mice and HepG2 cells (Okuda *et al.*, 2010; Ong *et al.*, 2007; Tirmenstein, 2002).

On the other hand, Porceddu *et al.* have reported that TGZ-induced mitochondrial membrane permeabilisation was not recorded in a mouse hepatocyte deficient in calcium pulse. Studies by Lim *et al.* using the human liver cell line HC-04 treated with TGZ (0 to 100 μ M) suggested that MPT pore opening was provoked by ROS production because of mitochondrial respiratory chain inhibition. Also, previous studies have reported that TGZ (12.5, 25 & 50 μ M) repressed all the mitochondrial respiratory chain complexes, but complex II (succinate dehydrogenase) has been reported to be less sensitive (Hu *et al.*, 2015; Nadanaciva *et al.*, 2012).

The results of this study show that TGZ stimulated ROS production in the Huh7 cell. ROS production could be attributed to the ability of TGZ to inhibit mitochondrial respiratory chain complex I, which might lead to increased ubiquinone formation, the primary electron donor in mitochondrial superoxide production. Also, TGZ-induced ROS development results in the oxidation within the mitochondria of crucial components, such as mtDNA. This DNA is much more susceptible than its nuclear equivalent to the damage induced by ROS as it does not have protective

histones and is closer to the source of ROS production (Bova *et al.*, 2005). The precise location of the initial oxidative stress caused by TGZ is poorly understood. ROS development candidates may be assumed to be mitochondria or membrane-based enzymes, for instance, NADPH oxidase or the TGZ redox itself. The oxidative damage of mtDNA increases ROS production (secondary ROS) due to a lack of coordination between mtDNA coded electron transport network components and nuclear DNA atypical respiratory complex formation.

ROS can trigger a vicious cycle in which it damages mtDNA to cause further impairment of the respiratory complexes. This might induce a further increase in ROS output and further damage to mtDNA; when the damage to mtDNA increases, ATP production decreases simultaneously due to the deficiency or a reduction of the two-electron. A decline in the transport of electrons causes a reduction in mitochondrial depolarisation, which has been linked to mtDNA damage and mitochondrial permeability (Santos *et al.*, 2005). Previous studies have also reported that MtDNA depletion inhibits ATP synthesis and causes disruptions in cellular activity (Li *et al.*, 2002; Santos *et al.*, 2005). Additionally, electron transportation chain dysfunction may result in excess ROS and secondary ROS generation, increasing cellular signals to activate cell death.

This disparity is attributable to the cell's respiration mechanism to maintain intracellular ATP levels. Cells that are more dependent on mitochondria for ATP die of necrosis because of insufficient energy. Cells with higher glycolysis die from apoptosis due to lower intracellular ATP levels, which are still sufficient for apoptosis. Another factor affecting modes of cell death may be the doses of toxic agents; these agents may cause apoptosis at lower doses. However, TGZ kills cells at higher levels by necrotic cell death at higher doses, mainly due to a collapse of cellular integrity, such as the loss of plasma membrane integrity of intracellular ATP depletion (Bova *et al.*, 2005). Sudden cell death cannot warn the host or disrupt apoptotic pathways. Therefore, as apoptosis is tightly regulated at genetic levels, diseases induced by enhanced apoptosis by drug-molecular mechanisms can be controlled. However, certain forms of necrosis are rescued by anti-apoptotic agents; it might be less critical to comprehend if cells die from apoptosis or necrosis than the mechanisms underlying cell death (Bova *et al.*, 2005).

Earlier studies using *in vivo* and *in vitro* systems have also reported that ROS could cause chemical alterations and injury to vital cellular molecules such as lipids, carbohydrates, or nucleic acids (Inoue *et al.*, 2003; Santo *et al.*, 2017). As a result, in a situation where ROS is being generated at levels enough to offset the normally resourceful defence methods, various deleterious effects can occur in both metabolic and cellular systems, resulting in hepatic or cellular injury, mutations, or cancer.

As drugs can cause oxidative stress, the study in this chapter aimed to determine the consequences of TGZ on cellular oxidative stress. The findings in this chapter focused on the effects of TGZ on ROS production in an *in vitro* cellular model of hepatic liver cells. However, there are many challenges in detecting reactive oxygen species because of the rate at which they react, mostly in a whole-cell experiment where there is competition with antioxidants. Also, superoxide ions particularity is challenging to detect because of the similarity of oxygen species' chemistry. However, using two methods to determine ROS generation, TGZ-treated cells were found to induce ROS production compared to control significantly. A pathophysiological level of TGZ was detected by the DCFH-DA probe and was confirmed by the assay that quantifies H₂O₂. The results from both methods produce an increase in H₂O₂, which indicates that ROS generation might be converted to H₂O₂. As ROS is produced by mitochondria under stressful conditions and can cause apoptosis or necrosis, the next step in our study was to determine the ROS generation in cells under experimental conditions. TGZ induces the activation of intrinsic apoptotic pathways in Huh7 cells. The puzzle is directed towards the exact mechanism by which TGZ causes excessive ROS production.

And as reported by previous studies, ROS has been evaluated in various cells and linked to the activation of apoptosis's intrinsic pathways (Dakubo, 2010; Inoue *et al.*, 2003; Peng & Jou, 2004; Santo *et al.*, 2017). To further identify how TGZ causes ROS generation in cells, Huh7 cells were exposed to a cytotoxic effect level of H₂O₂ as a positive control (Gülden *et al.*, 2010). 1 mM H₂O₂ elicited the maximum H₂O₂ activity in Huh7 cells. TGZ at 50 µM caused increased ROS and H₂O₂ outputs in Huh7 cells. The proposed mechanism of TGZ activity in this chapter was mitochondria facilitated parameters such as ROS, ATP levels, and other factors mentioned in the previous sections. In general, the mitochondrial transition pore

leads to cytochrome c release and activation of the intrinsic apoptotic cascade (Bernardi, 2013; Martinou & Youle, 2011; Scorrano, 2014).

One potential method of determining whether ROS production from TGZ caused cytotoxicity was antioxidants to TGZ in this study. If viability could be retained in the cell population, it would suggest that ROS was the cause of cytotoxicity. TGZ was assessed in the presence of an antioxidant (vitamin C). It was found that vitamin C maintained cell viability when cells were co-treated with both vitamin C and TGZ. Even at the highest concentration of TGZ, which caused about 80% of cell viability, the cell viability recorded was statistically insignificant compared to that of cells exposed only to the media. If viability could be retained in the cell population, it would suggest that ROS was the cause of cytotoxicity. Furthermore, the specific tailoring of antioxidants makes it possible to indicate the toxic oxidant species, as some antioxidants are radical specific. Exposing Huh7 to both TGZ and vitamin C, an antioxidant, inhibited TGZ-induced ROS production. It was observed that vitamin C could maintain some cell viability in Huh7 cells treated with TGZ. In humans, vitamin C is an essential micronutrient that plays multiple biological roles. It possesses double bonds with an associated electron deficiency, making it highly reactive to free radicals. Vitamin C can deactivate highly reactive molecules such as ROS, generated during various biological processes in cells (Dad *et al.*, 2016).

Substances that exhibit antioxidant properties emerge as putative preventives and co-adjuvants in preventing or rescuing cytotoxicity caused by excessive ROS generation. In line with this, a reduction in ROS production in Huh7 cells treated with vitamin C was recorded (Figure 4-5). These data are in line with a study by Li *et al.* who reported that Mn-SOD attenuated rotenone-induced apoptosis due to mitochondrial ROS production. Mn-SOD is the primary component of the molecular defence system against oxidative toxicity. It could react with hydrogen peroxide to form hydroxyl radicals, which are more toxic than superoxide and hydrogen peroxide (Li *et al.*, 2002).

Mn-SOD is the main enzyme required to transform superoxide into hydrogen peroxide in mitochondria (Li *et al.*, 2002). Also, Rachek *et al.* determined whether TGZ-induced ROS production was the mechanism behind cytotoxicity. Therefore,

they conducted a cell viability study by treating human liver cells with an antioxidant (NAC), a glutathione precursor that provides intracellular glutathione. They reported that NAC significantly reduced TGZ-induced cytotoxicity. Rachek *et al.* suggested that ROS production by TGZ was responsible for cell death. And to clarify this assumption, whether co-treatment of a toxicant with an antioxidant could rescue cell death, Huh7 cells were co-treated with vitamin C and TGZ. However, the co-treatment did not cause any significant death in Huh7 cells. This observation might support the argument that ROS production by TGZ is a causative factor in TGZ-induced liver injury. TGZ-induced mitochondrial impairment may be highlighted by reducing mitochondrial GSH levels, possibly due to lower GSH drift into mitochondria. The work described here adds to the weight of evidence that suggests that the non-receptor induced influences on TGZ function through a mitochondrial interaction (Feinstein *et al.*, 2005). When several cells, including hepatocytes, were exposed to TGZ, they recorded a rise in cytosolic calcium and mitochondrial swelling. They also stated that the loss of membrane potential was associated with a decrease in ATP. As a result of mitochondrial dysfunction, ROS production has been increased, with a subsequent increase in apoptosis induction (Bova *et al.*, 2005).

TZDs, in particular TGZ, are immediate and direct antagonists of the mitochondrial pyruvate carrier at physiologically relevant concentrations. Besides establishing that MPC is a target of TZDs, there is evidence that MPC activity inhibition can control cellular glucose metabolism. However, others suggest the involvement of PPAR γ in the insulin-sensitising impacts of TZDs. A biomass energy test combined with genetic depletion of either of the MPC isoforms showed that TZDs directly inhibited the uptake of mitochondrial pyruvate. According to the researchers, the impact occurred in permeabilised cells for a short period (Phelix *et al.*, 2017; Kirchheimer *et al.*, 2006). Although other previous studies have shown inhibition of complex I by TGZ, the concentration utilised in this case exceeded its physiological relevance (Brunmair *et al.*, 2006; Nadanaciva *et al.*, 2007). In this current study, a dose-dependent decrease in pyruvate in Huh7 cells exposed to various concentrations of TGZ was recorded. Even a 5 μ M concentration of TGZ in the treatment group did cause about a 34% reduction in pyruvate concentration in the Huh7 cells. And 50 μ M TGZ generated about a 70% reduction of pyruvate in Huh7 cells (Figure 4-9).

Feinstein and his group have reported that TZDs produce substrate-specificity in the respiration of isolated brain mitochondria (Feinstein *et al.*, 2005). Still, there is no substantial evidence that demonstrates that altered protein expression can modulate TGZ potency. A previous study by Brivet (2003) has characterised MPC1 and MPC2 activities. However, the clarity on whether evidence to date can distinguish between a well-defined function for the MPC complex in pyruvate transport as opposed to a separate role in overall pyruvate metabolism. While flow through the PDH-complex can affect pyruvate transport thresholds, there is evidence that excess methyl pyruvate can completely recover respiration from both MPC inhibition (Bricker *et al.*, 2012). Physiological drug concentrations cannot completely block the transport and oxidation of pyruvates, which may have a toxic effect. Although this interaction can validate toxicity, the proof that MPC inhibition may significantly increase the intake of glucose by TGZ and increased phosphorylation by AMPK shows that partial MPC inhibition may enhance the cellular utilisation of glucose.

The beneficial effects of TGZ on *in vivo* metabolism can also be due to MPC inhibition. Limited mitochondrial pyruvate uptake might block flux by pyruvate carboxylase, restricting the energy for hepatic glucose production (Natali & Ferrannini, 2006). This mechanism might also help explain why TGZ can decrease lipid accumulation in the liver and skeletal muscle (Teranishi *et al.*, 2007). By reducing its efflux, MPC inhibition may likely diminish the pool of intramitochondrial citrate by reducing its efflux and, in turn, acetyl-CoA to triglyceride for storage in fat (lipogenesis). This mechanism may further clarify why TGZ could reduce the deposition of lipid in the liver cells as well as the skeletal muscle (Teranishi *et al.*, 2007). Inhibition of MPC will possibly reduce the supply of intramitochondrial citrate, which in theory can reduce its efflux and, in effect, lipogenesis (Bandyopadhyay *et al.*, 2006; Teranishi *et al.*, 2007).

Reduced intramitochondrial pyruvate would probably improve amino acid oxidation to retain tricarboxylic acid cycles and the generation of ATP. It can also stimulate the mitochondrial malic enzyme, generate pyruvate from malate, and raise NAD(P)H levels. As evidenced by the fact that mild MPC inhibition can be insulin-sensitising

and would increase glucose uptake, the repression of the MPC might induce signalling through protein acetylation on either side of the mitochondrial inner membrane. Reduced mitochondrial pyruvate uptake would increase the level of pyruvate and therefore acetyl units in the cytoplasm (Bandyopadhyay *et al.*, 2006; Teranishi *et al.*, 2007).

Glutathione reduction is one of the characteristics of apoptosis and cytotoxicity and may be reduced by various mechanisms. Apoptosis caused by physiological stimuli such as death receptor activation or cytokine removal has been demonstrated to trigger GSH loss by activating a GSH plasma membrane efflux transport and not oxidising it to GSSG (Franco & Cidlowski, 2006; Lantz, 2001). Various apoptotic stimuli (death receptor), stress conditions (osmotic, hypoxic) and cytotoxicity (e.g., xenobiotics and pollutants) may generate or optimise ROS output either through organelle-mediated damage or simple chemical reactions which could respond to GSH reduction by oxidation (GSSG) or conjugation (Circu & Aw, 2010; Troyano *et al.*, 2003). The results in section 4.2.6 (Figure 4-6) of this current study indicate that lower doses of TGZ were recorded to be cytoprotective. Those low doses of TGZ also increase the levels of GSH in Huh7 cells (Figure 4-6). However, TGZ doses above 5 μM up to 7 μM did insignificantly decrease the levels of GSH in Huh7 cells. However, we recorded a significant decrease in Huh7 cells at 50 μM TGZ concentrations.

GSH depletion and ROS formation can cause an activation cascade using both increased ROS and GSH depletion. Besides, the mitochondrial GSH pool was shown to be an essential cell death regulator. The corresponding GSSG or GSH conjugates must be compressed by efflux pumps and are cytotoxic. This further decreases intracellular GSH pools by affecting GSSG GR and NADPH transformation into GSH. Finally, GSH depletion and ROS formation can regulate apoptosis or cytotoxicity through ROS-mediated signalling, thiol-exchange reactions, protein oxidation changes (S-glutathionylation, S-nitrosylation), or GSH (by GST). GSH-T, GSH depletion transporter via apoptosis (Circu & Aw, 2010; Franco & Cidlowski, 2006). GSH is needed to provide cellular protection against oxidative stress and its cellular reduction will make the cell more susceptible to toxic injury. The decrease of GSSG by the enzyme glutathione reductase can also generate

GSH. However, this mechanism involves reducing the strength of NADPH (Circu & Aw; 2010; DeBerardinis *et al.*, 2007; Franco & Cidlowski, 2006). Reduced nicotinamide intracellular levels, an NADPH precursor, can also reduce NADPH supply and raise GSH levels. Metabolite profiles harmonious with many of these effects have been demonstrated, and it could be assumed that TGZ might influence cellular and GSH energy production. Changes in metabolite rates may be underpinned by the recorded mitochondrial dysfunction and oxidative stress in TGZ-treated cells (Depeint *et al.*, 2006).

As discussed in the previous section, TGZ is biotransformed by CYP3A4, the major isoform of cytochrome P450 in the liver (Yamamoto *et al.*, 2002). A 5-fold induction was recorded when rifampicin was used as a potent inducer of CYP3A4 to induce CYP3A4 induction as a positive control compared with CYP3A4 induction by TGZ in Huh7 cells, and a 5-fold induction was recorded. In contrast, the positive control was about a 6-fold induction of CYP3A4 when compared to untreated cells. The role of TGZ metabolites remains unclear. However, Vignati *et al.* have reported the role of TGZ metabolites in toxicity in HepG2 cells. Cells were exposed to microsomes containing cDNA expressed CYP3A4 and HepG2 was transiently transfected with CYP3A4 expression plasmids. They recorded decreased cell viability relative to the control cells, indicating that TGZ metabolism was critical in producing toxicity. They also exposed the cells to a combined treatment with ketoconazole (a CYP3A4 inhibitor) that protected against the decrease in cell viability (Vignati *et al.*, 2005).

On the other hand, other studies dispute the report by Vignati and his team. For instance, the formation of epoxide and quinone-type metabolites of TGZ exhibited a less cytotoxic effect on HepG2 cells than the parent drug (Vignati *et al.*, 2005; Yamamoto *et al.*, 2002). Also, Tettey *et al.*, having exposed cells to another CYP3A4 inducer, dexamethasone, reported a minimal sensitivity to TGZ cytotoxicity. In line with this finding, Tirmenstein *et al.* exposed HepG2 to SKF-525AP450 (a non-selective inhibitor) with ketoconazole, a CYP3A4 inhibitor. They reported that the combined exposure did not rescue the cells from TGZ-provoked cell death.

As discussed in the previous section, TGZ is biotransformed by CYP3A4, the major isoform of cytochrome P450 in the liver (Yamamoto *et al.*, 2002). Rifampicin was

used as a potent inducer of CYP3A4 to induce CYP3A4 induction as a positive control compared with CYP3A4 induction by TGZ in Huh7 cells and a 5-fold induction was recorded. In contrast, the positive control was about a 6-fold induction of CYP3A4 when compared to untreated cells. The role of TGZ metabolites remains unclear. However, Vignati *et al.* have reported the role of TGZ metabolites in toxicity in HepG2 cells. Cells were exposed to microsomes containing cDNA expressed CYP3A4 and HepG2 was transiently transfected with CYP3A4 expression plasmids. They recorded decreased cell viability relative to the control cells, indicating that TGZ metabolism was critical in producing toxicity. They also exposed the cells to a combined treatment with ketoconazole (a CYP3A4 inhibitor) that protected against the decrease in cell viability (Vignati *et al.*, 2005).

On the other hand, other studies dispute the report by Vignati and his team. For instance, the formation of epoxide and quinone-type metabolites of TGZ exhibited a less cytotoxic effect on HepG2 cells than the parent drug (Vignati *et al.*, 2005; Yamamoto *et al.*, 2002). Also, Tettey *et al.*, having exposed cells to another CYP3A4 inducer, dexamethasone, reported a minimal sensitivity to TGZ cytotoxicity. In line with this finding, Tirmenstein *et al.* exposed HepG2 to SKF-525AP450 (a non-selective inhibitor) with ketoconazole, a CYP3A4 inhibitor. They reported that the combined exposure did not rescue the cells from TGZ-provoked cell death.

Chapter 5 The need for *in silico* system in drug discovery

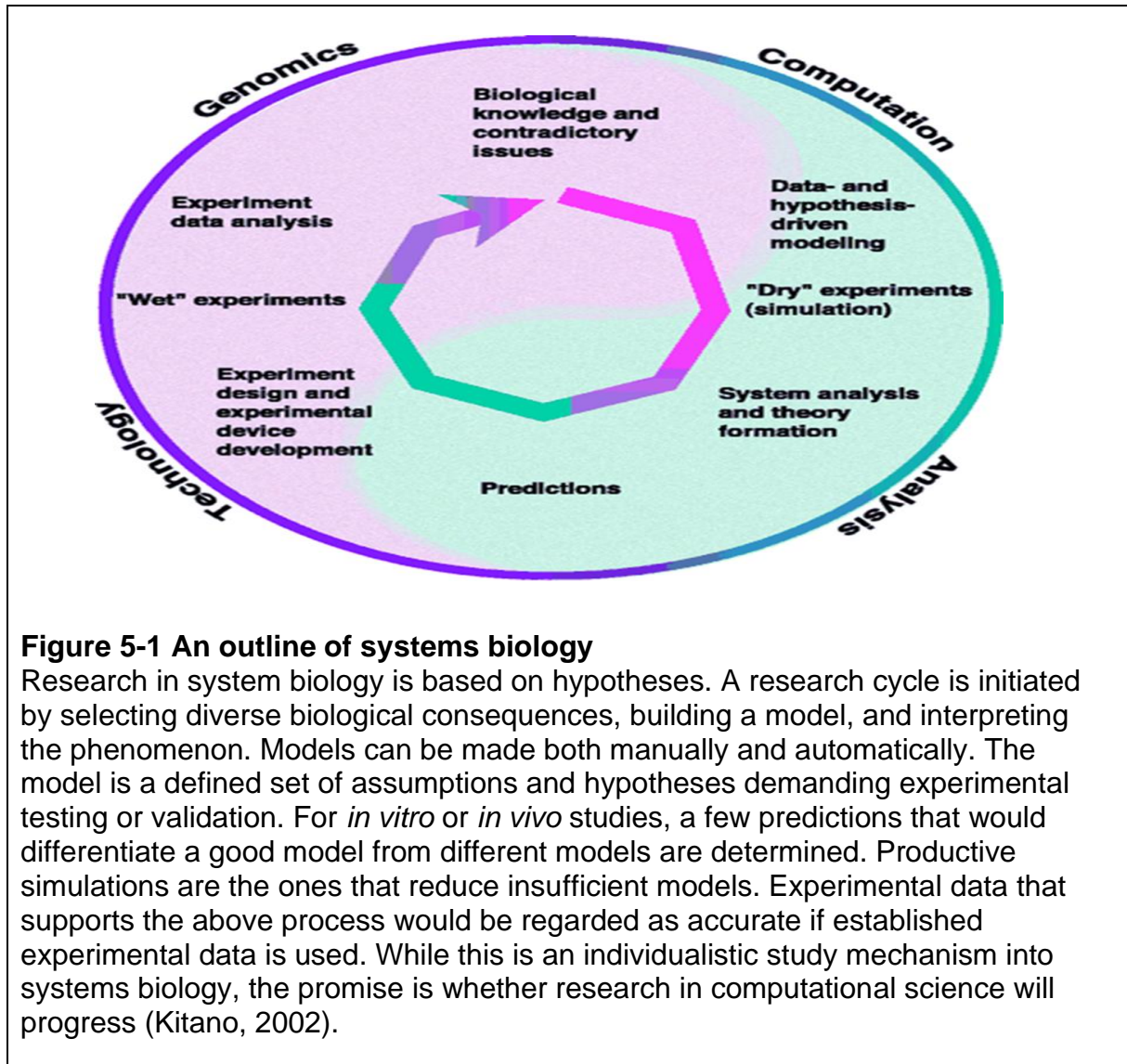
Despite the high expenditure over the last several decades, the development of new drugs and corrective approaches for disease improvement remains a highly unproductive process (Hay, 2014). Adverse drug reactions (ADRs), or drug-induced adverse events, are a common cause of preventable deaths globally. They have become a significant motive for the retraction of drugs from the market and the cessation of drug candidates in clinical trials (Hay, 2014; Plant, 2015). Currently, about 90% of drugs that undergo clinical trials do not get approval by the relevant agencies on account of lack of efficacy and/or unpredicted toxicity, even with advanced research as well as development costs (Aithal, 2015; 2019; Hay, 2014; Plant, 2015). For the above reasons, there is massive pressure on drug developers to produce novel, more efficient methods to isolate and remove drug candidates with insignificant safety profiles as early in development as practicable. As described in the previous section, animal models have failed to predict potential drug or drug candidate toxicity because they fail to repeat many aspects of human physiology and, thus, demonstrate the weak similarity between species (Driessen *et al.*, 2015). *In vitro* models that accurately replicate physiology have shown the possibility of being commercial options for an animal that improves the accuracy of predicting drug toxicity early in development. However, simple cellular models cannot incorporate all pharmacological contributions to toxicity, including the effects of serum binding drug clearance and they are unable to represent effective models for chronic toxicity mechanisms or responses that result from the interaction of multiple cell types. Therefore, pharmaceutical or toxicological settings need a reliable *in silico* model system to explore in drug development to predict the toxicity of a novel drug or a potential drug candidate. This is because they can combine data from various assays and predict the emerging behaviour from these interactions.

5.1 Systems Biology

Systems biology involves several approaches and models for exploring and understanding biological intricacy (Plant, 2015). Therefore, understanding physiological diseases from the level of biological pathways, regulatory cells, tissues, organs, or the entire organism and adverse effects triggered by xenobiotics forms a

critical driving force in modern system biology (Plant, 2015). Most researchers centre on building essential computational tools necessary to consolidate metabolomics data, gene expression, or metabolic pathways into models of the regulatory network and cell behaviour (Figure 5-1) (Kitano, 2002). As biological intricacy is a logarithmic function of the number of system units, the associations between them and increases at each additional level of configuration, the before-mentioned efforts are currently restricted to simple organisms or apparent theoretical pathways in higher organisms (Auffray *et al.*, 2011; Hunter & Borg, 2003; Ideker *et al.*, 2001; Kitano, 2002; Plant, 2015). Researchers can appropriately quantify molecules as well as their operational states and interactions. Therefore, approaches that explore data for applicability, for instance, biological perspective and, what is more, experimental awareness of cellular and complex level system reactions, will be essential to robustly distinguish different levels of organisation in systems biology studies (Ideker *et al.*, 2001; Noble, 2002; Plant, 2015). As discussed previously, there are several approaches to systems biology research. This current study focuses on three of the existing criteria: informatic integration of “omics” data files, computer modelling of pathologies, and organ response level data from the literature. Complex human cell systems to deduce and estimate the biological behaviours of xenobiotics, as well as gene targets or direct experimental approaches to cataloguing complex disease-related responses are complementary approaches (Ideker *et al.*, 2001; Plant, 2015). These systems must be integrated with the search for a hierarchical-to-systems level of knowledge of human pathologies that has a notable influence on drug development (Plant, 2015). The full understanding of the responses of a system involves understanding its fundamental constituents. Omic systems biology focuses on the building blocks of complex systems such as genes, proteins, or metabolites. Researchers can employ omic methods to determine what genes or proteins are expressed or upregulated in a disease process. For example, a multiparameter gene expression test that determines whether patients with breast cancer in the early stages are likely to benefit from chemo. This test and others have classified breast cancer into subtypes with varying diagnoses and therapeutic strategies (Matthews *et al.*, 2016; Weston & Hood, 2004; Ideker & Lauffenburger, 2003). Another example is the use of simple organisms and integrating analysis of time-series genome-scale mRNA expression data, large-scale perturbation analysis and detection of

simultaneously controlled parts, as well as protein-protein interaction for subsequent interaction networks. This provides knowledge about how the cell conveys data in response to triggers and actively develops the molecular machinery that is needed for life (Bar-Joseph *et al.*, 2003; Davidson, 2002).



5.1.1 Model Development

One of the fundamental goals of molecular biology is to define the biological pathways by which data are generated due to environmental signals, resulting in a particular phenotype. Mechanistic computational modelling is an essential tool given the large number of molecular elements of a cell and the unpredictable non-linear

existence of their interactions (Oberhardt *et al.*, 2011; Plant, 2015). The mechanistic models, as discussed previously, represent the current understanding of the cellular machinery that cells reflect. The molecules and the interactions included in the introduction of such models reflect the extent of the accompanying text of the genome sequence, with computer simulations used to predict the biology of systems. Such a neutral reflection of molecular interactions in mechanistic models is called reconstruction (Oberhardt *et al.*, 2009; Oberhardt *et al.*, 2011). Dynamic simulation of genome-scale molecular interaction networks will enable mechanistic prediction of interactions in both genotype and phenotype.

Notwithstanding the developments in quantitative biology, it is still not possible to pre-process the whole-cell models. Mechanisms of a mathematical model capable of using accessible qualitative data are necessary to build dynamic full-cell models across an algorithmic modelling system (Fisher *et al.*, 2013; Oberhardt *et al.*, 2011).

5.1.2 Results of model development and prediction

The first step of these processes was to identify relevant biological networks from the literature. Finally, such biological networks were automatically translated into the Petri-net notation. The final step was to fix the start configuration (give tokens to the places) and send the Petri-net to the simulation tool. A literature search has revealed that TGZ-induced liver toxicity results from a combination of two major pathways:(i) metabolic and (ii) non-metabolic (Kassahun *et al.*, 2001). Previous studies have reported that TGZ may cause toxicity through various metabolic pathways; for instance, the formation of quinone or sulphate metabolites as described in the previous section may contribute to TGZ-induced hepatotoxicity. Therefore, model objectives were set by reviewing the possible mechanisms that may contribute to TGZ-induced liver toxicity and representing these probable pathways diagrammatically (Figure 5-2).

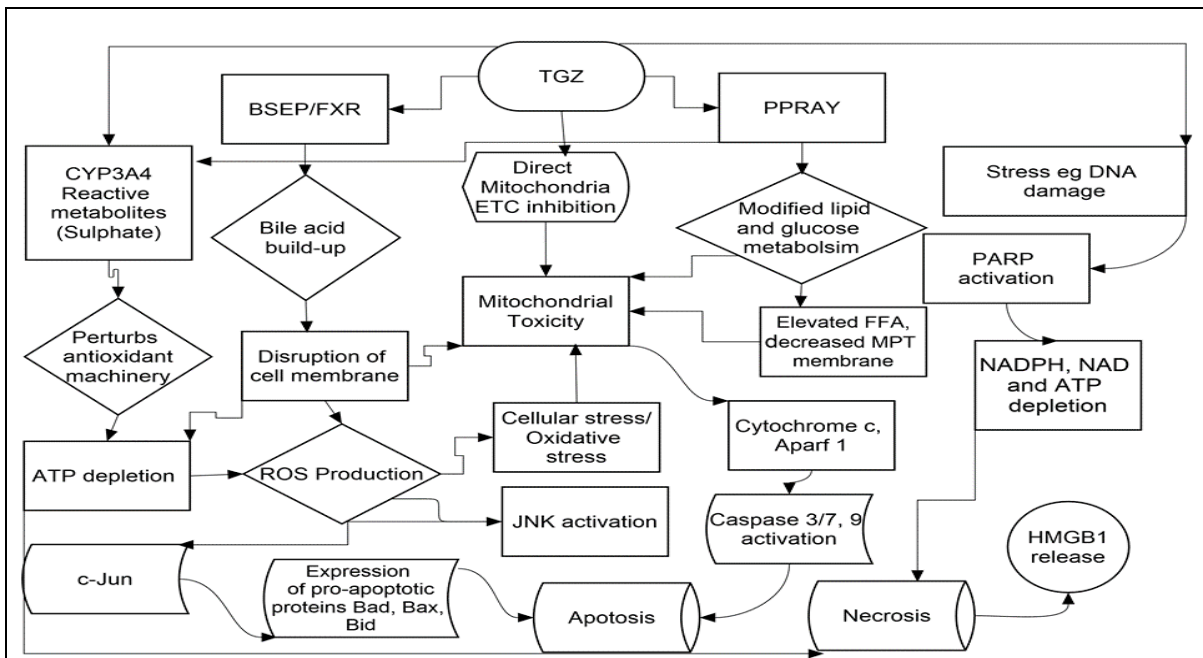


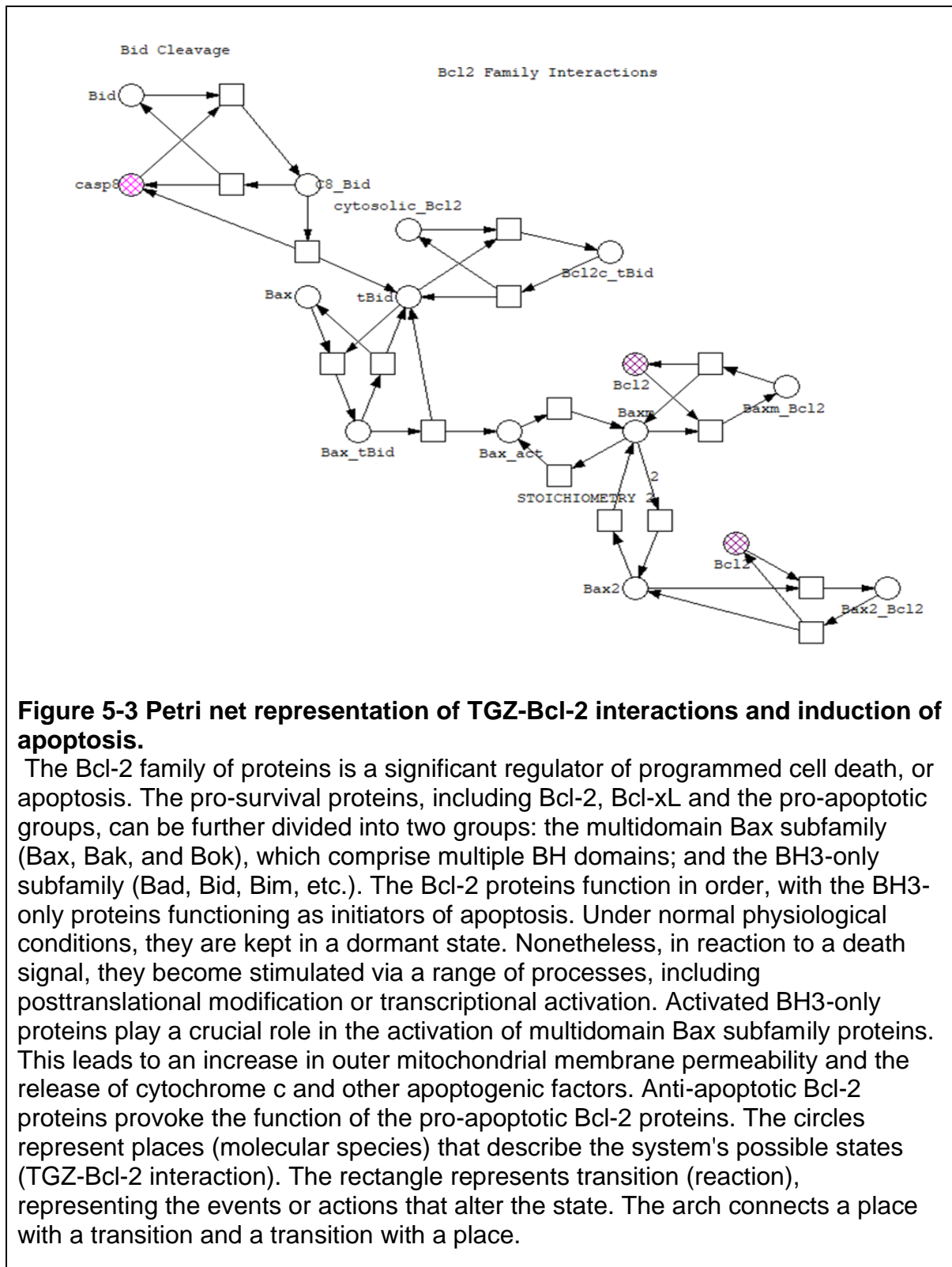
Figure 5-2 Probable pathways of TGZ-induced liver toxicity for model creation

TGZ activates PPAR, which in turn alters lipid and glucose metabolism. Alteration of lipid and glucose metabolism may lead to high FFA levels and a reduction of MPT to induce mitochondrial toxicity. TGZ may inhibit ETC, induction of mitochondrial toxicity, the release of cytochrome c and, in turn, caspase activation. Caspase activation leads to apoptosis. BSEP inhibition may cause accumulation of TGZ-sulphate, the major TGZ metabolite and a potent inhibitor of bile acid transport proteins in hepatocytes, which inhibits bile acid excretion, leading to bile acid accumulation and hepatotoxicity. Activation of FXR may cause a reduction in the synthesis of bile acids and increase expression of bile acid efflux transporters, BSEP, organic solute and steroid transporters. Inhibition of PXR by TGZ may cause an accumulation of bile acids. TGZ may induce ROS, or oxidative stress. ROS may cause lipid peroxidation, damage to the DNA repair process, or damage to a specific amino acid residue, which may control kinase signalling pathways. These pathways may detect oxidative stress and transduce signals to trigger a cellular response. However, if the balance shifts towards an excess of ROS over antioxidants, it may lead to oxidative stress and cause disruption of redox signalling. TGZ may cause CYP3A4 induction, which is accountable for the formation of quinone metabolites in humans. PARP1 uses NAD as an enzymatic substrate to produce poly-(ADP-ribose) polymers via PARylation. PARylation transfers signals from the nucleus to the mitochondria, releasing apoptosis-inducing factor that translocates to the nucleus, causes DNA damage, and further activates PARP-1. Depletion of NAD and ATP due to PARP-1 activation results in bioenergetic collapse and necrosis and the release of HMGB1 (Bae & Song, 2003; Funk *et al.*, 2001; Karin & Lin, 2002; Li & Chiang, 2017; Vignati *et al.*, 22005; Watkins 2013).

5.1.2.1 Petri net creation of TGZ apoptotic pathway

Different pro-apoptotic signals initially activate separate signalling pathways, which eventually converge into a common mechanism driven by a distinctive family of cysteine proteases (caspases) (Kluck, 2010; Shi, 2004). TGZ-Bcl-2 interaction on apoptosis in a Petri net was represented (Figure 5-3). Many sets of genes negatively control this process, with the Bcl2-family as a classic example. The Bcl-2 group is made up of members who are anti-apoptotic and pro-apoptotic and form heterodimers. The Bcl-2 family is characterised by three subfamilies. It depends entirely on the homology and functionalities of each protein (Bcl-2, Bcl-XL, and Bcl-W), all of which are active against cell death and BH (Bcl-2 homology) 1 through BH4. A second subfamily (Bak and Bax) shares series homology at BH1, BH2 and BH3 but not at BH4, although significant homology at BH4 is also marked in some members. Bcl-2 family proteins can form homodimers and heterodimers (Zhang *et al.*, 2004; Zucchini *et al.*, 2005). Heterodimerization between anti-apoptotic and pro-apoptotic members of this family is deemed to repress the biological activity of their partners (Zhang *et al.*, 2004), and this is triggered by the insertion of the BH3 region of a pro-apoptotic protein into a hydrophobic pocket composed of BH1, BH2 and BH3 from an anti-apoptotic protein (Zhang *et al.*, 2004). Bcl-2 and its closest homologs (Bcl-XL and Bcl-w) promote cell survival, but two other sub-groups promote apoptosis. The Bax and Bak domains are shared by one of these groups, whereas the other group (Bim, Bad, Bid, and so on) shares only the BH3 domains. When activated by stress signals, these BH3-only proteins insert an amphipathic alpha-helix into a hydrophobic groove on their pro-survival relatives (Hinds & Day, 2005; Zhang *et al.*, 2004). This coupling primes the cell for apoptosis, but commitment requires Bax or Bak activation, which then forms oligomers on intracellular membranes, including the mitochondrial outer membrane, thereby perturbing their integrity (Zhang *et al.*, 2004; Zong, 2001). The Bcl-2 family of proteins is a significant regulator of programmed cell death, or apoptosis. Pro-survival proteins including Bcl-2, Bcl-xL and the pro-apoptotic groups can be further grouped into two groups: the multidomain Bax subfamily (Bax, Bak, and Bok), which comprise multiple BH domains; and the BH3-only subfamily (Bad, Bid, Bim, etc.) (Zhang *et al.*, 2004). Also, the Bcl-2 proteins function in order, with the BH3-only

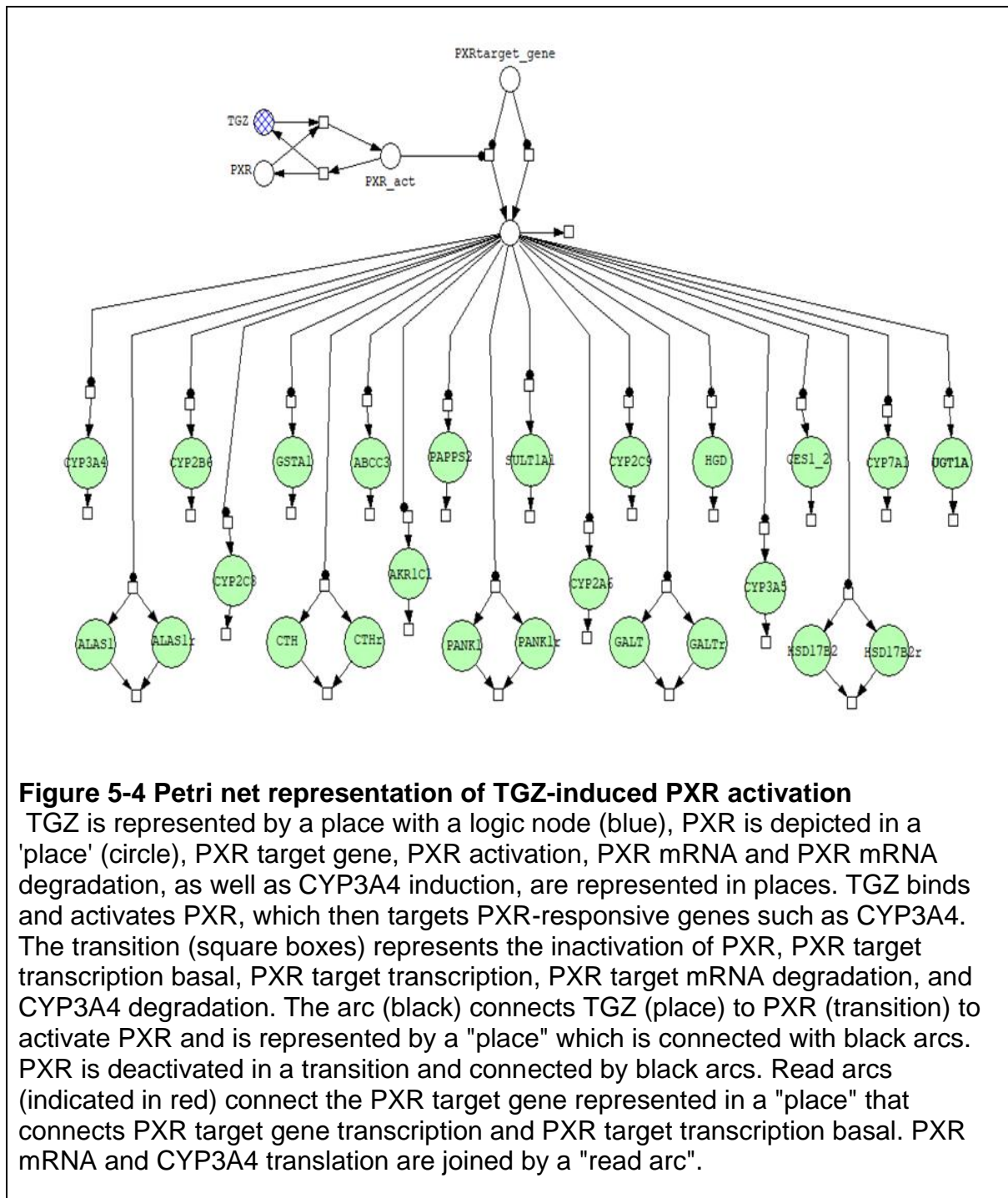
proteins operating as initiators of apoptosis. Under normal physiological conditions, they are kept in a dormant state.



5.1.2.2 Petri net representation of TGZ-induced PXR activation and its target genes

Although the systems responsible for PXR-mediated liver injury need further investigation (Hartley *et al.*, 2006), activation of PXR by agonists can enhance the expression of PXR target genes, including those encoding liver enzyme transporters and other enzymes involved in biosynthetic pathways. These might lead to the build-up of toxic metabolites or intermediate endogenous substances in the liver (Hartley *et al.*, 2006; Pan *et al.*, 2010). TGZ-induced PXR stimulation might be an underlying mechanism for its hepatotoxicity (Hartley *et al.*, 2006; Pan *et al.*, 2010). The activation of PXR by TGZ and its target genes is represented by the Petri net (Figure 5-4).

Various theoretical systems have obtained significant results in modelling mechanistically different cellular organisation levels such as metabolic, signalling, and gene regulatory networks. In this current study, the gene regulatory network using Petri net was established; for example, the transcription of genes encoding TGZ induces CYP3A through the activation of PXR was demonstrated. It forms part of PXR's target basal transcription factor (basic set of proteins required to stimulate gene transcription). The information in PXR DNA is transferred to a messenger RNA (mRNA) molecule by way of the transcription process. The PXR target mRNA is then translated. This then induces CYP3A4. Increased CYP3A4 activity is finally degraded.



5.1.2.3 Petri net representation of TGZ-induced cholesterol signalling

As discussed in the previous chapter, cholesterol is a vital part of cellular membranes and serves in other tissues as a precursor to steroid hormones, bile acids or vitamin D3. Yet, excess cholesterol levels can be cytotoxic. Thus,

cholesterol synthesis is usually strictly controlled by a feedback mechanism to control the physiologically acceptable cholesterol levels (Klopotek *et al.*, 2006).

A group of microsomal enzymes, such as the HMG-CoA synthase and reductase as the rate-limiting enzymes, catalyse cholesterol synthesis (Klopotek *et al.*, 2006). Their transcriptional control is regulated primarily by SREBP-2. SREBPs form a complex with SREBP-cleavage-activating protein (SCAP) following synthesis in ER membranes. SCAP escorts the SREBPs from the ER to the Golgi when cells are depleted of sterols (Horton *et al.*, 2002; Klopotek *et al.*, 2006). Within the Golgi, two resident proteases, site-1 protease and site-2 protease, sequentially cleave off the SREBPs, release the membrane-containing amino-terminal, essential helix-loop-helix proteins, enabling them to translocate to the nucleus and trigger transcription of their target genes. It characterised three SREBP isoforms: SREBP-1a, -1c, and -2. While SREBP-1c, the predominant isoform in the adult liver, activates the genes necessary for fatty acid synthesis preferentially, SREBP-2 activates the LDL receptor gene and various genes implicated in cholesterol synthesis, such as HMG-Coeducates (Horton *et al.*, 2002; Klopotek *et al.*, 2006). SREBP-1a activates both the biosynthetic cholesterol and fatty acid pathways but is found in the liver in far lower quantities than the other two types (Horton *et al.*, 2002). Insulin-induced genes (Insig)-1 and -2 are membrane proteins located in the ER and play a central role in SREBP cleavage control (Yang *et al.*, 2002). When the level of intracellular sterols increases, SCAP binds to Insigs, an action that prevents translocation of the SREBP-SCAP complex from the ER to the Golgi and proteolytic activation of SREBP. As a result, cholesterol synthesis and fatty acids decrease (Yang *et al.*, 2002). The above mechanism was represented by the Petri net (Figure 5-5).

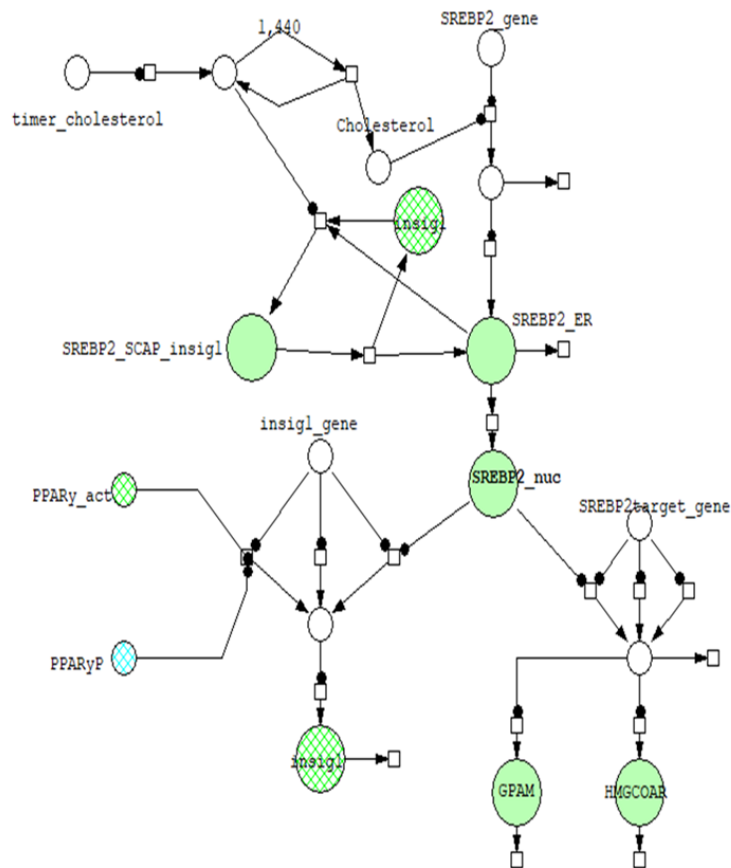


Figure 5-5 Petri net representation of cholesterol signalling

SREBP precursors are retained in the ER membrane via tight association with SCAP and proteins of the INSIG family. Once dissociated from INSIG, SCAP escorts the SREBP precursors from the ER to the Golgi apparatus; once in the Golgi apparatus, two proteases, S1P and S2P, sequentially cleave the precursor protein, releasing the mature form of SREBP into the cytoplasm.

5.1.3 Model simulation and prediction

A simulation is used to predict functional biological outcomes or to create results that can be used to check for reliability with existing data. It uses known inputs to generate a unique set of outputs. A simulation was run to explore the behaviour (prediction) of our model. And to run a simulation, a control file is required (see Appendix A). The control file is a small binary file that documents the physical database structure. The database cannot be mounted without the control file, and it

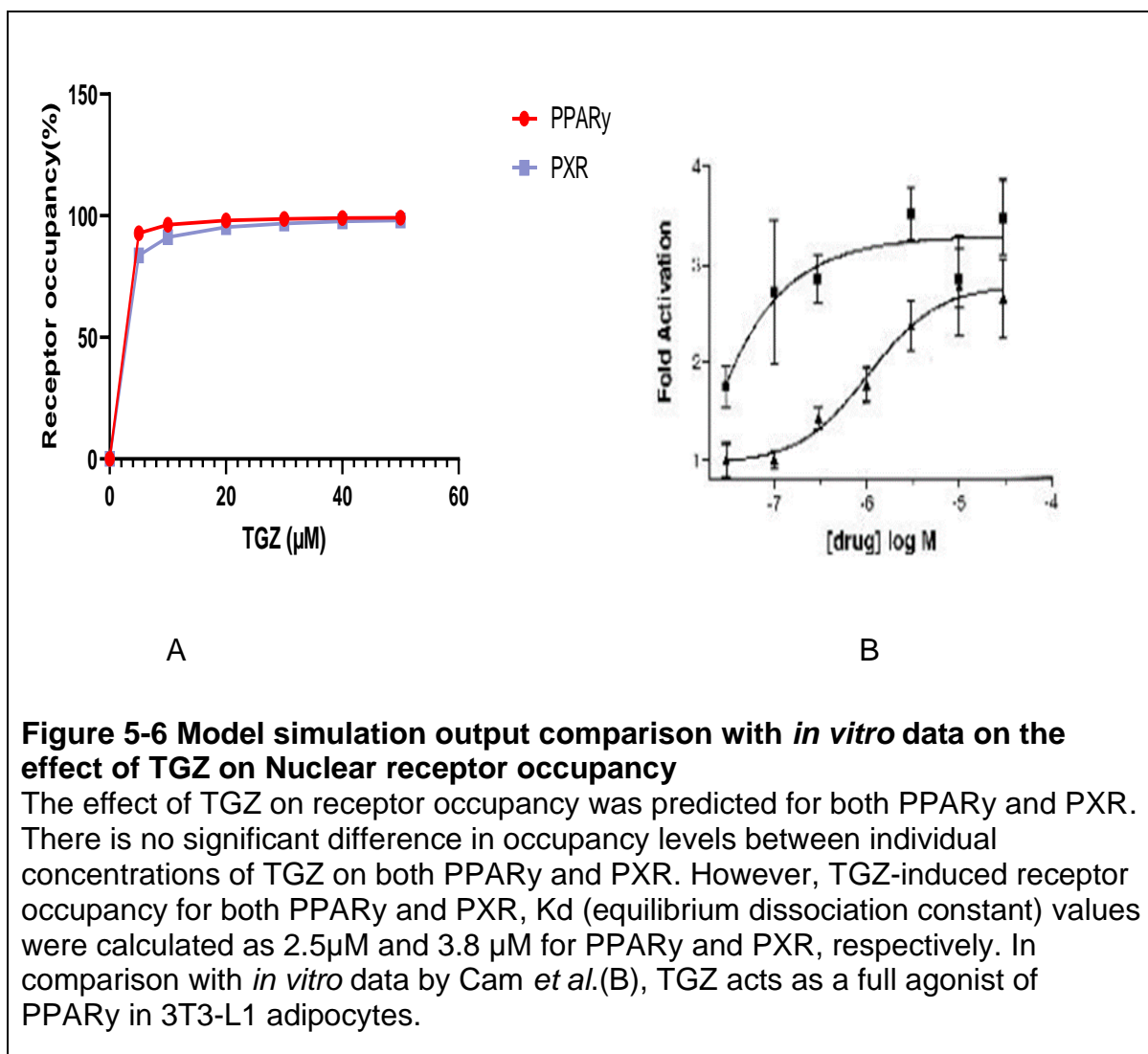
is difficult to recover. Care was taken to back up the file any time after a change in the database's physical structure was made. Such structural changes include adding, deleting, or renaming data files; adding, deleting a tablespace; or changing the read-write status of a tablespace, adding, deleting, or deleting redo log files or groups. The outcome of interest for this current was the prediction of TGZ-apoptotic pathways and the nuclear receptor occupancy by TGZ. Therefore, replication of the following was set out:

- The induction of apoptosis by TGZ through the various apoptotic pathways
- The effect of TGZ on CYP3A4 induction
- TGZ- quinone formation
- TGZ-sulphate formation
- The effect of TGZ on ATP production
- The effect of TGZ on mitochondrial respiratory chain complex
- The effect of TGZ on BSEP activity and bile acid homeostasis
- The effect of TGZ on PTEN levels
- Effect of TGZ on cholesterol levels
- The effect of TGZ on glucose formation
- TGZ nuclear receptor occupancy
- The effect of TGZ on cell number

5.1.4 TGZ receptor occupancy

The pharmaceutical industry has faced challenges over the past few decades, including rising research and development costs, lower approval rates, and improved drug safety (Beck *et al.*, 2014; Hrusovsky, 2008). Receptor occupancy experiments are used to evaluate the binding of therapeutics to targets on the cell surface. They are widely used in non-clinical and clinical trials of biological agents such as drugs to produce pharmacodynamic biomarker results. Many studies have shown that TGZ is a PPAR ligand, but little is known about its affinity for PXR (Bai *et al.*, 2007; Bailey, 2018; Baran, 2014; 2018; Bova *et al.*, 2005). TGZ's binding capacity to PPAR γ and PXR were determined through computer simulations over 3500 minutes, and it was recorded that at 5 μ M TGZ, the receptor occupancy for PPAR γ and PXR was 92 % and 83%, respectively. At 10 μ M TGZ, the receptor occupancy for PPAR γ and PXR

increased by 96 % and 91%, respectively. At 20 μM TGZ, the receptor occupancy for PPAR γ and PXR were 98% and 95%, respectively. At TGZ concentrations of 30 μM , 40 μM and 50 μM TGZ concentrations, there were no significant differences in the level of receptor occupancy between PPAR γ and PXR (98%, 99%, and 99%) and 96%, 97%, and 99%, respectively (Figure 5-6A).



5.1.5 TGZ apoptotic pathways

Having set out the above objectives, the model of apoptosis was downloaded from Biomodels (<https://www.biomodels.net>), which was based on a published model of apoptosis (Albeck *et al.*, 2008). To ensure that the model had been correctly imported into the Petri net formalism, the original SBML code was imported into the

Complex Pathway Simulator (COPASI). MuFINS software (QSSPN) was used separately and then simulated to see if they produced the same TGZ-JNK activation behaviour.

To check if our model reproduces biology (quality control), the model of apoptosis was compared with the above-published data that have been shown to reproduce biology (Figures 5-7 A to 5-7 D). Our model in QSSPN (Figures 5-7 A1 to 5-7D1) look the same as that of COPASI (Figures 5-7A-D). This is an indication that our model reproduces biology. However, the time sets in both COPASI and the QSSPN are not the same, for instance, between 0 to 200 minutes (Figure 5-7 A) and between 0 to 600 minutes (Figure 5-7 A1) as the level of cPARP stabilises at a steady state, so as the activation of PARP. And an explanation to different timing responses was due to a control period before any stimulation was added in the simulation for QSSPN.

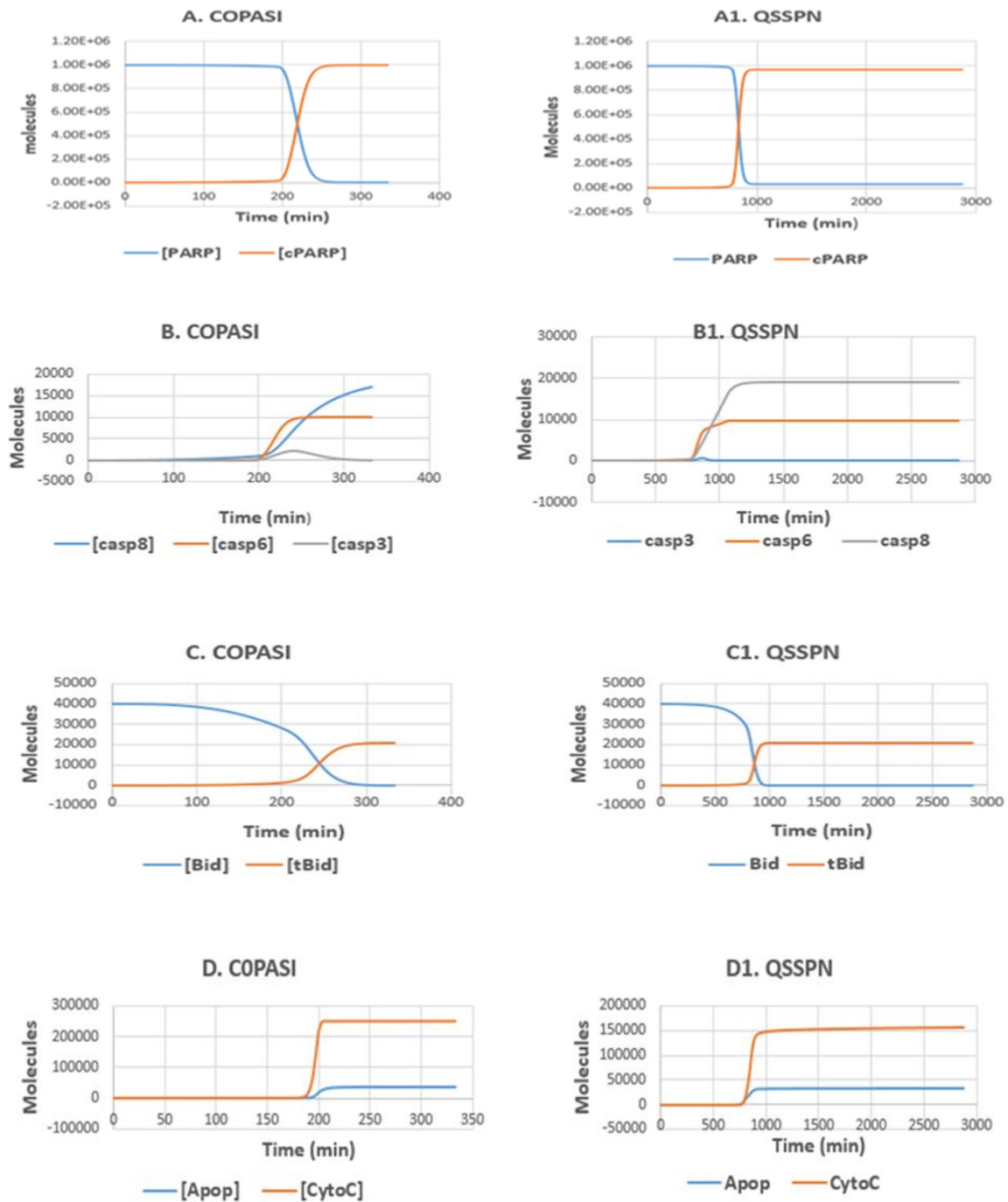


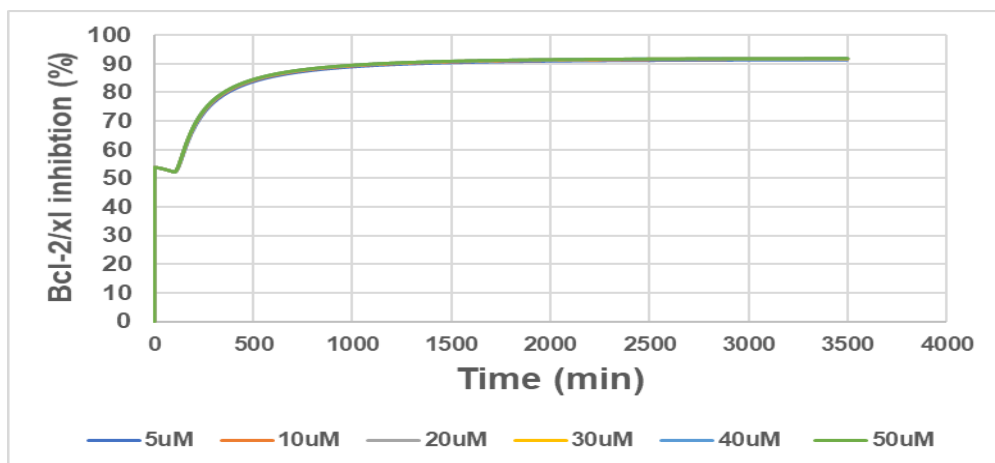
Figure 5-7 A- D and A1-D1 Comparison of simulation outputs

Comparison of the model with Albeck *et al.* apoptosis model, simulation using (A, B, C, and D) COPASI and (A1, B1, C1, and D1) MUFINS software. The molecular number over time was predicted for: (A) cleavage of PARP to form cPARP, a classical target of caspase-3; (B) production of active caspase-3, -6, and -8; (C) cleavage of bid to form tBid, a specific substrate of caspase 8, which may cause the release of cytochrome c and (D) release of cytochrome c into the cytoplasm and formation of the apoptosome (Apop).

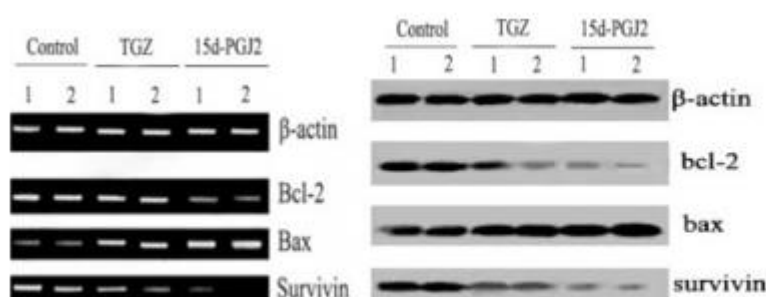
5.1.6 Effect of TGZ on Bcl-2/xL expression

The apoptotic Bcl-2/xL, a transmembrane molecule located in the mitochondria, plays a critical function in mitochondrial-dependent extrinsic and intrinsic pathways. Overexpression of Bcl-2/xL can inhibit apoptotic cell death. However, in a situation where Bcl-2/xL is inhibited, the pores in the cell become permeable to pro-apoptotic proteins and subsequent cell death (Cory *et al.*, 2003; Fiebig *et al.*, 2006).

This pathway is explored in the model to predict the impact of TGZ on Bcl-2/xL. Interestingly, similar levels of BCL-2/xL inhibition by the various concentrations of TGZ (5 μ M to 50 μ M) were observed at 57 minutes. The level of Bcl-2/xL was recorded at 53% by the various concentrations of TGZ. However, the various concentrations of TGZ (5 μ M to 50 μ M) would cause significant inhibition of Bcl-2/xl at 500 minutes; that is, all concentrations were predicted to lead to a near-complete (90%) inhibition (Figure 5-8A). Our model prediction is in line with the *in vitro* experiment by Liu *et al.*, who also reported significant inhibition of Bcl-2 by TGZ (Figure 5-8B). However, they only exposed the cells to 80 μ M TGZ, which was far higher than the concentrations of TGZ explored in our model (Liu *et al.*, 2005).



A



B

Figure 5-8A-B Comparison of model prediction and *in vitro* assessment of the effects of TGZ on Bcl-2/xL expression

The model prediction of the effect of TGZ on Bcl-2/xL expression was then compared (A) to Liu *et al.* *in vitro* reverse transcription (RT)–PCR and western blot assessment on the outcome of TGZ on Bcl-2/xL expression (B) and a significant inhibition of Bcl-2/xL similar to the *in vitro* recordings by Liu *et al.* was predicted.

5.1.7 Model simulation on the effect of TGZ on bile acid homeostasis

A drug's functionality to obstruct the bile salt export pump BSEP/ABCB11 has been attributed to drug-induced liver injury (DILI) (Dawson *et al.*, 2011). Also, DILI was associated with both the BSEP blockers and other bile acid transporters. TGZ was associated with liver toxicity and was the reason for its removal from the market (Bailey, 2018; Funk *et al.*, 2001; Jaeschke, 2007). Exceptionally, BSEP/ABCB11

antagonists have all been repeatedly proposed as other causes of hepatic toxic effects, which can undermine our understanding of TGZ-induced DILI more often than not (Bova *et al.*, 2005). Awareness of the consequences of BSEP/ABCB11 blockers on biotransformation of bile acid modification will substantiate a thorough understanding of the significance of BSEP/ABCB11 inhibition in DILI. Bile acids are molecules that help digest triglycerides and other fat-soluble nutrients. They are made in the liver and undergo successful enterohepatic recirculation (Hofmann, 2009; Pauli-Magnus, 2005).

Currently, there is no known qualitative data based on bile acid homeostasis. Also, there are still several aspects of bile acid transport for which there is inadequate scientific data available. Intestinal bacteria generate bile acids like deoxycholic acid (DCA) in the gut, but the rate of development and variability of this synthesis has not been assessed in any species (Duane, 2009; Hoffman, 2004; Li & Chiang, 2013).

Although some bile acids such as LCA and CDCA are much more cytotoxic than most other bile acids, the effect of these intrahepatic bile acid levels remains to be expounded on the liver cells (Hoffman, 2004; Hofmann & Hagey, 2008). The process of developing a DILI computer model generated from bile acid could be important for determining which data deficiencies should be answered first for maximum effect. Whereas any mechanistic model of DILI induced by bile acid will lack predictive precision due to large data gaps, computer modelling could be used to empirically describe traits of the mechanism that are likely to lead to DILI induced by bile acid. In this analysis, an *in silico* model to predict the effect of TGZ on both BSEP and CDCA levels was generated. At all concentrations of TGZ, it was predicted that 100% BSEP inhibition would be achieved, consistent with the *in vitro* data (Figure 5-9C) (Ogimura *et al.*, 2017). However, the predicted kinetics of these inhibition curves varied considerably. At the highest concentration of TGZ simulated, 98% inhibition is predicated upon the addition of TGZ, increasing to 100% inhibition after 900 mins. In contrast, simulation of 5uM TGZ predicted an initial 57% inhibition upon exposure, reaching 100% inhibition after 1000 minutes. These data are consistent with a concentration-dependent effect on BSEP inhibition by TGZ. Also, the accumulation of bile acid (CDCA) by TGZ was predicted. At 105 minutes, the model predicted 13.88 ng/ml for the various concentrations of TGZ (Figure 5-9B). However, at 500

minutes, bile acid levels were at 36.43 ng/ml at the lowest TGZ concentration (5 μ M) and 40.00 ng/ml at the highest TGZ concentration (50 μ M). In line with previous *in vitro* studies, TGZ at 50 μ M caused a significant accumulation of bile acid (CDCA) after 500 minutes (Ogimura *et al.*, 2017) (Figure 5-9D).

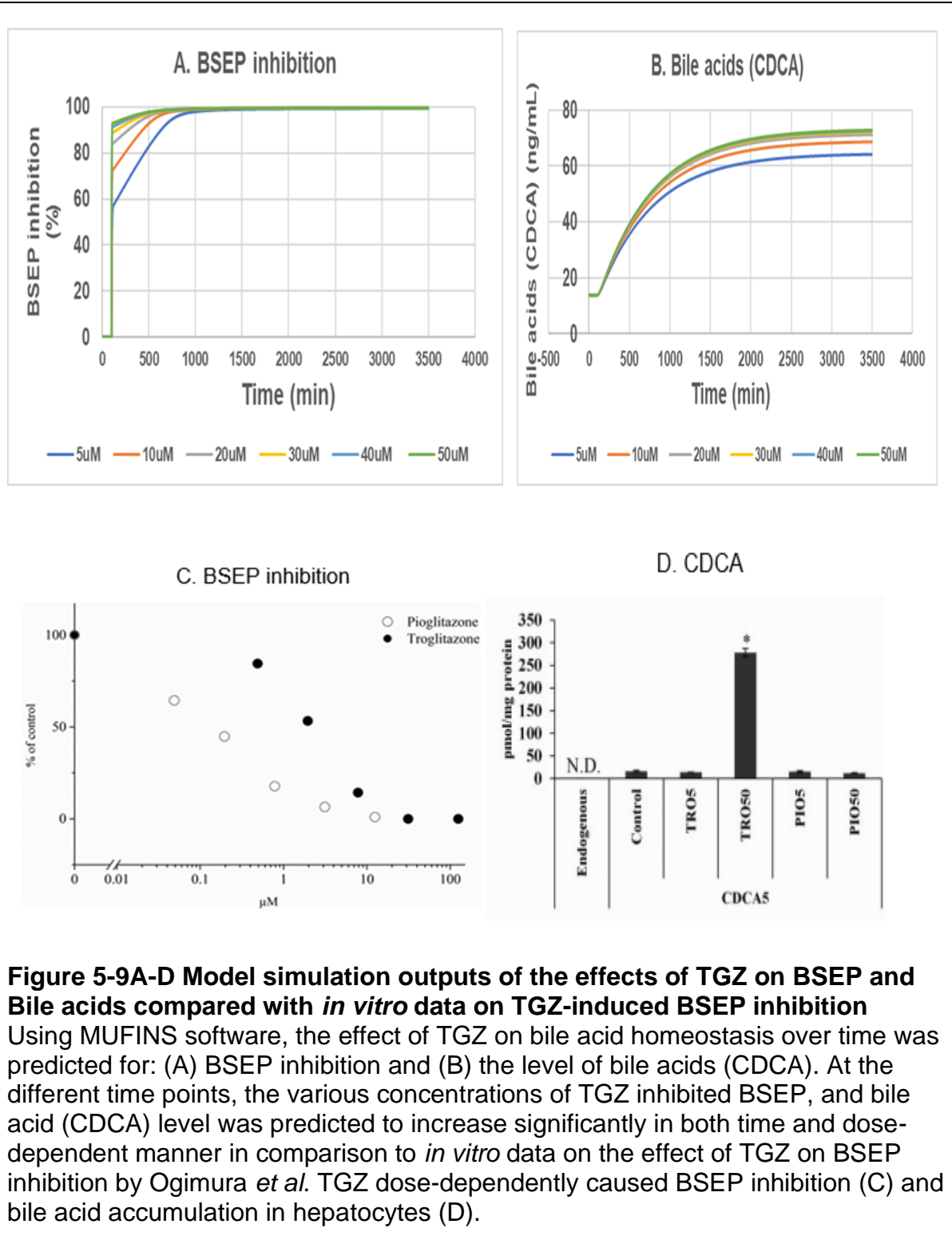


Figure 5-9A-D Model simulation outputs of the effects of TGZ on BSEP and Bile acids compared with *in vitro* data on TGZ-induced BSEP inhibition
 Using MUFINS software, the effect of TGZ on bile acid homeostasis over time was predicted for: (A) BSEP inhibition and (B) the level of bile acids (CDCA). At the different time points, the various concentrations of TGZ inhibited BSEP, and bile acid (CDCA) level was predicted to increase significantly in both time and dose-dependent manner in comparison to *in vitro* data on the effect of TGZ on BSEP inhibition by Ogimura *et al.* TGZ dose-dependently caused BSEP inhibition (C) and bile acid accumulation in hepatocytes (D).

5.1.8 The effect of TGZ on cholesterol synthesis

Physiological maintenance of cholesterol levels is important to retain cellular and systemic activities. Underlying cardiovascular disease and a growing array of other diseases or cancer might be a result of disrupted cholesterol levels (Luo *et al.*, 2019; Wong *et al.*, 2018). The cellular cholesterol level represents the complex equilibrium between biosynthesis, intake, distribution, and/or cholesterol in lipoprotein components converted to neutral cholesterol esters for storage in lipid droplets or secretions. Also, the LDL receptor pathway plays a significant role in controlling LDL plasma levels in humans (Klopotek *et al.*, 2006; Wong *et al.*, 2018). When clearance of LDL particles via the LDL receptor pathway, as in familial hypercholesterolemia, is substantially compromised or eliminated, there is a substantial increase in plasma LDL. On the other hand, the primary mechanism by which statins decrease plasma LDL is the more effective clearance of LDL particles through the LDL receptor pathway (Glassberg & Rader, 2008; Wong *et al.*, 2018). These modifications, therefore, are triggered by disease or pharmacological interference and do not display their physiological role in the LDL receptor pathway function (Glassberg & Rader, 2008). The speculation for the receptor pathway for LDL establishes the reciprocal relationship between the rate of cholesterol within an LDL particle in the cell and the levels of production of both cholesterol and the LDL receptors inside the cell (Glassberg & Rader, 2008; Luo *et al.*, 2019). The liver plays a central role in all the major cholesterol fluxes within the organism, with multiple lipoprotein receptor-mediated endocytic pathways that contribute cholesterol to the total hepatocyte cholesterol pool (Glassberg & Rader, 2008). There are also multiple outputs of cholesterol from the hepatocyte: cholesterol can be metabolised into bile acids, as well as dissolved in bile. Cholesterol and cholesterol ester might be synthesised in apolipoprotein B (apo B) containing very-low-density lipoprotein (VLDL) particles and transported from the liver cells' plasma membranes through the ATP-binding cassette transporter A1 as well as the ATP-binding cassette transporter G1 to apolipoprotein A-I and high-density lipoprotein (HDL) particles as well as specifically secreted with HDL (Makhouri & Ghasemi, 2018). Several *in silico* models simulating cholesterol metabolism have been generated for both human and animal models (Paalvast *et al.*, 2015; Worth, 2019). *In silico* modelling has proven to be a useful tool

in biology because it allows the study of interspecies variation and regulation of homeostasis and allows the integration of information from various sources (Makhouri & Ghasemi, 2018). In this work, a framework for predicting hepatic cholesterol levels was presented. The predictor is based on an algorithm for cholesterol metabolism simulation available in the literature. However, there are several modelling efforts on cholesterol (Ratushny *et al.*, 2003), an important biomarker for the risk of cardiovascular diseases as well as liver injury (Rosamond *et al.*, 2008). Most of these cholesterol modelling studies present models that focus on LDL cholesterol (LDL-C) metabolism in plasma (Adiels *et al.*, 2004; van Schalkwijk *et al.*, 2009) or on cellular cholesterol metabolism (Ratushny *et al.*, 2003).

In this study, the impact of TGZ on cholesterol concentrations was predicted, and an initial level of cholesterol of 0 to 100 mg/ml was observed with respect to all the TGZ concentrations (5 μ M to 50 μ M). Between 120 and 500 minutes, the level of cholesterol decreased to 23.95 ng/ml, 23.42 ng/ml, 22.96 ng/ml, 22.75 ng/ml, 22.25 ng/ml, and 21.49 ng/ml with respect to TGZ concentrations (5 μ M to 50 μ M). At 1000 minutes, the level of cholesterol relative to TGZ concentrations (5 μ M to 50 μ M) decreased to 20.19 ng/ml, 17.80 ng/ml, 16.66 ng/ml, 15.19 ng/ml, 14.80 ng/ml, and 14.14 ng/ml. At 1500 minutes, a further decrease in cholesterol levels with respect to the various concentrations of TGZ (5 μ M to 50 μ M) as 16.69 ng/ml, 13.36 ng/ml, 12.47 ng/ml, 11.59 ng/ml, 11.32 ng/ml, and 11.21 ng/ml was predicted. The levels of cholesterol with respect to TGZ concentrations (5 μ M to 50 μ M) at 2000 minutes were reduced to 14.67 ng/ml, 11.34 ng/ml, 10.27 ng/ml, 9.45 ng/ml, and 9.29 ng/ml. At 2500 minutes, the levels of cholesterol were reduced to 13.65 ng/ml, 10.31 ng/ml, 9.15 ng/ml, 8.20 ng/ml, 8.01 ng/ml, and 7.27 ng/ml with respect to TGZ concentrations (5 μ M to 50 μ M) (Figure 5-10).

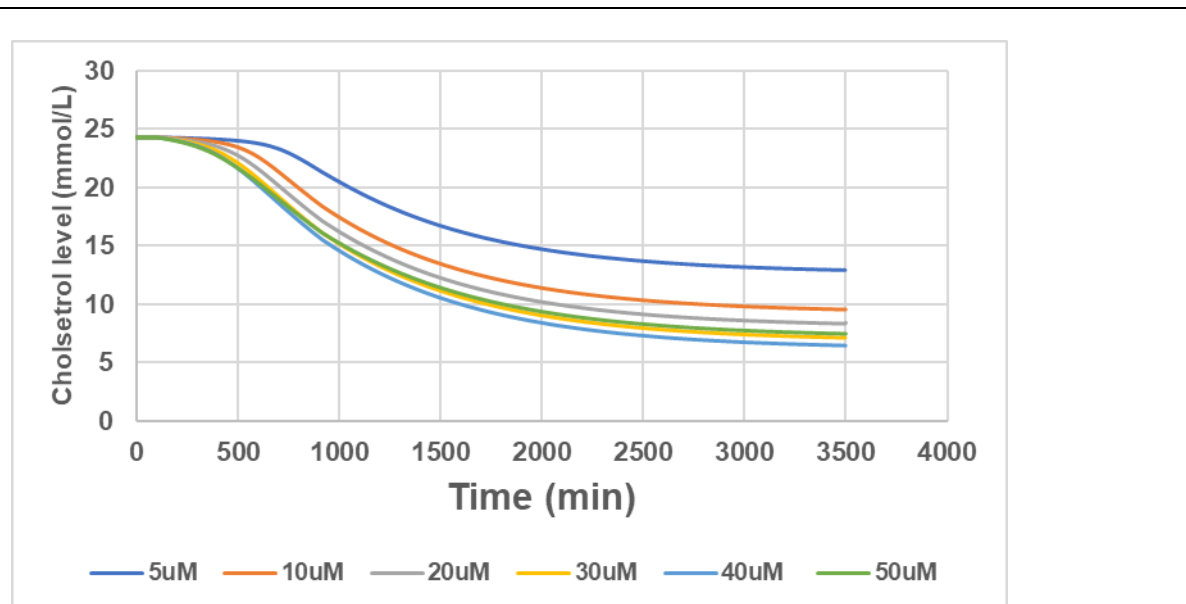


Figure 5-10 Model simulation output of the effect of TGZ on cholesterol levels at different time points.

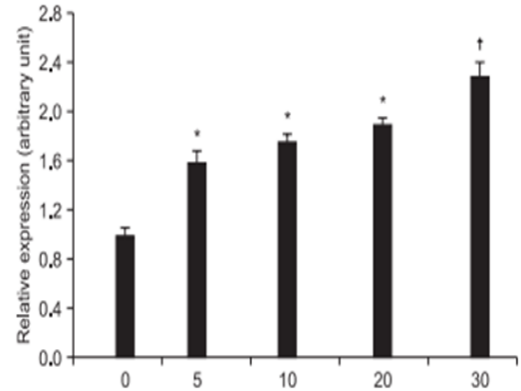
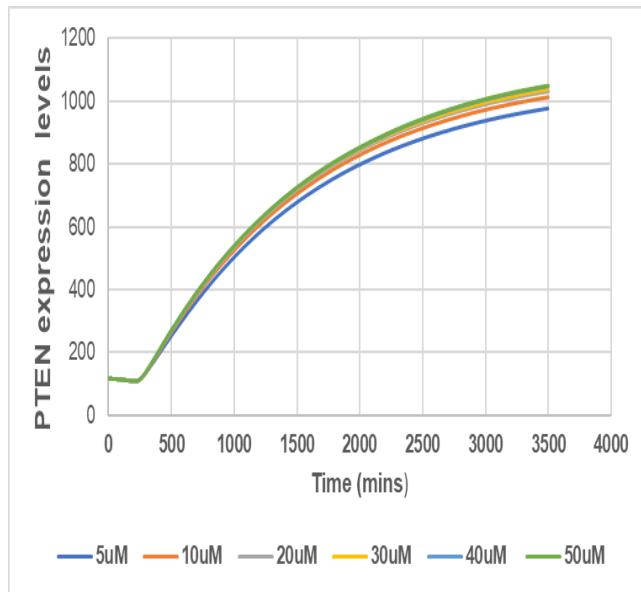
Using MuFINS software, the effect of TGZ on cholesterol homeostasis over time was predicted for cholesterol production; however, the level of cholesterol was observed to decrease significantly in both a time-dependent and dose-dependent manner.

5.1.9 Model simulation on the effect of TGZ on PTEN expression

PTEN (phosphatase and tensin homologue deleted from chromosome 10) or MMAC1, is a tyrosine phosphatase with folded protein and lipid phosphatase activity (Leslie & Downes, 2002; Lopez *et al.*, 2020; Wen *et al.*, 2001; Wishart *et al.*, 2002). PTEN accepts PIP3 as a substrate and detaches the D3 phosphate from the inositol ring. Inhibition of PTEN expression, as reported by Lopez *et al.* in cancers, might result in the build-up of PIP3, causing the constitutive stimulation of the phosphatidylinositol 3-kinase/Akt pathway. On the other hand, a surge in PTEN levels would be expected to decrease the levels of PIP3 and in turn block receptor-stimulated Akt activity (Lopez *et al.*, 2020).

PTEN also has reduced protein phosphatase activity, but the function as a tumour suppressor is essential. Cell cycle control might be implicated in PTEN protein phosphatase action to prevent cells from growing and dividing too quickly (Salmena

et al., 2008). Many PTEN protein substrates have been identified, including IRS1 (He, 2010; Shnitsar *et al.*, 2015). Therefore, this study explored the effects of TGZ on the expression levels of PTEN through computer simulations and found that the initial levels of PTEN were recorded at 116 minutes at all the various concentrations of TGZ (5 μ M to 50 μ M). Interestingly, as the time progressed to 240 minutes, the level of PTEN at the variable strengths of TGZ (5 μ M to 50 μ M) dropped to 111. However, between 240 minutes and 500 minutes, the level of PTEN increased to 268 at the various concentrations of TGZ. Between 500 minutes and 1000 minutes, it increased to 505, 528, 537, 538, and 538 at the different strengths of TGZ (5 μ M to 50 μ M), respectively. Between 1000 and 1500 minutes, the level of PTEN by TGZ concentrations increased to 679, 707, 720, 721, and 723, respectively. Between 1500 and 2000 minutes, the level of PTEN further increased to 820, 830, 843, 850, 853 and at the various concentrations of TGZ (5 μ M to 50 μ M), respectively. Between 2000 and 2500 minutes, the different concentrations of TGZ (5 μ M to 50 μ M) caused an increase in the PTEN levels at 880, 914, 930, 935, 941, and 944, respectively. The various concentrations of TGZ. Between 2500 minutes and 3000 minutes, the levels of PTEN also increased to 938, 972, 990, 996, 1004 and 1006 at TGZ concentrations of (5 μ M to 50 μ M) respectively (Figure 5-11A). 5 μ M to 50 μ M caused a further increase in PTEN levels at 938, 972, 990, 996, 1004 and 1006, respectively. Between 3000 minutes and 3500 minutes, the level of PTEN at the various concentrations of TGZ (5 μ M to 50 μ M) was increased to 976, 1012, 1030, 1037, 1046, and 1049, respectively. However, there was no significant difference between the PTEN expression levels induced by the various concentrations of TGZ at each simulation period. In line with our model prediction, Yoon *et al.* have reported a dose-dependent increase in PTEN expression by cells exposed to the various concentrations of TGZ (Figure 5-11B).



A

B

Figure 5-11 A-B Model simulation output and *in vitro* data on the effect of TGZ on PTEN expression levels

Using MUFINS software, the effect of TGZ on PTEN expression over time was predicted (A). The levels of PTEN increased as simulation time increased; however, the highest levels of PTEN were observed between 1500 minutes and 3500 minutes compared to the *in vitro* data by Yoon *et al.* have reported that TGZ dose-dependently caused an increase in PTEN expression (B).

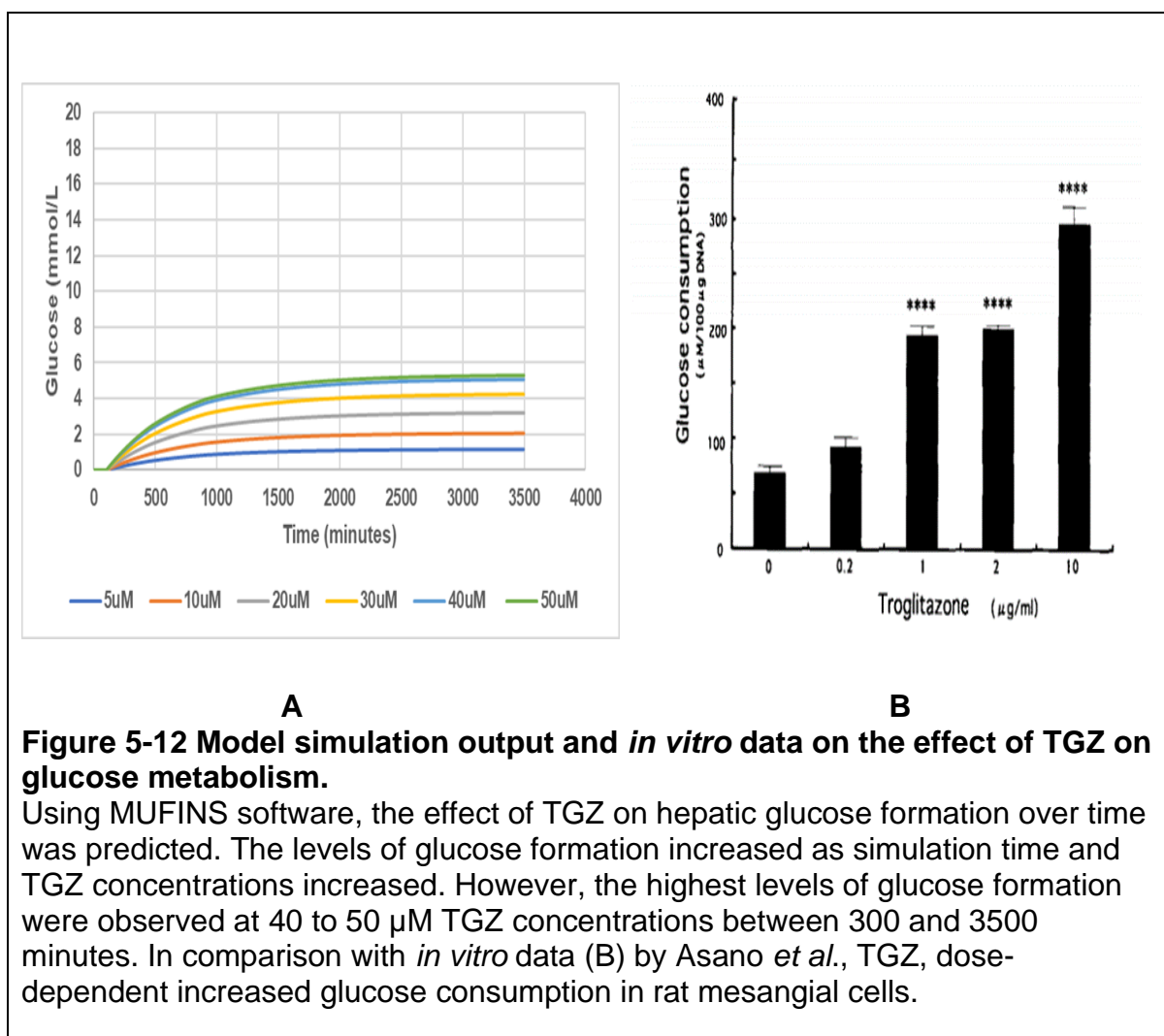
5.1.10 Model simulation on the effect of TGZ on glucose homeostasis

Variable glucose levels in the plasma have damaging effects on the whole organism. The primary energy source for the brain is glucose, and lower levels of plasma glucose can lead to impaired brain function and death (Alsahli *et al.*, 2017; Kruszynska *et al.*, 2004). Glucose homeostasis is regulated by intracellular nutrient sensing and hormonal signalling pathways that regulate the use and production of glucose. The liver, skeletal and cardiac muscles, and brain are part of the tissue that helps maintain normal blood glucose levels. More than 30% of blood glucose is absorbed into the liver after carbohydrate intake.

In comparison, over 30% is absorbed by adipose tissue and the muscle, whereas residual glucose is absorbed by the brain, kidney and red blood cells (Alsahli *et al.*, 2017; Kruszynska *et al.*, 2004). Insulin and glucagon are two essential counter-regulative hormones based on glucose that facilitate peripheral tissues' responses to regulate levels in the use and synthesis of glucose, whereby glycaemia is retained within limited ranges. However, the tissues' resistance to insulin leads significantly to the disruption of glucose homeostasis, resulting in hyperglycaemia and the progression of type 2 diabetes mellitus (Kruszynska *et al.*, 2004; König *et al.*, 2012).

In this chapter, the effects of TGZ on hepatic glucose formation were determined and recorded. All the various concentrations of TGZ (5 μ M to 50 μ M) did not cause glucose production between 0 and 100 minutes. However, between 100 minutes and 500 minutes, the various concentrations of TGZ (5 μ M to 50 μ M) caused hepatic glucose production of 0.54 mmol/L, 0.98 mmol/L, 1.56 mmol/L, 2.05 mmol/L, 2.46 mmol/L, and 2.61 mmol/L, respectively. Between 500 minutes and 1000 minutes, TGZ concentrations at (5 μ M to 50 μ M) did increase glucose formation by 0.80 mmol/L, 1.56 mmol/L, 2.47 mmol/L, and 3.27 mmol/L, respectively. Between 1000 minutes and 1500 minutes, the level of hepatic glucose production by the various concentrations of TGZ (5 μ M to 50 μ M) increased to 1.10 mmol/L, 1.81 mmol/L, 2.85 mmol/L, 3.77 mmol/L, 4.51 mmol/L, and 4.73 mmol/L, respectively. From 1500 minutes to 2000 minutes, hepatic glucose formation remained at 1.11 mmol/L, at 5 μ M TGZ. However, glucose production at TGZ concentrations (10 μ M to 50 μ M) increased to 1.94 mmol/L, 3.03 mmol/L, 4.02 mmol/L, 4.81 mmol/L, and 5.03 mmol/L, respectively. The level of glucose formation between 2000 and 2500-minutes simulation further increased to 1.12 mmol/L, 2.00 mmol/L, 3.12 mmol/L, 4.14 mmol/L, 4.95 mmol/L, and 5.11 mmol/L at the various concentrations of TGZ (5 μ M to 50 μ M) respectively. Also, between 2500 minutes and 3000 minutes, the levels of glucose formation by the various concentrations of TGZ (5 μ M to 50 μ M) were 1.14 mmol/L, 2.03 mmol/L, 3.17 mmol/L, 4.20 mmol/L, 5.03 mmol/L, and 5.25 mmol/L, respectively. Finally, between 3000 and 3500 minutes, glucose formation levels at TGZ concentrations (5 μ M to 50 μ M) were 1.15 mmol/L, 2.05 mmol/L, and 3.19 mmol/L, 4.23 mmol/L, 5.06 mmol/L, and 5.29 mmol/L, respectively (Figure 5-12A). A

previous *in vitro* experiment by Asona *et al.* reported a dose-dependent increase in glucose consumption by rat mesangial cells (Figure 5-12B).



5.1.11 TGZ metabolism and reactive metabolites

One of the possible causative roles is that of biotransformation of TGZ to a reactive metabolite. Kassahun *et al.* have reported that biotransformation of the TZDs ring of TGZ is an inducer of the CYP3A4 isoform in human liver cells. Also, He *et al.* reported that the oxidative ring-opening of the TGZ leads to the formation of quinone in an NADPH-dependent manner. The researchers also noted that the formation of TGZ-quinone was affected by co-treatment with catalase. This was partially blocked by superoxide dismutase. They then postulated that CYP3A4 catalysed TGZ-

quinone formation. The findings that TGZ could form some reactive intermediates led us to set our objective functions to predict TGZ on CYP3A4 induction, TGZ-SO₄ formation and TGZ-quinone formation.

5.1.11.1 The effect of TGZ on CYP3A4 induction

Having simulated the effects of TGZ on CYP3A4 induction, the level of CYP3A4 between 0 and 30 minutes at the various concentrations of TGZ was predicted at 100 and remained constant at 115 till 500 minutes. At 500 minutes, an increase in CYP3A4 at 296, 299, 300, 304, 309, and 312 concerning TGZ concentrations (5 μ M to 50 μ M) was predicted. TGZ concentrations (5 μ M to 50 μ M) at 1000 minutes caused a further increase in CYP3A4 levels at 398, 435, 446, 459, and 460, respectively. At 1500 minutes, the level of CYP3A4 was elevated to 454, 495, 510, 525, 528 and 530, respectively (5 μ M to 50 μ M). At 2000 minutes, CYP3A4 level predictions concerning TGZ concentrations increased to 492, 524, 543, 553, 557, and 558, respectively. At 2500 minutes, there was an increase in CYP3A4 levels at 504, 539, 558, 566, 571, and 552 at TGZ concentrations (5 μ M to 50 μ M). Between 3000 and 3500 minutes, the levels of CYP3A4 increased to 512, 548, 569, 580, 581, and 582 concerning TGZ concentrations (5 μ M to 50 μ M) (Figure 5-13).

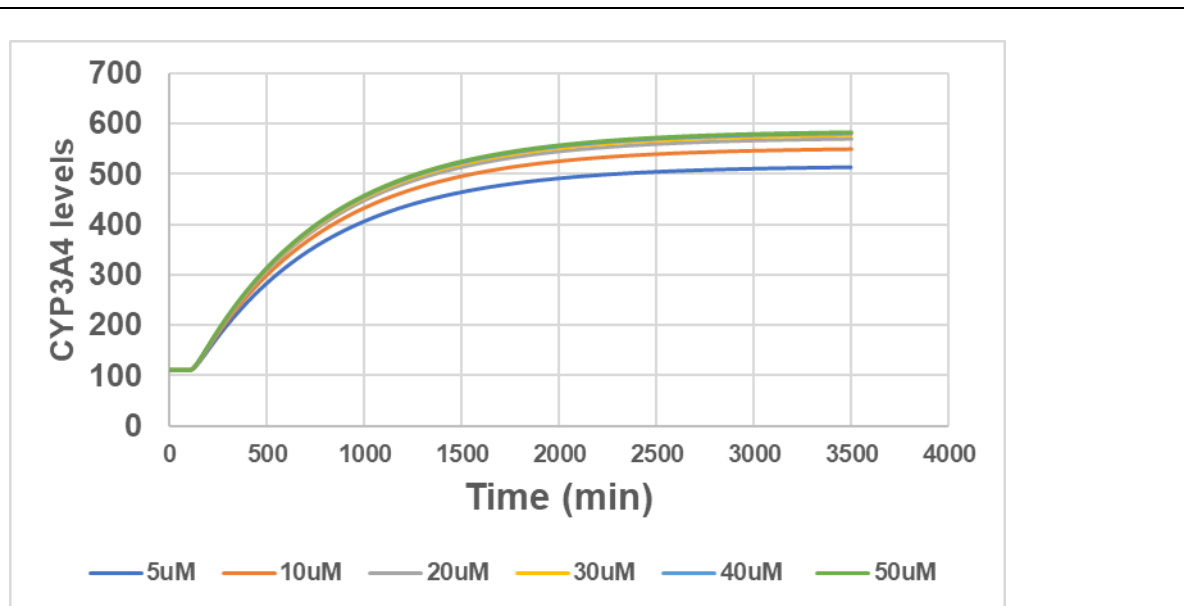
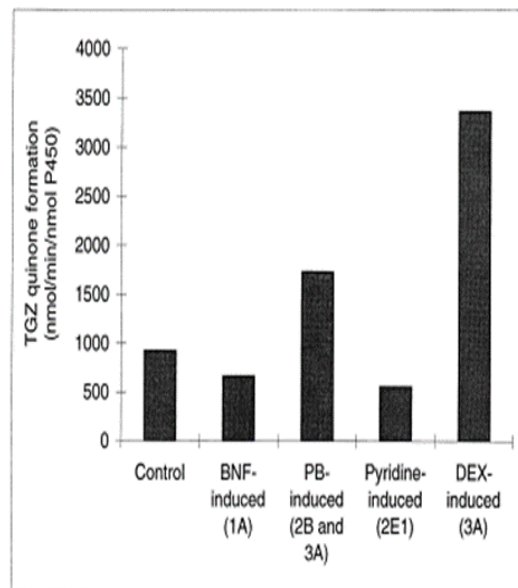
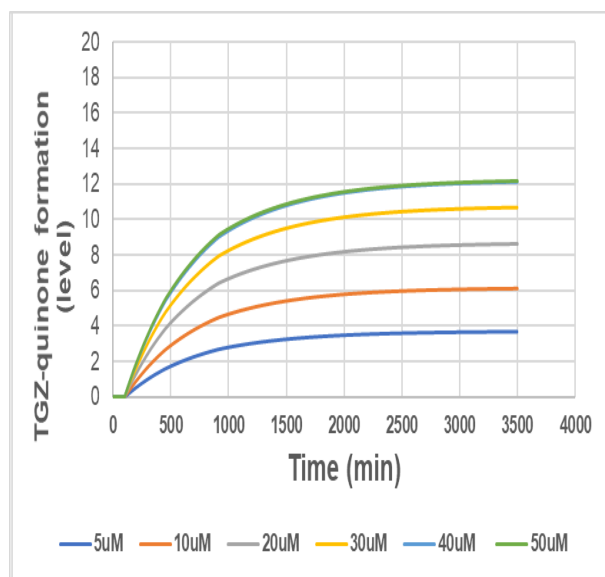


Figure 5-13 Model simulation output of the effect of TGZ on CYP3A4 levels
 The effect of TGZ on CYP3A4 induction over time was predicted. The level of CYP3A4 was observed to increase significantly in both time and dose-dependent manner.

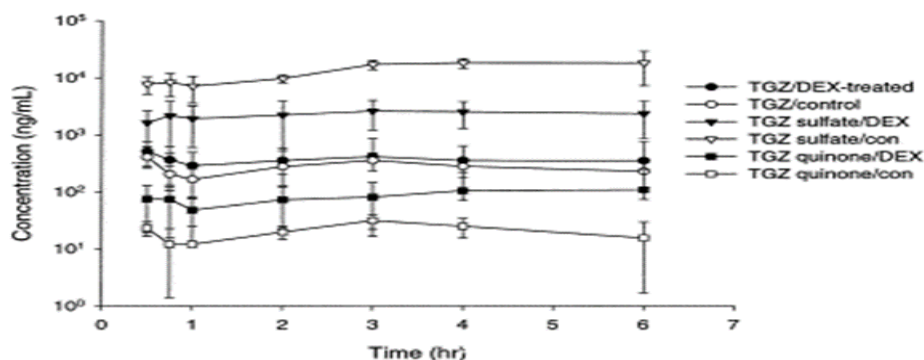
5.1.11.2 Metabolism of TGZ to TGZ-quinone formation

Between 0 and 500 minutes, a negligible TGZ-quinone formation by the various concentrations of TGZ; TGZ-quinone formation at 500 minutes as 1.82, 3.01, 3.59, 4.47, 5.73, and 6.03 with respect to TGZ concentrations (5 μ M to 50 μ M) was recorded. At 1000 minutes, TGZ-quinone formation levels for TGZ concentrations (5 μ M to 50 μ M) were 2.79, 4.65, 6.62, 9.23, 9.47, and 9.52. At 1500 minutes, the levels of TGZ-quinone at TGZ concentrations (5 μ M to 50 μ M) were 3.23, 5.40, 7.68, 9.58, 10.88, and 10.99. Between 2000 and 2500 minutes, TGZ-quinone formation levels at TGZ concentrations (5 μ M to 50 μ M) were predicted to be 3.58, 5.96, 8.43, 10.44, 11.60, and 11.90. TGZ-quinone formation was increased significantly in liver microsomes from rats pre-exposed to CYP3A inducers (Figure 5-14B). The engagement of CYP3A isoforms in TGZ-quinone production explored *in vivo* in rats led to a significant increase in TGZ quinone formation in animals pre exposed to DEX, an inducer of CYP3A enzymes (Figure 5-14C) (He *et al.*, 2001).



A

B



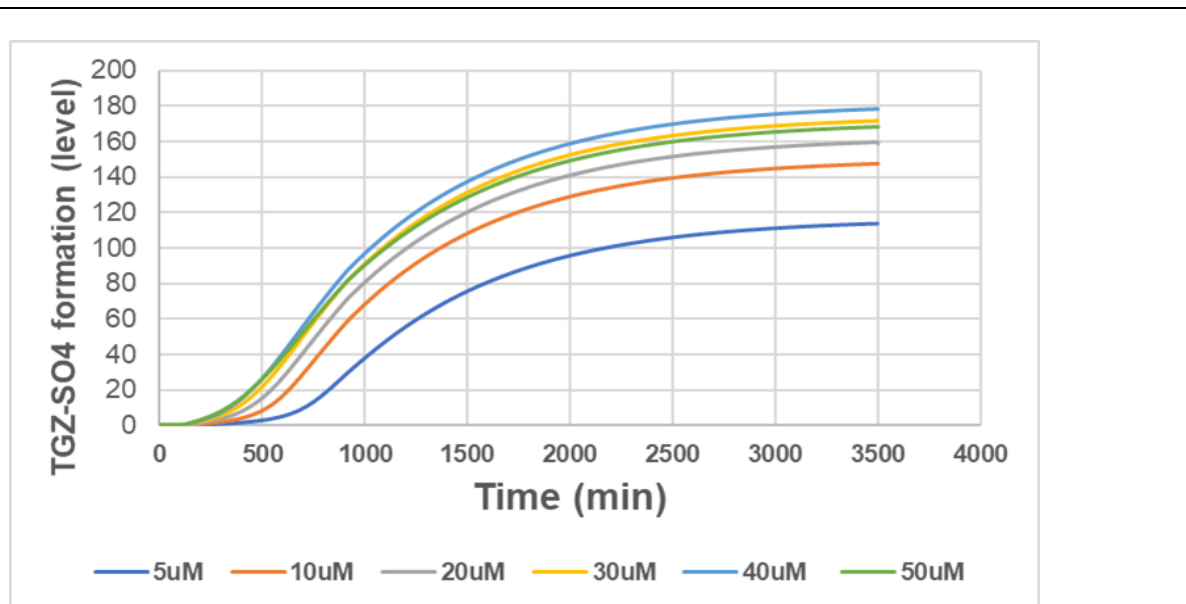
C

Figure 5-14 Model simulation output of the of TGZ-quinone formation compared with *in vitro* and *in vivo* data on the effects of TGZ-quinone formation

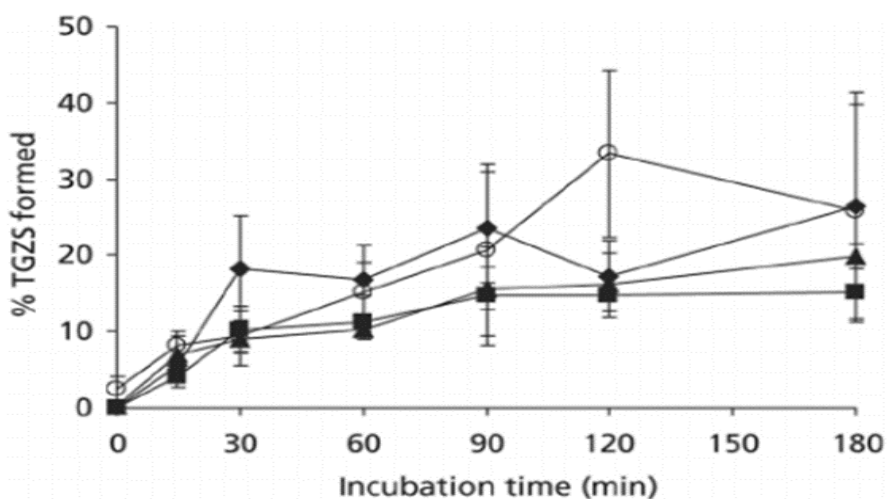
The effect of TGZ on quinone formation over time was predicted (A). TGZ dose-dependently increased TGZ-quinone formation. However, the level of TGZ-quinone formation between 1000 and 3500 minutes did not exhibit any significant difference in TGZ-quinone formation. In comparison to studies by He *et al.*, rat liver microsomes exposed to CYP inducers caused an increase in TGZ-quinone formation (B). Rats exposed to TGZ CYP3A4 inducer DEX *in vivo* caused TGZ-quinone formation (C).

5.1.11.3 Metabolism of TGZ to TGZ-SO₄

Between 0 and 500 minutes, a negligible TGZ-SO₄ formation by the various concentrations of TGZ. TGZ-SO₄ formation at 500 minutes as 1.82, 3.01, 3.59, 4.47, 5.73, and 6.03 with respect to TGZ concentrations (5 μM to 50 μM) was recorded. At 1000 minutes, TGZ-SO₄ formation levels at TGZ concentrations (5 μM to 50 μM) were 2.79, 4.65, 6.62, 9.23, 9.47, and 9.52, respectively. At 1500 minutes, the levels of TGZ-SO₄ at TGZ concentrations (5 μM to 50 μM) were 3.23, 5.40, 7.68, 9.58, 10.88, and 10.99, respectively. Between 2000 and 2500 minutes, TGZ-SO₄ formation levels at TGZ concentrations (5 μM to 50 μM) were 3.58, 5.96, 8.43, 10.44, 11.60, and 11.90, respectively. Between 3000 and 3500, there was no further increase in TGZ-SO₄ formation (Figure 5-15A). In line with *in vitro* studies, the researchers recorded TGZ-SO₄ formation in rat liver cells exposed to TGZ (Figure 5-15B) (Meechan *et al.*, 2006).



A



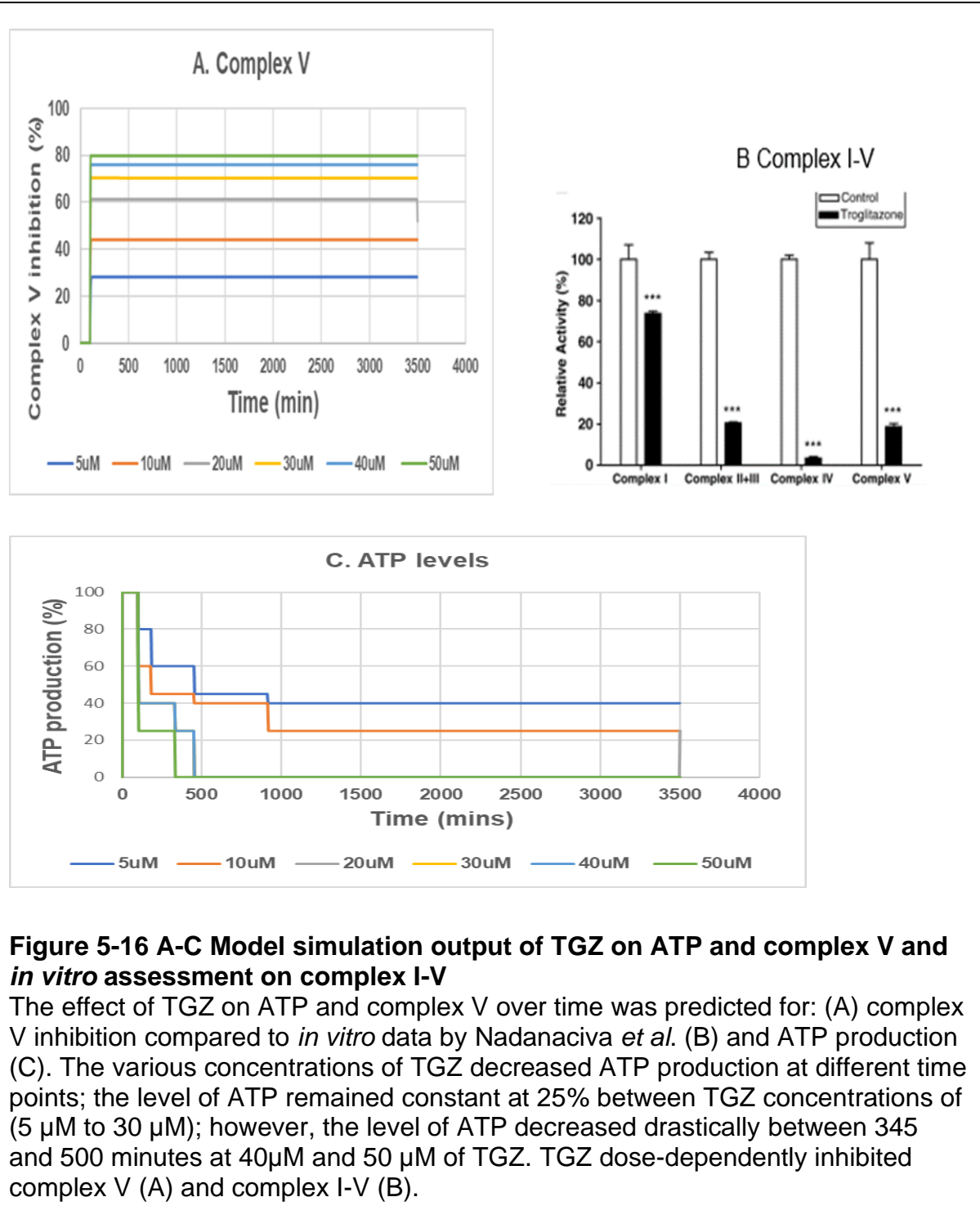
B

Figure 5-15 A-B Model simulation output of the effect of TGZ-SO4 formation
 The effect of TGZ metabolism on TGZ-SO4 formation over time was predicted. TGZ dose-dependently increased TGZ-SO4 formation significantly from 500 minutes to 3500 minutes (A). In line with *in vitro* studies between the time courses of forming the major metabolite TGZ-SO4 by Meechan *et al.*, TGZ was metabolised into TGZ-SO4 (B).

5.1.12 Mitochondrial complex inhibition and hepatic injury

Inhibition of any of the complexes of the mitochondria (I, II, III, IV, or V) could result in hepatic injury. For example, inhibiting the mitochondrial complexes that make up the OXPHOS will disrupt the OXPHOS (Bergman & Ben-Shachar, 2016). OXPHOS disturbance by the mitochondria can befall lower or no generation of ATP. In principle, OXPHOS perturbation and complex repression can lead to the accumulation of free electrons and, as such, will lead to ROS production, which can trigger injury to the mitochondria (Bergman & Ben-Shachar, 2016). When a certain level is reached, the mitochondria can no longer deal with stress-induced damage and will initiate cell death processes (apoptosis and necrosis depending on ATP availability), as described in the introduction chapter. Death gradually progresses to necrotic tissue and finally to hepatic damage. Hence, the effects of TGZ on MRCs complex V and ATP levels were predicted. Between 0 and 95 minutes, the various concentrations of TGZ (5 μM to 50 μM) would cause inhibition of complex V (Figure 5-16A), and this is in line with previous *in vitro* studies by Nadanaciva *et al.* TGZ did inhibit complex II-V (Figure 5-16B). However, at 95 minutes, the various concentrations (5 μM to 50 μM) of TGZ caused 28%, 44%, 60%, 70%, and 80%, respectively. The level of inhibition remained constant between 95 and 3500 minutes.

Also, the level of ATP between 115 and 325 at 50 μM TGZ was predicted to be 25%. Whereas between 325 and 345 minutes, the level of ATP dropped to 0% at 40 μM TGZ. At 40 μM TGZ concentration, the level of ATP between 115 and 325 was 40% and dropped to 25% between 325 and 445 minutes. At 500 minutes, the level of ATP at 40 μM TGZ dropped to 0%. Both 20 μM and 30 μM TGZ concentrations produced similar ATP levels between 0 and 174 minutes, which was 40% and dropped to 25% between 500 and 3500 minutes. A 60% ATP level at 10 μM between 0 and 174 minutes was recorded. Between 445 and 3500 minutes, there was a 44% reduction in ATP and a further 25% reduction between 445 and 3500 minutes. However, at 5 μM TGZ, the level of ATP was 80% between 0 and 174 minutes but dropped to 60% between 174 and 445 minutes (Figure 5-16C), as predicted.



5.1.13 Effect of TGZ on cell number

Having predicted that TGZ is a specific ligand of PPAR γ , the nuclear receptor that regulates cells' growth and differentiation at the transcriptional level. An effort was

made to determine the effect of TGZ on cell number through *in sillico* approach. Cell number or growth at TGZ concentrations of 5 μM 30 μM and 50 μM were explored. The initial cell numbers of the control (cells exposed only to the culture media) and the various TGZ concentrations were 100 cells. However, at 500 minutes, the cell numbers were 118 for both the control and 5 μM TGZ concentrations, whereas the number of cells at 30 μM and 50 μM TGZ concentrations was predicted at 114. At 1000 minutes, the predictions for the number of cells under the control condition and 5 μM TGZ concentration were 140 and 141, respectively. The number of cells at 1500 minutes for the control and the 5 μM TGZ were 168 and 143 for the 30 μM TGZ and 50 μM TGZ concentrations, respectively. 202 cells at the control condition, 200 cells under 5 μM TGZ, and 168 cells for both 30 μM TGZ and 50 μM TGZ concentrations have been predicted (Figure5-17).

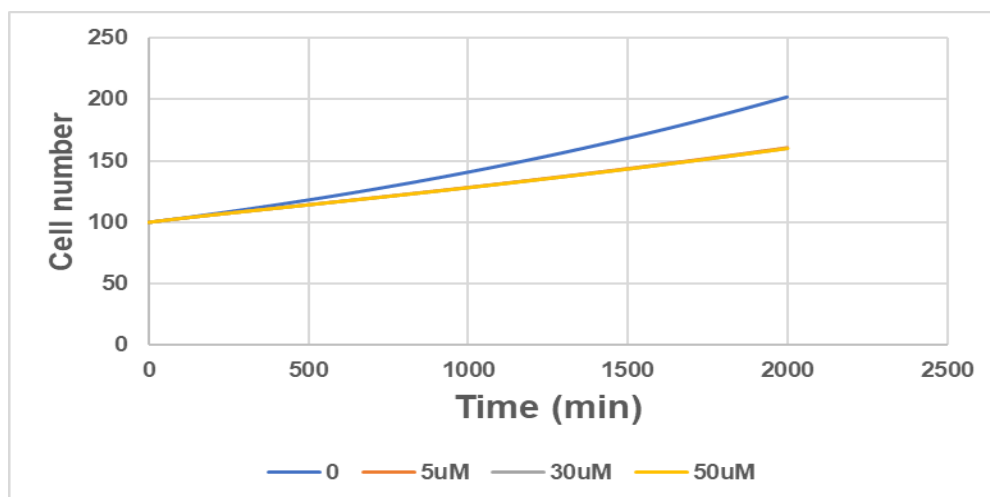


Figure 5-17 Model simulation output on the effect of TGZ on cell number

The effect of TGZ on cell number over time was predicted. Cells under the various conditions increased. However, cells under control and the 5 μM TGZ were predicted to increase significantly, whereas cells under 30 and 50 increased; however, these were 84 % less than the control and the 5 μM TGZ concentration.

5.2 Discussion

In silico models provide a systematic basis for knowing the underlying biological means that combine several biological experiments (Sakkalis *et al.*, 2014). New experiments can be planned by predicting the system's behaviour. In this way, the validation of computational modelling is an iterative process of improvement (Plant, 2015), which ends when an accurate, biologically feasible, and specific explanation of the system is found.

The TGZ-induced liver toxicity pathways were represented in the Petri net, for instance, TGZ-induced apoptosis (Figure 5-3), TGZ-induced PXR activation and its target genes (Figure 5-4), and TGZ-induced cholesterol signalling (Figure 5-5). As the method defines the dynamics of individual reactions and emphasises a discrete system-oriented approach, a mode of presentation for modelling metabolic pathways has been identified. Petri nets' simulation of biochemical processes is attractive because it is simple to execute, visually accessible and manipulative (Genrich *et al.*, 2001).

A qualitative study of a Petri net representation of a pathway will include comparing Petri net models with the properties identified earlier. This will be formally carried out by effectively replicating one Petri net onto another to maintain the maximum number of relationships between position and transformation. For instance, each part (a biological component of one pathway) corresponds perfectly to one element in the other pathway. Through a simple relationship of their architectures, an analysis of the differences in the properties of two Petri networks and the connection of these to structural differences (i.e., biological components and transformations) of the metabolic pathways described by the Petri nets in this study can be determined. In principle, the impact it has on the Petri nets' properties, could determine the position of each distinction in the biological structure. The properties of a Petri net pathway often provide useful information on the appropriate application method; for instance, the impact of TGZ-induced apoptosis through the Bcl-2 pathways was presented (Figure 5-3). In this study, Bcl-2 proteins provoke the function of the pro-apoptotic Bcl-2 proteins in that the circles represent molecular species, each surrounded by a circle, representing the possible states of TGZ-Bcl-2 interaction. And the rectangle

represents the transition reaction, which also means the events or actions that alter the condition. A transition reaction is an activity or event that describes activities or events that change the state, and the arch was used to connect a place with a transition and vice versa. This means that an investigation of a continuously operating Petri net of a metabolic pathway could produce a collection of transformations (reactions) and/or markings (essential biological components) that eventually result in such behaviour. To either improve or terminate this system's behaviour, an acceptable modification of only specific reactions or features is required (Sakkalis *et al.*, 2014).

In this current study, the effect of TGZ-induced apoptosis via the various probable pathways discussed in the previous sections has been explored. TGZ-JNK forms part of a non-metabolic pathway of TGZ-induced apoptosis. Based on *in vitro* data generated (Figures 3-4, 3-5, and 3-6), the effect of TGZ and apoptosis through other pathways such as caspases. Through the simulation of the model, it has been demonstrated that TGZ can activate JNK, which in turn may result in apoptosis. Consistent with recent work by Albeck *et al.*, JNK activation caused apoptosis through the activation of tumour necrosis factor, resulting in Bid's cleavage to produce a truncated Bid (tBid) (Figures 5-7A-D and 5-7A1-D1). tBid may translocate to the mitochondria and consequently induce the oligomerisation of Bax or Bak (apoptotic proteins), causing the release of cytochrome c, which is considered the commitment stage of apoptosis in many cells (Chai *et al.*, 2001; Chao, 2015; Denecker *et al.*, 2008; Dhanasekaran & Reddy, 2008; Houston, 2004; Riedl *et al.*, 2001; Uehara *et al.*, 2005).

As recorded in our *in vitro* data (Figure 3-2), TGZ decreased Huh7 cell viability, which might be due to apoptosis. It was proposed that TGZ-induced apoptosis could be activated via two main molecular pathways. For example, procaspase-8 recruitment promotes the formation of the death-inducing signalling complex (DISC) and mediates receptor-induced apoptosis (Lee, 2012). However, caspase-3 is a critical protease triggered by death signals to hydrolyse several important specific substrates (Almasan & Ashkenazi, 2003; Ghobrial *et al.*, 2005; Tsujimoto, 2003). Bcl-2, Bcl-xL, and Bcl-W are anti-apoptotic molecules that can be elevated in many tumours (Hunter *et al.*, 2007). Bax, Bak, and Bad, known as Bcl-2 family cell-death

mediators, promote apoptosis by external stimuli (Hunter *et al.*, 2007). Per our model prediction, an anti-apoptotic protein, Bcl-2, was downregulated by TGZ (Figure 5-8A). In our *in vitro* data (Figures 3-4 and 3-5), Apaf-1, a cell-death effector, acts as a downstream of Bcl-2 but upstream of caspase-3 (Liu, 2004; Ming, 2006) to stimulate caspase-3/7, leading to apoptosis as recorded in our *in vitro* data (Figures 3-4 and 3-5). A probable mechanism to explain our *in vitro* prediction might be as a result of TGZ-JNK activation. TGZ-JNK forms part of a non-metabolic pathway of TGZ-induced apoptosis. It has been demonstrated through the simulation of the model that TGZ may activate JNK, resulting in cell death or apoptosis. JNK's multiple signalling inputs support the extrinsic apoptotic pathway. Letai *et al.* have reported that during UV-induced apoptosis of HEK293 T cells, JNK's Bim and Bmf phosphorylation discharged them from the sequestering dynein and myosin V motor complexes. When released, Bim and Bmf will activate Bax or Bak to induce apoptosis (Donavan *et al.*, 2002; Letai *et al.*, 2002; Puthalakath & Strasser, 2002).

Also, PPAR γ activation may lead to transcription factors regulating cell differentiation and growth. The PPAR γ occupancy level predicted for TGZ was high, even at 5 μ M at 92%, whereas at 50 μ M, the occupancy level was predicted at 99%. However, in *in vitro* or *in vivo* studies, the receptor occupancy studies depend on the experimental setting; for instance, TGZ acts as a partial agonist for PPAR γ in the transfected muscle (C2C12) and kidney (HEK 293T) cells, producing a submaximal transcriptional response (Gautier *et al.*, 2012; Hanefeld *et al.*, 2011).

The researchers further reported that TGZ antagonised rosiglitazone stimulated PPAR γ transcriptional activity (Gautier *et al.*, 2012; Hanefeld *et al.*, 2011). The researchers also studied the mechanism whereby this induction occurs by specifically addressing whether potentiation of the transactivation function of PPAR γ leads to gene expression. TZDs, had differential effects, with TGZ inducing protein levels of PPAR γ , while the other TZDs, such as rosiglitazone, englitazone, and ciglitazone, produced no effect (Gautier *et al.*, 2012; Hanefeld *et al.*, 2011). They also reported that TGZ acted in adipocytes as a full PPAR γ agonist and demonstrated that TGZ and rosiglitazone control different but interacting genes in several cell types. Their finding was consistent with this current study's model prediction output, where TGZ exhibited high PPAR γ occupancy levels. However,

they stated that TGZ might act as a partial agonist under physiological conditions and, in others, as a full agonist. Such disparities can arise from variations in the number of cofactors, discrepancies in PPAR response elements, or the existence of different PPARy isoforms (Gautier *et al.*, 2012; Hanefeld *et al.*, 2011). However, further investigation of these other pathways could not be demonstrated in the current *in silico* studies. However, further exploration would provide an added advantage in understanding TGZ's affinity for the nuclear receptors.

Also, PPARy ligands can bind to the PPARy transcription factor and, in turn, generate a heterodimeric complex with the retinoid X receptor that functions as a central regulator of differentiation and modulator of cell growth (Ekins & Erickson, 2002; Hartley *et al.*, 2006). Other reports present evidence for the anti-tumorigenic activity of PPARy ligands (Gautier *et al.*, 2012; Hanefeld *et al.*, 2011; Masamune *et al.*, 2002; Wakino *et al.*, 2001; Yin *et al.*, 2001). Among PPARy ligands, the anti-tumorigenic activity of TGZ has been well established. For example, TGZ significantly inhibited the tumour proliferation of colorectal cancer cells (HCT-116), breast cancer cells (MCF-7) and prostate cancer cells (PC-3) in immunodeficient mice (Masamune *et al.*, 2002; Yin *et al.*, 2001). TGZ has specific functions, also as a PPARy agonist. For example, Hattori *et al.* reported that TGZ upregulates nitric oxide synthesis, whereas Okura *et al.* reported that TGZ induces the p53 pathway and inhibits cholesterol biosynthesis. Takeda *et al.* have also demonstrated that TGZ activates extracellular signal-regulated protein kinase (ERK) in a PPARy-independent manner.

For instance, TGZ, has been shown to bind and activate the PPARy receptor (Hartley *et al.*, 2006). Therefore, these insulin sensitisers are suggested to exert their anti-diabetic effects through PPARy activation (Ekins & Erickson, 2002; Hartley *et al.*, 2006). and supports our model's prediction recorded in this current study (Figure 5-6).

Interestingly, TGZ does not only activate PPARy, but it is also a PXR typical agonist and can induce CYP3A4 transcription through PXR-mediation (Ekins & Erickson, 2002; Hartley *et al.*, 2006). In line with the *in silico* data produced in this current study, TGZ-induced PXR activation can, therefore, be an underlying mechanism for

its liver toxicity. Our studies did predict that TGZ binds PXR even at 5 μM ; prediction of PXR occupancy of 84%, whereas the highest dose of 50 μM TGZ caused occupancy of PXR by 98%, an indication of TGZ being PXR activator. The activation of PXR thus improves the APAP-induced liver injury induction of CYP3A isoforms.

On the other hand, it also aids in the detoxification of APAP overdose by induction of phase II enzymes and transporters (Hinson, 2013). PXR activation can induce DILI by increasing the expression of enzymes metabolising drugs such as Phase I and Phase II. PXR can, therefore, facilitate drug bioactivation to form reactive metabolites. It may also cause a decrease in glucose cell use and an increase in lipid production and fatty acid uptake in the liver while decreasing fatty acid - oxidation, which can lead to lipid build-up and steatosis (He *et al.*, 2013; Hinson *et al.*, 2009; Zhang *et al.*, 2001). Based on our model prediction, it can therefore be suggested that TGZ might cause liver toxicity through the activation of PXR.

Also, a dose and time-dependent induction of CYP3A4 by TGZ (5-13), which was validated by our *in vitro* study on CYP3A4 induction by TGZ in Huh7 cells, had been predicted (Figure 4-7). In line with these current study results, other studies have also reported the fold induction of CYP3A4 by TGZ (Fahmi *et al.*, 2008). Consistent with *in vivo* studies, TGZ induced CYP3A4 activity in healthy subjects (Dimaraki & Jaffe, 2003). However, after normalisation with the fold-induction values of positive control agents, TGZ could be predicted within two limited errors in the induction of CYP3A4 in different loads of cryopreserved primary liver cells. Therefore, our model could be used to estimate the induction potency of P450 independently of liver cells. CYP is a primary source of variability in drug bioavailability and reactions (Zanger & Schwab, 2013). Each CYP's expression is affected by endogenous and exogenous factors such as diet or drug exposure (Kuramoto *et al.*, 2019; Sahi *et al.*, 2003).

Although the predictive models for CYP3A4 induction developed in this study fall into the category of just a few physiochemical variables established by several commercially produced software, our model allows us to predict TGZ as the potent inducer of CYP3A4.

Having predicted high PPAR γ affinity by TGZ, the effect of TGZ on glucose homeostasis by the liver was explored. In this study, glucose formation prediction at

the various concentrations of TGZ at 100 minutes was negligible. However, as time progressed, a gradual increase in glucose formation owing to the different concentrations of TGZ was predicted. Glucose production remained steady from 3000 minutes to 3500 minutes. However, our observation leads to the suggestion that glucose formation and fluxes in the presence of insulin or insulin sensitisers are dependent on time. For instance, in this current study, TGZ has been predicted to promote hepatic glucose formation, although its main activity is the stimulation of peripheral glucose utilisation. The liver plays an essential role in the metabolism of whole-body glucose through equilibrium between glucose production and glucose conservation in glycogen. About 80% of the output of endogenous glucose is by the liver and the rest is by the kidney (Alsahli *et al.*, 2017). In humans, the liver and the gut provide 25% of glucose utilisation under fasting conditions and 35% for oral glucose ingestion (Coate *et al.*, 2012; Kruszynska *et al.*, 2004).

Higher insulin levels stimulate insulin signalling cascades in the liver that inhibit glycogen breakdown and promote the storage of glycogen and lipogenesis (Coate *et al.*, 2012; Kruszynska *et al.*, 2004). However, blood FFA represses glucose absorption into the skeletal muscles (glucose fatty-acid cycle) and enhances glucose production by the liver (Costa *et al.*, 2010). PPAR γ is also an essential nuclear factor that promotes the differentiation of adipocytes (Downes *et al.*, 2007; Stiles *et al.*, 2004). TGZ-induced reduction in plasma glucose may affect adipose tissue and other tissues, such as the muscle in which PPAR γ agonists are upregulated (Costa *et al.*, 2010). However, in this current study, we only explored the effects of TGZ on glucose homeostasis. A further *in silico* prediction on this mechanism may improve our understanding of TGZ's impact on glucose homeostasis.

A dose and time-dependent increase in PTEN expression was predicted and is in line with *in vitro* data by Yoon *et al.* who reported that TGZ dose-dependently caused an increase in PTEN expression (Downes *et al.*, 2007; Stiles *et al.*, 2004).

Interestingly, Chen *et al.* reported that TNF failed to activate NF- κ B in cells exposed to ethanol. Still, when they decreased the levels of PTEN, they recorded a restored TNF-dependent NF- κ B stimulation. They further suggested that the levels of PTEN might be an essential mechanism by which ethanol blocks the defensive mechanisms in TNF-activated cells. In agreement with previous studies (hepatocytes

(Chen *et al.*, 2019; Mayo *et al.*, 2002; Puc *et al.*, 2005; Suzuki *et al.*, 2001; Tafani *et al.*, 2002). It could therefore be suggested that TGZ might cause liver toxicity through the elevation of PTEN in hepatocytes (Chen *et al.*, 2019; Mayo *et al.*, 2002; Puc *et al.*, 2005; Suzuki *et al.*, 2001; Tafani *et al.*, 2002).

An increase in PTEN levels would reduce PIP3 and inhibit receptor-activated activity (Abdulkareem & Blair, 2013; Pastorino *et al.*, 2003; Shi *et al.*, 2014; Worby & Dixon, 2014). These *in vitro* findings might also be linked to our model prediction of TGZ-induced PTEN expression. The model simulation output of TGZ on PTEN was increased levels of PTEN in a concentration and time-dependent manner. And to confirm if these reports were the result of a direct effect of TGZ on PTEN expression, Lee *et al.* explored the effects of TGZ on casein kinase 2 (CK2), a potent negative regulator of PTEN activity, and reported that TGZ dose-dependently repressed serum-induced proliferation of HUVEC.

In contrast, the phosphorylation of PTEN was declined with TGZ pretreatment, and this, according to Lee *et al.*, was indirectly related to CK2 activity. Furthermore, when they treated cells with a CK2 inhibitor, they recorded effects related to that of TGZ on Akt and its downstream signalling molecules. Lee *et al.* therefore suggested that TGZ inhibited the growth of HUVECs through the suppression of CK2 activity, making PTEN constantly stimulated. Consistent with other studies, the role of TGZ in the control of PTEN expression and cell death of PSMCs under hypoxic conditions was conducted by Pi *et al.*, who reported that cells treated with TGZ dose-dependently affected the growth rate of PSMCs. However, they recorded a substantial decrease in cell growth rate at TGZ concentrations above 20 μM under hypoxic conditions (Han *et al.*, 2003; Stambolic *et al.*, 2001). Therefore, this might lead to suggestions that TGZ causes cell death in hepatocytes by inhibiting the protective mechanisms pathways of the liver as a result of generating high levels of PTEN, and we can conclude that our model produces the known biology of the effects of TGZ on PTEN expression.

The *in silico* data on the doubling time of cell number matches that shown *in vitro* for the cells exposed to growth media. On the other hand, cells exposed to xenobiotics such as TGZ above 5 μM may decrease cell growth and reduce cell number, as

these compounds may kill all or about half of the cell population. and agrees with our *in vitro* studies.

A critical model in biological studies is the assessment of cells' responses to molecular disturbances. All such disturbances commonly control gene disruption or drug industry involvement to influence protein abundance or interaction. Reactions to such disturbances are also evaluated in cells relating to *in vitro* conditions on the basis that the predicted phenotypes might result in incomparable *in vivo* phenotypes (Maman & Witz, 2018). For instance, matrix structure, expressivity, and rigidity may influence cancer development (Paszek *et al.*, 2005). As a result, it is unclear how the effects of drug disruption on 2D assays might translate into more refined laboratory tests, which should reflect a much more complete *in vivo* microenvironment. Moreover, these sophisticated tests are deemed costly (Santo *et al.*, 2016; Wells, 2008). Generally, the analysis of parameters validates the significant effect of proliferation reported in Huh7 cell doubling time and highlights additional factors that could play an essential role in the growth of Huh7 cells.

Chapter 6 General discussion

Improvements in drug discovery over the past few decades have triggered a tremendous growth in available experimental data. Generating novel or insightful postulations from this enormous data is a significant challenge. The use of reliable predictive *in silico* models validated with experimental data is a field concerning both toxicity researchers and drug developers. To explore the prediction of TGZ-induced hepatotoxicity, *in vitro* data based on a literature review was used to construct the model. Computational modelling can be used to meet this challenge by providing a deeper understanding of the applicable events based on their fundamental mechanisms. Model simulations can help investigate a complete biological procedure as a replacement for the use of animals, direct future experiments, and predict a system's behaviour under given conditions. For instance, the successful creation of a Petri net representation of the possible TGZ-induced hepatotoxicity pathways has been demonstrated. In this case, future experiments could be efficiently executed by exploring the pathways demonstrated in the *in silico* data. This would also save researchers time and money by merely studying the predictive pathways of the model. Previously, a scientist had to conduct "try and error" experiments to come up with a possible underlying mechanism in a scientific puzzle before coming up with a solution to this puzzle. However, systems biology has provided a very predictable direction with computational modelling applied to many of the most significant biological objectives as it has the potential to scan vast databases and easily recommend evaluating molecules. There is a closer interaction between computational and *in vitro* systems. For instance, in this current study, our model predictions match our *in vitro* and other *in vitro* studies reported by previous researchers. Based on these comparisons, it can be stated that our model produces the known biology. However, the model could only be compared with *in vitro* studies and not *in vivo* studies because the basic idea of these studies was to test whether computational analyses could be used to predict TGZ-induced liver toxicity and validate it with *in vitro* data, as in the case of other studies that employ basic methods to understand a biological question before extrapolating it to *in vivo* studies. Furthermore, biological processes are nonlinear mechanisms that could lead to significant changes in system activity.

To the best of my knowledge, no computer programme entirely models the dynamics of biological systems, so this supports the assertion in the previous chapter that “we model what we can model”. Finally, computational biology will most probably become more complex and will probably demand some level of model integration. To have a much larger impact, *in silico* study methods must be incorporated into modern drug discovery studies, although training in modelling and informatics is required.

Current computational models have been developed using two methods. One is a related model using statistical algorithms that relate molecular descriptors to endpoints of toxicity without providing a mechanistic insight. A mechanistic model is a second approach related to our model, explaining the underlying toxicity mechanism (Venkatapathy & Wang, 2012). Statistical algorithms can produce mechanistic models, or computational biologists can develop them (Venkatapathy & Wang, 2012). Yet, models that cannot be interpreted mechanistically are still valuable if they make accurate predictions, which generally happens when they are correctly constructed from extensive datasets (Devillers, 2012). Models will usually justify user standards. If users expect models that provide mechanistic insight into toxicity, developers will aim to satisfy these requirements. Systems biology has continued to advance with the implementation of new methods and the improvement of existing tools. A perfect system for one toxicity endpoint or chemical, on the other hand, cannot be useful for another. If properly used, the toxicity of chemical substances via the *in silico* approach can be very efficient. However, it is crucial to recognise the strengths, weaknesses, applicability and understanding of the methods *in silico* models. To create a good model, the most appropriate method for the given problem must be selected, and the techniques for each condition must be adjusted when appropriate (Pletz *et al.*, 2018; Venkatapathy & Wang, 2012).

One of the leading methods in systems biology is the human hepatocyte model. An extended version of our QSSPN framework is used to incorporate a human GSMN, a robust kinetic model. However, *in vitro* laboratories demonstrate how systems biologists can use the MUFINS interface in the algorithmic stage of model development, making predictions, empirical confirmation, and model refinement. These have been shown with the model, which makes it an ideal system for this

current study. Also, MUFINS incorporates the constraint-based multi-formalism approach under an integrated network visualisation GUI. MUFINS is useful for creating and simulating multi-formalism models by a broad range of users, particularly systems biologists with limited experience in algorithmic frameworks and mathematical modelling settings.

In this current study, the objective was to determine the usefulness of *in silico* studies to predict potential TGZ toxicity pathways. Petri net, SurreyFBA, and MUFINS have been successfully used to model and predict the concurrent metabolic and non-metabolic pathways that might contribute to TGZ-induced hepatotoxicity. In this study, TGZ-induced BSEP inhibition and bile acid accumulation have been predicted, which correlates with other previous *in silico* studies and has been validated by *in vitro* studies (Notenboom *et al.*, 2016; Toroz *et al.*, 2019). Bile acids are essential endogenous molecules involved in the digestion and absorption of fats and the regulation of lipid and glucose homeostasis (Hofmann, 2008; Nguyen & Bouscarel, 2008). However, bile acids can exert toxic effects at above physiological levels through disruption of mitochondrial ATP synthesis, necrosis, and apoptosis. Previous *in vitro* and our *in vitro* data are correct with the prediction of TGZ-induced ATP production by our model. Thus, defects in excretion may lead to hepatic accumulation of bile acids and subsequent hepatotoxicity (Maillette de Buy Wenniger & Beuers, 2010; Perez & Briz, 2009). It can be concluded that BSEP inhibition, reported by other previous studies (Maillette de Buy Wenniger & Beuers, 2010; Perez & Briz, 2009), is one of the leading pathways involved in TGZ-induced liver toxicity. Based on literature reviews, TGZ causes hepatic injury through various pathways, which are in line with our data generated in this current study (Bradley, 2002; Bova *et al.*, 2005; Chojkier, 2005), and match our *in silico* predictions.

Most importantly, TGZ-induced apoptosis has been successfully modelled and predicted (i.e., our system works). In this case, the *in silico* system used is appropriate to explore TGZ-induced hepatotoxicity. Also, TGZ-induced sulphate, quinone formation, TGZ-induced PTEN levels predictions have been made, TGZ-induced glucose formation, prediction of TGZ cell population and cholesterol levels.

6.1 Future Work

The data produced in the current study has demonstrated the metabolic and non-metabolic effects of TGZ toxicity. These data promote further investigation of the mechanistic insights that further explain the results recorded in this study.

However, drug developers introduced screening mechanisms for chemically reactive metabolites at the early stage of drug development after reporting TGZ-induced liver toxicity (Ikeda, 2001). They considered the amount of covalent binding to proteins in *in vitro* systems to determine the physiological dose. In this case, an *in silico* model can be used to create many simulations from a "virtual population" where there are small modifications to each parameter. This would allow us to predict susceptible subjects to DILI.

By comparing the *in vitro* experiments with the *in silico* predictions, it was observed that although the proliferation rate is critical, experimental growth curves are not adequate to explain it. However, this is just an observation for our *in silico* studies because our modelling procedure does not indicate proliferation depth, which is a drawback of our methodology that needs to be addressed in future work. Intrinsically, there is no link between the response scale and the output scale. The minor differences between provisional settings that easily result in significant performance indicators need to be addressed in the future.

Time course analysis is popular during a triggered biological process, such as a cellular response to a stimulus or treatment, because the expression data, which is inexpensive to measure, can provide a vivid interpretation of the changes in cellular states over time (Duren *et al.*, 2020) In this study, we found that TGZ caused about 90% of cell death in cells exposed to TGZ concentration at 50 μM for 24 hrs and even about 98% of death in cells exposed to TGZ at 50 μM for 48 hrs. Technically, it would be expected that a complete cell death in cells exposed to 50 μM TGZ for 48 hrs would release minimal cellular contents. On the other hand, live cells would release their cellular contents in response to stimuli, but this was not the case in some of the data recorded in this study (chapter 4). It would be prudent to conduct time-course experiments to determine whether cells exposed to TGZ release their cellular contents at a certain time before death.

The use of the Huh7 cell line is one of the principal limitations of this study. While the cell line has similar features to primary hepatocytes (Choi *et al.*, 2009; Krelle *et al.*, 2013), drug metabolising enzymes are not articulated at the same levels as those seen *in vivo*. They cannot respond to xenobiotics or drugs in a comparable pattern, unlike primary cells. Extending this study to primary liver cell models will allow future studies to overcome the limitations encountered in this current study.

Considering that cytoprotective effects and inhibition of ROS production by vitamin C have been recorded during the study, it could be postulated that combining antioxidants with TGZ would protect against TGZ-induced hepatotoxicity; extending this study *in vivo* would allow future researchers to better understand TGZ-induced hepatotoxicity.

Another means by which drugs can induce an adverse reaction is an idiosyncratic response to the drug, for instance, TGZ. However, researchers find it challenging to study idiosyncratic drug reactions because of the scarcity of suitable animal models and erratic quality. Consequently, much of our mechanistic understanding of idiosyncratic drug reactions is determined by extrapolations from clinical characteristics instead of regulated mechanistic analyses. Therefore, we can extend this study by creating TGZ-induced immune responses and adverse outcome pathways by *in silico* studies in the future to overcome the difficulties in animal studies.

6.2 Conclusion

To the best of my knowledge and the understanding gained through this research, the above predictions made by the research model are novel. Therefore, it can be concluded that a combination of *in vitro* and *in silico* approaches can be used to explore liver cells' complex behaviour in response to TGZ exposure: the emergent biological response, identifying which biological processes are causative and which are consequential of toxicity.

Chapter 7 References

Abasht, B., Mutryn, M. F., Michalek, R. D., & Lee, W. R. (2016). Oxidative stress and metabolic perturbations in wooden breast disorder in chickens. *PLOS ONE*, 11(4), e0153750.

Abdulkareem, I., & Blair, M. (2013). Phosphatase and tensin homologue deleted on chromosome 10. *Nigerian Medical Journal*, 54(2), 79.

Abete, P., Calabrese, E. J., Ji, L. L., Kristensen, T. N., Le Bourg, E., Loeschcke, V., Vaiserman, A. M. (2008). Mild Stress and Healthy Aging: Perspectives for Human Beings. *Mild Stress and Healthy Aging*, 171-183.

Acharya, A., & Garg, L. C. (2016). Drug target identification and prioritization for treatment of ovine foot rot: An *In Silico* Approach. *International Journal of Genomics*, 2016, 1-8.

Adams, D. H., & Eksteen, B. (2006). Aberrant homing of mucosal T cells and extra-intestinal manifestations of inflammatory bowel disease. *Nature Reviews Immunology*, 6(3), 244-251.

Adams, L. A. (2005). Nonalcoholic fatty liver disease. *Canadian Medical Association Journal*, 172(7), 899-905.

Adeva, M. M., Souto, G., Blanco, N., & Donapetry, C. (2012). Ammonium metabolism in humans. *Metabolism*, 61(11), 1495-1511.

Adiels, M., Packard, C., Caslake, M. J., Stewart, P., Soro, A., Westerbacka, J., Borén, J. (2004). A new combined multicompartamental model for apolipoprotein B-100 and triglyceride metabolism in VLDL subfractions. *Journal of Lipid Research*, 46(1), 58-67.

Agledal, L., Niere, M., & Ziegler, M. (2010). The phosphate makes a difference: Cellular functions of NADP. *Redox Report*, 15(1), 2-10.

Agoram, B. M. (2009). Use of pharmacokinetic/ pharmacodynamic modelling for starting dose selection in first-in-human trials of high-risk biologics. *British Journal of Clinical Pharmacology*, 67(2), 153-160.

Ahsan W. (2019). The Journey of Thiazolidinediones as Modulators of PPARs for the Management of Diabetes: A Current Perspective. *Current pharmaceutical design*, 25(23), 2540–2554.

Aithal, G. P. (2015). Pharmacogenetic testing in idiosyncratic drug-induced liver injury: current role in clinical practice. *Liver International*, 35(7), 1801-1808.

Aithal, G. P. (2019). Drug-induced liver injury. *Medicine*, 47(11), 734-739.

Aithal, G. P., & Daly, A. K. (2010). Preempting and preventing drug-induced liver injury. *Nature Genetics*, 42(8), 650-651.

Aithal, G. P., Ramsay, L., Daly, A. K., Sonchit, N., Leathart, J. B., Alexander, G., Kenna, J. G., Caldwell, J., & Day, C. P. (2004). Hepatic adducts, circulating antibodies, and cytokine polymorphisms in patients with diclofenac hepatotoxicity. *Hepatology*, 39(5), 1430-1440.

Akasaki, Y., Liu, G., Matundan, H. H., Ng, H., Yuan, X., Zeng, Z., Yu, J. S. (2005). A Peroxisome Proliferator-activated Receptor- γ Agonist, Troglitazone, Facilitates Caspase-8 and -9 Activities by Increasing the Enzymatic Activity of Protein-tyrosine Phosphatase-1B on Human Glioma Cells. *Journal of Biological Chemistry*, 281(10), 6165-6174.

Akinyeke, T. O., & Stewart, L. V. (2011). Troglitazone suppresses C-MyC levels in human prostate cancer cells via a PPAR γ -independent mechanism. *Cancer Biology & Therapy*, 11(12), 1046-1058.

Albeck, J. G., Burke, J. M., Aldridge, B. B., Zhang, M., Lauffenburger, D. A., & Sorger, P. K. (2008). Quantitative Analysis of Pathways Controlling Extrinsic Apoptosis in Single Cells. *Molecular Cell*, 30(1), 11-25.

Alempijevic, T., Zec, S., & Milosavljevic, T. (2017). Drug-induced liver injury: Do we know everything? *World Journal of Hepatology*, 9(10), 491.

Allard, J., Le Guillou, D., Begriche, K., & Fromenty, B. (2019). Drug-induced liver injury in obesity and nonalcoholic fatty liver disease. *Advances in Pharmacology*, 75-107.

Almasan, A., & Ashkenazi, A. (2003). Apo2L/TRAIL: apoptosis signaling, biology, and potential for cancer therapy. *Cytokine & Growth Factor Reviews*, 14(3-4), 337-348.

Alsahli, M., Shrayyef, M. Z., & Gerich, J. E. (2017). Normal glucose homeostasis. *Principles of Diabetes Mellitus*, 23-42.

Amacher, D. E. (2012). The primary role of hepatic metabolism in idiosyncratic drug-induced liver injury. *Expert Opinion on Drug Metabolism & Toxicology*, 8(3), 335-347.

Andrews, E., Armstrong, M., Tugwood, J., Swan, D., Glaves, P., Pirmohamed, M., Daly, A. K. (2010). A role for the Pregnane X receptor in flucloxacillin-induced liver injury. *Hepatology*, 51(5), 1656-1664.

Annaert, P., Brouwers, J., Bijmens, A., Lammert, F., Tack, J., & Augustijns, P. (2010). *Ex vivo* permeability experiments in excised rat intestinal tissue and *in vitro* solubility measurements in aspirated human intestinal fluids support age-dependent oral drug absorption. *European Journal of Pharmaceutical Sciences*, 39(1-3), 15-22.

Aravinthan, A. D., Fateen, W., Doyle, A. C., Venkatachalapathy, S. V., Issachar, A., Galvin, Z., Sapisochin, G., Cattral, M. S., Ghanekar, A., McGilvray, I. D., Selzner, M., Grant, D. R., Selzner, N., Lilly, L. B., Renner, E. L., & Bhat, M. (2019). The impact of Preexisting and post-transplant diabetes mellitus on outcomes following liver transplantation. *Transplantation*, 103(12), 2523-2530.

- Arndtz, K., & Hirschfield, G. M. (2016). The pathogenesis of autoimmune liver disease. *Digestive Diseases*, 34(4), 327-333.
- Aroda, V. R., & Ratner, R. E. (2012). Interventional Trials to Prevent Diabetes: Diabetes Prevention Program. *Prevention of Type 2 Diabetes*, 143-166.
- Aronoff, S. L., Berkowitz, K., Shreiner, B., & Want, L. (2004). Glucose Metabolism and Regulation: Beyond Insulin and Glucagon. *Diabetes Spectrum*, 17(3), 183-190.
- Artika, I. M. (2019). Current understanding of structure, function, and biogenesis of yeast mitochondrial ATP synthase. *Journal of Bioenergetics and Biomembranes*, 51(5), 315-328.
- Asano, T., Wakisaka, M., Yoshinari, M., Nakamura, S., Doi, Y., & Fujishima, M. (2000). Troglitazone enhances glycolysis and improves intracellular glucose metabolism in rat mesangial cells. *Metabolism*, 49(3), 308-313.
- Aslantürk, Ö. S. (2018). *In Vitro* Cytotoxicity and Cell Viability Assays: Principles, Advantages, and Disadvantages. *Genotoxicity – A Predictable Risk to Our Actual World*.
- Assanga, I. (2013). Cell growth curves for different cell lines and their relationship with biological activities. *International Journal of Biotechnology and Molecular Biology Research*, 4(4), 60-70.
- Auffray, C., Ideker, T., Galas, D. J., & Hood, L. (2011). The Hallmarks of Cancer Revisited Through Systems Biology and Network Modelling. *Cancer Systems Biology, Bioinformatics and Medicine*, 245-266.
- Azarias, G., Perreten, H., Lengacher, S., Poburko, D., Demaurex, N., Magistretti, P. J., & Chatton, J. (2011). Glutamate Transport Decreases Mitochondrial pH and Modulates Oxidative Metabolism in Astrocytes. *Journal of Neuroscience*, 31(10), 3550-3559.
- Bae, M., & Song, B. J. (2003). Critical Role of c-Jun N-Terminal Protein Kinase Activation in Troglitazone-Induced Apoptosis of Human HepG2 Hepatoma Cells. *Molecular Pharmacology*, 63(2), 401-408.
- Bai, P., Houten, S. M., Huber, A., Schreiber, V., Watanabe, M., Kiss, B., Murcia, J. M. (2007). Peroxisome Proliferator-activated Receptor (PPAR)-2 Controls Adipocyte Differentiation and Adipose Tissue Function through the Regulation of the Activity of the Retinoid X Receptor/PPAR γ Heterodimer. *Journal of Biological Chemistry*, 282(52), 37738-37746.
- Bailey, C. J. (2018). The rise and fall of troglitazone Diabetic Medicine. 17, 414-415.
- Balaban, R. S., Nemoto, S., & Finkel, T. (2005). Mitochondria, Oxidants, and Aging. *Cell*, 120(4), 483-495.
- Balls, M., & Clothier, R. (2010). A Frame Response to the European Commission Consultation on the Draft Report on Alternative (Non-animal) Methods for Cosmetics

Testing: Current Status and Future Prospects — 2010. *Alternatives to Laboratory Animals*, 38(5), 345-353.

Balti, E. V., Ngo-Nemb, M. C., Lontchi-Yimagou, E., Atogho-Tiedeu, B., Effoe, V. S., Akwo, E. A., Sobngwi, E. (2015). Association of HLA class II markers with autoantibody-negative ketosis-prone atypical diabetes compared to type 2 diabetes in a population of sub-saharan African patients. *Diabetes Research and Clinical Practice*, 107(1), 31-36.

Bandyopadhyay, G. K., Yu, J. G., Ofrecio, J., & Olefsky, J. M. (2006). Increased Malonyl-CoA levels in muscle from obese and type 2 diabetic subjects lead to decreased fatty acid oxidation and increased lipogenesis; thiazolidinedione treatment Reverses these defects. *Diabetes*, 55(8), 2277-2285.

Baran, K. (2014). Peroxisome Proliferator-Activated Receptors (PPARs). *Encyclopedia of Toxicology*, 812-814.

Baranyi, J., & Roberts, T. A. (1994). A dynamic approach to predicting bacterial growth in food. *International Journal of Food Microbiology*, 23(3-4), 277-294.

Bar-Joseph, Z., Gerber, G. K., Lee, T. I., Rinaldi, N. J., Yoo, J. Y., Robert, F., Gifford, D. K. (2003). Computational discovery of gene modules and regulatory networks. *Nature Biotechnology*, 21(11), 1337-1342.

Barton, M., Baretella, O., & Meyer, M. R. (2012). Obesity and risk of vascular disease: Importance of endothelium-dependent vasoconstriction. *British Journal of Pharmacology*, 165(3), 591-602. Pi, W., Guo, X., Su, L., & Xu, W. (2013). Troglitazone upregulates PTEN expression and induces the apoptosis of pulmonary artery smooth muscle cells under hypoxic conditions. *International Journal of Molecular Medicine*, 32(5), 1101-1109.

Beck, B., Iversen, P., & Sashegyi, A. (2014). Combining Information for Quantitative Decision-making in Drug Development. *Journal of Multi-Criteria Decision Analysis*, 21(3-4), 139-151.

Begrache, K., Massart, J., Robin, M., Borgne-Sanchez, A., & Fromenty, B. (2011). Drug-induced toxicity on mitochondria and lipid metabolism: Mechanistic diversity and deleterious consequences for the liver. *Journal of Hepatology*, 54(4), 773-794.

Belcher, G., & Matthews, D. (2000). Safety and tolerability of pioglitazone. *Experimental and Clinical Endocrinology & Diabetes*, 108(Sup. 2), 267-273.

Belfiore, A., Malaguarnera, R., Vella, V., Lawrence, M. C., Sciacca, L., Frasca, F., Vigneri, R. (2017). Insulin receptor Isoforms in physiology and disease: An updated view. *Endocrine Reviews*, 38(5), 379-431.

Belmokhtar, C. A., Hillion, J., & Ségal-Bendirdjian, E. (2001). Staurosporine induces apoptosis through both caspase-dependent and caspase-independent mechanisms. *Oncogene*, 20(26), 3354-3362.

- Benbow, S., & Gallagher, M. (2004). Brittle diabetes in the elderly. *Unstable and Brittle Diabetes*, 179-196.
- Beraud, C., Henzel, W. J., & Baeuerle, P. A. (1999). Involvement of regulatory and catalytic subunits of phosphoinositide 3-kinase in NF-kappa B activation. *Proceedings of the National Academy of Sciences*, 96(2), 429-434.
- Bergman, O., & Ben-Shachar, D. (2016). Mitochondrial oxidative phosphorylation system (OXPHOS) deficits in schizophrenia. *The Canadian Journal of Psychiatry*, 61(8), 457-469.
- Bernardi, P. (2013). The mitochondrial permeability transition pore: a mystery solved? *Frontiers in Physiology*, 4.
- Bilzer, M., Roggel, F., & Gerbes, A. L. (2006). Role of Kupffer cells in host defence and liver disease. *Liver International*, 26(10), 1175-1186.
- Birney, E. (2002). Citric acid cycle (TCA cycle). *Reactome—a curated knowledgebase of biological pathways*, 01.
- Björnsson, E. (2014). Epidemiology and Risk Factors for Idiosyncratic Drug-Induced Liver Injury. *Seminars in Liver Disease*, 34(02), 115-122.
- Björnsson, H., & Björnsson, E. (2021). Drug-induced liver injury: Pathogenesis, epidemiology, clinical features, and practical management. *European Journal of Internal Medicine*.
- Boelsterli, U. A., & Lim, P. L. (2007). Mitochondrial abnormalities—A link to idiosyncratic drug hepatotoxicity? *Toxicology and Applied Pharmacology*, 220(1), 92-107.
- Bolden, A., Bernard, L., Jones, D., Akinyeke, T., & Stewart, L. V. (2012). The PPAR Gamma Agonist Troglitazone Regulates Erk 1/2 Phosphorylation via a PPARγ-Independent, MEK-Dependent Pathway in Human Prostate Cancer Cells. *PPAR Research*, 2012, 1-9.
- Bolton, J. L., & Dunlap, T. (2016). Formation and Biological Targets of Quinones: Cytotoxic versus Cytoprotective Effects. *Chemical Research in Toxicology*, 30(1), 13-37.
- Bosl, W. J. (2007). Systems biology by the rules: hybrid intelligent systems for pathway modeling and discovery. *BMC Systems Biology*, 1(1).
- Botman, D., Tigchelaar, W., & Van Noorden, C. J. (2014). Determination of Glutamate Dehydrogenase Activity and Its Kinetics in Mouse Tissues using Metabolic Mapping (Quantitative Enzyme Histochemistry). *Journal of Histochemistry & Cytochemistry*, 62(11), 802-812.
- Bova, M. P., Tam, D., McMahon, G., & Mattson, M. N. (2005). Troglitazone induces a rapid drop of mitochondrial membrane potential in liver HepG2 cells. *Toxicology Letters*, 155(1), 41-50.

- Boysen, G., Goel, S., & Georgieva, N. (2011). Profiling the internal dose of reactive compounds and their metabolites using N-terminal valine adducts. *Toxicology Letters*, 205, S40-S41.
- Bradbury, D., Simmons, T., Slater, K., & Crouch, S. (2000). Measurement of the ADP:ATP ratio in human leukemic cell lines can be used as an indicator of cell viability, necrosis, and apoptosis. *Journal of Immunological Methods*, 240(1-2), 79-92.
- Bradley, C. (2002). The glitazones: a new treatment for type 2 diabetes mellitus. *Intensive and Critical Care Nursing*, 18(3), 189-191. Nonalcoholic Fatty Liver Disease and Hepatocellular Carcinoma. (2017).
- Bradshaw, P. (2019). Cytoplasmic and mitochondrial NADPH-coupled redox systems in the regulation of aging. *Nutrients*, 11(3), 504.
- Brenner, C., Cadiou, H., Vieira, H. L., Zamzami, N., Marzo, I., Xie, Z., Kroemer, G. (2000). Bcl-2 and Bax regulate the Channel activity of the mitochondrial adenine nucleotide translocator. *Oncogene*, 19(3), 329-336.
- Brewer, C. T., & Chen, T. (2016). PXR variants: The impact on drug metabolism and therapeutic responses. *Acta Pharmaceutica Sinica B*, 6(5), 441-449
- Bricker, D. K., Taylor, E. B., Schell, J. C., Orsak, T., Boutron, A., Chen, Y., Rutter, J. (2012). A mitochondrial pyruvate carrier required for pyruvate uptake in yeast, drosophila, and humans. *Science*, 337(6090), 96-100.
- Bridges, J. P., Schehr, A., Wang, Y., Huo, L., Besnard, V., Ikegami, M., Xu, Y. (2014). Epithelial SCAP/INSIG/SREBP Signaling Regulates Multiple Biological Processes during Perinatal Lung Maturation. *PLoS ONE*, 9(5), e91376.
- Brivet, M. (2003). Impaired mitochondrial pyruvate importation in a patient and a fetus at risk. *Molecular Genetics and Metabolism*, 78(3), 186-192.
- Brookes, P. S. (2005). Mitochondrial H⁺ leak and ROS generation: An odd couple. *Free Radical Biology and Medicine*, 38(1), 12-23.
- Brown, A. J., Sun, L., Feramisco, J. D., Brown, M. S., & Goldstein, J. L. (2002). Cholesterol Addition to ER Membranes Alters Conformation of SCAP, the SREBP Escort Protein that Regulates Cholesterol Metabolism. *Molecular Cell*, 10(2), 237-245.
- Browning, J. D., Szczepaniak, L. S., Dobbins, R., Nuremberg, P., Horton, J. D., Cohen, J. C., Hobbs, H. H. (2004). Prevalence of hepatic steatosis in an urban population in the United States: Impact of ethnicity. *Hepatology*, 40(6), 1387-1395.
- Brunmair, B., Staniek, K., Gras, F., Scharf, N., Althaym, A., Clara, R., Fornsinn, C. (2004). Thiazolidinediones, Like Metformin, Inhibit Respiratory Complex I: A Common Mechanism Contributing to Their Antidiabetic Actions? *Diabetes*, 53(4), 1052-1059.

- Bu, Z., & Callaway, D. J. (2011). Proteins MOVE! Protein dynamics and long-range allostery in cell signaling. *Protein Structure and Diseases*, 163-221.
- Budak, Y., & Akdog, M. (2011). Retinal Ganglion Cell Death. *Glaucoma – Basic and Clinical Concepts*.
- Bulutoglu, B., Rey-Bedón, C., Mert, S., Tian, L., Jang, Y., Yarmush, M. L., & Usta, O. B. (2020). A comparison of hepato-cellular *in vitro* platforms to study CYP3A4 induction. *PLOS ONE*, 15(2), e0229106.
- Byrne, J. A., Strautnieks, S. S., Mieli-Vergani, G., Higgins, C. F., Linton, K. J., & Thompson, R. J. (2002). The human bile salt export pump: Characterization of substrate specificity and identification of inhibitors. *Gastroenterology*, 123(5), 1649-1658.
- Calabrese, E. J. (2009). Hormesis: Once Marginalized, Evidence Now Supports Hormesis as the Most Fundamental Dose Response. *Hormesis*, 15-56.
- Calabrese, E. J., Bachmann, K. A., Bailer, A. J., Bolger, P. M., Borak, J., Cai, L., Mattson, M. P. (2007). Biological stress response terminology: Integrating the concepts of adaptive response and preconditioning stress within a hormetic dose–response framework. *Toxicology and Applied Pharmacology*, 222(1), 122-128.
- Cardoso, A. R., Queliconi, B. B., & Kowaltowski, A. J. (2010). Mitochondrial Reactive Oxygen Species in Myocardial Pre- and Postconditioning. *Studies on Cardiovascular Disorders*, 109-123.
- Carnahan, V., & Redinbo, M. (2005). Structure and Function of the Human Nuclear Xenobiotic Receptor PXR. *Current Drug Metabolism*, 6(4), 357-367.
- CarrÃƒ, M. T., Valle, C., Bozzo, F., & Cozzolino, M. (2015). Oxidative stress and mitochondrial damage: importance in non-SOD1 ALS. *Frontiers in Cellular Neuroscience*, 9.
- Castro, M., Wenzel, S. E., Bleecker, E. R., Pizzichini, E., Kuna, P., Busse, W. W., Raible, D. G. (2014). Benralizumab, an anti-interleukin 5 receptor α monoclonal antibody, versus placebo for uncontrolled eosinophilic asthma: a phase 2b randomised dose-ranging study. *The Lancet Respiratory Medicine*, 2(11), 879-890.
- Chai, J., Wu, Q., Shiozaki, E., Srinivasula, S. M., Alnemri, E. S., & Shi, Y. (2001). Crystal structure of a procaspase-7 zymogen. *Cell*, 107(3), 399-407.
- Chalasanani, N., & Björnsson, E. (2010). Risk Factors for Idiosyncratic Drug-Induced Liver Injury. *Gastroenterology*, 138(7), 2246-2259.
- Chan, K., Jensen, N., & O'Brien, P. J. (2008). Structure–activity relationships for thiol reactivity and rat or human hepatocyte toxicity induced by substituted-benzoquinone compounds. *Journal of Applied Toxicology*, 28(5), 608-620.

Chandra, V., Huang, P., Hamuro, Y., Raghuram, S., Wang, Y., Burris, T., & Rastinejad, F. (2008). Intact PPAR gamma – RXR alpha Nuclear Receptor Complex on DNA bound with Rosiglitazone, 9-cis Retinoic Acid and NCOA2 Peptide.

Chao, Y., Shiozaki, E. N., Srinivasula, S. M., Rigotti, D. J., Fairman, R., & Shi, Y. (2005). Engineering a Dimeric Caspase-9: A Re-evaluation of the Induced Proximity Model for Caspase Activation. *PLoS Biology*, 3(6), e183.

Charbonnel, B. (2007). Oral combination therapy with thiazolidinediones and sulfonylureas in type 2 diabetes. *International Journal of Clinical Practice*, 61, 1-2.

Charlebois, D. A., Intosalmi, J., Fraser, D., & Kærn, M. (2011). An Algorithm for the Stochastic Simulation of Gene Expression and Heterogeneous Population Dynamics. *Communications in Computational Physics*, 9(1), 89-112.

Chastre, A., Jiang, W., Desjardins, P., & Butterworth, R. F. (2010). Ammonia and proinflammatory cytokines modify expression of genes coding for astrocytic proteins implicated in brain oedema in acute liver failure. *Metabolic Brain Disease*, 25(1), 17-21.

Chaudhry, F. A. (2001). Coupled and uncoupled proton movement by amino acid transport system N. *The EMBO Journal*, 20(24), 7041-7051.

Chawla, A., Boisvert, W. A., Lee, C., Laffitte, B. A., Barak, Y., Joseph, S. B., Tontonoz, P. (2001). A PPAR γ -LXR-ABCA1 Pathway in Macrophages Is Involved in Cholesterol Efflux and Atherogenesis. *Molecular Cell*, 7(1), 161-171.

Chen, C., Kuo, L., Chang, Y., Wu, W., Goldbach, C., Ross, M. A., Qian, S. (2006). *In vivo* immune modulatory activity of hepatic stellate cells in mice. *Hepatology*, 44(5), 1171-1181.

Chen, D. (2018). The mitochondrial metabolic checkpoint, stem cell aging and rejuvenation. *Free Radical Biology and Medicine*, 120, S18.

Chen, M., Suzuki, A., Borlak, J., Andrade, R. J., & Lucena, M. I. (2015). Drug-induced liver injury: Interactions between drug properties and host factors. *Journal of Hepatology*, 63(2), 503-514.

Chen, W. W., Freinkman, E., Wang, T., Birsoy, K., & Sabatini, D. M. (2016). Absolute quantification of matrix metabolites reveals the dynamics of mitochondrial metabolism. *Cell*, 166(5), 1324-1337.e11.

Chen, Y., Zhu, D., Gao, J., Xu, Z., Tao, S., Yin, W., Zhang, C. (2019). Diminished membrane recruitment of Akt is instrumental in alcohol-associated osteopenia via the PTEN /Akt/ GSK -3 β / β -catenin axis. *The FEBS Journal*, 286(6), 1101-1119.

Chen, Z., Trotman, L. C., Shaffer, D., Lin, H., Dotan, Z. A., Niki, M., Paolo Pandolfi, P. (2005). Crucial role of p53-dependent cellular senescence in suppression of PTEN-deficient tumorigenesis. *Nature*, 436(7051), 725-730.

- Chen, Z., Vigueira, P. A., Chambers, K. T., Hall, A. M., Mitra, M. S., Qi, N., Finck, B. N. (2012). Insulin Resistance and Metabolic Derangements in Obese Mice Are Ameliorated by a Novel Peroxisome Proliferator-activated Receptor γ -sparing Thiazolidinedione. *Journal of Biological Chemistry*, 287(28), 23537-23548.
- Cheng, A. Y. (2005). Oral antihyperglycemic therapy for type 2 diabetes mellitus. *Canadian Medical Association Journal*, 172(2), 213-226.
- Chiang, J. Y. (2009). Bile acids: regulation of synthesis. *Journal of Lipid Research*, 50(10), 1955-1966.
- Chiang, J. Y. (2017). Bile acid metabolism and signaling in liver disease and therapy. *Liver Research*, 1(1), 3-9.
- Chinenov, Y., Gupte, R., & Rogatsky, I. (2013). Nuclear receptors in inflammation control: Repression by GR and beyond. *Molecular and Cellular Endocrinology*, 380(1-2), 55-64.
- Chinetti, G., Griglio, S., Antonucci, M., Torra, I. P., Delerive, P., Majd, Z., Staels, B. (1998). Activation of Proliferator-activated Receptors α and γ Induces Apoptosis of Human Monocyte-derived Macrophages. *Journal of Biological Chemistry*, 273(40), 25573-25580.
- Cho, J., Lim, H., Suh, Y., Chung, J., Hong, K., Yi, S., Shin, S. (2005). Pharmacokinetics of Rosiglitazone according to CYP2C8 genotype in Korean population. *Journal of Korean Society for Clinical Pharmacology and Therapeutics*, 13(2), 142.
- Choi, J. H., Banks, A. S., Estall, J. L., Kajimura, S., Boström, P., Laznik, D., Spiegelman, B. M. (2010). Anti-diabetic drugs inhibit obesity-linked phosphorylation of PPAR γ by Cdk5. *Nature*, 466(7305), 451-456.
- Chojkier, M. (2005). Troglitazone and liver injury: In search of answers. *Hepatology*, 41(2), 237-246.
- Ciana, P., Biserni, A., Tatangelo, L., Tiveron, C., Sciarroni, A. F., Ottobrini, L., & Maggi, A. (2007). A novel Peroxisome proliferator-activated receptor responsive element-luciferase reporter mouse reveals gender specificity of Peroxisome proliferator-activated receptor activity in liver. *Molecular Endocrinology*, 21(2), 388-400.
- Circu, M. L., & Aw, T. Y. (2010). Reactive oxygen species, cellular redox systems, and apoptosis. *Free Radical Biology and Medicine*, 48(6), 749-762.
- Clerk, L. H., Vincent, M. A., Lindner, J. R., Clark, M. G., Rattigan, S., & Barrett, E. J. (2004). The vasodilatory actions of insulin on resistance and terminal arterioles and their impact on muscle glucose uptake. *Diabetes/Metabolism Research and Reviews*, 20(1), 3-12.
- Coate, K. C., Kraft, G., Irimia, J. M., Smith, M. S., Farmer, B., Neal, D. W., Cherrington, A. D. (2012). Portal vein glucose entry triggers a coordinated cellular

response that potentiates hepatic glucose uptake and storage in normal but not high-fat/high-fructose-Fed dogs. *Diabetes*, 62(2), 392-400.

Coleman, M. D. (2010). *Human Drug Metabolism: An Introduction*. Hoboken, NJ: John Wiley & Sons

Colmers, I., Bowker, S., & Johnson, J. (2012). Thiazolidinedione use and cancer incidence in type 2 diabetes: A systematic review and meta-analysis. *Diabetes & Metabolism*, 38(6), 475-484.

Colquitt, R. B., Colquhoun, D. A., & Thiele, R. H. (2011). *In silico* modelling of physiologic systems. *Best Practice & Research Clinical Anaesthesiology*, 25(4), 499-510.

Costa, V., Gallo, M. A., Letizia, F., Aprile, M., Casamassimi, A., & Ciccodicola, A. (2010). PPAR γ : Gene expression regulation and next-generation sequencing for unsolved issues. *PPAR Research*, 2010, 1-17.

Craig, M. E., Jefferies, C., Dabelea, D., Balde, N., Seth, A., & Donaghue, K. C. (2014). Definition, epidemiology, and classification of diabetes in children and adolescents. *Paediatric Diabetes*, 15(S20), 4-17.

Crespi, C. L., Zuo, R., Li, F., Parikh, S., Cooper, K., Liu, J., Patten, C. J. (2017). Characterizations of corning® hepatocells as a novel *in vitro* tool for drug metabolism and hepatotoxicity studies. *Drug Metabolism and Pharmacokinetics*, 32(1), S106.

Cubitt, H. E., Houston, J. B., & Galetin, A. (2011). Prediction of Human Drug Clearance by Multiple Metabolic Pathways: Integration of Hepatic and Intestinal Microsomal and Cytosolic Data. *Drug Metabolism and Disposition*, 39(5), 864-873.

Cui, J. Y., & Klaassen, C. D. (2016). RNA-Seq reveals common and unique PXR- and CAR-target gene signatures in the mouse liver transcriptome. *Biochimica et Biophysica Acta (BBA) - Gene Regulatory Mechanisms*, 1859(9), 1198-1217

Cui, Y., König, J., Leier, I., Buchholz, U., & Keppler, D. (2000). Hepatic uptake of bilirubin and its conjugates by the human organic anion transporter SLC21A6. *Journal of Biological Chemistry*, 276(13), 9626-9630.

Cui, Y., Wang, Y., Liu, M., Qiu, L., Xing, P., Wang, X., Li, B. (2017). Determination of glucose deficiency-induced cell death by mitochondrial ATP generation-driven proton homeostasis. *Journal of Molecular Cell Biology*, 9(5), 395-408.

Cumming, J. G., Davis, A. M., Muresan, S., Haerberlein, M., & Chen, H. (2013). Chemical predictive modelling to improve compound quality. *Nature Reviews Drug Discovery*, 12(12), 948-962.

Cummings, B. S., Wills, L. P., & Schnellmann, R. G. (2012). Measurement of Cell Death in Mammalian Cells. *Current Protocols in Pharmacology*, 56(1), 12.8.1-12.8.24.

Dad, Z., Ismail, A., & Sarmadi, B. (2016). Ascorbic Acid: Physiology and Health Effects. *Encyclopedia of Food and Health*, 266-274.

Daisy, P., & Saipriya, K. (2012). BCL-2 Family Proteins: The Mitochondrial Apoptotic Key Regulators. *Current Cancer Therapy Reviews*, 8(2), 133-140.

Dakubo, G. D. (2010). The Role of Mitochondrial Reactive Oxygen Species in Cancer. *Mitochondrial Genetics and Cancer*, 237-256.

Daly, A. K., Donaldson, P. T., Bhatnagar, P., Shen, Y., Pe'er, I., Floratos, A., Daly, M. J., Goldstein, D. B., John, S., Nelson, M. R., Graham, J., Park, B. K., Dillon, J. F., Bernal, W., Cordell, H. J., Pirmohamed, M., Aithal, G. P., & Day, C. P. (2009). HLA-b*5701 genotype is a major determinant of drug-induced liver injury due to flucloxacillin. *Nature Genetics*, 41(7), 816-819.

D'Apolito, M., Colia, A. L., Lasalvia, M., Capozzi, V., Falcone, M. P., Pettoello-Mantovani, M., Giardino, I. (2017). Urea-induced ROS accelerate senescence in endothelial progenitor cells. *Atherosclerosis*, 263, 127-136.

D'Apolito, M., Du, X., Pisanelli, D., Pettoello-Mantovani, M., Campanozzi, A., Giacco, F., Giardino, I. (2015). Urea-induced ROS cause endothelial dysfunction in chronic renal failure. *Atherosclerosis*, 239(2), 393-400.

Dara, L., & Kaplowitz, N. (2017). Cell death in drug-induced liver injury. *Cellular Injury in Liver Diseases*, 1-35.

Davidson, E. H. (2002). A Genomic Regulatory Network for Development. *Science*, 295(5560), 1669-1678.

Davies, C., & Tournier, C. (2012). Exploring the function of the JNK (c-Jun N-terminal kinase) signalling pathway in physiological and pathological processes to design novel therapeutic strategies. *Biochemical. Society. Transactions*, 40(1), 85-89.

Davis, J. W., & Kramer, J. A. (2006). Genomic-based biomarkers of drug-induced nephrotoxicity. *Expert Opinion on Drug Metabolism & Toxicology*, 2(1), 95-101.

Dawson, S., Stahl, S., Paul, N., Barber, J., & Kenna, J. G. (2011). *In Vitro* Inhibition of the Bile Salt Export Pump Correlates with Risk of Cholestatic Drug-Induced Liver Injury in Humans. *Drug Metabolism and Disposition*, 40(1), 130-138.

De Meyts, P. (2008). The insulin receptor: A prototype for dimeric, allosteric membrane receptors? *Trends in Biochemical Sciences*, 33(8), 376-384.

DeBerardinis, R. J., Mancuso, A., Daikhin, E., Nissim, I., Yudkoff, M., Wehrli, S., & Thompson, C. B. (2007). Beyond aerobic glycolysis: Transformed cells can engage in glutamine metabolism that exceeds the requirement for protein and nucleotide synthesis. *Proceedings of the National Academy of Sciences*, 104(49), 19345-19350.

- DeFronzo, R. A., & Abdul-Ghani, M. A. (2011). Preservation of β -cell function: The key to diabetes prevention. *The Journal of Clinical Endocrinology & Metabolism*, 96(8), 2354-2366.
- DeFronzo, R. A., Mandarino, L., & Ferrannini, E. (2003). *Metabolic and Molecular Pathogenesis of Type 2 Diabetes Mellitus*. International Textbook of Diabetes Mellitus.
- Del Prato, S. (2009). Role of glucotoxicity and lipotoxicity in the pathophysiology of Type 2 diabetes mellitus and emerging treatment strategies. *Diabetic Medicine*, 26(12), 1185-1192.
- DeLeve, L. D. (2013). Liver sinusoidal endothelial cells and liver injury. *Drug-Induced Liver Disease*, 135-146.
- Demirovic, D., De Toda, I., & Rattan, S. (2014). Molecular stress response pathways as the basis of Hormesis. *Oxidative Stress and Disease*, 225-240.
- Denecker, G., Ovaere, P., Vandenabeele, P., & Declercq, W. (2008). Caspase-14 reveals its secrets. *Journal of Cell Biology*, 180(3), 451-458.
- Deng, R. (2018). Bile Salt Export Pump: Drug-Induced Liver Injury and Assessment Approaches. *Methods in Pharmacology and Toxicology*, 301-329.
- Depeint, F., Bruce, W. R., Shangari, N., Mehta, R., & O'Brien, P. J. (2006). Mitochondrial function and toxicity: Role of the B vitamin family on mitochondrial energy metabolism. *Chemico-Biological Interactions*, 163(1-2), 94-112.
- Derks, T. G., Van Dijk, T. H., Grefhorst, A., Rake, J., Smit, G. P., Kuipers, F., & Reijngoud, D. (2008). Inhibition of mitochondrial fatty acid oxidation *in vivo* only slightly suppresses gluconeogenesis but enhances clearance of glucose in mice. *Hepatology*, 47(3), 1032-1042.
- Devendra, D., Liu, E., & Eisenbarth, G. S. (2004). Type 1 diabetes: recent developments. *BMJ*, 328(7442), 750-754.
- Devillers, J. (2012). Methods for Building QSARs. *Methods in Molecular Biology*, 3-27.
- Dhanasekaran, D. N., & Reddy, E. P. (2008). JNK signaling in apoptosis. *Oncogene*, 27(48), 6245-6251.
- Di Cristofano, A., & Pandolfi, P. P. (2000). The multiple roles of PTEN in tumour suppression. *Cell*, 100(4), 387-390.
- Dias-da-Silva, D., Arbo, M., Valente, M., Bastos, M., & Carmo, H. (2015). Hepatotoxicity of piperazine designer drugs: Comparison of different *in vitro* models. *Toxicology in Vitro*, 29(5), 987-996.

- Díaz, L. F., Chiong, M., Quest, A. F., Lavandero, S., & Stutzin, A. (2005). Mechanisms of cell death: molecular insights and therapeutic perspectives. *Cell Death & Differentiation*, 12(11), 1449-1456.
- Diers, A., Broniowska, K., Chang, C., & Hogg, N. (2012). Pyruvate fuels mitochondrial respiration and proliferation of breast cancer cells: Effect of monocarboxylate transporter inhibition. *Biochemical Journal*, 444(3), 561-571.
- Dikalov, S., Nazarewicz, R., Panov, A., Harrison, D. G., & Dikalova, A. (2011). Crosstalk Between Mitochondrial ROS and NADPH Oxidases in Cardiovascular and Degenerative Diseases: Application of Mitochondria-Targeted Antioxidants. *Free Radical Biology and Medicine*, 51, S85-S86.
- Dimaraki, E. V., & Jaffe, C. A. (2003). Troglitazone Induces CYP3A4 Activity Leading to Falsely Abnormal Dexamethasone Suppression Test. *The Journal of Clinical Endocrinology & Metabolism*, 88(7), 3113-3116.
- DiMauro, S. (2002). Treatment of mitochondrial diseases. *Mitochondrial Disorders*, 307-325.
- Dimovasili, C., Aschner, M., Plaitakis, A., & Zaganas, I. (2015). Differential interaction of hGDH1 and hGDH2 with manganese: Implications for metabolism and toxicity. *Neurochemistry International*, 88, 60-65.
- Ding, W., & Yin, X. (2009). The Bcl-2 Family Proteins. *Essentials of Apoptosis*, 25-61.
- Divakaruni, A. S., & Murphy, A. N. (2012). A mitochondrial mystery, solved. *Science*, 337(6090), 41-43.
- Donato, M., Jover, R., & Gómez-Lechón, M. (2013). Hepatic cell lines for drug Hepatotoxicity testing: Limitations and strategies to upgrade their metabolic competence by gene engineering. *Current Drug Metabolism*, 14(9), 946-968.
- Donato, M., Rigamonti, C., & Colombo, M. (2010). Can protocol liver biopsy be avoided to evaluate post-transplant hepatitis C recurrence? Transient elastography makes it possible. *Digestive and Liver Disease*, 42(4), 307.
- Donovan, N., Becker, E. B., Konishi, Y., & Bonni, A. (2002). JNK Phosphorylation and Activation of BAD Couples the Stress-activated Signaling Pathway to the Cell Death Machinery. *Journal of Biological Chemistry*, 277(43), 40944-40949.
- Dooley, T. P., Haldeman-Cahill, R., Joiner, J., & Wilborn, T. W. (2000). Expression Profiling of Human Sulfotransferase and Sulfatase Gene Superfamilies in Epithelial Tissues and Cultured Cells. *Biochemical and Biophysical Research Communications*, 277(1), 236-245.
- Downes, C. P., Ross, S., Maccario, H., Perera, N., Davidson, L., & Leslie, N. R. (2007). Stimulation of PI 3-kinase signaling via inhibition of the tumour suppressor phosphatase, PTEN. *Advances in Enzyme Regulation*, 47(1), 184-194.

Dranoff, J. A., Ogawa, M., Kruglov, E. A., Gaça, M. D., Sévigny, J., Robson, S. C., & Wells, R. G. (2004). Expression of P2Y nucleotide receptors and ectonucleotidases in quiescent and activated rat hepatic stellate cells. *American Journal of Physiology-Gastrointestinal and Liver Physiology*, 287(2), G417-G424.

Driessen, M., Vitins, A. P., Pennings, J. L., Kienhuis, A. S., Water, B. V., & Van der Ven, L. T. (2015). A transcriptomics-based hepatotoxicity comparison between the zebrafish embryo and established human and rodent *in vitro* and *in vivo* models using cyclosporine A, amiodarone, and acetaminophen. *Toxicology Letters*, 232(2), 403-412.

Druet, C., Tubiana-Rufi, N., Chevenne, D., Rigal, O., Polak, M., & Levy-Marchal, C. (2006). Characterization of Insulin Secretion and Resistance in Type 2 Diabetes of Adolescents. *The Journal of Clinical Endocrinology & Metabolism*, 91(2), 401-404.

Du, M., Chen, S., Liu, Y., Liu, Y., & Yang, J. (2011). MHC polymorphism and disease resistance to vibrio anguillarum in 8 families of half-smooth tongue sole (*Cynoglossus semilaevis*). *BMC Genetics*, 12(1).

Duane, W. C. (2009). Bile acids: developments new and very old. *Journal of Lipid Research*, 50(8), 1507-1508.

Duren, Z., Chen, X., Xin, J., Wang, Y., & Wong, W. H. (2020). Time course regulatory analysis based on paired expression and chromatin accessibility data. *Genome Research*, 30(4), 622-634.

Eckland, D., & Danhof, M. (2000). Clinical pharmacokinetics of pioglitazone. *Experimental and Clinical Endocrinology & Diabetes*, 108(Sup. 2), 234-242.

Edlich, F. (2018). BCL-2 proteins and apoptosis: Recent insights and unknowns. *Biochemical and Biophysical Research Communications*, 500(1), 26-34.

Elrod, H. A., & Sun, S. (2008). PPAR γ and Apoptosis in cancer. *PPAR Research*, 2008, 1-12.

Enami, S., Sakamoto, Y., & Colussi, A. J. (2013). Fenton chemistry at aqueous interfaces. *Proceedings of the National Academy of Sciences*, 111(2), 623-628.

Engel, P. C. (2013). Glutamate Dehydrogenases: The Why and How of Coenzyme Specificity. *Neurochemical Research*, 39(3), 426-432.

Engelking, L., McFarlane, M. R., Li, C., & Liang, G. (2013). 942 insig-mediated regulation of intestinal Lipogenesis. *Gastroenterology*, 144(5), S-169-S-170.

Espenshade, P. J., & Hughes, A. L. (2007). Regulation of Sterol Synthesis in Eukaryotes. *Annual Review of Genetics*, 41(1), 401-427

Evan, G. I., & Vousden, K. H. (2001). Proliferation, cell cycle and apoptosis in cancer. *Nature*, 411(6835), 342-348.

Evans, D. C., Watt, A. P., Nicoll-Griffith, D. A., & Baillie, T. A. (2004). Drug-Protein adducts: An industry perspective on minimizing the potential for drug Bioactivation in drug discovery and development. *Chemical Research in Toxicology*, 17(1), 3-16.

Fahmi, O. A., Kish, M., Boldt, S., & Obach, R. S. (2010). Cytochrome P450 3A4 mRNA Is a More Reliable Marker than CYP3A4 Activity for Detecting Pregnane X Receptor-Activated Induction of Drug-Metabolizing Enzymes. *Drug Metabolism and Disposition*, 38(9), 1605-1611.

Fahmi, O. A., Maurer, T. S., Kish, M., Cardenas, E., Boldt, S., & Nettleton, D. (2008). A Combined Model for Predicting CYP3A4 Clinical Net Drug-Drug Interaction Based on CYP3A4 Inhibition, Inactivation, and Induction Determined *in Vitro*. *Drug Metabolism and Disposition*, 36(8), 1698-1708.

Fan, J., Chen, S., C.Y. Chow, E., & Sandy Pang, K. (2010). PBPK Modeling of Intestinal and Liver Enzymes and Transporters in Drug Absorption and Sequential Metabolism. *Current Drug Metabolism*, 11(9), 743-761.

Feige, J. N., Gelman, L., Michalik, L., Desvergne, B., & Wahli, W. (2006). From molecular action to physiological outputs: Peroxisome proliferator-activated receptors are nuclear receptors at the crossroads of key cellular functions. *Progress in Lipid Research*, 45(2), 120-159.

Feinstein, D., Spagnolo, A., Akar, C., Weinberg, G., Murphy, P., Gavrilyuk, V., & Russo, C. D. (2005). Receptor-independent actions of PPAR thiazolidinedione agonists: Is mitochondrial function the key? *Biochemical Pharmacology*, 70(2), 177-188.

Fernie, A. R., Trethewey, R. N., Krotzky, A. J., & Willmitzer, L. (2004). Metabolite profiling: From diagnostics to systems biology. *Nature Reviews Molecular Cell Biology*, 5(9), 763-769.

Ferreira-Silva, V., Rodrigues, A. C., Hirata, T. D., Hirabara, S. M., & Curi, R. (2008). Effects of 15-deoxy- Δ 12, 14 prostaglandin J2 and ciglitazone on human cancer cell cycle progression and death: The role of PPAR γ . *European Journal of Pharmacology*, 580(1-2), 80-86.

Fiebig, A. A., Zhu, W., Hollerbach, C., Leber, B., & Andrews, D. W. (2006). Bcl-XL is qualitatively different from and ten times more effective than Bcl-2 when expressed in a breast cancer cell line. *BMC Cancer*, 6(1).

Fisher, C. P., Plant, N. J., Moore, J. B., & Kierzek, A. M. (2013). QSSPN: dynamic simulation of molecular interaction networks describing gene regulation, signalling and whole-cell metabolism in human cells. *Bioinformatics*, 29(24), 3181-3190.

Florez, J. C., Jablonski, K. A., Bayley, N., Pollin, T. I., De Bakker, P. I., Shuldiner, A. R., Altshuler, D. (2006). TCF7L2 Polymorphisms and Progression to Diabetes in the Diabetes Prevention Program. *New England Journal of Medicine*, 355(3), 241-250

- Fong, D. S., & Contreras, R. (2009). Glitazone use associated with diabetic macular oedema. *American Journal of Ophthalmology*, 147(4), 583-586.e1.
- Fontana, R., & Hayashi, P. (2014). Clinical features, diagnosis, and natural history of drug-induced liver injury. *Seminars in Liver Disease*, 34(02), 134-144
- Franco, R., & Cidlowski, J. A. (2006). SLCO/OATP-like Transport of Glutathione in FasL-induced Apoptosis. *Journal of Biological Chemistry*, 281(40), 29542-29557.
- Franco, R., & Cidlowski, J. A. (2012). Glutathione Efflux and Cell Death. *Antioxidants & Redox Signaling*, 17(12), 1694-1713.
- Freeman, D. A., & Romero, A. (2003). Effects of troglitazone on intracellular cholesterol distribution and cholesterol-dependent cell functions in MA-10 Leydig tumour cells. *Biochemical Pharmacology*, 66(2), 307-313.
- Freeman, D. J., McDorman, K., Ogbagabriel, S., Kozlosky, C., Yang, B., Doshi, S., Radinsky, R. (2012). Tumour penetration and epidermal growth factor receptor saturation by panitumumab correlate with antitumor activity in a preclinical model of human cancer. *Molecular Cancer*, 11(1), 47.
- Freshney, R. I. (2010). *Culture of animal cells: A manual of basic technique and specialised applicatoins*, Wiley-Blackwell, New Jersey.
- Friday, E., Oliver, R., Welbourne, T., & Turturro, F. (2010). Glutaminolysis and glycolysis regulation by troglitazone in breast cancer cells: Relationship to mitochondrial membrane potential. *Journal of Cellular Physiology*, 226(2), 511-519.
- Fritsch, M., Günther, S. D., Schwarzer, R., Albert, M., Schorn, F., Werthenbach, J. P., Kashkar, H. (2019). Caspase-8 is the molecular switch for apoptosis, necroptosis and pyroptosis. *Nature*, 575(7784), 683-687.
- Frohlich, E. (2005). Action of thiazolidinediones on differentiation, proliferation and apoptosis of normal and transformed thyrocytes in culture. *Endocrine Related Cancer*, 12(2), 291-303.
- Fujita, M., Hasegawa, A., Yamamori, M., & Okamura, N. (2017). *In vitro* and *in vivo* cytotoxicity of troglitazone in pancreatic cancer. *Journal of Experimental & Clinical Cancer Research*, 36(1).
- Fujiwara, R., Sumida, K., Kutsuno, Y., Sakamoto, M., & Itoh, T. (2015). UDP-glucuronosyltransferase (UGT) 1A1 mainly contributes to the glucuronidation of trovafloxacin. *Drug Metabolism and Pharmacokinetics*, 30(1), 82-88.
- Fulda, S. (2009). Apoptosis in Cancer Biology and Cancer Therapeutics. *Essentials of Apoptosis*, 581-596.
- Fulda, S., & Debatin, K. (2006). Extrinsic versus intrinsic apoptosis pathways in anticancer chemotherapy. *Oncogene*, 25(34), 4798-4811.

- Fulgencio, J., Kohl, C., Girard, J., & Pegorier, J. (1996). Troglitazone inhibits fatty acid oxidation and esterification, and gluconeogenesis in isolated Hepatocytes from starved rats. *Diabetes*, 45(11), 1556-1562.
- Funk, C., Ponelle, C., Scheuermann, G., & Pantze, M. (2001). Cholestatic Potential of Troglitazone as a Possible Factor Contributing to Troglitazone-Induced Hepatotoxicity: *In Vivo* and *in Vitro* Interaction at the Canalicular Bile Salt Export Pump (Bsep) in the Rat. *Molecular Pharmacology*, 59(3), 627-635.
- Fürnsinn, C., Neschen, S., Noe, C., Bisschop, M., Roden, M., Vogl, C., Waldhäusl, W. (1997). Acute non-insulin-like stimulation of rat muscle glucose metabolism by troglitazone *in vitro*. *British Journal of Pharmacology*, 122(7), 1367-1374.
- Gaillard, D. (1995). Thiazolidinediones and Fatty Acids Convert Myogenic Cells into Adipose-like Cells. *Journal of Biological Chemistry*, 270(47), 28183-28187.
- Gallelli, L., Gallelli, G., Codamo, G., Argentieri, A., Michniewicz, A., Siniscalchi, A., De Sarro, G. (2016). Recognizing severe adverse drug reactions: Two case reports after switching therapies to the same generic company. *Current Drug Safety*, 11(1), 104-108.
- Gan, J., Qu, Q., He, B., Shyu, W., Rodrigues, A., & He, K. (2008). Troglitazone Thiol Adduct Formation in Human Liver Microsomes: Enzyme Kinetics and Reaction Phenotyping. *Drug Metabolism Letters*, 2(3), 184-189.
- Gao, H., & Zhao, C. (2017). Analysis of Protein–DNA interaction by chromatin Immunoprecipitation and DNA tiling Microarray (chip-on-chip). *Chromatin Immunoprecipitation*, 43-51.
- Garbuzova-Davis, S., Ehrhart, J., Sanberg, P., & Borlongan, C. (2018). Potential Role of Humoral IL-6 Cytokine in Mediating Pro-Inflammatory Endothelial Cell Response in Amyotrophic Lateral Sclerosis. *International Journal of Molecular Sciences*, 19(2), 423.
- García, H. E., Laudet, V., & Robinson-Rechavi, M. (2003). Nuclear receptors are markers of animal genome evolution. *Genome Evolution*, 177-184.
- García-Compean, D., Jaquez-Quintana, J. O., & Maldonado-Garza, H. (2009). Hepatogenous diabetes. Current views of an ancient problem. *Annals of Hepatology*, 8(1), 13-20.
- Garza, A. S., Khan, S. H., Moure, C. M., Edwards, D. P., & Kumar, R. (2011). Binding-folding induced regulation of AF1 Transactivation domain of the glucocorticoid receptor by a cofactor that binds to its DNA binding domain. *PLoS ONE*, 6(10), e25875.
- Garzel, B., Yang, H., Zhang, L., Huang, S., Polli, J. E., & Wang, H. (2013). The role of bile salt export pump gene repression in drug-induced Cholestatic liver toxicity. *Drug Metabolism and Disposition*, 42(3), 318-322.

- Gautier, E. L., Chow, A., Spanbroek, R., Marcelin, G., Greter, M., Jakubzick, C., Randolph, G. J. (2012). Systemic analysis of PPAR γ in mouse macrophage populations reveals marked diversity in expression with critical roles in resolution of inflammation and airway immunity. *The Journal of Immunology*, 189(5), 2614-2624.
- Genrich, H., Küffner, R., & Voss, K. (2001). Executable petri net models for the analysis of metabolic pathways. *International Journal on Software Tools for Technology Transfer*, 3(4), 394-404.
- Genuth, S. (2014). Should Sulfonylureas Remain an Acceptable First-Line Add-on to Metformin Therapy in Patients with Type 2 Diabetes? No, It is Time to Move On! *Diabetes Care*, 38(1), 170-175.
- Gevorgyan, A., Bushell, M. E., Avignone-Rossa, C., & Kierzek, A. M. (2010). SurreyFBA: A command line tool and graphics user interface for constraint-based modeling of genome-scale metabolic reaction networks. *Bioinformatics*, 27(3), 433-434.
- Ghobrial, I. M., Witzig, T. E., & Adjei, A. A. (2005). Targeting Apoptosis Pathways in Cancer Therapy. *CA: A Cancer Journal for Clinicians*, 55(3), 178-194.
- Gibson, G. G., & Skett, P. (2013). *Introduction to Drug Metabolism*. Basingstoke, England: Springer.
- Glassberg, H., & Rader, D. J. (2008). Management of lipids in the prevention of cardiovascular events. *Annual Review of Medicine*, 59(1), 79-94.
- Glintborg, B., Andersen, S. E., & Dalhoff, K. (2005). Drug-drug interactions among recently hospitalised patients – frequent but mostly clinically insignificant. *European Journal of Clinical Pharmacology*, 61(9), 675-681.
- Go, Y., Uppal, K., Walker, D. I., Tran, V., Dury, L., Strobel, F. H., Jones, D. P. (2014). Mitochondrial Metabolomics using high-resolution fourier-transform mass spectrometry. *Methods in Molecular Biology*, 43-73.
- Gong, H., Singh, S. V., Singh, S. P., Mu, Y., Lee, J. H., Saini, S. P., Xie, W. (2006). Orphan Nuclear Receptor Pregnane X Receptor Sensitizes Oxidative Stress Responses in Transgenic Mice and Cancerous Cells. *Molecular Endocrinology*, 20(2), 279-290.
- Good, C. B., & Pogach, L. M. (2018). Should Metformin Be First-line Therapy for Patients with Type 2 Diabetes and Chronic Kidney Disease? *JAMA Internal Medicine*, 178(7), 911.
- Gotoh, S., & Negishi, M. (2013). Serum- and Glucocorticoid-Regulated Kinase 2 Determines Drug-Activated Pregnane X Receptor to Induce Gluconeogenesis in Human Liver Cells. *Journal of Pharmacology and Experimental Therapeutics*, 348(1), 131-140.
- Gourmaud, S., Paquet, C., Dumurgier, J., Pace, C., Bouras, C., Gray, F., Laplanche, J., Meurs, E. F., Mouton-Liger, F., & Hugon, J. (2015). Increased levels of

cerebrospinal fluid JNK3 associated with amyloid pathology: Links to cognitive decline. *Journal of Psychiatry and Neuroscience*, 40(3), 151-161.

Graham, D. J., Green, L., Senior, J. R., & Nourjah, P. (2003). Troglitazone-induced liver failure: a case study. *The American Journal of Medicine*, 114(4), 299-306.

Graham, D. J., Ouellet-Hellstrom, R., MaCurdy, T. E., Ali, F., Sholley, C., Worrall, C., & Kelman, J. A. (2010). Risk of acute myocardial infarction, stroke, heart failure, and death in elderly Medicare patients treated with Rosiglitazone or Pioglitazone. *JAMA*, 304(4), 411.

Gras, F., Brunmair, B., Roden, M., Waldhäusl, W., & Fürnsinn, C. (2003). Differences in troglitazone action on glucose metabolism in freshly isolated long-term incubated rat skeletal muscle. *British Journal of Pharmacology*, 138(6), 1140-1146.

Grattagliano, I., Portincasa, P., Palmieri, V. O., & Palasciano, G. (2002). Overview on the mechanisms of drug-induced liver cell death. *Annals of Hepatology*, 1(4), 162-168.

Grimaldi, M., Karaca, M., Latini, L., Brioudes, E., Schalch, T., & Maechler, P. (2017). Identification of the molecular dysfunction caused by glutamate dehydrogenase S445L mutation responsible for hyperinsulinism/hyperammonaemia. *Human Molecular Genetics*, 26(18), 3453-3465.

Guengerich, F. P. (2001). Common and Uncommon Cytochrome P450 Reactions Related to Metabolism and Chemical Toxicity. *Chemical Research in Toxicology*, 14(6), 611-650.

Guha, A., Narayanru, S., Kaley, N. M., Rao, D. K., Mondal, J., & Narayanan, T. (2019). Mechanistic insight into high yield electrochemical nitrogen reduction to ammonia using lithium ions

Gülden, M., Jess, A., Kammann, J., Maser, E., & Seibert, H. (2010). Cytotoxic potency of H₂O₂ in cell cultures: Impact of cell concentration and exposure time. *Free Radical Biology and Medicine*, 49(8), 1298-1305.

Guo, G. L. (2004). Enhanced Acetaminophen Toxicity by Activation of the Pregnane X Receptor. *Toxicological Sciences*, 82(2), 374-380.

Guo, W., Wang, A., & Gao, C. (2009). Apoptosis and expression of apoptosis-related proteins Bcl-2, Bcl-xL and Bcl-w in human colon adenocarcinoma. *World Chinese Journal of Digestology*, 17(25), 2589.

Gupta, D., Venkatesh, M., Wang, H., Kim, S., Sinz, M., Goldberg, G. L., Mani, S. (2008). Expanding the Roles for Pregnane X Receptor in Cancer: Proliferation and Drug Resistance in Ovarian Cancer. *Clinical Cancer Research*, 14(17), 5332-5340.

Gupta, Y., Gupta, P., & Gupta, V. (2012). Phase I clinical trials of anticancer drugs in healthy volunteers: Need for critical consideration. *Indian Journal of Pharmacology*, 44(4), 540.

- Gurnell, M., Savage, D. B., Chatterjee, V. K., & O'Rahilly, S. (2003). The metabolic syndrome: Peroxisome proliferator-activated receptor γ and its therapeutic modulation. *The Journal of Clinical Endocrinology & Metabolism*, 88(6), 2412-2421.
- Haeusler, R. A., McGraw, T. E., & Accili, D. (2017). Biochemical and cellular properties of insulin receptor signalling. *Nature Reviews Molecular Cell Biology*, 19(1), 31-44.
- Hakkola, J., Rysä, J., & Hukkanen, J. (2016). Regulation of hepatic energy metabolism by the nuclear receptor PXR. *Biochimica et Biophysica Acta (BBA) - Gene Regulatory Mechanisms*, 1859(9), 1072-1082.
- Halban, P. A., Polonsky, K. S., Bowden, D. W., Hawkins, M. A., Ling, C., Mather, K. J., Weir, G. C. (2014). β -Cell Failure in Type 2 Diabetes: Postulated Mechanisms and Prospects for Prevention and Treatment. *Diabetes Care*, 37(6), 1751-1758.
- Haliakon, S., Doare, L., Foufelle, F., Kergoat, M., Guerre-Millo, M., Berthault, M., Ferre, P. (1997). Pioglitazone induces *in vivo* Adipocyte differentiation in the obese Zucker Fa/Fa rat. *Diabetes*, 46(9), 1393-1399.
- Hamasaki, H. (2012). Hyperinsulinemia and insulin resistance in a patient with type 2 diabetes complicated with myelofibrosis. *World Journal of Diabetes*, 3(8), 156.
- Han, B., Dong, Z., Liu, Y., Chen, Q., Hashimoto, K., & Zhang, J. (2003). Regulation of constitutive expression of mouse PTEN by the 5'-untranslated region. *Oncogene*, 22(34), 5325-5337.
- Han, S. J., Lonard, D. M., & O'Malley, B. W. (2009). Multi-modulation of nuclear receptor coactivators through posttranslational modifications. *Trends in Endocrinology & Metabolism*, 20(1), 8-15.
- Hanefeld, M., Pfützner, A., Forst, T., Kleine, I., & Fuchs, W. (2011). Double-blind, randomized, multicentre, and active comparator controlled investigation of the effect of Pioglitazone, metformin, and the combination of both on cardiovascular risk in patients with type 2 diabetes receiving stable basal insulin therapy: The PIOCMB study. *Cardiovascular Diabetology*, 10(1), 65.
- Hariparsad, N., Chu, X., Yabut, J., Labhart, P., Hartley, D. P., Dai, X., & Evers, R. (2009). Identification of pregnane-X receptor target genes and coactivator and corepressor binding to promoter elements in human hepatocytes. *Nucleic Acids Research*, 37(4), 1160-1173.
- Harper, N., Hughes, M., MacFarlane, M., & Cohen, G. M. (2003). Fas-associated Death Domain Protein and Caspase-8 Are Not Recruited to the Tumour Necrosis Factor Receptor1 Signaling Complex during Tumour Necrosis Factor-induced Apoptosis. *Journal of Biological Chemistry*, 278(28), 25534-25541.
- Hartley, D. P., Dai, X., Yabut, J., Chu, X., Cheng, O., Zhang, T., Evans, D. C. (2006). Identification of potential pharmacological and toxicological targets differentiating structural analogs by a combination of transcriptional profiling and promoter analysis

in LS-180 and caco-2 adenocarcinoma cell lines. *Pharmacogenetics and Genomics*, 16(8), 579-599.

Hashimoto, Y., Naruyama, Y., Tozawa, K., & Kohri, K. (2007). MP-17.10: Peroxisome proliferator-activated receptor-gamma ligands inhibit cell growth of human prostate cancer. *Urology*, 70(3), 132-133.

Haskins, J., Rowse, P., Rahbari, R., & De la Iglesia, F. (2001). Thiazolidinedione toxicity to isolated hepatocytes revealed by coherent multiprobe fluorescence microscopy and correlated with multiparameter flow cytometry of peripheral leukocytes. *Archives of Toxicology*, 75(7), 425-438.

Hata, M., Hirano, Y., Hoshino, T., & Tsuda, M. (2001). Monooxygenation Mechanism by Cytochrome P-450. *Journal of the American Chemical Society*, 123(26), 6410-6416.

Hattori, Y., Hattori, S., & Kasai, K. (1999). Troglitazone Upregulates nitric oxide synthesis in vascular smooth muscle cells. *Hypertension*, 33(4), 943-948.

Hay, M., Thomas, D. W., Craighead, J. L., Economides, C., & Rosenthal, J. (2014). Clinical development success rates for investigational drugs. *Nature Biotechnology*, 32(1), 40-51.

He, J., Gao, J., Xu, M., Ren, S., Stefanovic-Racic, M., O'Doherty, R. M., & Xie, W. (2013). PXR Ablation Alleviates Diet-Induced and Genetic Obesity and Insulin Resistance in Mice. *Diabetes*, 62(6), 1876-1887.

He, K., Woolf, T. F., Kindt, E. K., Fielder, A. E., & Talaat, R. E. (2001). Troglitazone quinone formation catalysed by human and rat CYP3A: an atypical CYP oxidation reaction☆. *Biochemical Pharmacology*, 62(2), 191-198.

He, L. (2010). Posttranscriptional regulation of PTEN dosage by Noncoding RNAs. *Science Signaling*, 3(146), pe39-pe39

Heikkinen, S., Argmann, C. A., Champy, M., & Auwerx, J. (2007). Evaluation of Glucose Homeostasis. *Current Protocols in Molecular Biology*.

Heiner, M., Herajy, M., Liu, F., Rohr, C., & Schwarick, M. (2012). Snoopy – A Unifying Petri Net Tool. *Lecture Notes in Computer Science*, 398-407.

Hengartner, M. O. (2000). The biochemistry of apoptosis. *Nature*, 407(6805), 770-776.

Heppner, K. M., Habegger, K. M., Day, J., Pfluger, P. T., Perez-Tilve, D., Ward, B., Tschöp, M. (2010). Glucagon regulation of energy metabolism. *Physiology & Behavior*, 100(5), 545-548

Herbert, K. E., Fletcher, S., Chauhan, D., Ladapo, A., Nirwan, J., Munson, S., & Mistry, P. (2005). Dietary supplementation with different vitamin C doses: no effect on oxidative DNA damage in healthy people. *European Journal of Nutrition*, 45(2), 97-104.

Herzig, S., Raemy, E., Montessuit, S., Veuthey, J., Zamboni, N., Westermann, B., Martinou, J. (2012). Identification and Functional Expression of the Mitochondrial Pyruvate Carrier. *Science*, 337(6090), 93-96.

Hewitt, N. J., Lloyd, S., Hayden, M., Butler, R., Sakai, Y., Springer, R., Li, A. P. (2002). Correlation between troglitazone cytotoxicity and drug metabolic enzyme activities in cryopreserved human hepatocytes. *Chemico-Biological Interactions*, 142(1-2), 73-82.

Hinds, M. G., & Day, C. L. (2005). Regulation of apoptosis: uncovering the binding determinants. *Current Opinion in Structural Biology*, 15(6), 690-699.

Hinson, J. A. (2013). Mechanisms of Acetaminophen-Induced Liver Disease. *Drug-Induced Liver Disease*, 305-329.

Hinson, J. A., Roberts, D. W., & James, L. P. (2009). Mechanisms of Acetaminophen-Induced Liver Necrosis. *Handbook of Experimental Pharmacology*, 369-405.

Hoedemakers, R. M., Morselt, H. W., Scherphof, G. L., & Daemen, T. (2008). Heterogeneity in secretory responses of rat liver macrophages of different size. *Liver*, 15(6), 313-319

Hofmann, A. F. (2004). Detoxification of Lithocholic Acid, A Toxic Bile Acid: Relevance to Drug Hepatotoxicity. *Drug Metabolism Reviews*, 36(3-4), 703-722.

Hofmann, A. F. (2009). The enterohepatic circulation of bile acids in mammals: form and functions. *Frontiers in Bioscience*, Volume (14), 2584.

Hofmann, A. F., & Hagey, L. R. (2008). Bile Acids: Chemistry, Pathochemistry, Biology, Pathobiology, and Therapeutics. *Cellular and Molecular Life Sciences*, 65(16), 2461-2483.

Holt, M. P., & Ju, C. (2006). Mechanisms of drug-induced liver injury. *The AAPS Journal*, 8(1), E48-E54.

Honma, W. (2002). Phenol Sulfotransferase, ST1A3, as the Main Enzyme Catalyzing Sulfation of Troglitazone in Human Liver. *Drug Metabolism and Disposition*, 30(8), 944-949.

Horikoshi, H., & Yoshioka, T. (1998). Troglitazone — a novel antidiabetic drug for treating insulin resistance. *Drug Discovery Today*, 3(2), 79-88.

Horton, J. D., Goldstein, J. L., & Brown, M. S. (2002). SREBPs: Activators of the complete program of cholesterol and fatty acid synthesis in the liver. *Journal of Clinical Investigation*, 109(9), 1125-1131.

Hotchkiss, R. S., Strasser, A., McDunn, J. E., & Swanson, P. E. (2009). Cell Death. *New England Journal of Medicine*, 361(16), 1570-1583.

- Houston, A. (2004). The Fas signalling pathway and its role in the pathogenesis of cancer. *Current Opinion in Pharmacology*, 4(4), 321-326.
- Hrusovsky, K. (2006). Getting on the critical path: better evaluation tools for drug discovery and development. *Drug Discovery Today*, 11(17-18), 773-774.
- Hu, C., & Li, L. (2015). *In vitro* culture of isolated primary hepatocytes and stem cell-derived hepatocyte-like cells for liver regeneration. *Protein & Cell*, 6(8), 562-574.
- Hu, G., Xu, C., & Staudinger, J. L. (2010). Pregnane X Receptor Is SUMOylated to Repress the Inflammatory Response. *Journal of Pharmacology and Experimental Therapeutics*, 335(2), 342-350.
- Hu, N., & Ren, J. (2016). Reactive Oxygen Species Regulate Myocardial Mitochondria through Post-Translational Modification. *Reactive Oxygen Species*.
- Hu, Q., Wood, C. R., Cimen, S., Venkatachalam, A. B., & Alwayn, I. P. (2015). Mitochondrial Damage-Associated Molecular Patterns (MTDs) Are Released during Hepatic Ischemia Reperfusion and Induce Inflammatory Responses. *PLOS ONE*, 10(10), e0140105.
- Hua, F., Comer, G. M., Stockert, L., Jin, B., Nowak, J., Pleasic-Williams, S., Beebe, J. S. (2013). Anti-IL21 receptor monoclonal antibody (ATR-107): Safety, pharmacokinetics, and pharmacodynamic evaluation in healthy volunteers: A phase I, first-in-human study. *The Journal of Clinical Pharmacology*, 54(1), 14-22.
- Huang, R., Xia, M., Sakamuru, S., Zhao, J., Shahane, S. A., Attene-Ramos, M., Simeonov, A. (2016). Modelling the Tox21 10 K chemical profiles for *in vivo* toxicity prediction and mechanism characterization. *Nature Communications*, 7(1).
- Hubbard, S. R. (2013). The insulin receptor: Both a prototypical and atypical receptor tyrosine kinase. *Cold Spring Harbor Perspectives in Biology*, 5(3), a008946-a008946.
- Hubert, J., Nuzillard, J., & Renault, J. (2015). Dereplication strategies in natural product research: How many tools and methodologies behind the same concept? *Phytochemistry Reviews*, 16(1), 55-95.
- Hughes, T. B., Dang, N. L., Miller, G. P., & Swamidass, S. J. (2016). Modeling Reactivity to Biological Macromolecules with a Deep Multitask Network. *ACS Central Science*, 2(8), 529-537.
- Hunter, A. M., LaCasse, E. C., & Korneluk, R. G. (2007). The inhibitors of apoptosis (IAPs) as cancer targets. *Apoptosis*, 12(9), 1543-1568.
- Hunter, P. J., & Borg, T. K. (2003). Integration from proteins to organs: the Physiome Project. *Nature Reviews Molecular Cell Biology*, 4(3), 237-243.
- Huss, J. M., Imahashi, K., Dufour, C. R., Weinheimer, C. J., Courtois, M., Kovacs, A., Kelly, D. P. (2007). The nuclear receptor ERR α is required for the Bioenergetic and functional adaptation to cardiac pressure overload. *Cell Metabolism*, 6(1), 25-37.

- Hüttemann, M., Pecina, P., Rainbolt, M., Sanderson, T. H., Kagan, V. E., Samavati, L., Lee, I. (2011). The multiple functions of cytochrome c and their regulation in life and death decisions of the mammalian cell: From respiration to apoptosis. *Mitochondrion*, 11(3), 369-381.
- Ideker, T., & Lauffenburger, D. (2003). Building with a scaffold: emerging strategies for high- to low-level cellular modeling. *Trends in Biotechnology*, 21(6), 255-262.
- Ideker, T., Galitski, T., & Hood, L. (2001). A NEW APPROACH TO DECODING LIFE: Systems Biology. *Annual Review of Genomics and Human Genetics*, 2(1), 343-372.
- Iida, K. T., Kawakami, Y., Suzuki, H., Sone, H., Shimano, H., Toyoshima, H., ... Yamada, N. (2002). PPAR γ ligands, troglitazone and pioglitazone, up-regulate expression of HMG-CoA synthase and HMG-CoA reductase gene in THP-1 macrophages. *FEBS Letters*, 520(1-3), 177-181.
- Ikeda, T. (2011). Drug-induced idiosyncratic Hepatotoxicity: Prevention strategy developed after the Troglitazone case. *Drug Metabolism and Pharmacokinetics*, 26(1), 60-70.
- Inoue, M., Sato, E. F., Nishikawa, M., Park, A., Kira, Y., Imada, I., & Utsumi, K. (2003). Mitochondrial Generation of Reactive Oxygen Species and its Role in Aerobic Life. *Current Medicinal Chemistry*, 10(23), 2495-2505.
- Intapa, C., & Jabra Rizk, M. A. (2014). Farnesol-induced apoptosis in oral squamous carcinoma cells is mediated by MRP1 extrusion and depletion of intracellular glutathione. *Pathology*, 46, S94-S95.
- Iorga, A., & Dara, L. (2019). Cell death in drug-induced liver injury. *Advances in Pharmacology*, 31-74.
- Iryna, K., Helen, M., & Elena, S. (2015). Drug-induced Liver Disease in Patients with Diabetes Mellitus. *Euroasian Journal of Hepato-Gastroenterology*, 5(2), 83-86.
- Isshiki, K., Haneda, M., Koya, D., Maeda, S., Sugimoto, T., & Kikkawa, R. (2000). Thiazolidinedione compounds ameliorate glomerular dysfunction independent of their insulin-sensitizing action in diabetic rats. *Diabetes*, 49(6), 1022-1032.
- Jack, J., Wambaugh, J., & Shah, I. (2013). Systems Toxicology from Genes to Organs. *Methods in Molecular Biology*, 375-397.
- Jackson, J. P., Freeman, K. M., St. Claire, R. L., Black, C. B., & Brouwer, K. R. (2018). Cholestatic drug induced liver injury: A function of bile salt export pump inhibition and Farnesoid X receptor antagonism. *Applied In Vitro Toxicology*, 4(3), 265-279.
- Jaeschke, H. (2007). Troglitazone Hepatotoxicity: Are We Getting Closer to Understanding Idiosyncratic Liver Injury? *Toxicological Sciences*, 97(1), 1-3.
- Jaeschke, H., McGill, M. R., & Ramachandran, A. (2012). Oxidant stress, mitochondria, and cell death mechanisms in drug-induced liver injury: Lessons

learned from acetaminophen hepatotoxicity. *Drug Metabolism Reviews*, 44(1), 88-106.

Jagota, A., Thummadi, N. B., & Kukkemann, K. (2019). Circadian Regulation of Hormesis for Health and Longevity. *The Science of Hormesis in Health and Longevity*, 223-233.

Janowski, B. A. (2002). The hypocholesterolemic agent LY295427 up-regulates INSIG-1, identifying the INSIG-1 protein as a mediator of cholesterol homeostasis through SREBP. *Proceedings of the National Academy of Sciences*, 99(20), 12675-12680.

Javadov, S., Jang, S., & Agostini, B. (2014). Crosstalk between mitogen-activated protein kinases and mitochondria in cardiac diseases: Therapeutic perspectives. *Pharmacology & Therapeutics*, 144(2), 202-225.

Jia, B., Yu, Z., Duan, Z., Lü, X., Li, J., Liu, X., Kan, Q. (2013). Hyperammonaemia induces hepatic injury with alteration of gene expression profiles. *Liver International*, 34(5), 748-758.

Jia, L., & Liu, X. (2007). The Conduct of Drug Metabolism Studies Considered Good Practice (II): *In Vitro* Experiments. *Current Drug Metabolism*, 8(8), 822-829.

John, W. G., Hillson, R., & Alberti, S. G. (2012). Use of haemoglobin A1c (HbA1c) in the diagnosis of diabetes mellitus. The implementation of world health organisation (WHO) guidance 2011. *Practical Diabetes*, 29(1), 12-12a.

Johnell, K., & Klarin, I. (2007). The relationship between number of drugs and potential drug-drug interactions in the elderly. *Drug Safety*, 30(10), 911-918.

Johnson, E. (2016). Reactive Oxygen Species, Oxidative Stress, and Cardiovascular Disease. *Reactive Oxygen Species in Biology and Human Health*, 279-286.

Jones, D. P., Lemasters, J. J., Han, D., Boelsterli, U. A., & Kaplowitz, N. (2010). Mechanisms of Pathogenesis in Drug Hepatotoxicity Putting the Stress on Mitochondria. *Molecular Interventions*, 10(2), 98-111.

Jorgensen, I., Rayamajhi, M., & Miao, E. A. (2017). Programmed cell death as a defence against infection. *Nature Reviews Immunology*, 17(3), 151-164.

Jove, M., Salla, J., Planavila, A., Cabrero, À., Michalik, L., Wahli, W., Vázquez-Carrera, M. (2003). Impaired expression of NADH dehydrogenase subunit 1 and PPAR γ coactivator-1 in skeletal muscle of ZDF rats. *Journal of Lipid Research*, 45(1), 113-123.

Judson, P. N., Cooke, P. A., Doerrer, N. G., Greene, N., Hanzlik, R. P., Hardy, C., Zeiger, E. (2005). Towards the creation of an international toxicology information centre. *Toxicology*, 213(1-2), 117-128.

Julien, O., & Wells, J. A. (2017). Caspases and their substrates. *Cell Death & Differentiation*, 24(8), 1380-1389.

Kahanovitz, L., Sluss, P. M., & Russell, S. J. (2017). Type 1 Diabetes—A Clinical Perspective. *Point of Care: The Journal of Near-Patient Testing & Technology*, 16(1), 37-40.

Kakinuma, Y., Kimura, T., & Watanabe, Y. (2017). Possible Involvement of Liver Resident Macrophages (Kupffer Cells) in the Pathogenesis of Both Intrahepatic and Extrahepatic Inflammation. *Canadian Journal of Gastroenterology and Hepatology*, 2017, 1-10.

Kakizaki, S., Yamazaki, Y., Takizawa, D., & Negishi, M. (2008). New insights on the xenobiotic-sensing nuclear receptors in liver diseases – CAR and PXR-. *Current Drug Metabolism*, 9(7), 614-621.

Kalgutkar, A. S., Dalvie, D., Obach, R. S., & Smith, D. A. (2012). *Reactive Drug Metabolites*. Hoboken, NJ: John Wiley & Sons.

Kalkavan, H., & Green, D. R. (2017). MOMP, cell suicide as a BCL-2 family business. *Cell Death & Differentiation*, 25(1), 46-55.

Kanavouras, K., Mastorodemos, V., Borompokas, N., Spanaki, C., & Plaitakis, A. (2007). Properties and molecular evolution of human GLUD2 (neural and testicular tissue-specific) glutamate dehydrogenase. *Journal of Neuroscience Research*, 85(15), 3398-3406.

Kanno, Y., Tanuma, N., Yazawa, S., Zhao, S., Inaba, M., Nakamura, S., Inouye, Y. (2016). Differences in gene regulation by dual ligands of nuclear receptors constitutive Androstane receptor (CAR) and Pregnane X receptor (PXR) in HepG2 cells stably expressing CAR/PXR. *Drug Metabolism and Disposition*, 44(8), 1158-1163.

Kaplowitz, N. (2006). Liver biology and pathobiology. *Hepatology*, 43(S1), S235-S238.

Kaplowitz, N. (2013). Avoiding idiosyncratic DILI: Two is better than one. *Hepatology*, 58(1), 15-17.

Kaplowitz, N. (2013). Drug-Induced Liver Injury. *Drug-Induced Liver Disease*, 3-14.

Kappas, A. (2003). A method for interdicting the development of severe jaundice in newborns by inhibiting the production of bilirubin. *PEDIATRICS*, 113(1), 119-123.

Karin, M., & Lin, A. (2002). NF- κ B at the crossroads of life and death. *Nature Immunology*, 3(3), 221-227.

Karr, J., Sanghvi, J., Macklin, D., Gutschow, M., Jacobs, J., Bolival, B., Covert, M. (2012). A Whole-Cell Computational Model Predicts Phenotype from Genotype. *Cell*, 150(2), 389-401.

Kassahun, K., Pearson, P. G., Tang, W., McIntosh, I., Leung, K., Elmore, C., Baillie, T. A. (2001). Studies on the Metabolism of Troglitazone to Reactive Intermediates *in Vitro* and *in Vivo*. Evidence for Novel Biotransformation Pathways Involving Quinone

Methide Formation and Thiazolidinedione Ring Scission. *Chem. Res. Toxicol*, 14(1), 62-70.

Kast-Woelbern, H. R., Dana, S. L., Cesario, R. M., Sun, L., De Grandpre, L. Y., Brooks, M. E., Leibowitz, M. D. (2004). Rosiglitazone Induction of Insig-1 in White Adipose Tissue Reveals a Novel Interplay of Peroxisome Proliferator-activated Receptor γ and Sterol Regulatory Element-binding Protein in the Regulation of Adipogenesis. *Journal of Biological Chemistry*, 279(23), 23908-23915.

Kavlock, R., & Dix, D. (2010). Computational toxicology as implemented by the U.S. EPA: Providing high throughput decision support tools for screening and assessing chemical exposure, hazard and risk. *Journal of Toxicology and Environmental Health, Part B*, 13(2-4), 197-217.

Kegel, V., Deharde, D., Pfeiffer, E., Zeilinger, K., Seehofer, D., & Damm, G. (2016). Protocol for Isolation of Primary Human Hepatocytes and Corresponding Major Populations of Non-parenchymal Liver Cells. *Journal of Visualized Experiments*, (109).

Kelts, J. L., Cali, J. J., Duellman, S. J., & Shultz, J. (2015). Altered cytotoxicity of ROS-inducing compounds by sodium pyruvate in cell culture medium depends on the location of ROS generation. *SpringerPlus*, 4(1).

Kennedy, L. (2006). Prevention of Type 2 Diabetes with Troglitazone in the Diabetes Prevention Program. *Yearbook of Medicine*, 2006, 474-476.

Kharroubi, A. T. (2015). Diabetes mellitus: The epidemic of the century. *World Journal of Diabetes*, 6(6), 850.

Kim, E., & Kim, A. (2012). Apigenin Sensitizes Huh-7 Human Hepatocellular Carcinoma Cells to TRAIL-induced Apoptosis. *Biomolecules and Therapeutics*, 20(1), 62-67.

Kim, H., Haluzik, M., Gavrilova, O., Yakar, S., Portas, J., Sun, H., LeRoith, D. (2004). Thiazolidinediones improve insulin sensitivity in adipose tissue and reduce the hyperlipidaemia without affecting the hyperglycaemia in a transgenic model of type 2 diabetes. *Diabetologia*, 47(12), 2215-2225.

Kim, J. H., Choi, S., Jung, J., Roh, E., & Kim, H. (2006). Capacitative Ca^{2+} entry is involved in regulating soluble amyloid precursor protein (sAPP α) release mediated by muscarinic acetylcholine receptor activation in neuroblastoma SH-SY5Y cells. *Journal of Neurochemistry*, 97(1), 245-254.

Kim, J. W., Choi, E., & Joe, C. O. (2000). Activation of death-inducing signaling complex (DISC) by pro-apoptotic C-terminal fragment of RIP. *Oncogene*, 19(39), 4491-4499.

King-Jones, K., & Thummel, C. S. (2005). Nuclear receptors — a perspective from drosophila. *Nature Reviews Genetics*, 6(4), 311-323.

- Kirchheimer, J., Thomas, S., Bauer, S., Tomalikscharte, D., Hering, U., Doroshenko, O., Meineke, I. (2006). Pharmacokinetics and pharmacodynamics of rosiglitazone in relation to CYP2C8 genotype. *Clinical Pharmacology & Therapeutics*, 80(6), 657-667.
- Kirchmair, J., Göller, A. H., Lang, D., Kunze, J., Testa, B., Wilson, I. D., Schneider, G. (2015). Predicting drug metabolism: Experiment and/or computation? *Nature Reviews Drug Discovery*, 14(6), 387-404.
- Kitano, H. (2002). Systems Biology: A Brief Overview. *Science*, 295(5560), 1662-1664.
- Kitano, M., & Bloomston, P. (2016). Hepatic Stellate Cells and microRNAs in Pathogenesis of Liver Fibrosis. *Journal of Clinical Medicine*, 5(3), 38.
- Klopotek, A., Hirche, F., & Eder, K. (2006). PPAR γ ligand Troglitazone lowers cholesterol synthesis in HepG2 and caco-2 Cells via a reduced concentration of nuclear SREBP-2. *Experimental Biology and Medicine*, 231(8), 1365-1372.
- Kluck, R. (2010). Bcl-2 family-regulated apoptosis in health and disease. *Cell Health and Cytoskeleton*, 9.
- Kmieć, Z. (2001). Cooperation of Liver Cells in the Process of Liver Fibrosis. *Cooperation of Liver Cells in Health and Disease*, 97-105.
- Kocarek, T. A., Schuetz, E. G., & Guzelian, P. S. (1993). Transient induction of cytochrome P450 1a1 mRNA by culture medium component in primary cultures of adult rat hepatocytes. *In Vitro Cellular & Developmental Biology - Animal*, 29(1), 62-66.
- Kodera, Y., Takeyama, K., Murayama, A., Suzawa, M., Masuhiro, Y., & Kato, S. (2013). Ligand type-specific interactions of peroxisome proliferator-activated receptor γ with transcriptional coactivators. *Journal of Biological Chemistry*, 288(42), 30505-30505.
- König, M., Bulik, S., & Holzhütter, H. (2012). Quantifying the contribution of the liver to glucose homeostasis: A detailed kinetic model of human hepatic glucose metabolism. *PLoS Computational Biology*, 8(6), e1002577.
- Konrad, D., Rudich, A., Bilan, P. J., Patel, N., Richardson, C., Witters, L. A., & Klip, A. (2005). Troglitazone causes acute mitochondrial membrane depolarisation and an AMPK-mediated increase in glucose phosphorylation in muscle cells. *Diabetologia*, 48(5), 954-966.
- Koppe, L., Nyam, E., Vivot, K., Manning Fox, J. E., Dai, X., Nguyen, B. N., Poitout, V. (2016). Urea impairs β cell glycolysis and insulin secretion in chronic kidney disease. *Journal of Clinical Investigation*, 126(9), 3598-3612.
- Koppel, N., Maini Rekdal, V., & Balskus, E. P. (2017). Chemical transformation of xenobiotics by the human gut microbiota. *Science*, 356(6344), eaag2770.

- Krämer, S., & Testa, B. (2008). The biochemistry of drug metabolism - An introduction. *Chemistry & Biodiversity*, 5(12), 2465-2578.
- Krause, K. (2018). Role of NOX-generated reactive oxygen species in health and disease. *Free Radical Biology and Medicine*, 120, S7.
- Kroemer, G., Galluzzi, L., & Brenner, C. (2007). Mitochondrial Membrane Permeabilization in Cell Death. *Physiological Reviews*, 87(1), 99-163.
- Krstic, J., Galhuber, M., Schulz, T., Schupp, M., & Prokesch, A. (2018). p53 as a Dichotomous Regulator of Liver Disease: The Dose Makes the Medicine. *International Journal of Molecular Sciences*, 19(3), 921.
- Kruszynska, Y. T. (2004). Type 2 diabetes mellitus: Etiology, pathogenesis and clinical manifestations. *Principles of Diabetes Mellitus*, 179-199.
- Krysko, D. V., Denecker, G., Festjens, N., Gabriels, S., Parthoens, E., D'Herde, K., & Vandenabeele, P. (2006). Macrophages use different internalization mechanisms to clear apoptotic and necrotic cells. *Cell Death & Differentiation*, 13(12), 2011-2022.
- Kubitz, R., Dröge, C., Stindt, J., Weissenberger, K., & Häussinger, D. (2012). The bile salt export pump (BSEP) in health and disease. *Clinics and Research in Hepatology and Gastroenterology*, 36(6), 536-553.
- Kubota, N., Terauchi, Y., Kubota, T., Kumagai, H., Itoh, S., Satoh, H., Kadowaki, T. (2006). Pioglitazone Ameliorates Insulin Resistance and Diabetes by Both Adiponectin-dependent and -independent Pathways. *Journal of Biological Chemistry*, 281(13), 8748-8755.
- Kullak-ublick, G. A., Stieger, B., & Meier, P. J. (2004). Enterohepatic bile salt transporters in normal physiology and liver disease. *Gastroenterology*, 126(1), 322-342
- Kumar, S. (2006). Caspase function in programmed cell death. *Cell Death & Differentiation*, 14(1), 32-43.
- Kuo, L., Kuo, C., Lin, C., Hung, M., Shen, J., & Hwang, T. (2014). Intracellular Glutathione depletion by Oridonin leads to Apoptosis in hepatic stellate cells. *Molecules*, 19(3), 3327-3344.
- Kuramoto, S., Kato, M., Shindoh, H., & Ishigai, M. (2019). Quantitative prediction of CYP3A4 Induction using simple relative factor approach. *Drug Metabolism and Pharmacokinetics*, 34(1), S42-S43.
- Kusminski, C. M., Shetty, S., Orci, L., Unger, R. H., & Scherer, P. E. (2009). Diabetes and apoptosis: lipotoxicity. *Apoptosis*, 14(12), 1484-1495.
- Kwon, Y., Garcia-Bassets, I., Hutt, K. R., Cheng, C. S., Jin, M., Liu, D., Fu, X. (2007). Sensitive ChIP-DSL technology reveals an extensive estrogen receptor -binding program on human gene promoters. *Proceedings of the National Academy of Sciences*, 104(12), 4852-4857.

- Labbe, G., Pessayre, D., & Fromenty, B. (2008). Drug-induced liver injury through mitochondrial dysfunction: mechanisms and detection during preclinical safety studies. *Fundamental & Clinical Pharmacology*, 22(4), 335-353.
- Lakhani, S. A. (2006). Caspases 3 and 7: Key mediators of mitochondrial events of Apoptosis. *Science*, 311(5762), 847-851.
- Lammert, C., Bjornsson, E., Niklasson, A., & Chalasani, N. (2009). Oral medications with significant hepatic metabolism at higher risk for hepatic adverse events. *Hepatology*, 51(2), 615-620.
- Lange, C. M., Bojunga, J., Hofmann, W. P., Wunder, K., Mihm, U., Zeuzem, S., & Sarrazin, C. (2009). Severe lactic acidosis during treatment of chronic hepatitis B with entecavir in patients with impaired liver function. *Hepatology*, 50(6), 2001-2006.
- Lantz, R. C. (2001). Rapid Reduction of Intracellular Glutathione in Human Bronchial Epithelial Cells Exposed to Occupational Levels of Toluene Diisocyanate. *Toxicological Sciences*, 60(2), 348-355.
- Lawrence, J. M., Imperatore, G., Dabelea, D., Mayer-Davis, E. J., Linder, B., Saydah, S., D'Agostino, R. B. (2014). Trends in Incidence of Type 1 Diabetes Among Non-Hispanic White Youth in the U.S., 2002–2009. *Diabetes*, 63(11), 3938-3945.
- Lee, E., Kim, J., Ahn, Y., Seo, J., Ko, A., Jeong, M., Song, J. (2012). Ubiquitination and degradation of the FADD adaptor protein regulate death receptor-mediated apoptosis and necroptosis. *Nature Communications*, 3(1).
- Lee, J. K., Marion, T. L., Abe, K., Lim, C., Pollock, G. M., & Brouwer, K. L. (2009). Hepatobiliary Disposition of Troglitazone and Metabolites in Rat and Human Sandwich-Cultured Hepatocytes: Use of Monte Carlo Simulations to Assess the Impact of Changes in Biliary Excretion on Troglitazone Sulfate Accumulation. *Journal of Pharmacology and Experimental Therapeutics*, 332(1), 26-34.
- Lee, K., Park, J., Lee, S., Lim, H., Jang, Y., & Park, H. (2006). Troglitazone inhibits endothelial cell proliferation through suppression of casein kinase 2 activity. *Biochemical and Biophysical Research Communications*, 346(1), 83-88.
- Lee, T. I., Johnstone, S. E., & Young, R. A. (2006). Chromatin immunoprecipitation and microarray-based analysis of protein location. *Nature Protocols*, 1(2), 729-748.
- Leist, M., Hasiwa, N., Daneshian, M., & Hartung, T. (2012). Validation and quality control of replacement alternatives –current status and future challenges. *Toxicology Research*, 1(1), 8.
- Lennernas, H. (2007). Modeling Gastrointestinal Drug Absorption Requires More *In Vivo* Biopharmaceutical Data: Experience from *In Vivo* Dissolution and Permeability Studies in Humans. *Current Drug Metabolism*, 8(7), 645-657.
- Leslie, N. R., & Downes, C. (2002). PTEN: The downside of PI 3-kinase signalling. *Cellular Signalling*, 14(4), 285-295.

- Leslie, R. D. (2010). Predicting adult-onset autoimmune diabetes: Clarity from complexity. *Diabetes*, 59(2), 330-331.
- Letai, A., Bassik, M. C., Walensky, L. D., Sorcinelli, M. D., Weiler, S., & Korsmeyer, S. J. (2002). Distinct BH3 domains either sensitize or activate mitochondrial apoptosis, serving as prototype cancer therapeutics. *Cancer Cell*, 2(3), 183-192.
- Lewis, C., Griffiths, B., Santos, C., Pende, M., & Schulze, A. (2011). Regulation of the SREBP transcription factors by mTORC1. *Biochemical Society Transactions*, 39(2), 495-499.
- Li, L., Jick, H., & Jick, S. S. (2009). Updated study on risk of cholestatic liver disease and flucloxacillin. *British Journal of Clinical Pharmacology*, 68(2), 269-270.
- Li, M., Li, C., Allen, A., Stanley, C. A., & Smith, T. J. (2013). Glutamate Dehydrogenase: Structure, allosteric regulation, and role in insulin homeostasis. *Neurochemical Research*, 39(3), 433-445.
- Li, N., Ragheb, K., Lawler, G., Sturgis, J., Rajwa, B., Melendez, J. A., & Robinson, J. P. (2002). Mitochondrial Complex I Inhibitor Rotenone Induces Apoptosis through Enhancing Mitochondrial Reactive Oxygen Species Production. *Journal of Biological Chemistry*, 278(10), 8516-8525.
- Li, T., & Apte, U. (2015). Bile Acid Metabolism and Signaling in Cholestasis, Inflammation, and Cancer. *Cytochrome P450 Function and Pharmacological Roles in Inflammation and Cancer*, 263-302.
- Li, T., & Chiang, J. Y. (2013). Nuclear receptors in bile acid metabolism. *Drug Metabolism Reviews*, 45(1), 145-155.
- Li, T., & Chiang, J. Y. (2017). Bile Acid-Induced Liver Injury in Cholestasis. *Cellular Injury in Liver Diseases*, 143-172.
- Liao, X., Wang, Y., & Wong, C. (2010). Troglitazone induces cytotoxicity in part by promoting the degradation of peroxisome proliferator-activated receptor γ co-activator-1 α protein. *British Journal of Pharmacology*, 161(4), 771-781.
- Lim, D., Fedrizzi, L., Tartari, M., Zuccato, C., Cattaneo, E., Brini, M., & Carafoli, E. (2007). Calcium Homeostasis and Mitochondrial Dysfunction in Striatal Neurons of Huntington Disease. *Journal of Biological Chemistry*, 283(9), 5780-5789.
- Lim, J. S., Brown, J. S., & De Bono, J. S. (2018). Can Early Clinical Trials Help Deliver More Precise Cancer Care? Novel Designs of Early Phase Trials for Cancer Therapeutics, 115-128.
- Lin, H., & Accili, D. (2011). Hormonal regulation of hepatic glucose production in health and disease. *Cell Metabolism*, 14(1), 9-19.
- Ling, Z., Shu, N., Xu, P., Wang, F., Zhong, Z., Sun, B., Liu, X. (2016). Involvement of pregnane X receptor in the impaired glucose utilization induced by atorvastatin in hepatocytes. *Biochemical Pharmacology*, 100, 98-111.

Liu, J. (2004). Apoptosis-Dependent and Apoptosis-Independent Functions Bim in Prostate Cancer Cells.

Liu, W., Zeng, X., Liu, Y., Liu, J., Li, C., Chen, L., Chen, H., & Ouyang, D. (2021). The immunological mechanisms and immune-based biomarkers of drug-induced liver injury. *Frontiers in Pharmacology*, 12.

Liu, Z., Govindarajan, S., Okamoto, S., & Dennert, G. (2001). Fas-mediated Apoptosis causes elimination of virus-specific cytotoxic T cells in the virus-infected liver. *The Journal of Immunology*, 166(5), 3035-3041.

Lonard, D. M., & O'Malley, B. W. (2007). Nuclear receptor Coregulators: Judges, juries, and executioners of cellular regulation. *Molecular Cell*, 27(5), 691-700.

Lopez, G., Noale, M., Corti, C., Gaudio, G., Sajjadi, E., Venetis, K., Fusco, N. (2020). PTEN expression as a complementary Biomarker for mismatch repair testing in breast cancer. *International Journal of Molecular Sciences*, 21(4), 1461.

López-Hernández, F. J., Ortiz, M. A., & Piedrafita, F. J. (2006). The extrinsic and intrinsic apoptotic pathways are differentially affected by temperature upstream of mitochondrial damage. *Apoptosis*, 11(8), 1339-1347.

López-Velázquez, J. A., Carrillo-Córdova, L. D., Chávez-Tapia, N. C., Uribe, M., & Méndez-Sánchez, N. (2012). Nuclear Receptors in Nonalcoholic Fatty Liver Disease. *Journal of Lipids*, 2012, 1-10.

Lu, P., & Xie, W. (2017). Xenobiotic receptors in the crosstalk between drug metabolism and energy metabolism. *Drug Metabolism in Diseases*, 257-278.

Luo, J., Jiang, L., Yang, H., & Song, B. (2019). Intracellular cholesterol transport by sterol transfer proteins at membrane contact sites. *Trends in Biochemical Sciences*, 44(3), 273-292.

Macherey, A., & Dansette, P. M. (2015). Biotransformations leading to toxic metabolites. *The Practice of Medicinal Chemistry*, 585-614.

Mack, A., Fürmann, C., & Häcker, G. (2000). Detection of caspase-activation in intact lymphoid cells using standard caspase substrates and inhibitors. *Journal of Immunological Methods*, 241(1-2), 19-31.

Madan, A. K., Bajaj, S., & Dureja, H. (2012). Classification Models for Safe Drug Molecules. *Methods in Molecular Biology*, 99-124.

Madsen, K. G., Grönberg, G., Skonberg, C., Jurva, U., Hansen, S. H., & Olsen, J. (2008). Electrochemical Oxidation of Troglitazone: Identification and Characterization of the Major Reactive Metabolite in Liver Microsomes. *Chem. Res. Toxicology*, 21(10), 2035-2041.

Madsen, M., Aarup, A., Albinsson, S., Hartvigsen, K., Sørensen, C. M., Turczynska, K., Pedersen, T. X. (2017). Uraemia modulates the phenotype of aortic smooth muscle cells. *Atherosclerosis*, 257, 64-70.

Maglich, J. M., Stoltz, C. M., Goodwin, B., Hawkins-Brown, D., Moore, J. T., & Kliewer, S. A. (2002). Nuclear Pregnane X Receptor and Constitutive Androstane Receptor Regulate Overlapping but Distinct Sets of Genes Involved in Xenobiotic Detoxification. *Molecular Pharmacology*, 62(3), 638-646.

Maher, J. J. (2001). Interactions between Hepatic Stellate Cells and the Immune System. *Seminars in Liver Disease*, 21(03), 417-426.

Maianski, N. A., Geissler, J., Srinivasula, S. M., Alnemri, E. S., Roos, D., & Kuijpers, T. W. (2003). Functional characterization of mitochondria in neutrophils: a role restricted to apoptosis. *Cell Death & Differentiation*, 11(2), 143-153.

Maillette de Buy Wenniger, L., & Beuers, U. (2010). Bile salts and cholestasis. *Digestive and Liver Disease*, 42(6), 409-418.

Makhouri, F. R., & Ghasemi, J. B. (2018). *In Silico* studies in drug research against neurodegenerative diseases. *Current Neuropharmacology*, 16(6), 664-725.

Malarkey, D. E., Johnson, K., Ryan, L., Boorman, G., & Maronpot, R. R. (2005). New Insights into Functional Aspects of Liver Morphology. *Toxicologic Pathology*, 33(1), 27-34.

Malsy, M., Bitzinger, D., Graf, B., & Bundscherer, A. (2019). Staurosporine induces apoptosis in pancreatic carcinoma cells PaTu 8988t and Panc-1 via the intrinsic signaling pathway. *European Journal of Medical Research*, 24(1).

Maman, S., & Witz, I. P. (2018). A history of exploring cancer in context. *Nature Reviews Cancer*, 18(6), 359-376.

Manivannan, A., Soundararajan, P., & Jeong, B. R. (2017). Role of reactive oxygen species signaling in cell proliferation and differentiation. *Reactive Oxygen Species in Plants*, 319-329.

Mansouri, A., Tarhuni, A., Larosche, I., Reyl-Desmars, F., Demeilliers, C., Degoul, F., Pessayre, D. (2010). MnSOD Overexpression Prevents Liver Mitochondrial DNA Depletion after an Alcohol Binge but Worsens This Effect after Prolonged Alcohol Consumption in Mice. *Digestive Diseases*, 28(6), 756-775.

Marco-Lázaro, R., Pérez-Martos, A., Fernández-Silva, P., & Enriquez, J. (2011). Reconstitution of the mitochondrial inner membrane protein Cox10 by using inteins. *Mitochondrion*, 11(4), 677.

Marí, M., Morales, A., Colell, A., García-Ruiz, C., & Fernández-Checa, J. C. (2009). Mitochondrial Glutathione, a Key Survival Antioxidant. *Antioxidants & Redox Signaling*, 11(11), 2685-2700.

Maritim, A. C., Sanders, R. A., & Watkins, J. B. (2003). Diabetes, oxidative stress, and antioxidants: A review. *Journal of Biochemical and Molecular Toxicology*, 17(1), 24-38.

- Marks, D., & Harbord, M. (2013). Drug-induced liver injury. *Emergencies in Gastroenterology and Hepatology*, 291-30.
- Martinou, J., & Youle, R. (2011). Mitochondria in Apoptosis: Bcl-2 Family Members and Mitochondrial Dynamics. *Developmental Cell*, 21(1), 92-101.
- Masamune, A., Satoh, K., Sakai, Y., Yoshida, M., Satoh, A., & Shimosegawa, T. (2002). Ligands of Peroxisome Proliferator-activated Receptor- γ Induce Apoptosis in AR42J Cells. *Pancreas*, 24(2), 130-138.
- Masclaux-Daubresse, C., Reisdorf-Cren, M., Pageau, K., Lelandais, M., Grandjean, O., Kronenberger, J., Suzuki, A. (2006). Glutamine Synthetase-Glutamate Synthase Pathway and Glutamate Dehydrogenase Play Distinct Roles in the Sink-Source Nitrogen Cycle in Tobacco. *Plant Physiology*, 140(2), 444-456.
- Massart, J., Borgne-Sanchez, A., & Fromenty, B. (2018). Drug-Induced Mitochondrial Toxicity. *Mitochondrial Biology and Experimental Therapeutics*, 269-295.
- Masubuchi, Y., Kano, S., & Horie, T. (2006). Mitochondrial permeability transition as a potential determinant of hepatotoxicity of antidiabetic thiazolidinediones. *Toxicology*, 222(3), 233-239.
- Mathers, C. D., & Loncar, D. (2006). Projections of Global Mortality and Burden of Disease from 2002 to 2030. *PLoS Med*, 3(11), e442.
- Mathieu, J., & Ruohola-Baker, H. (2017). Metabolic remodelling during the loss and acquisition of pluripotency. *Development*, 144(4), 541-551.
- Matsumoto, S. (2011). Autologous islet cell transplantation to prevent surgical diabetes. *Journal of Diabetes*, 3(4), 328-336.
- Matsumura, K., Saito, T., Takahashi, Y., Ozeki, T., Kiyotani, K., Fujieda, M., ... Kamataki, T. (2004). Identification of a Novel Polymorphic Enhancer of the Human CYP3A4 Gene. *Molecular Pharmacology*, 65(2), 326-334.
- Matteucci, E., & Giampietro, O. (2014). Epidemiology of Cardiovascular Disease in Patients with Type 1 Diabetes: European Perspective. *Experimental and Clinical Endocrinology & Diabetes*, 122(04), 208-214.
- Matthews, H., Hanison, J., & Nirmalan, N. (2016). "Omics"-Informed Drug and Biomarker Discovery: Opportunities, Challenges and Future Perspectives. *Proteomes*, 4(3), 28.
- Mayo, M. W., Madrid, L. V., Westerheide, S. D., Jones, D. R., Yuan, X., Baldwin, A. S., & Whang, Y. E. (2002). PTEN blocks tumour necrosis factor-induced NF- κ B-dependent transcription by inhibiting the Transactivation potential of the p65 subunit. *Journal of Biological Chemistry*, 277(13), 11116-11125.
- McCommis, K., & Finck, B. (2015). Mitochondrial pyruvate transport: a historical perspective and future research directions. *Biochemical Journal*, 466(3), 443-454.

- McDonnell, M. A., Wang, D., Khan, S. M., Vander Heiden, M. G., & Kelekar, A. (2003). Caspase-9 is activated in a cytochrome c-independent manner early during TNF α -induced apoptosis in murine cells. *Cell Death and Differentiation*, 10(9), 1005-1015.
- McGill, M. R., Ramachandran, A., & Jaeschke, H. (2014). Oxidant Stress and Drug-Induced Hepatotoxicity. *Systems Biology of Free Radicals and Antioxidants*, 1757-1785.
- McIlwain, D. R., Berger, T., & Mak, T. W. (2013). Caspase Functions in Cell Death and Disease. *Cold Spring Harbor Perspectives in Biology*, 5(4), a008656-a008656
- McPherson, R., & Gauthier, A. (2004). Molecular regulation of SREBP function: The Insig-SCAP connection and isoform-specific modulation of lipid synthesis. *Biochemistry and Cell Biology*, 82(1), 201-211.
- Meechan, A. J., Henderson, C., Bates, C. D., Grant, M. H., & Tettey, J. N. (2006). Metabolism of troglitazone in hepatocytes isolated from experimentally induced diabetic rats. *Journal of Pharmacy and Pharmacology*, 58(10), 1359-1365.
- Menini, S., Amadio, L., Oddi, G., Ricci, C., Pesce, C., Pugliese, F., Pugliese, G. (2006). Deletion of p66Shc Longevity Gene Protects Against Experimental Diabetic Glomerulopathy by Preventing Diabetes-Induced Oxidative Stress. *Diabetes*, 55(6), 1642-1650.
- Méry, B., Guy, J., Vallard, A., Espenel, S., Ardail, D., Rodriguez-Lafrasse, C., Rancoule, C., & Magné, N. (2017). *In vitro* cell death determination for drug discovery: A landscape review of real issues. *Journal of Cell Death*, 10, 117967071769125.
- Michiels, C. (2003). Endothelial cell functions. *Journal of Cellular Physiology*, 196(3), 430-443.
- Miller, B. W., Willett, K. C., & Desilets, A. R. (2011). Rosiglitazone and Pioglitazone for the treatment of Alzheimer's disease. *Annals of Pharmacotherapy*, 45(11), 1416-1424.
- Miller, M. A., & Zachary, J. F. (2017). Mechanisms and morphology of cellular injury, adaptation, and death. *Pathologic Basis of Veterinary Disease*, 2-43. e19.
- Ming, M. (2006). Effect of ligand troglitazone on peroxisome proliferator-activated receptor γ expression and cellular growth in human colon cancer cells. *World Journal of Gastroenterology*, 12(45), 7263.
- Mitsugi, R., Sumida, K., Fujie, Y., Tukey, R. H., Itoh, T., & Fujiwara, R. (2016). Acyl-glucuronide as a Possible Cause of Trovafloxacin-Induced Liver Toxicity: Induction of Chemokine (C-X-C Motif) Ligand 2 by Trovafloxacin Acyl-glucuronide. *Biological & Pharmaceutical Bulletin*, 39(10), 1604-1610.

- Monte, M. J., Marin, J. J., Antelo, A., & Vazquez-Tato, J. (2009). Bile acids: Chemistry, physiology, and pathophysiology. *World Journal of Gastroenterology*, 15(7), 804.
- Moochhala, S., & Lee, E. (1991). Effects of recombinant human interferon alpha on aryl hydrocarbon hydroxylase activity in cultured human peripheral lymphocytes. *Life Sciences*, 48(18), 1715-1719.
- Moore, J. T., Moore, L. B., Maglich, J. M., & Kliewer, S. A. (2003). Functional and structural comparison of PXR and CAR. *Biochimica et Biophysica Acta (BBA) - General Subjects*, 1619(3), 235-238.
- Moore, K. L., Dalley, A. F., & Agur, A. M. (2010). *Clinically Oriented Anatomy*. Philadelphia, PA: Lippincott Williams & Wilkins.
- Moreno, S., Farioli-Vecchioli, S., & Cerù, M. (2004). Immunolocalization of peroxisome proliferator-activated receptors and retinoid x receptors in the adult rat CNS. *Neuroscience*, 123(1), 131-145.
- Morgan, E. T., Li-Masters, T., & Cheng, P. (2002). Mechanisms of cytochrome P450 regulation by inflammatory mediators. *Toxicology*, 181-182, 207-210.
- Morgan, R. E., Trauner, M., Van Staden, C. J., Lee, P. H., Ramachandran, B., Eschenberg, M., Hamadeh, H. K. (2010). Interference with Bile Salt Export Pump Function Is a Susceptibility Factor for Human Liver Injury in Drug Development. *Toxicological Sciences*, 118(2), 485-500.
- Morgan, S., Grootendorst, P., Lexchin, J., Cunningham, C., & Greyson, D. (2011). The cost of drug development: A systematic review. *Health Policy*, 100(1), 4-17.
- Moses, R. (2009). Fixed combination of repaglinide and metformin in the management of type 2 diabetes. *Diabetes, Metabolic Syndrome and Obesity: Targets and Therapy*, 101.
- Moutinho, M., Codocedo, J. F., Puntambekar, S. S., & Landreth, G. E. (2019). Nuclear receptors as therapeutic targets for neurodegenerative diseases: Lost in translation. *Annual Review of Pharmacology and Toxicology*, 59(1), 237-261.
- Mudaliar, S., & Henry, R. R. (2001). New oral therapies for type 2 diabetes mellitus: The Glitazones or insulin sensitizers. *Annual Review of Medicine*, 52(1), 239-257.
- Muralidhara, S., Ramanathan, R., Mehta, S. M., Lash, L. H., Acosta, D., & Bruckner, J. V. (2001). Acute, Subacute, and Subchronic Oral Toxicity Studies of 1,1-Dichloroethane in Rats: Application to Risk Evaluation. *Toxicological Sciences*, 64(1), 135-145.
- Murphy, A. N. (2020). Beneficial effects of inhibition of the mitochondrial pyruvate carrier and the mechanism of action of Thiazolidinediones. *The FASEB Journal*, 34(S1), 1-1.

Murphy, M. (2008). How mitochondria produce reactive oxygen species. *Biochemical Journal*, 417(1), 1-13.

Nadanaciva, S., Dykens, J. A., Bernal, A., Capaldi, R. A., & Will, Y. (2007). Mitochondrial impairment by PPAR agonists and statins identified via immunocaptured OXPHOS complex activities and respiration. *Toxicology and Applied Pharmacology*, 223(3), 277-287.

Nadanaciva, S., Rana, P., Beeson, G. C., Chen, D., Ferrick, D. A., Beeson, C. C., & Will, Y. (2012). Assessment of drug-induced mitochondrial dysfunction via altered cellular respiration and acidification measured in a 96-well platform. *Journal of Bioenergetics and Biomembranes*, 44(4), 421-437.

Nagamine, M., Okumura, T., Tanno, S., Sawamukai, M., Motomura, W., Takahashi, N., & Kongo, Y. (2003). PPAR γ ligand-induced apoptosis through a p53-dependent mechanism in human gastric cancer cells. *Cancer Science*, 94(4), 338-343.

Naifeh J, Varacallo M. (2018). *Biochemistry, Aerobic Glycolysis*. Treasure Island (FL): StatPearls Publishing.

Nakagawa, Y., & Medina, J. (2018). The role of the glucose-sensing receptor in glucose-induced insulin secretion in pancreatic β -cells. *Glucose-sensing Receptor in Pancreatic Beta-cells*, 61-71.

Nakamura, K., Moore, R., Negishi, M., & Sueyoshi, T. (2007). Nuclear Pregnane X Receptor Cross-talk with FoxA2 to Mediate Drug-induced Regulation of Lipid Metabolism in Fasting Mouse Liver. *Journal of Biological Chemistry*, 282(13), 9768-9776.

Nakayama, S., Atsumi, R., Takakusa, H., Kobayashi, Y., Kurihara, A., Nagai, Y., Okazaki, O. (2009). A zone classification system for risk assessment of idiosyncratic drug toxicity using daily dose and covalent binding. *Drug Metabolism and Disposition*, 37(9), 1970-1977.

Nancy, Q., & Troy, A. (2013). *Programmed Cell Death in T Cell Development*. Apoptosis.

Narayanan, P. K., Hart, T., Elcock, F., Zhang, C., Hahn, L., McFarland, D., Bugelski, P. (2003). Troglitazone-induced intracellular oxidative stress in rat hepatoma cells: A flow cytometric assessment. *Cytometry*, 52A (1), 28-35.

Natali, A., & Ferrannini, E. (2006). Effects of metformin and thiazolidinediones on suppression of hepatic glucose production and stimulation of glucose uptake in type 2 diabetes: A systematic review. *Diabetologia*, 49(3), 434-441. Ekins, S., & Erickson, J. A. (2002). A Pharmacophore for Human Pregnane X Receptor Ligands. *Drug Metabolism and Disposition*, 30(1), 96-99.

Newell, D., Silvester, J., McDowell, C., & Burtles, S. (2004). The Cancer Research UK experience of pre-clinical toxicology studies to support early clinical trials with novel cancer therapies. *European Journal of Cancer*, 40(6), 899-906.

Nguyen, A., & Bouscarel, B. (2008). Bile acids and signal transduction: Role in glucose homeostasis. *Cellular Signalling*, 20(12), 2180-2197.

Nicoletti, P., Aithal, G. P., Bjornsson, E. S., Andrade, R. J., Sawle, A., Arrese, M., Barnhart, H. X., Bondon-Guitton, E., Hayashi, P. H., Bessone, F., Carvajal, A., Cascorbi, I., Cirulli, E. T., Chalasani, N., Conforti, A., Coulthard, S. A., Daly, M. J., Day, C. P., Dillon, J. F., Daly, A. K. (2017). Association of liver injury from specific drugs, or groups of drugs, with polymorphisms in HLA and other genes in a genome-wide association study. *Gastroenterology*, 152(5), 1078-1089.

Noble, D. (2002). Modeling the Heart--from Genes to Cells to the Whole Organ. *Science*, 295(5560), 1678-1682.

Nogueira, V., & Hay, N. (2013). Molecular Pathways: Reactive Oxygen Species Homeostasis in Cancer Cells and Implications for Cancer Therapy. *Clinical Cancer Research*, 19(16), 4309-4314.

Norris, A. W., Chen, L., Fisher, S. J., Szanto, I., Ristow, M., Jozsi, A. C., Kahn, C. R. (2003). Muscle-specific PPAR γ -deficient mice develop increased adiposity and insulin resistance but respond to thiazolidinediones. *Journal of Clinical Investigation*, 112(4), 608-618.

Notenboom, S., Weigand, K. M., Proost, J. H., Lipzig, M. M., Van de Steeg, E., Van den Broek, P. H., Groothuis, G. M. (2016). Development of a mechanistic biokinetic model describing hepatic bile acid handling to predict possible cholestatic effects of drugs. *Toxicology Letters*, 258, S47.

Oakes, N. D., Thalen, P. G., Jacinto, S. M., & Ljung, B. (2001). Thiazolidinediones Increase Plasma-Adipose Tissue FFA Exchange Capacity and Enhance Insulin-Mediated Control of Systemic FFA Availability. *Diabetes*, 50(5), 1158-1165.

Oberhardt, M. A., Chavali, A. K., & Papin, J. A. (2009). Flux Balance Analysis: Interrogating Genome-Scale Metabolic Networks. *Methods in Molecular Biology*, 61-80.

Oberhardt, M. A., Puchalka, J., Martins dos Santos, V. A., & Papin, J. A. (2011). Reconciliation of Genome-Scale Metabolic Reconstructions for Comparative Systems Analysis. *PLoS Computational Biology*, 7(3), e1001116.

Ogimura, E., Nakagawa, T., Deguchi, J., Sekine, S., Ito, K., & Bando, K. (2017). Troglitazone inhibits bile acid Amidation: A possible risk factor for liver injury. *Toxicological Sciences*, 158(2), 347-355.

Ogimura, E., Sekine, S., & Horie, T. (2011). Bile salt export pump inhibitors are associated with bile acid-dependent drug-induced toxicity in sandwich-cultured

hepatocytes. *Biochemical and Biophysical Research Communications*, 416(3-4), 313-317.

Okuda, T., Norioka, M., Shitara, Y., & Horie, T. (2010). Multiple mechanisms underlying troglitazone-induced mitochondrial permeability transition. *Toxicology and Applied Pharmacology*, 248(3), 242-248.

Okura, T., Nakamura, M., Takata, Y., Watanabe, S., Kitami, Y., & Hiwada, K. (2000). Troglitazone induces apoptosis via the p53 and Gadd45 pathway in vascular smooth muscle cells. *European Journal of Pharmacology*, 407(3), 227-235.

Oliver III, R., Friday, E., Turturro, F., & Welbourne, T. (2008). Troglitazone induced Cytosolic acidification via Extracellular signal-response kinase activation and mitochondrial depolarization: Complex I proton pumping regulates Ammoniogenesis in proximal tubule-like LLC-PK1 -cells. *Cellular Physiology and Biochemistry*, 22(5-6), 475-486.

Oliver III, R., Friday, E., Turturro, F., & Welbourne, T. (2010). Troglitazone regulates anaplerosis via a pull/Push effect on glutamate Dehydrogenase mediated glutamate Deamination in kidney-derived epithelial cells, Implications for the Warburg effect. *Cellular Physiology and Biochemistry*, 26(4-5), 619-628.

Omicinski, C. J., Vanden Heuvel, J. P., Perdew, G. H., & Peters, J. M. (2010). Xenobiotic Metabolism, Disposition, and Regulation by Receptors: From Biochemical Phenomenon to Predictors of Major Toxicities. *Toxicological Sciences*, 120(Supplement 1), S49-S75.

Ong, M. M., Latchoumycandane, C., & Boelsterli, U. A. (2007). Troglitazone-Induced Hepatic Necrosis in an Animal Model of Silent Genetic Mitochondrial Abnormalities. *Toxicological Sciences*, 97(1), 205-213.

Ott, P., Ranek, L., & Young, M. A. (1998). Pharmacokinetics of troglitazone, a PPAR- γ agonist, in patients with hepatic insufficiency. *European Journal of Clinical Pharmacology*, 54(7), 567-571.

Paalvast, Y., Kuivenhoven, J. A., & Groen, A. K. (2015). Evaluating computational models of cholesterol metabolism. *Biochimica et Biophysica Acta (BBA) - Molecular and Cell Biology of Lipids*, 1851(10), 1360-1376.

Pai, M. P. (2012). Drug dosing based on weight and body surface area: Mathematical assumptions and limitations in obese adults. *Pharmacotherapy: The Journal of Human Pharmacology and Drug Therapy*, 32(9), 856-868.

Pan, D., Kather, M., Willmann, L., Schlimpert, M., Bauer, C., Lagies, S., Kammerer, B. (2016). Metabolic response to XD14 treatment in human breast cancer cell line MCF-7. *International Journal of Molecular Sciences*, 17(10), 1772.

Pan, Y., Li, L., Kim, G., Ekins, S., Wang, H., & Swaan, P. W. (2010). Identification and validation of novel human Pregnane X receptor activators among prescribed

drugs via ligand-based virtual screening. *Drug Metabolism and Disposition*, 39(2), 337-344.

Park, B. K., Boobis, A., Clarke, S., Goldring, C. E., Jones, D., Kenna, J. G., Baillie, T. A. (2011). Managing the challenge of chemically reactive metabolites in drug development. *Nature Reviews Drug Discovery*, 10(4), 292-306.

Park, J., Zarnegar, R., Kanauchi, H., Wong, M. G., Hyun, W. C., Ginzinger, D. G., Clark, O. H. (2005). Troglitazone, the Peroxisome Proliferator-Activated Receptor- γ Agonist, Induces Antiproliferation and Redifferentiation in Human Thyroid Cancer Cell Lines. *Thyroid*, 15(3), 222-231.

Parker, G. A., & Picut, C. A. (2005). Liver Immunobiology. *Toxicologic Pathology*, 33(1), 52-62.

Parker, J. C. (2002). Troglitazone: the discovery and development of a novel therapy for the treatment of Type 2 diabetes mellitus. *Advanced Drug Delivery Reviews*, 54(9), 1173-1197.

Parrish, A. B., Freel, C. D., & Kornbluth, S. (2013). Cellular Mechanisms Controlling Caspase Activation and Function. *Cold Spring Harbor Perspectives in Biology*, 5(6), a008672-a008672.

Parulkar, A. A., Pendergrass, M. L., Granda-Ayala, R., Lee, T. R., & Fonseca, V. A. (2001). Nonhypoglycemic effects of Thiazolidinediones. *Annals of Internal Medicine*, 134(1), 61.

Pastorino, J. G., Shulga, N., & Hoek, J. B. (2003). TNF- α -induced cell death in ethanol-exposed cells depends on p38 MAPK signaling but is independent of bid and caspase-8. *American Journal of Physiology-Gastrointestinal and Liver Physiology*, 285(3), G503-G516.

Paszek, M. J., Zahir, N., Johnson, K. R., Lakins, J. N., Rozenberg, G. I., Gefen, A., Weaver, V. M. (2005). Tensional homeostasis and the malignant phenotype. *Cancer Cell*, 8(3), 241-254.

Pate, M., Damarla, V., Chi, D. S., Negi, S., & Krishnaswamy, G. (2010). Endothelial Cell Biology. *Advances in Clinical Chemistry*, 109-130.

Pauli-Magnus, C., Stieger, B., Meier, Y., Kullak-Ublick, G. A., & Meier, P. J. (2005). Enterohepatic transport of bile salts and genetics of cholestasis. *Journal of Hepatology*, 43(2), 342-357.

Paulsen, G., Cumming, K. T., Holden, G., Hallén, J., Rønnestad, B. R., Sveen, O., Raastad, T. (2014). Vitamin C and E supplementation hampers cellular adaptation to endurance training in humans: a double-blind, randomised, controlled trial. *The Journal of Physiology*, 592(8), 1887-1901.

Peng, T., & Jou, M. (2004). Mitochondrial Swelling and Generation of Reactive Oxygen Species Induced by Photoirradiation Are Heterogeneously Distributed. *Mitochondrial Pathogenesis*, 112-122.

Perez, M. J., & Briz, O. (2009). Bile-acid-induced cell injury and protection. *World Journal of Gastroenterology*, 15(14), 1677.

Perry, A., & Ofek, I. (1984). Inhibition of blood clearance and hepatic tissue binding of *Escherichia coli* by liver lectin-specific sugars and glycoproteins. *Infection and Immunity*, 43(1), 257-262.

Pessayre, D., Fromenty, B., Berson, A., Robin, M., Lettéron, P., Moreau, R., & Mansouri, A. (2012). Central role of mitochondria in drug-induced liver injury. *Drug Metabolism Reviews*, 44(1), 34-8.

Petersen, M. C., & Shulman, G. I. (2018). Mechanisms of insulin action and insulin resistance. *Physiological Reviews*, 98(4), 2133-2223.

Petunina, N. A., & Telnova, M. E. (2018). Diabetes and obesity. The role of agonists glucagon-like peptide-1 of in the treatment of type 2 diabetes. *Diabetes mellitus*, 21(4), 293-300.

Pfizenmaier, J., Junghans, L., Teleki, A., & Takors, R. (2016). Hyperosmotic stimulus study discloses benefits in ATP supply and reveals miRNA/mRNA targets to improve recombinant protein production of CHO cells. *Biotechnology Journal*, 11(8), 1037-1047.

Phelix, C. F., Bourdon, A. K., Dugan, J. L., Villareal, G., & Perry, G. (2017). MSDC-0160 and MSDC-0602 Binding with Human Mitochondrial Pyruvate Carrier (MPC) 1 and 2 Heterodimer. *International Journal of Knowledge Discovery in Bioinformatics*, 7(2), 43-67.

Phimister, A. J., Williams, K. J., Van Winkle, L. S., & Plopper, C. G. (2005). Consequences of abrupt Glutathione depletion in murine Clara cells: Ultrastructural and biochemical investigations into the role of Glutathione loss in naphthalene cytotoxicity. *Journal of Pharmacology and Experimental Therapeutics*, 314(2), 506-513.

Phypers, B., & Pierce, J. T. (2006). Lactate physiology in health and disease. *Continuing Education in Anesthesia Critical Care & Pain*, 6(3), 128-132.

Pi, W., Guo, X., Su, L., & Xu, W. (2013). Troglitazone upregulates PTEN expression and induces the apoptosis of pulmonary artery smooth muscle cells under hypoxic conditions. *International Journal of Molecular Medicine*, 32(5), 1101-1109.

Plaitakis, A., Kalef-Ezra, E., Kotzamani, D., Zaganas, I., & Spanaki, C. (2017). The Glutamate Dehydrogenase Pathway and Its Roles in Cell and Tissue Biology in Health and Disease. *Biology*, 6(4), 11.

Plaitakis, A., Zaganas, I., & Spanaki, C. (2013). Deregulation of glutamate dehydrogenase in human neurologic disorders. *Journal of Neuroscience Research*, 91(8), 1007-1017.

Plant, N. J. (2004). Strategies for using *in vitro* screens in drug metabolism. *Drug Discovery*.

Plant, N. J. (2015). An introduction to systems toxicology. *Toxicology Research*, 4(1), 9-22.

Plant, N., & Aouabdi, S. (2009). Nuclear receptors: The controlling force in drug metabolism of the liver? *Xenobiotica*, 39(8), 597-605.

Pletz, J., Ebbrell, D., Enoch, S., Firman, J., Madden, J., Webb, S., & Cronin, M. (2018). Development of a Robust *In Silico* Profiler to Screen for Nephrotoxicity Endpoints. *Toxicology Letters*, 295, S97.

Poirier, Y., Antonenkov, V. D., Glumoff, T., & Hiltunen, J. K. (2006). Peroxisomal β -oxidation—A metabolic pathway with multiple functions. *Biochimica et Biophysica Acta (BBA) - Molecular Cell Research*, 1763(12), 1413-1426.

Poole, R. (2015). Type 1 diabetes in adults: New NICE guidance on diagnosis and management. *Practical Diabetes*, 32(8), 279-280.

Porceddu, M., Buron, N., Roussel, C., Labbe, G., Fromenty, B., & Borgne-Sanchez, A. (2012). Prediction of Liver Injury Induced by Chemicals in Human with a Multiparametric Assay on Isolated Mouse Liver Mitochondria. *Toxicological Sciences*, 129(2), 332-345.

Porstmann, T., Santos, C. R., Griffiths, B., Cully, M., Wu, M., Leever, S., Schulze, A. (2008). SREBP Activity Is Regulated by mTORC1 and Contributes to Akt-Dependent Cell Growth. *Cell Metabolism*, 8(3), 224-236.

Prabhu, S., Fackett, A., Lloyd, S., McClellan, H. A., Terrell, C. M., Silber, P. M., & Li, A. P. (2002). Identification of glutathione conjugates of troglitazone in human hepatocytes. *Chemico-Biological Interactions*, 142(1-2), 83-97.

Pratley, R. E. (2013). The Early Treatment of Type 2 Diabetes. *The American Journal of Medicine*, 126(9), S2-S9.

Premchaiswadi, W., & Jongsawat, N. (2012). Building a Bayesian network model based on the combination of structure learning algorithms and weighting expert opinions scheme. *Bayesian Networks*.

Pridgeon, C., Wong, M. W., & Goldring, C. (2017). Development of stem cell derived hepatocyte-like cells: 3D co-culture with primary non-parenchymal liver cells and low-oxygen culture. *Toxicology Letters*, 280, S298.

Produit-Zengaffinen, N., Davis-Lameloise, N., Perreten, H., Bécard, D., Gjinovci, A., Keller, P. A., Assimacopoulos-Jeannet, F. (2006). Increasing uncoupling protein-2 in pancreatic beta cells does not alter glucose-induced insulin secretion but decreases production of reactive oxygen species. *Diabetologia*, 50(1), 84-93.

Puc, J., Keniry, M., Li, H. S., Pandita, T. K., Choudhury, A. D., Memeo, L., Parsons, R. (2005). Lack of PTEN sequesters CHK1 and initiates genetic instability. *Cancer Cell*, 7(2), 193-204.

- Puche, J. E., Lee, Y. A., Jiao, J., Aloman, C., Fiel, M. I., Muñoz, U., Friedman, S. L. (2013). A novel murine model to deplete hepatic stellate cells uncovers their role in amplifying liver damage in mice. *Hepatology*, 57(1), 339-350.
- Puhl, A. C., Bernardes, A., Silveira, R. L., Yuan, J., Campos, J. L., Saidemberg, D. M., Polikarpov, I. (2012). Mode of Peroxisome Proliferator-Activated Receptor Activation by Luteolin. *Molecular Pharmacology*, 81(6), 788-799.
- Pusl, T., Wild, N., Vennegeerts, T., Wimmer, R., Göke, B., Brand, S., & Rust, C. (2008). Free fatty acids sensitize hepatocytes to bile acid-induced apoptosis. *Biochemical and Biophysical Research Communications*, 371(3), 441-445.
- Puthalakath, H., & Strasser, A. (2002). Keeping killers on a tight leash: Transcriptional and post-translational control of the pro-apoptotic activity of BH3-only proteins. *Cell Death & Differentiation*, 9(5), 505-512.
- Puthalakath, H., Huang, D. C., O'Reilly, L. A., King, S. M., & Strasser, A. (1999). The Proapoptotic Activity of the Bcl-2 Family Member Bim Is Regulated by Interaction with the Dynein Motor Complex. *Molecular Cell*, 3(3), 287-296.
- Qian, Y., Feldman, E., Pennathur, S., Kretzler, M., & Brosius, F. C. (2008). From fibrosis to sclerosis: Mechanisms of Glomerulosclerosis in diabetic nephropathy. *Diabetes*, 57(6), 1439-1445.
- Rachek, L. I., Yuzefovych, L. V., LeDoux, S. P., Julie, N. L., & Wilson, G. L. (2009). Troglitazone, but not rosiglitazone, damages mitochondrial DNA and induces mitochondrial dysfunction and cell death in human hepatocytes. *Toxicology and Applied Pharmacology*, 240(3), 348-354.
- Rang, H. P., Dale, M. M., Ritter, J. M., Flower, R. J., & Henderson, G. (2012). Drug metabolism and elimination. *Rang & Dale's Pharmacology*, 115-122.
- Rathod, S. D., Crampin, A. C., Musicha, C., Kayuni, N., Banda, L., Saul, J., Nyirenda, M. J. (2018). Glycated haemoglobin A1c(HbA1c) for detection of diabetes mellitus and impaired fasting glucose in Malawi: a diagnostic accuracy study. *BMJ Open*, 8(5), e020972.
- Ratushny, A., Likhoshvai, V., Ignatieva, E., Goryanin, I., & Kolchanov, N. (2003). Resilience of cholesterol concentration to a wide range of mutations in the cell. *Complexus*, 1(3), 142-148.
- Raunio, H. (2011). *In Silico Toxicology-Non-Testing Methods*. *Frontiers in Pharmacology*, 2.
- Reynolds, M., & Clem, B. (2014). Troglitazone suppresses tumour cell growth and glutamine metabolism through a PPAR-independent mechanism. *Cancer & Metabolism*, 2(S1).
- Riedl, S., Renatus, M., Schwarzenbacher, R., Zhou, Q., Sun, C., Fesik, S., Salvesen, G. (2001). Crystal structure of the complex of xiap-bir2 and caspase 3.

Ritschel, T., Hermans, S. M., Schreurs, M., Van den Heuvel, J. J., Koenderink, J. B., Greupink, R., & Russel, F. G. (2014). *In Silico* identification and *in vitro* validation of potential Cholestatic compounds through 3D ligand-based Pharmacophore modeling of BSEP inhibitors. *Chemical Research in Toxicology*, 27(5), 873-881.

Rodrigues, A. D., Lai, Y., Cvijic, M. E., Elkin, L. L., Zvyaga, T., & Soars, M. G. (2013). Drug-induced perturbations of the bile acid pool, Cholestasis, and Hepatotoxicity: Mechanistic considerations beyond the direct inhibition of the bile salt export pump. *Drug Metabolism and Disposition*, 42(4), 566-574.

Roede, J. R., Park, Y., Li, S., Strobel, F. H., & Jones, D. P. (2012). Detailed mitochondrial Phenotyping by high resolution Metabolomics. *PLoS ONE*, 7(3), e33020.

Roglic, G. (2016). WHO global report on diabetes: A summary. *International Journal of Noncommunicable Diseases*, 1(1), 3.

Rogue, A., Lambert, C., Jossé, R., Antherieu, S., Spire, C., Claude, N., & Guillouzo, A. (2011). Comparative Gene Expression Profiles Induced by PPAR γ and PPAR α/γ Agonists in Human Hepatocytes. *PLoS ONE*, 6(4), e18816.

Rohr, C., Marwan, W., & Heiner, M. (2010). Snoopy--a unifying Petri net framework to investigate biomolecular networks. *Bioinformatics*, 26(7), 974-975.

Rosamond, W., Flegal, K., Furie, K., Go, A., Greenlund, K., & Hong, Y. (2008). Heart disease and stroke statistics—2008 update. *Circulation*, 117(4).

Rosenfeld, M. G., & Glass, C. K. (2001). Coregulator codes of transcriptional regulation by nuclear receptors. *Journal of Biological Chemistry*, 276(40), 36865-36868

Rowland, A., Miners, J. O., & Mackenzie, P. I. (2013). The UDP-glucuronosyltransferases: Their role in drug metabolism and detoxification. *The International Journal of Biochemistry & Cell Biology*, 45(6), 1121-1132.

Rusmann, S., Kullak-Ublick, G., & Grattagliano, I. (2009). Current concepts of mechanisms in drug-induced Hepatotoxicity. *Current Medicinal Chemistry*, 16(23), 3041-3053

Ryter, S. W., Alam, J., & Choi, A. M. (2006). Heme oxygenase-1/Carbon monoxide: From basic science to therapeutic applications. *Physiological Reviews*, 86(2), 583-650.

Ryter, S. W., Kim, H. P., Hoetzel, A., Park, J. W., Nakahira, K., Wang, X., & Choi, A. M. (2007). Mechanisms of Cell Death in Oxidative Stress. *Antioxidants & Redox Signaling*, 9(1), 49-89.

Sachs, J. R., Mayawala, K., Gadamsetty, S., Kang, S. P., & De Alwis, D. P. (2015). Optimal Dosing for Targeted Therapies in Oncology: Drug Development Cases Leading by Example. *Clinical Cancer Research*, 22(6), 1318-1324.

Sahi, J., Black, C. B., Hamilton, G. A., Zheng, X., Jolley, S., Rose, K. A., Sinz, M. W. (2003). Comparative Effects of Thiazolidinediones on *in Vitro* P450 Enzyme Induction and Inhibition. *Drug Metabolism and Disposition*, 31(4), 439-446.

Sakkalis, V., Sfakianakis, S., Tzamali, E., Marias, K., Stamatakos, G., Misichroni, F., Graf, N. (2014). Web-based workflow planning platform supporting the design and execution of complex Multiscale cancer models. *IEEE Journal of Biomedical and Health Informatics*, 18(3), 824-831.

Salmena, L., Carracedo, A., & Pandolfi, P. P. (2008). Tenets of PTEN tumour suppression. *Cell*, 133(3), 403-414.

Samoilova, R. I., Crofts, A. R., & Dikanov, S. A. (2011). Reaction of Superoxide Radical with Quinone Molecules. *The Journal of Physical Chemistry A*, 115(42), 11589-11593.

Santo, A., Zhu, H., & Li, Y. R. (2016). Free Radicals: From Health to Disease. *Reactive Oxygen Species*.

Santo, V. E., Rebelo, S. P., Estrada, M. F., Alves, P. M., Boghaert, E., & Brito, C. (2016). Drug screening in 3D *in vitro* tumour models: overcoming current pitfalls of efficacy read-outs. *Biotechnology Journal*, 12(1), 1600505.

Santos, J. H., Hunakova, L., Chen, Y., Bortner, C., & Van Houten, B. (2002). Cell Sorting Experiments Link Persistent Mitochondrial DNA Damage with Loss of Mitochondrial Membrane Potential and Apoptotic Cell Death. *Journal of Biological Chemistry*, 278(3), 1728-1734.

Sarup, P., Sørensen, P., & Loeschcke, V. (2014). The long-term effects of a life-prolonging heat treatment on the *Drosophila melanogaster* transcriptome suggest that heat shock proteins extend lifespan. *Experimental Gerontology*, 50, 34-39.

Schapira, A. H. (2006). Mitochondrial disease. *The Lancet*, 368(9529), 70-82.

Scheen, A. J. (2004). Combined Thiazolidinedione-Insulin Therapy. *Drug Safety*, 27(12), 841-856.

Schenone, M., Dančák, V., Wagner, B. K., & Clemons, P. A. (2013). Target identification and mechanism of action in chemical biology and drug discovery. *Nature Chemical Biology*, 9(4), 232-240.

Schieber, M., & Chandel, N. (2014). ROS Function in Redox Signaling and Oxidative Stress. *Current Biology*, 24(10), R453-R462.

Schindler, A. E., & Pasqualini, J. R. (2005). Progesterone and Progestins in Human Pregnancy and Breast Cancer. *The Journal of Steroid Biochemistry and Molecular Biology*, 97(5), 385.

Schmeding, M., Neumann, U., Boas-Knoop, S., Spinelli, A., & Neuhaus, P. (2007). Erythropoietin reduces ischemia-reperfusion injury in the rat liver. *European Surgical Research*, 39(3), 189-197.

- Schmeding, M., Rademacher, S., Boas-Knoop, S., Roecken, C., Lendeckel, U., Neuhaus, P., & Neumann, U. P. (2010). RHuEPo reduces ischemia-reperfusion injury and improves survival after transplantation of fatty livers in rats. *Transplantation*, 89(2), 161-168.
- Schmitz, G., & Torzewski, M. (2002). Cellular effects of HMG-CoA reductase inhibitors on blood cells (monocytes, macrophages, platelets). *HMG-CoA Reductase Inhibitors*, 55-80.
- Scorrano, L. (2014). Mitochondrial Apoptosis Regulation by Bcl-2 Family Members. *Pathobiology of Human Disease*, 170-174.
- Shaffer, S. M., Dunagin, M. C., Torborg, S. R., Torre, E. A., Emert, B., Krepler, C., Raj, A. (2017). Rare cell variability and drug-induced reprogramming as a mode of cancer drug resistance. *Nature*, 546(7658), 431-435.
- Shah, I., Liu, J., Judson, R. S., Thomas, R. S., & Patlewicz, G. (2016). Systematically evaluating read-across prediction and performance using a local validity approach characterized by chemical structure and bioactivity information. *Regulatory Toxicology and Pharmacology*, 79, 12-24.
- Sharma, R., Majer, F., Peta, V. K., Wang, J., Keaveney, R., Kelleher, D., Gilmer, J. F. (2010). Bile acid toxicity structure–activity relationships: Correlations between cell viability and lipophilicity in a panel of new and known bile acids using an oesophageal cell line (HET-1A). *Bioorganic & Medicinal Chemistry*, 18(18), 6886-6895.
- Shehu, A. I., Ma, X., & Venkataramanan, R. (2017). Mechanisms of drug-induced Hepatotoxicity. *Clinics in Liver Disease*, 21(1), 35-54.
- Sheu, S., Kaya, T., Waxman, D. J., & Vajda, S. (2005). Exploring the Binding Site Structure of the PPAR γ Ligand-Binding Domain by Computational Solvent Mapping†. *Biochemistry*, 44(4), 1193-1209.
- Shi, Y. (2004). Caspase activation, inhibition, and reactivation: A mechanistic view. *Protein Science*, 13(8), 1979-1987.
- Shi, Y., Wang, J., Chandarlapaty, S., Cross, J., Thompson, C., Rosen, N., & Jiang, X. (2014). PTEN is a protein tyrosine phosphatase for IRS1. *Nature Structural & Molecular Biology*, 21(6), 522-527.
- Shipkova, M., Armstrong, V. W., Oellerich, M., & Wieland, E. (2003). Acyl Glucuronide Drug Metabolites: Toxicological and Analytical Implications. *Therapeutic Drug Monitoring*, 25(1), 1-16.
- Shnitsar, I., Bashkurov, M., Masson, G. R., Ogunjimi, A. A., Mosessian, S., Cabeza, E. A., Barrios-Rodiles, M. (2015). PTEN regulates cilia through dishevelled. *Nature Communications*, 6(1).

- Shoda, L. K., Woodhead, J. L., Siler, S. Q., Watkins, P. B., & Howell, B. A. (2013). Linking physiology to toxicity using DILIsym®, a mechanistic mathematical model of drug-induced liver injury. *Biopharmaceutics & Drug Disposition*, 35(1), 33-49.
- Siminerio, L. M., Zgibor, J., & Zimecki, S. (2000). Screening for type 2 diabetes in the Pittsburgh community. *Diabetes Research and Clinical Practice*, 50, 409.
- Slivac, I., Blajić, V., Radošević, K., Kniewald, Z., & Gaurina Srček, V. (2010). Influence of different ammonium, lactate and glutamine concentrations on CCO cell growth. *Cytotechnology*, 62(6), 585-594.
- Śliwka, L., Wiktorska, K., Suchocki, P., Milczarek, M., Mielczarek, S., Lubelska, K., Chilmonczyk, Z. (2016). The comparison of MTT and CVS assays for the assessment of Anticancer agent interactions. *PLOS ONE*, 11(5), e0155772.
- Smith, M. T. (2003). Mechanisms of Troglitazone Hepatotoxicity. *Chemical Research in Toxicology*, 16(6), 679-687
- Snow, K. L., & Moseley, R. H. (2007). Effect of thiazolidinediones on bile acid transport in rat liver. *Life Sciences*, 80(8), 732-740.
- Sokal, P., Jastrzębski, Z., Jaskulska, E., Sokal, K., Jastrzębska, M., Radzimiński, Ł., Zieliński, P. (2013). Differences in Blood Urea and Creatinine Concentrations in Earthed and Unearthed Subjects during Cycling Exercise and Recovery. *Evidence-Based Complementary and Alternative Medicine*, 2013, 1-6.
- Sood, V., Costello, B. A., & Burge, M. R. (2001). How low can you go? Chronic hypoglycaemia versus normal glucose homeostasis. *Journal of Investigative Medicine*, 49(2), 205-209.
- Sousa, J. S., D'Imprima, E., & Vonck, J. (2018). Mitochondrial respiratory chain complexes. *Subcellular Biochemistry*, 167-227.
- Spanaki, C., Zaganas, I., Kleopa, K. A., & Plaitakis, A. (2010). Human GLUD2 Glutamate Dehydrogenase Is Expressed in Neural and Testicular Supporting Cells. *Journal of Biological Chemistry*, 285(22), 16748-16756.
- Spinelli, J. B., Yoon, H., Ringel, A. E., Jeanfavre, S., Clish, C. B., & Haigis, M. C. (2017). Metabolic recycling of ammonia via glutamate dehydrogenase supports breast cancer biomass. *Science*, 358(6365), 941-946.
- Stallard, N., Whitehead, A., & Ridgway, P. (2002). Statistical evaluation of the revised fixed-dose procedure. *Human & Experimental Toxicology*, 21(4), 183-196.
- Stambolic, V., MacPherson, D., Sas, D., Lin, Y., Snow, B., Jang, Y., Mak, T. (2001). Regulation of PTEN transcription by p53. *Molecular Cell*, 8(2), 317-325.
- Stampella, A., Rizzitelli, G., Donati, F., Mazzarino, M., De la Torre, X., Botrè, F., ... Massimi, M. (2015). Human hepatoma cell lines on gas foaming templated alginate scaffolds for *in vitro* drug-drug interaction and metabolism studies. *Toxicology in Vitro*, 30(1), 331-340.

- Starkov, A. A. (2008). The role of mitochondria in reactive oxygen species metabolism and signaling. *Annals of the New York Academy of Sciences*, 1147(1), 37-52.
- Stepan, A. F., Walker, D. P., Bauman, J., Price, D. A., Baillie, T. A., Kalgutkar, A. S., & Aleo, M. D. (2011). Structural alert/Reactive metabolite concept as applied in medicinal chemistry to mitigate the risk of idiosyncratic drug toxicity: A perspective based on the critical examination of trends in the top 200 drugs marketed in the United States. *Chemical Research in Toxicology*, 24(9), 1345-1410.
- Stiles, B., Groszer, M., Wang, S., Jiao, J., & Wu, H. (2004). PTENless means more. *Developmental Biology*, 273(2), 175-184.
- Stockert, J. C., Blázquez-Castro, A., Cañete, M., Horobin, R. W., & Villanueva, Á. (2012). MTT assay for cell viability: Intracellular localization of the formazan product is in lipid droplets. *Acta Histochemica*, 114(8), 785-796.
- Suga, T., Yamaguchi, H., Sato, T., Maekawa, M., Goto, J., & Mano, N. (2017). Preference of Conjugated Bile Acids over Unconjugated Bile Acids as Substrates for OATP1B1 and OATP1B3. *PLOS ONE*, 12(1), e0169719.
- Sun, Z. (2003). Hepatic allograft-derived Kupffer cells regulate T cell response in rats. *Liver Transplantation*, 9(5), 489-497.
- Susukida, T., Sekine, S., Ogimura, E., Aoki, S., Oizumi, K., Horie, T., & Ito, K. (2015). Basal efflux of bile acids contributes to drug-induced bile acid-dependent hepatocyte toxicity in rat sandwich-cultured hepatocytes. *Toxicology in Vitro*, 29(7), 1454-1463.
- Suzuki, A., Yamaguchi, M. T., Ohteki, T., Sasaki, T., Kaisho, T., Kimura, Y., Mak, T. W. (2001). T cell-specific loss of PTEN leads to defects in central and peripheral tolerance. *Immunity*, 14(5), 523-534.
- Swayne, T. C., Boldogh, I. R., & Pon, L. A. (2009). Imaging of the cytoskeleton and mitochondria in fixed budding yeast cells. *Cytoskeleton Methods and Protocols*, 171-184.
- Szabo, M., Veres, Z., Baranyai, Z., Jakab, F., & Jemnitz, K. (2013). Comparison of Human Hepatoma HepaRG Cells with Human and Rat Hepatocytes in Uptake Transport Assays in Order to Predict a Risk of Drug Induced Hepatotoxicity. *Public Library of Science*, 8(3), e59432.
- Tacke, F., & Weiskirchen, R. (2012). Update on hepatic stellate cells: Pathogenic role in liver fibrosis and novel isolation techniques. *Expert Review of Gastroenterology & Hepatology*, 6(1), 67-80.
- Tafani, M., Karpinich, N. O., Hurster, K. A., Pastorino, J. G., Schneider, T., Russo, M. A., & Farber, J. L. (2002). Cytochrome C release upon Fas receptor activation depends on translocation of full-length bid and the induction of the mitochondrial permeability transition. *Journal of Biological Chemistry*, 277(12), 10073-10082.

- TaheriChadorneshin, H., Cheragh-Birjandi, S., Goodarzy, S., & Ahmadabadi, F. (2019). The impact of high intensity interval training on serum chemerin, tumour necrosis factor-alpha and insulin resistance in overweight women. *Obesity Medicine*, 14, 100101.
- Tailor, A., Faulkner, L., Naisbitt, D., & Park, B. (2015). The chemical, genetic and immunological basis of idiosyncratic drug-induced liver injury. *Human & Experimental Toxicology*, 34(12), 1310-1317.
- Takeda, K., Ichiki, T., Tokunou, T., Iino, N., & Takeshita, A. (2001). 15-Deoxy- $\Delta^{12,14}$ -prostaglandin J₂ and Thiazolidinediones activate the MEK/ERK pathway through Phosphatidylinositol 3-Kinase in vascular smooth muscle cells. *Journal of Biological Chemistry*, 276(52), 48950-48955.
- Takeuchi, Y., Nakayama, Y., Fukusaki, E., & Irino, Y. (2018). Glutamate production from ammonia via glutamate dehydrogenase 2 activity supports cancer cell proliferation under glutamine depletion. *Biochemical and Biophysical Research Communications*, 495(1), 761-767.
- Takita, M., Seven, N., F., M., & Naziruddi, B. (2013). Beta Cell Function After Islet Transplantation. *Type 1 Diabetes*.
- Tamaki, N., Hatano, E., Taura, K., Tada, M., Kodama, Y., Nitta, T., Uemoto, S. (2008). CHOP deficiency attenuates cholestasis-induced liver fibrosis by reduction of hepatocyte injury. *American Journal of Physiology-Gastrointestinal and Liver Physiology*, 294(2), G498-G505.
- Taub, R. (2004). Liver regeneration: from myth to mechanism. *Nature Reviews Molecular Cell Biology*, 5(10), 836-847.
- Taylor, R. C., Cullen, S. P., & Martin, S. J. (2008). Apoptosis: controlled demolition at the cellular level. *Nature Reviews Molecular Cell Biology*, 9(3), 231-241.
- Teng, S., & Piquette-Miller, M. (2004). The Involvement of the Pregnane X Receptor in Hepatic Gene Regulation during Inflammation in Mice. *Journal of Pharmacology and Experimental Therapeutics*, 312(2), 841-848.
- Teranishi, T., Ohara, T., Maeda, K., Zenibayashi, M., Kouyama, K., Hirota, Y., Kasuga, M. (2007). Effects of pioglitazone and metformin on intracellular lipid content in liver and skeletal muscle of individuals with type 2 diabetes mellitus. *Metabolism*, 56(10), 1418-1424.
- Testa, B. (2014). Metabolism in drug development. *Methods and Principles in Medicinal Chemistry*, 1-26.
- Testa, B., Pedretti, A., & Vistoli, G. (2012). Reactions and enzymes in the metabolism of drugs and other xenobiotics. *Drug Discovery Today*, 17(11-12), 549-560.

- Tettey, J. N., Maggs, J. L., Rapeport, W. G., Pirmohamed, M., & Park, B. K. (2001). Enzyme-Induction Dependent Bioactivation of Troglitazone and Troglitazone Quinone *In Vivo*. *Chem. Res. Toxicol*, 14(8), 965-974.
- Tezcan, S., Ulu Ozturk, F., Ayvazoglu Soy, E., Uslu, N., & Haberal, M. (2019). Portal Venous Flow Alterations in Hepatic Artery Thrombosis Following Liver Transplant. *Experimental and Clinical Transplantation*.
- Thompson, R. A., Isin, E. M., Li, Y., Weidolf, L., Page, K., Wilson, I., Kenna, J. G. (2012). *In vitro* approach to assess the potential for risk of idiosyncratic adverse reactions caused by candidate drugs. *Chemical Research in Toxicology*, 25(8), 1616-1632.
- Thompson, R. A., Isin, E. M., Ogese, M. O., Mettetal, J. T., & Williams, D. P. (2016). Reactive metabolites: Current and emerging risk and hazard assessments. *Chemical Research in Toxicology*, 29(4), 505-533.
- Tildón, J. T., & Zielke, H. R. (2018). Glutamine. *Glutamine and Glutamate in Mammals*, 167-182.
- Tirmenstein, M. A. (2002). Effects of Troglitazone on HepG2 Viability and Mitochondrial Function. *Toxicological Sciences*, 69(1), 131-138.
- Tobias, D. K., Zhang, C., Chavarro, J., Olsen, S., Bao, W., Bjerregaard, A. A., Hu, F. B. (2016). Healthful dietary patterns and long-term weight change among women with a history of gestational diabetes mellitus. *International Journal of Obesity*, 40(11), 1748-1753.
- Toroz, D., Khanna, T., & Gould, I. R. (2019). Modeling the Effect of BSEP Inhibitors in Lipid Bilayers by Means of All-Atom Molecular Dynamics Simulation. *ACS Omega*, 4(2), 3341-3350.
- Toyoda, M., Takagi, H., Horiguchi, N., Takayama, H., Sato, K., & Mori, M. (2002). Activation of PPAR γ inhibits cell growth and induces apoptosis in human liver cancer cells. *Gastroenterology*, 118(4), A921.
- Trécherel, E., Godin, C., Louandre, C., Benchitrit, J., Poirot, S., Mazière, J., Galmiche, A. (2012). Upregulation of BAD, a pro-apoptotic protein of the BCL2 family, in vascular smooth muscle cells exposed to uremic conditions. *Biochemical and Biophysical Research Communications*, 417(1), 479-483.
- Tripathy, D., Mohanty, P., Dhindsa, S., Syed, T., Ghanim, H., Aljada, A., & Dandona, P. (2003). Elevation of free fatty acids induces inflammation and impairs vascular reactivity in healthy subjects. *Diabetes*, 52(12), 2882-2887.
- Troyano, A., Sancho, P., Fernández, C., De Blas, E., Bernardi, P., & Aller, P. (2003). The selection between apoptosis and necrosis is differentially regulated in hydrogen peroxide-treated and glutathione-depleted human promonocytic cells. *Cell Death & Differentiation*, 10(8), 889-898.

- Tsujimoto, Y. (2003). Cell death regulation by the Bcl-2 protein family in the mitochondria. *Journal of Cellular Physiology*, 195(2), 158-167.
- Turrens, J. F. (2007). Formation of Reactive Oxygen Species in Mitochondria. *Mitochondria*, 185-196.
- Tuso, P. (2014). Prediabetes and Lifestyle Modification: Time to Prevent a Preventable Disease. *The Permanente Journal*, 88-93.
- Tyagi, S., Sharma, S., Gupta, P., Saini, A., & Kaushal, C. (2011). The peroxisome proliferator-activated receptor: A family of nuclear receptors role in various diseases. *Journal of Advanced Pharmaceutical Technology & Research*, 2(4), 236.
- Uehara, T., Bennett, B., Sakata, S. T., Satoh, Y., Bilter, G. K., Westwick, J. K., & Brenner, D. A. (2005). JNK mediates hepatic ischemia reperfusion injury. *Journal of Hepatology*, 42(6), 850-859.
- Utrecht, J. (2019). Mechanisms of idiosyncratic drug-induced liver injury. *Advances in Pharmacology*, 133-163.
- Utrecht, J., & Naisbitt, D. J. (2013). Idiosyncratic adverse drug reactions: Current concepts. *Pharmacological Reviews*, 65(2), 779-808.
- Van de Poll, M. C., Soeters, P. B., Deutz, N. E., Fearon, K. C., & Dejong, C. H. (2004). Renal metabolism of amino acids: its role in interorgan amino acid exchange. *The American Journal of Clinical Nutrition*, 79(2), 185-197.
- Van Schalkwijk, D. B., De Graaf, A. A., Van Ommen, B., Van Bochove, K., Rensen, P. C., Havekes, L. M., Freidig, A. P. (2009). Improved cholesterol phenotype analysis by a model relating lipoprotein life cycle processes to particle size. *Journal of Lipid Research*, 50(12), 2398-2411.
- Van Vranken, J. G., & Rutter, J. (2016). The whole (Cell) is less than the sum of its parts. *Cell*, 166(5), 1078-1079.
- Vander Heiden, M. G., & DeBerardinis, R. J. (2017). Understanding the Intersections between Metabolism and Cancer Biology. *Cell*, 168(4), 657-669.
- Veling, M. T., Reidenbach, A. G., Freiburger, E. C., Kwiecien, N. W., Hutchins, P. D., Drahnak, M. J., Pagliarini, D. J. (2017). Multi-omic Mitoprotease profiling defines a role for Oct1p in coenzyme Q production. *Molecular Cell*, 68(5), 970-977.e11.
- Venditti, E. M., & Kramer, M. K. (2013). Diabetes Prevention Program Community Outreach. *American Journal of Preventive Medicine*, 44(4), S339-S345.
- Venkatapathy, R., & Wang, N. C. (2012). Developmental Toxicity Prediction. *Methods in Molecular Biology*, 305-340.
- Vermeulen, K., Berneman, Z. N., & Van Bockstaele, D. R. (2003). Cell cycle and apoptosis. *Cell Proliferation*, 36(3), 165-175.

- Verrax, J., Dejeans, N., Sid, B., Glorieux, C., & Calderon, P. B. (2011). Intracellular ATP levels determine cell death fate of cancer cells exposed to both standard and redox chemotherapeutic agents. *Biochemical Pharmacology*, 82(11), 1540-1548.
- Versari, D., Daghini, E., Viridis, A., Ghiadoni, L., & Taddei, S. (2009). Endothelial dysfunction as a target for prevention of cardiovascular disease. *Diabetes Care*, 32(suppl_2), S314-S321.
- Vignati, L., Turlizzi, E., Monaci, S., Grossi, P., Kanter, R. D., & Monshouwer, M. (2005). An *in vitro* approach to detect metabolite toxicity due to CYP3A4-dependent bioactivation of xenobiotics. *Toxicology*, 216(2-3), 154-167.
- Wakino, S., Kintscher, U., Liu, Z., Kim, S., Yin, F., Ohba, M., & Kuroki, T. (2001). Peroxisome Proliferator-activated Receptor γ Ligands Inhibit Mitogenic Induction of p21Cip1 by Modulating the Protein Kinase C δ Pathway in Vascular Smooth Muscle Cells. *Journal of Biological Chemistry*, 276(50), 47650-47657.
- Walgren, J. L., Mitchell, M. D., & Thompson, D. C. (2005). Role of metabolism in drug-induced idiosyncratic Hepatotoxicity. *Critical Reviews in Toxicology*, 35(4), 325-361.
- Wallace, D. C., & Fan, W. (2010). Energetics, epigenetics, mitochondrial genetics. *Mitochondrion*, 10(1), 12-31.
- Walsh, J. G., Cullen, S. P., Sheridan, C., Luthi, A. U., Gerner, C., & Martin, S. J. (2008). Executioner caspase-3 and caspase-7 are functionally distinct proteases. *Proceedings of the National Academy of Sciences*, 105(35), 12815-12819.
- Wan, X. S., Zhou, Z., & Kennedy, A. R. (2003). Adaptation of the Dichlorofluorescein Assay for Detection of Radiation-Induced Oxidative Stress in Cultured Cells. *Radiation Research*, 160(6), 622-630.
- Wang, K., & Lin, B. (2013). Pathophysiological Significance of Hepatic Apoptosis. *ISRN Hepatology*, 2013, 1-14.
- Wang, P., Shehu, A. I., & Ma, X. (2017). The opportunities of Metabolomics in drug safety evaluation. *Current Pharmacology Reports*, 3(1), 10-15.
- Wang, S., & Yang, C. (2018). From Apoptosis to Regulated Necrosis: An Evolving Understanding of Acute Kidney Injury. *Current Understanding of Apoptosis - Programmed Cell Death*.
- Wang, X., Pei, D., Xu, J., Guan, Q., Sun, Y., Liu, X., & Zhang, G. (2007). Opposing effects of Bad phosphorylation at two distinct sites by Akt1 and JNK1/2 on ischemic brain injury. *Cellular Signalling*, 19(9), 1844-1856.
- Ward, E., Mittereder, N., Kuta, E., Sims, G. P., Bowen, M. A., Dall'Acqua, W., Herbst, R. (2011). A glycoengineered anti-CD19 antibody with potent antibody-dependent cellular cytotoxicity activity *in vitro* and lymphoma growth inhibition *in vivo*. *British Journal of Haematology*, 155(4), 426-437.

- Wärnmark, A., Treuter, E., Wright, A. P., & Gustafsson, J. (2003). Activation functions 1 and 2 of nuclear receptors: Molecular strategies for transcriptional activation. *Molecular Endocrinology*, 17(10), 1901-1909.
- Wasmuth, H., Tacke, F., & Trautwein, C. (2010). Chemokines in Liver Inflammation and Fibrosis. *Seminars in Liver Disease*, 30(03), 215-225.
- Watanabe, Y. (2002). Troglitazone Glucuronidation in Human Liver and Intestine Microsomes: High Catalytic Activity of UGT1A8 and UGT1A10. *Drug Metabolism and Disposition*, 32), 1462-1469.
- Watford, M. (2018). Long-term regulation of hepatic glutaminase and the urea cycle enzymes. *Nutrition and Gene Expression*, 335-352.
- Watkins, P. B. (2013). Biomarkers for Drug-Induced Liver Injury. *Drug-Induced Liver Disease*, 275-286.
- Watkins, P. B. (2019). Idiosyncratic drug-induced liver injury in patients: Detection, severity assessment, and regulatory implications. *Advances in Pharmacology*, 165-193.
- Weiskirchen, R., & Tacke, F. (2016). Liver fibrosis: From pathogenesis to novel therapies. *Digestive Diseases*, 34(4), 410-422.
- Welbourne, T., Routh, R., Yudkoff, M., & Nissim, I. (2001). The glutamine/Glutamate couplet and cellular function. *Physiology*, 16(4), 157-160.
- Wells, R. G. (2008). The role of matrix stiffness in regulating cell behaviour. *Hepatology*, 47(4), 1394-1400.
- Wen, S., Stolarov, J., Myers, M. P., Su, J. D., Wigler, M. H., Tonks, N. K., & Durden, D. L. (2001). PTEN controls tumour-induced angiogenesis. *Proceedings of the National Academy of Sciences*, 98(8), 4622-4627.
- Weston, A. D., & Hood, L. (2004). Systems Biology, Proteomics, and the Future of Health Care: Toward Predictive, Preventative, and Personalized Medicine. *Journal of Proteome Research*, 3(2), 179-196.
- Westphal, D., Kluck, R. M., & Dewson, G. (2013). Building blocks of the apoptotic pore: how Bax and Bak are activated and oligomerize during apoptosis. *Cell Death Differentiation*, 21(2), 196-205.
- Weyer, C. (2001). Hypoadiponectinemia in Obesity and Type 2 Diabetes: Close Association with Insulin Resistance and Hyperinsulinemia. *Journal of Clinical Endocrinology & Metabolism*, 86(5), 1930-1935.
- Whicher, C. A., O'Neill, S., & Holt, R. I. (2020). Diabetes in the UK: 2019. *Diabetic Medicine*, 37(2), 242-247.
- Whitebread, S., Fekete, A., Jin, H., Armstrong, D., & Urban, L. (2017). Inhibition of Bile Salt Export Pump (BSEP) in Relation to Systemic Exposure: A Risk Factor for

- Drug Induced Liver Injury (DILI). *Journal of Pharmacological and Toxicological Methods*, 88, 215.
- Wilkinson, J. J., Force, R. W., & Cady, P. S. (2004). Impact of Safety Warnings on Drug Utilization: Marketplace Life Span of Cisapride and Troglitazone. *Pharmacotherapy*, 24(8), 978-986.
- Wishart, D. S., Feunang, Y. D., Marcu, A., Guo, A. C., Liang, K., Vázquez-Fresno, R., Scalbert, A. (2017). HMDB 4.0: The human metabolome database for 2018. *Nucleic Acids Research*, 46(D1), D608-D617.
- Wishart, M. J., & Dixon, J. E. (2002). PTEN and myotubularin phosphatases: From 3-phosphoinositide dephosphorylation to disease. *Trends in Cell Biology*, 12(12), 579-585.
- Withington, L. (2002). High-throughput epithelial cell culture systems for screening drug intestinal permeability. *Cell Culture Models of Biological Barriers*, 94-111.
- Wolf, K. K. (2005). Role of the nuclear receptor PXR in acetaminophen hepatotoxicity. *Drug Metabolism and Disposition*.
- Wong, L. H., Gatta, A. T., & Levine, T. P. (2018). Lipid transfer proteins: The lipid commute via shuttles, bridges and tubes. *Nature Reviews Molecular Cell Biology*, 20(2), 85-101.
- Woodhead, J. L., Yang, K., Siler, S. Q., Watkins, P. B., Brouwer, K. L., Barton, H. A., & Howell, B. A. (2014). Exploring BSEP inhibition-mediated toxicity with a mechanistic model of drug-induced liver injury. *Frontiers in Pharmacology*, 5.
- Worby, C. A., & Dixon, J. E. (2014). PTEN. *Annual Review of Biochemistry*, 83(1), 641-669.
- Worth, A. P. (2019). The future of *in silico* chemical safety and beyond. *Computational Toxicology*, 10, 60-62.
- Wright, M. (2006). The impact of pregnane X receptor activation on liver fibrosis. *Biochemical Society Transactions*, 34(6), 1119-1123.
- Wu, H., Von Kamp, A., Leoncikas, V., Mori, W., Sahin, N., Gevorgyan, A., Kierzek, A. M. (2016). MUFINS: Multi-formalism interaction network simulator. *npj Systems Biology and Applications*, 2(1).
- Yamada, H., Suzuki, D., & Kakei, M. (2016). Close Association of Hypoadiponectinemia and Increased Insulin Resistance in Non-Obese Japanese Type 2 Diabetes with Visceral Adiposity. *Journal of Metabolic Syndrome*, 05(04).
- Yamamoto, Y. (2002). Formation of a Novel Quinone Epoxide Metabolite of Troglitazone with Cytotoxic to HepG2 Cells. *Drug Metabolism and Disposition*, 30(2), 155-160.

- Yamazaki, H., Suzuki, M. & Tane, K. (2000). *In vitro* inhibitory effects of troglitazone and its metabolites on drug oxidation activities of human cytochrome P450 enzymes: comparison with pioglitazone and rosiglitazone. *Xenobiotica*, 30(1), 61-70.
- Yang, C., Ko, B., Hensley, C., Jiang, L., Wasti, A., Kim, J., DeBerardinis, R. (2014). Glutamine oxidation maintains the TCA cycle and cell survival during impaired mitochondrial pyruvate transport. *Molecular Cell*, 56(3), 414-424.
- Yang, H., Li, J., Wu, Z., Li, W., Liu, G., & Tang, Y. (2017). Evaluation of Different Methods for Identification of Structural Alerts Using Chemical Ames Mutagenicity Data Set as a Benchmark. *Chemical Research in Toxicology*, 30(6), 1355-1364.
- Yang, H., Sun, L., Li, W., Liu, G., & Tang, Y. (2018). *In Silico* Prediction of Chemical Toxicity for Drug Design Using Machine Learning Methods and Structural Alerts. *Frontiers in Chemistry*, 6. d
- Yang, K., Woodhead, J. L., Watkins, P. B., Howell, B. A., & Brouwer, K. L. (2014). Systems Pharmacology Modeling Predicts Delayed Presentation and Species Differences in Bile Acid-Mediated Troglitazone Hepatotoxicity. *Clinical Pharmacology & Therapeutics*, 96(5), 589-598.
- Yang, T., Espenshade, P. J., Wright, M. E., Yabe, D., Gong, Y., Aebersold, R., Brown, M. S. (2002). Crucial step in cholesterol homeostasis. *Cell*, 110(4), 489-500.
- Yang, V., Pedrosa, S. S., Fernandes, R., Maurício, A. C., Kokschi, B., Gärtner, F., Vale, N. (2019). Synthesis of PEGylated methotrexate conjugated with a novel CPP6, *in silico* structural insights and activity in MCF-7 cells. *Journal of Molecular Structure*, 1192, 201-207.
- Yang, Y., & Sauve, A. A. (2016). NAD + metabolism: Bioenergetics, signaling and manipulation for therapy. *Biochimica et Biophysica Acta (BBA) - Proteins and Proteomics*, 1864(12), 1787-1800.
- Yao, Y., Richman, L., Higgs, B. W., Morehouse, C. A., De los Reyes, M., Brohawn, P., Jallal, B. (2009). Neutralization of interferon- α/β -inducible genes and downstream effect in a phase I trial of an anti-interferon- α monoclonal antibody in systemic lupus erythematosus. *Arthritis & Rheumatism*, 60(6), 1785-1796.
- Yim, S., Yun, C., Ahn, T., Jung, H., & Pan, J. (2005). A Continuous Spectrophotometric Assay for NADPH-cytochrome P450 Reductase Activity Using 3-(4,5-Dimethylthiazol-2-yl)-2,5-diphenyltetrazolium Bromide. *BMB Reports*, 38(3), 366-369.
- Yin, C., Evason, K. J., Asahina, K., & Stainier, D. Y. (2013). Hepatic stellate cells in liver development, regeneration, and cancer. *Journal of Clinical Investigation*, 123(5), 1902-1910.
- Yin, F., Wakino, S., Liu, Z., Kim, S., Hsueh, W. A., Collins, A. R., Law, R. E. (2001). Troglitazone Inhibits Growth of MCF-7 Breast Carcinoma Cells by Targeting G1 Cell

Cycle Regulators. *Biochemical and Biophysical Research Communications*, 286(5), 916-922.

Yki-Järvinen, H. (2004). Thiazolidinediones. *New England Journal of Medicine*, 351(11), 1106-1118.

Yokoi, T. (2011). *Current Topics in Drug Metabolism and Drug Toxicity. Drug Metabolism and Pharmacokinetics*, 26(1), 1-2.

Yoon, S. J., Zhou, L., & Kim, J. R. (2011). Over-expression of PTEN involved in troglitazone-induced Apoptosis in human osteosarcoma cells. *The Journal of the Korean Bone and Joint Tumour Society*, 17(1), 23.

Youn, H., Jung, S., Park, M., & Yoon, J. (2008). Peroxisome proliferator-activated receptor-gamma agonist, troglitazone has anticancer effect on breast cancer cells. *European Journal of Cancer Supplements*, 6(7), 84.

Youssef, J. A., & Badr, M. Z. (2013). Peroxisome Proliferator-Activated Receptors. *Peroxisome Proliferator-Activated Receptors*, 15-23.

Yu, C., Minemoto, Y., Zhang, J., Liu, J., Tang, F., Bui, T. N., Lin, A. (2004). JNK Suppresses Apoptosis via Phosphorylation of the Proapoptotic Bcl-2 Family Protein BAD. *Molecular Cell*, 13(3), 329-340.

Yu, M., Chen, C., Liang, X., Wang, L., Gandhi, C. R., Fung, J. J., Qian, S. (2004). Inhibition of T-cell responses by hepatic stellate cells via B7-H1-mediated T-cell apoptosis in mice. *Hepatology*, 40(6), 1312-1321.

Yuan, G., & Hegele, R. A. (2007). Treating hypertriglyceridemia. *Canadian Medical Association Journal*, 177(6), 604.2-605. doi:10.1503/cmaj.1070076

Yuan, L., & Kaplowitz, N. (2013). Mechanisms of drug-induced liver injury. *Clinics in Liver Disease*, 17(4), 507-518.

Zaganas, I., & Plaitakis, A. (2002). Single Amino Acid Substitution (G456A) in the Vicinity of the GTP Binding Domain of Human Housekeeping Glutamate Dehydrogenase Markedly Attenuates GTP Inhibition and Abolishes the Cooperative Behavior of the Enzyme. *Journal of Biological Chemistry*, 277(29), 26422-26428.

Zaganas, I., Pajęcka, K., Wendel Nielsen, C., Schousboe, A., Waagepetersen, H. S., & Plaitakis, A. (2013). The effect of pH and ADP on ammonia affinity for human glutamate dehydrogenases. *Metabolic Brain Disease*, 28(2), 127-131.

Zanger, U. M., & Schwab, M. (2013). Cytochrome P450 enzymes in drug metabolism: Regulation of gene expression, enzyme activities, and impact of genetic variation. *Pharmacology & Therapeutics*, 138(1), 103-141.

Zhang, J., Kuehl, P., Green, E. D., Touchman, J. W., Watkins, P. B., Daly, A., Boguski, M. S. (2001). The human pregnane X receptor: genomic structure and identification and functional characterization of natural allelic variants. *Pharmacogenetics*, 11(7), 555-572.

- Zhang, X., Liu, F., Chen, X., Zhu, X., & Uetrecht, J. (2011). Involvement of the immune system in idiosyncratic drug reactions. *Drug Metabolism and Pharmacokinetics*, 26(1), 47-59.
- Zhang, Z., Lapolla, S. M., Annis, M. G., Truscott, M., Roberts, G. J., Miao, Y., Lin, J. (2004). Bcl-2 Homodimerization Involves Two Distinct Binding Surfaces, a Topographic Arrangement That Provides an Effective Mechanism for Bcl-2 to Capture Activated Bax. *Journal of Biological Chemistry*, 279(42), 43920-43928.
- Zhao, W., Zitzow, J. D., Ehresman, D. J., Chang, S., Butenhoff, J. L., Forster, J., & Hagenbuch, B. (2015). Na⁺/Taurocholate Cotransporting Polypeptide and Apical Sodium-Dependent Bile Acid Transporter Are Involved in the Disposition of Perfluoroalkyl Sulfonates in Humans and Rats. *Toxicological Sciences*, 146(2), 363-373.
- Zhao, Y., Seefeldt, T., Chen, W., Wang, X., Matthees, D., Hu, Y., & Guan, X. (2009). Effects of glutathione reductase inhibition on cellular thiol redox state and related systems. *Archives of Biochemistry and Biophysics*, 485(1), 56-62.
- Zhou, J., Liu, M., Zhai, Y., & Xie, W. (2008). The Antiapoptotic Role of Pregnane X Receptor in Human Colon Cancer Cells. *Molecular Endocrinology*, 22(4), 868-880.
- Zhou, J., Zhai, Y., Mu, Y., Gong, H., Uppal, H., Toma, D., Xie, W. (2006). A Novel Pregnane X Receptor-mediated and Sterol Regulatory Element-binding Protein-independent Lipogenic Pathway. *Journal of Biological Chemistry*, 281(21), 15013-15020.
- Zhou, Y., Wen, Y., Kang, X., Qian, H., Yang, J., & Yin, Z. (2008). Troglitazone, a peroxisome proliferator-activated receptor γ ligand, induces growth inhibition and apoptosis of HepG2 human liver cancer cells. *World Journal of Gastroenterology*, 14(14), 2168.
- Zhu, R., Wang, Y., Zhang, L., & Guo, Q. (2012). Oxidative stress and liver disease. *Hepatology Research*, 42(8), 741-749.
- Zong, W. (2001). BH3-only proteins that bind pro-survival Bcl-2 family members fail to induce apoptosis in the absence of Bax and Bak. *Genes & Development*, 15(12), 1481-1486. doi:10.1101/gad.897601
- Zucchini, N., De Sousa, G., Bailly-Maitre, B., Gugenheim, J., Bars, R., Lemaire, G., & Rahmani, R. (2005). Regulation of Bcl-2 and Bcl-xL anti-apoptotic protein expression by nuclear receptor PXR in primary cultures of human and rat hepatocytes. *Biochimica et Biophysica Acta (BBA) - Molecular Cell Research*, 1745(1), 48.

Appendix A.

Control file for simulations

```

*TGZv11.ctrl - Notepad
File Edit Format View Help
MODEL ./recon2_xt.PIPES.CORE.TGZ.sfba
NUMBER_OF_SAMPLES 1
SEED 761

TIME_MAX 1440
MAXIMAL_TIMESTEP 0.01
MAX_CHANGE 0.01
OUTPUT ./outputv11.xls
LOG ./log_low.txt
MONITOR 10000
PROGRESS 10000

INITIAL_STATE
TGZ 100
Hepatocytes 21.6273
RBC 400
Glucose 4.5
Lactate 1.5
Urea 4.0
PARP 1E+6
CytoC_m 500000
M 500000
Apaf 100000
Bax 100000
proC9 100000
Smac_m 100000
XIAP 100000
Bid 40000

PROPENSITY_FUNCTION
PPARtarget_transcription_PPAR
PPARytarget_gene*12*
(PPARy_act-PPARyP)
END
*/ MONITORS */

PETRI_NET_MONITORS
TGZ
PXR
PXR_act
PPARy
PPARy_act
PPARyP
JNK
JNK_act
Trx_Ask1
Trx_Ask1act
Test_O2s

RBC
Hepatocytes

Glucose
Urea
Lactate

Glucose_liver_flux
Lactate_liver_flux
urea_liver_flux

PPARytarget_mRNA
FABP1
insig1
insig1_mRNA
SREBP1c_SCAP_insig1
SREBP1_mRNA
SREBP1c_ER
SREBP1c_nuc
FAS
HMGCOAR
FABP1
Cholesterol
FAS100COA_flux
HMGCOARc_flux
FABP1_flux
TGZquinone_flux
TGZglc_flux
TGZS04_flux
TGZ_ext_flux
O2s_flux
casp8
casp6
casp3
PARP
cPARP
Bid
tBid
Apop
Bcl2_mRNA
END
SIMULATION

```

The control file includes the name of the database, the names, and destinations of the related data files, the time frame for creating the file, and the checkpoint information

